Radiosurgery of Brain Arteriovenous Malformations

Buis, D. R.

Published: 01/01/2010

Document Version
Publisher's PDF, also known as Version of record

Citation for pulished version (APA):
Buis, D. R. (2010). *Radiosurgery of Brain Arteriovenous Malformations: From Target Delineation to Obliteration*. [Phd-Thesis - Research and graduation external, Vrije Universiteit: Faculteit Geneeskunde].

Radiosurgery of brain arteriovenous malformations: from target delineation to obliteration Dennis Robert Buis

Radiosurgery of brain arteriovenous malformations: from target delineation to obliteration

Dennis Robert Buis

Radiosurgery of brain arteriovenous malformations: from target delineation to obliteration

Dennis Robert Buis

The studies described in this thesis were conducted at the Departments of Neurosurgery, Radiation Oncology and Radiology of the VU University Medical Center, Amsterdam, The Netherlands.

Radiosurgery of brain arteriovenous malformations:
from target delineation to obliteration
Buis, Dennis R.
Amsterdam: VU Universiteit, Faculteit Geneeskunde
Thesis VU University, with a summary in Dutch
ISBN: 978-90-9025748-8
Cover image: The Great Wave off Kanagawa, Katsushika Hokusai, ca. 1829 – 32,
Library of Congress, Washington DC
Cover design and lay-out: Esther Beekman (www.estherontwerpt.nl)
Printed by: Ipskamp Groep

Financial support for publication of this thesis from following sources is gratefully acknowledged: B. Braun Medical B.V.; Carl Zeiss B.V.; Codman Johnson & Johnson; Elekta B.V.; Integra LS; Neurosurgical Center Amsterdam; Nycomed B.V.; Promedics Medical Systems B.V.; The Netherlands Heart Foundation and the Van Leersum Fund, Royal Netherlands Academy of Arts and Sciences.

VRIJE UNIVERSITEIT

Radiosurgery of Brain Arteriovenous Malformations: From Target Delineation to Obliteration

ACADEMISCH PROEFSCHRIFT

ter verkrijging van de graad Doctor aan
de Vrije Universiteit Amsterdam,
op gezag van de rector magnificus
prof.dr. L.M. Bouter,
in het openbaar te verdedigen
ten overstaan van de promotiecommissie
van de faculteit der Geneeskunde
op donderdag 11 november 2010 om 11.45 uur
in de aula van de universiteit,
De Boelelaan 1105

door
Dennis Robert Buis
geboren te Amsterdam

promotoren: prof.dr. W.P. Vandertop
prof.dr. B.J. Slotman
copromotoren: prof.dr. C.M.F. Dirven
prof.dr. F. Barkhof

If I could write the beauty of your eyes,
And in fresh numbers number all your graces,
The age to come would say 'This poet lies;
Such heavenly touches ne'er touch'd earthly faces.'

William Shakespeare, Sonnet XVII

Once our hearts get broken, they never fully heal. They always ache. But perhaps a broken heart is a more loving instrument. Perhaps only after our hearts have cracked wide open, have finally and totally unclenched, can we truly know love without boundaries.

Fred J. Epstein, neurosurgeon, 1937 - 2006

Aan mijn ouders

Table of contents

Chapter 1

General Introduction and Outline of This Thesis

D.R. Buis

BRAIN ARTERIOVENOUS MALFORMATIONS: DIAGNOSIS

Introduction

A brain arteriovenous malformation (bAVM) is a network of abnormal channels between the arterial feeders and the draining veins[446]. This network is called the nidus (Figure 1.1). A bAVM is caused by a structural defect in the formation of the primitive arteriolar-capillary system. The absence of this capillary system results in low resistance within this network and induces an exaggerated blood flow, causing a shortened arteriovenous transit time and therefore a shunt.

BAVMs are thought to be caused by either persistence of a primitive arteriovenous connection, or by reopening after its initial closure. It has been proposed that bAVMs are formed when the embryo is in the 40 – 80 mm stage, that is before three months' gestation, when multiple pial-to-dura arachnoidal veins are being absorbed[318]. Other authors have suggested that they may be the result of a biological dysfunction of the remodelling process at the junction of capillaries and veins[254]. Therefore, early mutations in embryogenesis may lead to large metameric bAVMs or cerebral-facial syndromes such as CAMS or Wyburn-Mason[36], or multiple bAVMs as in hereditary hemorrhagic teleangiectasias[243] or familial occurrence[30], while smaller bAVMs are caused by later causative events. This theory is further supported by the finding of an association of polymorphism in the ALK1 gene that causes hereditary hemorrhagic teleangiectasias, among patients with a sporadic bAVM[357]. Such a mutation may result in a 10.000 fold increased risk of developing a bAVM[227].

As the bAVM originates due to a single event, bAVMs should not grow. Observed growth is therefore likely to be caused by a secondary angiopathy, or angiogenesis after ischemia, or hemorrhage.

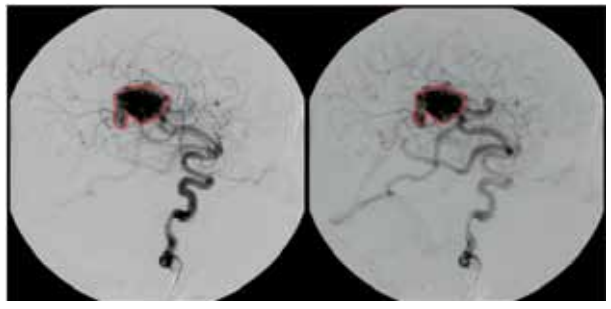

Figure 1.1
Lateral digital subtraction angiography (DSA) in a 46 year old female with a Spetzler-Martin grade III bAVM. The nidus is encircled in red. There is deep drainage in the direction of the straight sinus (black arrow), and superficial drainage in the direction of the Vein of Labbé (white arrow).

BAVM vessels exhibit a wide spectrum of vascular phenotypes. Macroscopically, feeding arteries and draining veins are generally mature, normal-appearing vessels that may exhibit some degree of wall thickening. Microscopically, the arteries demonstrate smooth muscle hyperplasia associated with fibroblasts and hyalinized connective tissue elements[54, 143, 202]. Venous elements are dilated due to exposure to elevated pressure[32, 50]. They tend to have thin collagenous walls, whereas arterial feeders have muscular elastic walls[50]. The intranidal vessels may participate in direct connections between the arterial and venous circulations[446], and often lack normal periendothelial support structures[289, 477]. Parenchymal elements within the bAVM tend to be gliotic, hemosiderin-stained and not functional[50]. BAVM vessels exhibit abnormal expression of Tie-2 and Vascular Endothelial Growth Factor (VEGF) Receptor which may contribute to its aberrant vascular phenotype[173].

Epidemiology

In the New York Islands AVM Study, 284 prospective bAVM patients were found during 21.216.467 person-years of observation. Hence the incidence, i.e. the annual number of new patients presenting with a bAVM was 1.34 (95% CI, 1.18 to 1.49) per 100.000 person-years[432]. Comparable numbers were found in Scotland, Sweden, The Netherlands Antilles and Northern California with an annual incidence of 1.12 (95% CI, 0.90 to 1.37), 1.24, 1.1 and 1.4 per 100.000 adults, respectively[5, 137, 186, 208]. In a prevalence study, on a given day, 93 patients with a previously diagnosed bAVM were encountered among a population of 628.788 persons over 16 years old, resulting in a prevalence of 18 per 100.000 persons[6].

Extrapolating these data to the adult population of the Netherlands, this frequency estimates approximately 180 new patients each year, and 3000 prevalent patients alive with a bAVM at any given day[9]. However, it is of interest to note that five bAVMs were found in a cohort of 2.563 healthy applicants for German military flying duty who underwent MR-imaging of the brain[464], suggesting that the actual prevalence (0.2%) is probably higher, but that not all bAVMs present clinically.

Clinical presentation

An intracerebral hemorrhage is the main mode of presentation for a bAVM[6, 134, 189], with around 53 - 71 percent of all patients presenting with an initial hemorrhage[88, 340]. Hemorrhage from a bAVM accounts for approximately 1.4 percent of all intracranial hemorrhages, however, in children this percentage may reach up to 61 percent[348, 431]. Intracerebral hemorrhage from a bAVM has a prevalence of 0.68 per 100.000 and an incidence of 0.51 per 100.000 person years[5, 432]. Patients presenting with a hemorrhage tend to be younger, with a median age at presentation of 28 years for a hemorrhagic and 38 years for a non-hemorrhagic

presentation[432]. The first hemorrhage is fatal in nearly 5 percent[21]. Factors thought to be associated with a hemorrhagic presentation are an increased age[216], small bAVM size[211], deep bAVM location[117, 436] and exclusive deep venous drainage, venous outflow restriction[104, 433] or a small number of draining veins[436], high arterial input pressure[104] and feeding artery aneurysms[434].

Seizures are the second most common form of presentation. Approximately 30 – 40 percent of bAVMs presents with epileptic seizures[189, 293, 430]. Not unexpectedly, a bAVM size larger than three centimeters and a temporal location are factors found to be associated with seizures at presentation[190]. In case of an unruptured bAVM, seizures usually start before the age of 60[430].

Headache is the presenting symptom in 4 – 16 percent of patients[149, 189, 293]. Headache preceded a hemorrhage in 12.6 percent and was found to be an early warning when it increased in frequency, intensity and duration[149]. BAVM-related headaches are non-pulsating and are only rarely accompanied by nausea, vomiting, photo- or phonophobia[149]. Focal neurological deficits, defined as deficits that are neither attributable to a migrainous aura, nor postictal, nor related to a hemorrhage or infarction after radiological investigation, are reported in 7 – 15 percent of the patient population, and more often in women[73, 189, 293]. They are associated with an increasing age, a deep, or brainstem location, or venous ectasias[73].

Natural history and risk of hemorrhage

In a prospective study of 160 patients with an untreated bAVM, a major hemorrhage was seen in 64 patients (40 percent) during a follow up interval of 23.7 years[340]. The risk of hemorrhage after presentation varies and seems to depend on the type of presentation and the angiographic characteristics of the bAVM[370]. The annual risk is estimated to be 1.3 – 3.9 percent after an initial non-hemorrhagic presentation[53, 88, 152, 340]. Patients presenting with epilepsy, but without hemorrhage, are thought to have an annual risk of hemorrhage of 1.5 – 4.0 percent[88, 296, 340]. The annual risk after an initial, clinical hemorrhage is approximately comparable, ranging annually from 0.9 – 3.9 percent[88, 152, 203, 340], but has been reported to be as high as 6.0 – 18 percent in the first year after clinical presentation[134, 152, 203, 478]. However, this annual hemorrhage rate may be as high as 34 percent[433] in individual cases where the bAVM demonstrates factors known to be associated with bleeding, such as a large bAVM size or a Spetzler-Martin grade IV or V[206, 216, 433, 437] (see Imaging, page 14), increasing age[216, 433], deep brain location[433, 437], and hypertension[252]. Patient-related factors that seem to predispose for hemorrhage after an initial diagnosis of a bAVM include the presence of the Apo E and TNF-alpha-238 AG genotype[3, 356].

Several risk prediction formulas have been proposed in order to estimate a patients life time cumulative risk of hemorrhage[51, 238]. These models are based on the patients age and a 3-4 percent annual risk of hemorrhage. In general, the patients' cumulative chance of staying hemorrhage-free for life from a bAVM is equal to the following: (1 – (1-risk of hemorrhage) $^{\text{expected years of remaining life}}$)[238]. Put differently, the cumulative life time risk of bleeding (at least once) for a 3 percent annual risk is: (1 – $0.97^{\text{expected years of remaining life}}$). A more simple way of approximating the lifetime risk of hemorrhage for patients with bAVMs, again based on a 3 percent annual risk of hemorrhage and the patients age, is 105 minus the patients' age in years[51]. Using either model, the estimated lifetime risk of a hemorrhage for, e.g. a 25-year-old with a newly diagnosed bAVM after a first hemorrhage is approximately 80 percent.

Reports regarding the clinical outcome after hemorrhage from a bAVM have demonstrated different results. A large and prospective, study demonstrated that the clinical outcome after bleeding from a bAVM is mild when compared to patients suffering from a spontaneous, non-bAVM-related hemorrhage[74, 77]. Although presentation with a first hemorrhage is an important predictor for a subsequent hemorrhage, a second bAVM-related hemorrhage in general does not result in a worse disability[74, 161]. Although a modified Rankin score ≤ 3 has been reported in 33 percent of patients by the time of hospital discharge, the long term disability seems less gloomy[161], with no neurological deficits in 47 percent, and an additional 37 percent independent in their daily life after a mean follow-up of sixteen months after initial hemorrhage[169]. Several problems with these studies have been addressed, including the large amount of intraventricular and subarachnoid bleedings, in which the outcome is better due to absence of parenchymal damage. Furthermore, a short follow-up varying between 55 days and 16.1 months, and the long interval before the patients were referred to these tertiary referral centers, suggest a selection bias[9, 77, 78, 311]. Other studies demonstrate less optimistic data: 7.4% mortality was reported among 27 Spetzler-Martin grade I and II patients who presented with a bleeding and were operated on acutely[355]. Moreover, a combined prospective and retrospective study in a single hospital in Perth, Western Australia, showed less optimistic data, with 8.8 percent bAVM-related mortality, including 3.9 percent mortality during active management, and 24.6 percent during expectative management[21].

It has been observed that approximately 1 percent of bAVMs regresses spontaneously and completely during follow-up[1, 353]. This phenomenon is poorly understood, although the closing of the (single) venous drainage pathway seems to play an important role in this process[347, 397]. As no angiographic, or other radiological data have been found that can predict spontaneous regression, this option of spontaneous regression should not be considered realistic in the management of bAVMs[265]. Although careful follow-up has been recommended

after spontaneous regression in order to diagnose bAVM reappearance early[188], no cases of bleeding after spontaneous regression have been reported. After complete eradication or obliteration of the bAVM the risk of (re-)bleeding decreases impressively, although not completely to zero. In a retrospective study of 500 patients undergoing radiosurgery for a bAVM, 318 patients bled during 32 follow-up years before radiosurgery, eleven patients bled during three follow-up years in the interval period before obliteration, and two patients bled during 4.8 years follow-up after obliteration[291, 292]. The risk of hemorrhage was reduced by 86 percent after obliteration, compared with the period before radiosurgery. Therefore, complete obliteration of the bAVM, without introducing new morbidity should be the goal of treatment[118, 129, 336].

Imaging

The aim of imaging is first to find, or exclude, a bAVM and to distinguish it from other intracranial vascular pathologies. When diagnosed, the neuroradiological examination can supply the basis for its treatment[418]. Neuroradiological studies should identify feeding arteries and draining veins, but also evaluate the angioarchitecture and other particularities of the nidus, its proximity to eloquent brain tissue, as well as the different manifestations of high-flow angiopathy, the associated parenchymatous lesions, or other incidental and clinically asymptomatic cerebral pathologies. From the hemodynamic point of view, flow velocities in the different vascular compartments and global modification of the cerebral circulation should be evaluated in detail[17].

High resolution digital subtraction angiography (DSA) with a high frame rate, remains the gold standard for analyzing the precise angio-architecture of a bAVM, including the presence or absence of related aneurysms and the pattern of venous outflow[17, 129, 181, 343, 418, 455]. Although DSA is an invasive investigation and not without risk, large prospective studies have shown it to be a safe procedure with transient neurologic complications occurring in 0.3 – 2.6 percent and permanent neurological complications in 0 – 0.5 percent[76, 94, 221, 474]. On DSA the bAVM consists of tightly packed, pyramidal tangle of enlarged feeding arteries and dilated draining veins, with characteristic arteriovenous shunting (Figure 1.1)[343]. Associated abnormalities include flow induced angiopathy, or flow-related aneurysms[343]. These aneurysms may be located in the nidus, or on a feeding vessel[299]. In order to rule out dural contribution to the bAVM the angiographic series should always include the external carotid vessels. Other neurovascular pathologies that may resemble a bAVM on DSA include Developmental Venous Anomalies (DVA)[198, 475], cerebral proliferative angiopathy[258], or highly vascularized primary brain tumors[343].

MRI is very sensitive, showing an inhomogeneous signal void on T_1- and T_2-weighted sequences, commonly with hemosiderin deposits, suggesting prior hemorrhage (Figure 1.2)[196, 344]. In comparison to CT, MRI permits better visualization of the exact location of the bAVM and its relation with surrounding cerebral structures[129, 376, 415]. In comparison to DSA, 3D dynamic MR digital subtraction angiography was able to detect all nidi[144]. Evaluation of size of the nidus by both techniques was similar, but on 3D dynamic MR angiograms, veins were correctly analyzed in only 89 percent[144]. Other neurovascular pathologies that may resemble a bAVM on MRI include cavernomas[363] or vascularized primary brain tumors[343]

On CT irregularly hyperdense areas with spotlike contrast enhancement can be seen[376]. CT-Angiography provides better vascular detail than MR-Angiography[344], whereas CT, with and without contrast, may be necessary to improve depiction of previously embolized parts of the nidus[165].

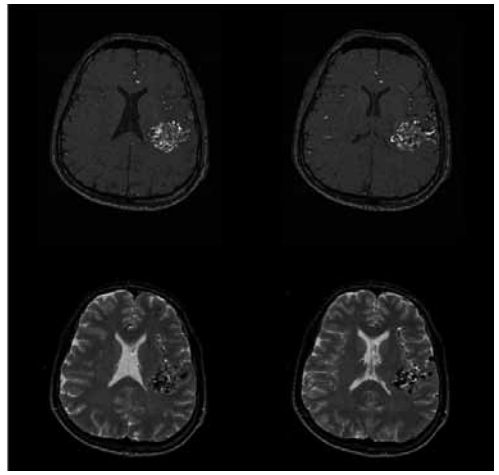

Figure 1.2
MR-Angiography and T_2-weighted MR-images of the same left parietal bAVM as depicted in figure 1.1 On MR-angiography (upper row) the bAVM is characterized by hyperintense flow signal. On T_2-sequences (bottom row) there are flow voids in the same region, with some intranidal hyperintensity.

Although a non-contrast enhanced CT-scan has a low sensitivity for detecting bAVMs, it is the modality of choice for demonstrating an initial hemorrhage[415]. In the acute phase after a hemorrhage, CT-angiography can be very useful to demonstrate the original site of bleeding such as an intranidal aneurysm or venous pouch[97, 234, 444]. As a surrounding hematoma may partially compress the nidus, timing is a major concern. Intranidal aneurysms are known to be associated with early rebleeding, hence an early DSA[299], preferably performed within one week, should be made in order to assess the possibility of endovascular treatment of the intranidal aneurysm. In the absence of an intranidal aneurysm DSA should preferably be done at least six weeks to three months after the hemorrhage, depending on the resorption rate of the hematoma[153, 187, 473].

In 1986, Spetzler and Martin proposed a simple grading system on the basis of bAVM size, pattern of venous drainage and neurological eloquence of adjacent brain (table 1)[423]. This

Table 1.1: Spetzler-Martin bAVM grading system[423]

Size	Points
Small (< 3 cm)	1
Medium (3-6 cm)	2
Large (> 6 cm)	3
Eloquence of adjacent brain‡	
non-eloquent	0
eloquent	1
Pattern of venous drainage!!	
Superficial only	0
Deep	1

‡ Eloquent brain: sensorimotor; language and visual cortex; hypothalamus and thalamus; internal capsule; brainstem; cerebellar peduncles; deep cerebellar nuclei

!! Venous drainage is considered superficial if all drainage is through the cortical venous system; it is considered deep if any or all is through internal cerebral veins, basal veins, or precentral cerebellar vein

Table 1.2: Percentage good clinical outcome after surgery, correlated to Spetzler-Martin grade (SMG)[185]

SMG	Good clincal outcome
I	100
II	94,3
III	88,6
IV	61
V	28,6
VI	N/A

grading system awards a maximum of five points, based on three categories (size, drainage pattern, and eloquent cerebral location) to each bAVM. Application of this system is possible using DSA, as well as MR-angiography[383]. Retrospective application of this grading system showed a correlation with the incidence of postoperative neurological complications (table 2) [185, 423]. In 2003, a modification of the heterogeneous group of grade III bAVMs was proposed in order to improve on its usefulness to predict surgical risks for new neurological deficits or death[259].

BRAIN ARTERIOVENOUS MALFORMATIONS: TREATMENT

Although bAVM-related seizures seem to respond well to medical therapy with good control in 75 percent[345], treatment of the bAVM itself is indicated when the risk of treatment-induced neurological morbidity is expected to be lower than the morbidity incurred during the natural

history of a specific bAVM in a specific patient. Factors that predispose an individual patient to either a low or high hemorrhage risk should be taken into consideration when managing a bAVM[370]. The goal of treatment should be aimed at complete eradication or obliteration of the bAVM in order to minimize the chance of intracerebral hemorrhage[336]. Modalities for treatment of a bAVM include microsurgical resection, endovascular embolization, and stereotactic radiosurgery, or any combination of these three. Each modality has its own indication and advantages, as well as its disadvantages.

Neurosurgery

Historically, there is a strong tradition in surgery of bAVMs since the first complete excision by Olivecrona in 1932[484], made possible by the development of cerebral angiography by Moniz in 1927[102, 127, 277]. Introduction of the operating microscope by Yaşargil in the 1960s greatly improved the possibilities of surgery for bAVMs. After the introduction of the Spetzler-Martin classification (Table 1)[423], the surgical risk could be approximated reliably, and microneurosurgery of Spetzler-Martin grade I and II bAVMs is now frequently performed with good results (Table 2)[92, 171, 185, 312, 423]. As the rate of neurological complications increases to 12.2 and 38.4 percent respectively in Spetzler-Martin grade IV and V, no surgical treatment is recommended for these grades nowadays[167, 183, 185, 233, 422, 424]. In addition to bAVM-related determining factors, a female gender, and non-hemorrhagic presentation appear to be significantly associated with treatment-related neurological deficits[170, 171]. A favorable functional outcome was reached in 85% of patients who were operated on immediately

Endovascular embolization

In addition to microneurosurgery, endovascular embolization has been introduced in order to reduce the flow in bAVMs. From the 1960's and '70's catheters were developed, based on the belief that higher flow in the vessels supplying the bAVM could be used to direct emboli into the nidus[48]. Various materials, including polymer threads, 6-0 silk sutures, gelatin particles and autologous clot have been used as embolic agents. However, many of these agents were either difficult to control during delivery, associated with high rates of recanalization or induced vasculitis. Currently N-butyl cyanoacrylate (NBCA) is used. NBCA polymerizes rapidly on contact with blood, but is easy to cut, which makes the guiding catheter less prone to being cast into the glue. A relatively new agent is a combination of ethylene-vinyl alcohol copolymer and dimethyl sulfoxide (Onyx®), which is thick enough to fill vessels, but does not adhere to the catheter, although the microcatheter might still get trapped within the embolization material[24]. The ultimate goal of treatment of a bAVM, complete obliteration, is rarely reached after embolization alone, because many small vessels cannot be catheterized, and most series report five to 28 percent complete obliteration[177, 220, 390]. In a retrospective study, in which 192 patients were endovascularly treated in 489

embolization sessions with mainly NBCA, >75 percent nidus reduction was reached in 32 percent[207]. Permanent disabling and non-disabling complications occurred in 1.6 and 2.6 percent, respectively. The number of embolized feeders (>3), Spetzler-Martin grade III – V bAVMs, and periprocedural hemorrhage have been associated with an increased chance of complications[228, 261].

The appropriate role of endovascular embolization has been under debate. Currently, endovascular embolization is useful as a preoperative treatment in appropriately selected patients in order to reduce bAVM size, eliminate surgically inaccessible vessels and prevent excessive intraoperative blood loss[115, 465]. Other goals of presurgical embolization are to occlude intranidal aneurysms in the initial phase after a hemorrhage and high-flow fistulas in order to promote progressive thrombosis of the nidus of the bAVM[115, 336]. Too proximal occlusion of feeding vessels and failure to occlude the nidus with embolic agents may have a deleterious effect on surgery because of the inevitable development of cortical and transdural collaterals[459]. Embolization before radiosurgery aims to reduce bAVM size, decreasing the volume of the radiation field and improving conformal dosing, thereby increasing the rate of obliteration[336]. In case of a small bAVM with a single feeder embolization can serve as definitive treatment.

Stereotactic Radiosurgery

In 1949, Leksell, a Swedish neurosurgeon, (Figure 1.3) devised a stereotactic guiding device[267], which was based on the arc-center principle and consisted of an arc mounted onto a headframe, in such a way that the center of the arc always coincided with the target (Figure 1.3). Using this device, he was able to determine the exact coordinates of every structure within the framework of the stereotactic device. Subsequently, he developed a method for rotating an orthovoltage x-ray tube around his stereotactic instrument, thereby focusing its beam on the target in the center[268]. This results in a very steep dose gradient, which makes it possible to deliver a larger and more efficacious dose to the target, without exceeding the radiation tolerance of adjacent normal tissue. In 1967 this concept resulted in the first Gamma-knife.

Originally, the Gamma-knife was used to treat functional cases primarily. However, the advent of CT in the 1970s and MRI in the 1980s made treatment of tumors and bAVMs possible. The increase in indications for radiosurgery resulted in modifications in standard medical linear accelerators in order to also use these for radiosurgery. Although the process of treatment and the accuracy between a gamma-knife and a stereotactic linear accelerator (linac) are comparable, the method of delivery of radiation differs. The Gamma-knife uses a hemispheric collimator helmet with 201 conical channels in which a Cobalt 60 radiation

Figure 1.3
Lars Leksell (left), a Swedish neurosurgeon who developed a stereotactic apparatus for human functional neurosurgery in 1949. The arc is mounted on a headframe in such a way that the center of the arc always coincides with the target (middle). When this principle is used in a Gamma-knife the patient is placed under a helmet with 201 conical channels right) in which the Cobalt 60 radiation source is placed (photo: Elekta/Neurosurgery-Online).

Figure 1.4
A linac crossfires a photon beam by moving in arc shaped paths around the patients head (left), hence the radiation beams converge towards the unit center point, which is defined as the point of intersection of the axis of the individual source beams (right) (photo: BrainLAB/VU University Medical Center.

source is placed (Figure 1.3)[192]. A linac crossfires a photon beam by moving in arc shaped paths around the patients head (Figure 1.4), thereby minimizing irradiation of normal tissue[192]. In both cases, the radiation beams converge towards the unit center point, which is defined as the point of intersection of the axis of the individual source beams (Figure 1.4).

In order to stereotactically localize the target, a derivative of Leksells stereotactic device is attached to the patients skull under local anesthetics (Figure 1.5). A combination of CT-, or MR-imaging, and stereotactic DSA is performed in order to depict the target and to provide

the 3D image data set used to develop a treatment plan for radiation delivery. Using the stereotactic base ring, the patient is placed in such a way that the point of intersection of the radiation beams coincides with the intended target point in the brain, i.e. the bAVM.

Successful radiosurgery of a bAVM results in slow, but progressive endothelial proliferation with hyalin and calcium deposition in the vessel walls, and finally in complete obliteration of the bAVM[67, 401, 439]. In recent publications this process succeeds in between 67 – 81 percent after four years and between 87 – 91 percent after five to six years[291, 411, 487, 489]. In the interval after radiosurgery, but before complete obliteration, the overall risk of hemorrhage decreases by 54 percent. After obliteration this risk decreases further by 88 percent[291]. After repeat radiosurgery, in case of failure of initial radiosurgery, the chance of successful obliteration is comparable to that of the initial radiosurgery, with reported obliteration rates varying between 35 and 86 percent[372, 382].

Figure 1.5
The stereotactic base ring is attached to the patients skull under local anesthetics (photo: Elekta).

Although an increased marginal radiation dose has been associated with increased bAVM obliteration, increasing the dose is limited by an increased risk of radiation-induced complications. Radiation induced image changes, consisting of an area of hyperintensity surrounding the bAVM, on T_2-weighted or FLAIR MR-images, have been reported in up to 60 percent of all patients[166, 282, 372]. These changes occur from two to 36 months after treatment[282, 372], and resulted in permanent neurological deficits in 5.1 percent[166]. However, radiological radiation necrosis was seen in 11.2% with a mean time to onset of eighteen months[39]. A larger bAVM-volume and the volume of tissue receiving radiation in excess of 12 Gy were found to be significantly related to adverse radiation effects[131, 140]. Longer term complications include the formation of cysts, which occurred in 3.4 percent after a mean latency period of 6.8 years[109, 204, 367, 479]. After a second radiosurgical treatment, moderate-grade radiation changes on MRI have been reported to increase from 57.7 to 88.2 percent[400]. However, this

was not found to be significant. Neither was a significant increase in necrosis-like changes found[400].
Based on eight patients who developed radiation necrosis among 74 patients with a bAVM treated with proton beam therapy, Kjellberg was the first to construct a radiation-dose vs. volume plot that would predict a 1 percent chance of radiation necrosis[231]. However, extended follow-up demonstrated that this model seriously underpredicted the actual risks of permanent complications[28]. Newer models based on the integrated logistic formula and the relative seriality model as developed by Flickinger and Karlsson *et al.* used prescription doses that ensure low levels (less than 3 percent) of expected complications[119, 214]. These models suggest that the prescribed dose has to be reduced as the nidus volume increases. However, only an increasing marginal dose was found to be strongly correlated with successful treatment, there is therefore no independent volume effect[111, 121, 123, 487, 497]. The latest, and most regularly used model to predict patient outcome after radiosurgery was published by Pollock *et al.* in 2002[368, 369]. This model calculates the bAVM-score based on numerical values for bAVM volume, location, and the patients age (Table 1.3). All patients with a bAVM score of one or lower had an excellent outcome compared with only 39 percent of patients with a bAVM score higher than two[368].

Table 1.3: bAVM score according to Pollock[369]

bAVM score = (0.1)(bAVM volume, mL) + (0.02)(patient age, yr) + (0.5)(bAVM location†)

† bAVM location:	Points
Hemispheric, Corpus Callosum, Cerebellum	0
Basal ganglia, thalamic, or brainstem	1

Although treatment failure after radiosurgery may be caused by several factors, such as inappropriately selecting too large bAVMs for radiosurgery[166], using an inefficient radiation dose, radioresistence in case of a fistulous bAVM[250], or inaccurate target delineation[375]. Target delineation is impeded due to observer-, imaging-, and bAVM-related factors[121, 122, 165, 497]. Observer-related factors are mainly the consequence of the absence of a common definition of the nidus. Imaging-related factors reflect the quality of the DSA and the angiographic phase in which the nidus is determined[43, 288]. BAVM-related factors include the presence of a high-flow bAVM with almost simultaneous filling and overlap of feeding arteries, nidus, and draining veins, a history of prior embolization[15, 121], or a diffuse bAVM structure with associated neovascularity[497].

Staged Volume Radiosurgery and Hypofractionated Stereotactic Radiotherapy (HSRT)
Due to the dose-volume relationship for bAVMs, radiosurgery is suitable for bAVMs smaller than 3 cm in diameter, or less than 15 ml volume. In patients with larger bAVMs, estimated at a high risk for surgical excision, and in which endovascular volume reduction is not possible, staged volume radiosurgery, or HSRT has been investigated as a treatment option[373].

In staged volume radiosurgery, a strategy is formulated that virtually divides the bAVM in several components of preferably equal volume. Each component is treated in a separate fraction with intervals of about six months in order to give the brain tissue surrounding the bAVM time to repair radiation-induced injury[209]. During each fraction a minimum dose of 16 Gy to the bAVM margin is used because the obliteration rate associated with this dose is around 70 percent after an interval of three years[122, 132]. However, in order to prevent permanent symptomatic radiation related complications the volume of neural tissue within the 12 Gy volume should be as small as possible[123, 140]. Typically, this results in several 10 – 15 ml components. The component of the bAVM containing the majority of draining vessels is treated last, in order to prevent an increase in hemorrhage risk[373].

In a prospective series of 37 patients with a mean bAVM volume of 24.9 ml who underwent radiosurgery in two or three stages, using a marginal dose of 16 Gy each stage, seven patients, out of fourteen with a follow-up longer than 36 months, reached complete obliteration[413]. Using staged volume radiosurgery the 12-Gy volume decreased by an average of eleven percent, and the non-12 Gy volume by an average of 27 percent[373].

So far staged-volume radiosurgery of large bAVMs seems to result in less radiation exposure to the normal brain, when compared to single stage radiosurgery. Further follow-up is needed to determine whether this technique provides a comparable rate of bAVM obliteration and to optimize variables such as minimum dose, interval between stages, and volume per segment[209].

In HSRT, the advantage of spatial precision of radiosurgery is combined with the potential radiobiological advantage of better sparing of late-responding tissue when a large bAVM is treated in multiple fractions[491]. Most studies regarding HSRT use a treatment regime based on the linear-quadratic formula for late complications without correcting for slow repair[46]. Using this formula, a dose of 35 Gy and 28 Gy in four fractions, respectively, would have the same effect as 18.4 Gy and 14.2 Gy in a single exposure of irradiation.

Different outcomes after HSRT have been published[20, 68, 281, 491]. Aoyama *et al.* delivered 35 Gy in four fractions to 26 patients with bAVMs larger than 2.5 cm, or located in eloquent brain, and compared his results with those in 27 patients who underwent radiosurgery for a bAVM ≤ 2.5 cm[20]. A three-year actuarial obliteration-rate of 53 percent was found, compared to 71 percent for radiosurgery. No patients treated with HSRT experienced late radiation effects, but radiation-induced necrosis was seen in two radiosurgically treated patients. However, an intracranial hemorrhage was seen in five patients: two had been treated with radiosurgery, and three with HSRT. Zabel-du Bois *et al.* used HSRT in fifteen patients with bAVMs larger than 4 cm, and compared the outcome with 33 patients who underwent regular radiosurgery[491]. She administered 4 – 5 fractions of 6.5 Gy on consecutive days, and reports a 4-year actuarial complete obliteration-rate of 33 percent after HSRT and 60 percent after radiosurgery. Intracranial hemorrhage occurred after HSRT in three patients after a median of 18 months, and after radiosurgery in seven patients after a median of 17 months. As large bAVMs seem to hemorrhage more often, and they take a long interval to obliterate after radiosurgery, or HSRT, the additional value of HSRT has not been clearly determined yet.

Multimodality treatment of large bAVMs
Large bAVMs are usually treated by multiple, subsequent treatment modalities. This may be planned, in the case of a large bAVM which is treated in a single or multiple endovascular sessions, followed by surgical resection or radiosurgery, or this may be unplanned, e.g. after failure of the initial treatment[336]. In larger series, treatment indications and outcome vary widely[42, 320, 425, 456, 458, 465, 496]. As there is no evidence that partial treatment protects from a bAVM-related hemorrhage[167], the target of multimodality treatment is the same as in single modality treatment, i.e. complete obliteration of the bAVM, without inducing new neurological deficits.

These large and complex bAVMs have been reported to bleed more frequently, with an annual hemorrhage rate of 10.4%[206, 216, 437]. Due to the larger size of the bAVM, with its inherent more complex structure, as well as the use of subsequent treatment modalities, multimodality treatment may be more hazardous in comparison to single modality treatment of smaller bAVMs. Earlier series report a complete obliteration-rate of 30 - 36 percent, with a combined morbidity and mortality rate of 30 percent[66, 206, 416]. Furthermore an annual bleeding risk of 10.4 – 14.6 percent after partial treatment has been reported, suggesting that partial treatment may increase the odds of bleeding[167, 303]. These treatment results were regarded to worse than the natural history of these large bAVMs.
For these reasons, many physicians now recommend no treatment for most grade IV or V bAVMs, except in the specific circumstances of arterial or intranidal aneurysms or progressive neurological deficits related to vascular steal[167, 183, 184, 233, 422]. Nevertheless, complete treatment is warranted for patients with progressive neurological deficits caused by one or several hemorrhages from a large bAVM[167].

Recent studies show more promising results: an overall decrease in annual hemorrhage-rate from 10.4 percent before, to 6.1 percent after multimodality treatment in a cohort of 61 patients with Spetzler-Martin grade IV or V bAVMs, has been reported[206]. After treatment a modified Rankin score of zero to two had been reached in 51 patients. The authors concluded that initiation of treatment does not appear to increase the rate of subsequent hemorrhage, and, treatment may be warranted, given the poor natural history of these lesions. In another study 52 percent complete obliteration was reached, and a good or excellent outcome in 81 percent after multimodality treatment of Spetzler-Martin grade III – V bAVMs located in the posterior fossa[222]. Although this study was criticized for consisting mostly of Spetzler-Martin grade III bAVMs, which are relatively easy to treat[184], in this series multimodality therapy nearly tripled the cure-rate. While it remains difficult to predict which patient may benefit from multimodality treatment these novel studies demonstrate that multimodality treatment of large bAVMs may be justified.

Longer term effects of treatment remain unclear

Although treatment results are promising, population-based studies did not yet demonstrate a clearly improved outcome in treated patients. In a prospective Scottish study, the baseline and three-year outcome were analyzed among 63 patients who received interventional treatment for their bAVM, and 51 who were treated expectatively[466]. The risk of poor outcome, defined as 2 – 6 on the Oxford Handicap Scale, was greater after three years in patients who had interventional treatment than in those who did not and was also greater in patients with a larger nidus. The authors concluded that the longer term effects of intervention are unclear[466]. It was however, pointed out that only 23 patients in the untreated and 30 in the treated cohort remained at risk at the two year point, suggesting inherent bias[52].

In a Cochrane database review, no randomized controlled trials were found to guide the choice of interventional treatment for bAVMs in clinical practice[8]. The authors concluded that at least two types of randomized controlled trial are warranted: one comparing a policy of interventional treatment versus no interventional treatment for unruptured bAVMs, and a second trial comparing different interventions against each other for ruptured bAVMs. The first trial is currently taking place in form of the ARUBA trial, which is a prospective, multi-center, parallel design, randomized, controlled trial, designed to evaluate whether medical management or interventional therapy will reduce the risk of bAVM-related death or stroke by at least 40 percent (www.arubastudy.org)[307].

Future research

Although the molecular etiology of bAVMs is unknown, recently several genes and molecules

involved in the etiology and pathogenesis of bAVMs and bAVM-related hemorrhages have been found.

In mice increased expression of the Notch 4 gene causes vascular abnormalities with the characteristics of a bAVM, implying that increased Notch 4 activation is a potential molecular cause of bAVMs[319].

Interleukin-6 (IL-6) is a potent proangiogenic cytokine, which participates in angiogenesis during tumor progression, wound healing, and brain vascular system development[113]. IL-6 promotes matrix metalloproteinase-9 (MMP-9) activation and induces release of Vascular Endothelial Growth Factor (VEGF) from cultured endothelial cells and tumor cells[79, 467, 482]. In bAVM patients the GG genotype of IL-6-174G>C promoter polymorphism is associated with an almost threefold increase in risk of a hemorrhagic presentation[358]. Further studies demonstrated that IL-6 protein levels were increased in bAVM tissue from patients with hemorrhagic presentation compared with patients without hemorrhagic presentation[71]. Both findings implicate that inflammatory processes are involved in causing a bAVM-related hemorrhage[358].

One of the proteins stimulated by IL-6, VEGF has the ability to increase vascular permeability and cause vasodilation. As such, it has been associated with various cerebral hemorrhagic disorders, such as hemorrhagic transformation of ischemic stroke, and metastatic brain tumor-related intracranial hemorrhage[178, 495]. BAVM vessels also exhibit abnormal expression of VEGF Receptor[173]. Like IL-6, focal hyperstimulation of VEGF stimulated MMP-9 in mice[263, 481]. MMP-9 is a tissue protease known to degrade important structures in the vascular wall, including extracellular matrix proteins, cell surface molecules, and other pericellular substances[22, 164, 309]. Therefore, MMP-9 is implicated in the disruption of neurovascular structures, leading to vascular rupture and hemorrhage. In a mouse model, adenoviral vector-mediated VEGF induced MMP-9 levels sixfold and increased brain tissue hemoglobin, which was used as an index of intracranial hemorrhage. Tetracycline derivatives, such as doxycycline and minocycline, and pyrrolidine dithiocarbamate administration suppressed MMP-9 activity in mice and in cultured bAVM tissue[174]. In patients, oral administration of doxycycline for as short as one week prior to resection of the bAVM, resulted in a decrease in MMP-9 within the nidus[174]. These results suggest that tetracycline derivatives may have a therapeutic potential to reduce MMP-9 activity in bAVM tissues and stabilize blood vessels that are prone to rupture. However, larger clinical trials are necessary to study these effects, as well as those of IL-6- and MMP- inhibitors in preventing bAVM hemorrhage.

BAVM and pregnancy

Although obstetric causes of maternal mortality have declined since the 1920's[251], non-

obstetric causes of maternal morbidity and mortality have increased. Among these neurovascular events may play an important role. The uncertainties, associated with the fear of adverse effects of treatment and etiological investigations on the mother and the unborn fetus, justify special attention regarding this topic.

In the Île de France study sixteen patients with an intraparenchymal hemorrhage were found among 348.295 pregnant patients, for a prevalence of 4.6 per 100.000 deliveries[405]. Two of these hemorrhages were due to a bAVM (0.6/100.000 deliveries). Surprisingly bAVM related hemorrhages during pregnancy occur nearly ten times as often in Taiwan with a prevalence of 6.0/100.000[274]. Assuming that the French situation is representative for the Netherlands situation as well, this would mean 1.1 annual bAVM related hemorrhages during pregnancy, with 185.057 deliveries in 2006. Pregnancy itself does not appear to increase the likelihood of a first hemorrhage from a bAVM[93, 114, 195]. Most pregnant patients with a bAVM are primiparous, and multiparous patients with a bAVM often have had a complicated obstetric history[387]. Based on these findings a bAVM vulnerability factor for rupture has been suggested, leaving a subset of more 'robust' lesions which can survive several pregnancies[453].

It does not become clear whether a bAVM-related intracranial hemorrhage during pregnancy increases morbidity or mortality in comparison to an intracranial hemorrhage in a not pregnant woman, although some authors report an increased chance of rebleeding[100, 253, 387]. BAVMs have been reported to bleed more often at third trimester of pregnancy when cardiac output is at its greatest[99, 126, 325, 470]. Among 154 patients with a verified intracranial hemorrhage from an identified intracranial lesion during pregnancy only four patients bled during labour or delivery[99]. Two had bAVMs, the others had brain aneurysms. For those patients with a lesion not operated on, caesarean delivery afforded no better maternal or fetal outcome than did vaginal delivery[100]. It has been recommended that the decision to operate after a bAVM-related bleeding during pregnancy should be based upon neurosurgical principles, whereas the method of delivery should be based upon obstetrical considerations[100]. Adjunctive measures that decrease the risk of recurrent hemorrhage during vaginal delivery include epidural anesthesia, a shortening of the second stage of delivery, and a low forceps delivery[93]. Caesarean delivery should be reserved for obstetric indications and for fetal salvage when the mother becomes moribund in the third trimester[99]. Post partum spontaneous regression of the bAVM has been reported[360].

BAVM and children

A substantial proportion of bAVM patients are in the pediatric age group, with ten percent of all bAVMs being discovered before the age of ten, and sixteen percent between the age of ten and twenty[189, 255, 388, 408, 449]. In children the arteriovenous shunt seems to be different than in adults[328] with an increased frequency of multifocal niduses[197, 255, 257] and induced remote arteriovenous shunts[141, 197]. On the other hand high flow angiopathic changes or flow-related aneurysms are only seen rarely[162, 226, 256]. This seems to result in a less favourable prognosis than bAVMs in adults, with a mortality rate after hemorrhage of greater than 20 percent[65, 98, 236, 315]. Moreover a significantly increased number of initial hemorrhages (56 – 71 percent) was found in children in comparison to adults (43 – 52 percent), although there was no increased risk for a subsequent hemorrhage[133, 328]. Because the cumulative morbidity in children is obviously larger than in adults, as they are at risk for a prolonged period of time, the necessity for treatment is more compelling.

In contrast to adults, children seem to fare quite well after surgery of a bAVM, with good outcomes (mRS Scores 0–2, living independently) in 90.6 percent of children, versus 71.4 percent of adults[394]. This discrepancy does not seem to be explained by differences in bAVM anatomy, lesion rupture rates, presenting neurological condition or treatment techniques[232, 394]. After radiosurgery the obliteration rate in children is comparable with the obliteration rate in adults, although bAVMs in children tend to obliterate faster, with a median time to obliteration of 25.7 months in children, vs. 28.2 months in adults[329].

Guidelines for treatment

Trials are underway evaluating whether a conservative approach of medical management only, or a more aggressive approach of interventional therapy reduces the risk of bAVM-related death or stroke. Pending these results, the following guidelines seem creditable: in general, microsurgical resection should be strongly considered as the primary mode of therapy for Spetzler-Martin grade I and II lesions because radical resection is rapidly obtained in over 95% of cases with low morbidity and mortality. For bAVMs that cannot be reached surgically and which are smaller than 3 centimeter in diameter, stereotactic radiosurgery is an excellent alternative leading with an obliteration rate of 60-90% in 4 years. Embolization as stand-alone treatment is only indicated in a minority of patients, but is a very useful adjunct preceding surgery or radiosurgery in Spetzler-Martin Grade II or III bAVMs, either in order to decrease the bAVM volume, or to obliterate intranidal sources of hemorrhage. Spetzler-Martin Grade IV or V bAVMs should be treated only after hemorrhaging or in case of a progressive neurological deficit.

AIMS AND OUTLINE OF THIS THESIS

The different aspects of the diagnosis, natural history and radiosurgical treatment of bAVMs are subject of this thesis.

Spontaneous regression of a bAVM is a known, but very rare phenomenon. After spontaneous regression the patient seems to be cured from his bAVM, and no further treatment needs to be carried out. In order to discover which factors are associated with, or predictive for, spontaneous regression of a bAVM, we describe in **Chapter 2** the rare finding of spontaneous regression of a bAVM in an adult male patient and present an overview of all previously published cases.

Several factors play a role in the treatment failure of radiosurgery. When the target is delineated accurately, only a higher marginal dose has been found to strongly correlate with successful treatment. However, accurate target delineation is impeded due to observer-, imaging-, and bAVM-related factors. Observer-related factors are mainly the consequence of the absence of a common definition of the nidus. Imaging-related factors reflect the quality of the DSA and the angiographic phase in which the nidus is determined. BAVM-related factors include the presence of a high-flow bAVM with almost simultaneous filling and overlap of feeding arteries, nidus, and draining veins, a history of prior embolization, or a diffuse bAVM structure with associated neovascularity. These factors all cause ambiguity in delineating bAVMs for the purpose of radiosurgical planning. In **Chapter 3** and **4** we investigated the extent of interobserver variability when delineating bAVMs on stereotactic DSA (**Chapter 3**), or MR-angiography (**Chapter 4**). Subsequently, we evaluated its possible dosimetric, and therefore future clinical consequences.

During actual radiosurgical planning, detailed examination of numerous consecutive angiography images is needed to study the various components of the bAVM. Usually, only a single early phase of DSA is selected for delineation of the nidus in the radiosurgery planning system. However, practical considerations limit the reliability of contouring the nidus in a single biplanar angiographic phase because not all shunt areas in the nidus exhibit the same pace of flow and, more importantly, because biplanar angiography is a two-dimensional imaging modality, overprojecting arteries and veins may sometimes obscure the actual nidus. These factors further contribute to interobserver variations during nidus delineation. In the **appendix**, we present an effective method for color coding the time that contrast arrives at any location in the brain vasculature in a single composite image. This patented method, arrival-time color intensity projection (CIP), combines the information contained in a number of sequential angiographic images into a single composite color image. This composite image represents the arrival time of contrast at each pixel with each pixel's hue, brightness, and saturation conveying the intensity and intensity variation, respectively, of the pixel over the angiographic component images. In **Chapter 5** we investigated the extent of interobserver variability, as well as its possible dosimetric consequences, when delineating bAVMs on these color intensity projection-images.

In contrast to adult bAVMs, pediatric bAVMs are more often located in deep or eloquent locations, making surgical resection less attractive as a treatment option. In children, radiosurgery alone, or in combination with other modalities, has been reported to result in a complete angiographic obliteration varying between 54 percent three years after radiosurgery to 65 percent five years after radiosurgery. The actuarial rate of hemorrhage after radiosurgery, before obliteration has been obtained, varies between 2.7 and 4.3 percent/patient/year. In children, no adverse effects of radiosurgery on cognitive and neuropsychological functions have been found after long-term follow-up. These findings suggest that radiosurgery is an equally successful, but less invasive alternative to surgery of a small pediatric bAVM. Therefore, in our institute it has been the policy to treat small bAVMs with radiosurgery, regardless of its intracranial location. In **Chapter 6** we evaluated the clinical and radiological outcome after radiosurgically treating 22 children for bAVMs.

Complications of radiosurgery may be related to the adverse effects of the radiation itself, usually resulting in circumscribed perinidal gliosis. In some cases however, more extensive MR-signal intensity changes occur in the white matter far beyond the target area and these may be associated with new neurological symptoms. In previous reports, obstruction of the venous outflow of the bAVM was held responsible for these MR-signal intensity changes and the term 'occlusive hyperemia' was proposed, in analogy with changes seen after surgical resection of bAVMs, in which hyperemia due to acute thrombosis of the draining vein was found to be responsible for the clinical deterioration and the MR signal intensity changes. **Chapter 7** regards the clinical outcome in the subclass of patients who demonstrated hyperintensity on T_2-weighted MR-images, after radiosurgery. The relationships between hyperintensity and treatment dose, as well as drainage pattern are investigated.

Although DSA remains the gold standard to both diagnose the bAVM, as well as complete obliteration, DSA is an invasive and expensive investigation. Nevertheless, patients with a bAVM treated in the VU University medical center undergo at least three DSA investigations: one for diagnosis, one shortly before radiosurgery, and finally one to diagnose obliteration. MRI is very sensitive in detecting bAVMs, showing an inhomogeneous signal void on T_1- and T_2-weighted sequences. Therefore MRI is the imaging modality of choice for providing information on the exact location of the bAVM and its relation with surrounding cerebral structures. Potentially MRI can be used to assess obliteration as well. In **Chapter 8** the results of a study to assess the additional value of both T_2-weighted MR-images, as well as MR-Angiography in predicting complete obliteration are described. Final considerations about radiosurgery for bAVMs and its future are given in **Chapter 9**. Summaries in English and Dutch conclude this thesis (**Chapter 10**).

Chapter 2

Spontaneous Regression of Brain Arteriovenous Malformations

D.R. Buis
R. van den Berg
G.J. Lycklama à Nijeholt
H.B. van der Worp
C.M.F. Dirven
W.P. Vandertop

Adapted from: Buis DR, van den Berg R, Lycklama G, van der Worp HB, Dirven CM, Vandertop WP. Spontaneous regression of brain arteriovenous malformations--a clinical study and a systematic review of the literature. **J Neurol.** 2004 Nov;251(11):1375-82.

Abstract

Purpose

Complete spontaneous obliteration of a brain arteriovenous malformation (bAVM) is a rare event, with 67 angiographically proven cases in the world literature. We present a new case and a systematic literature review to determine possible mechanisms underlying this unusual phenomenon.

Presentation

One patient with a bAVM was referred for radiosurgical treatment. Shortly before treatment however, complete spontaneous regression occurred. This patient had experienced a hemorrhage in the months before referral.

Results

We found 38 articles in which 67 cases of complete and spontaneous regression of a bAVM were presented. Male to female ratio was 1.2,with a mean age of 37 years (range 1–81). Regression occurred in 72% without new neurological events. Median size of the nidus was 2 cm (range 1–7). There was a single arterial feeder in 46 % and a single draining vein in 59%.

Conclusion

Spontaneous regression of a bAVM is the result of multiple interacting factors. Intracranial hemorrhage and the presence of a single draining vein seem to play a major role in this process.

Key Words

Angiography, digital subtraction • Cerebral angiography • Intracranial arteriovenous malformations • Intracranial arteriosclerosis • Intracranial thrombosis

Introduction

The prevalence of brain arteriovenous malformations (bAVM) is 0.02 %[6], with an incidence of between 1.1 and 1.3 per 100.000 persons-years[5, 432]. An intracerebral hemorrhage is the main mode of presentation[134, 189, 210, 365, 449] with a prevalence of 0.68 per 100.000 and an incidence of 0.51 per 100.000 person-years[5, 432]. The median age of presentation is 28 and 38 years for a hemorrhagic and a non-hemorrhagic presentation, respectively[432]. Spontaneous and complete regression of an BAVM is a well recognized, but rare phenomenon, with an estimated prevalence of 0.8 to 1.3 %[1, 353]. Several causes of spontaneous regression have been postulated, such as premature atherosclerosis[41], embolus[249], turbulence in feeding vessels[106], elevated estrogens[412], hemodynamic changes associated with surgery[286] and mass effect due to haemorrhage from the bAVM[306]. We describe the case of an adult patient, referred to our clinic for treatment of his bAVM, by whom complete regression had occurred, and present a systematic review of the literatur

Methods

A computerized search of both the National Library of Medicine database of literature and Embase was performed. The search was limited to human studies. We used the medical subject heading ‘intracranial arteriovenous malformations’ combined with the terms ‘regression’ and ‘obliteration’. Regression was defined as the disappearance of a bAVM without prior intervention or therapy. Obliteration was defined as the disappearance of a bAVM after prior therapy. Thrombosis of a bAVM was only used when this was pathologically demonstrated. BAVMs were defined as parenchymal or pial AVMs. Excluded were articles that dealt with cases other than bAVMs, cases of partial regression and all cases in which patients had undergone treatment. Treatment was defined as surgical, endovascular or radiation therapy to the bAVM and included removal of an bAVM related hematoma and clipping of aneurysms proximal to the bAVM. VP-Shunt placement or exploratory surgery in which the bAVM was not manipulated was not regarded as treatment. Duplicate references, as well as redundant publications were discarded. The abstracts were reviewed, and articles unrelated to the specific topic were excluded. To identify additional eligible studies, the reference lists were screened for journal articles.

An analysis of clinical, radiological, and pathological features of all cases was performed. Details included were: patient age at diagnosis of regression, gender, clinical presentation which led to the diagnosis of the bAVM, localization and lateralisation of the bAVM, previous treatment, nidus size, Spetzler-Martin classification, number of arterial feeders, pattern of venous drainage, and number of draining veins (single or multiple). Events possibly leading to regression and timespan between diagnosis of the bAVM and diagnosis of regression

were noted. In our database of over 300 patients with a bAVM, referred for stereotactic radiosurgery, we identified one patient in whom complete spontaneous regression had occurred.

Case Report

A 51-year old male (patient 1, Table 2.1) presented with seizures, attributed to a left-temporal bAVM, Spetzler-Martin grade II (Figures 2.1A and B),with drainage in the direction of the transverse sinus (Figure 2.1C). Two months later the patient had an acute moment of complete disorientation, with hemianopia and dysphasia, without headaches, nausea, vomiting, or loss of consciousness. Four months after this episode, he was referred to our institute for radiosurgical treatment. The preplanning-MR-angiography showed remains of an old hematoma, surrounded by gliosis, but no aberrant vessels. The planning DSA confirmed these findings (Figures 2.1D and E). MR-angiography one year later confirmed lasting regression.

Results

We found 38 articles[1, 23, 27, 61, 63, 75, 83, 95, 106, 110, 116, 150, 155, 163, 179, 194, 241, 265, 269, 286, 290, 298, 302, 305, 306, 324, 334, 338, 339, 351-353, 393, 395, 402, 443, 462, 463] in which 67 cases of complete regression of brain arteriovenous malformations are reported (Table 2.1). Combined with the case described in the present paper, a total of 68 patients form the core of this review. In all selected reports age at diagnosis of regression, gender, neurological symptoms that resulted in the diagnosis of a bAVM, localization and lateralisation of the bAVM were mentioned (Table 2.1). Nidus size was mentioned in 52 cases, while Spetzler-Martin classification was mentioned in only six of the 45 cases published after 1986. From the available information in the figures, legends, and results the Spetzler-Martin classification could be determined in three further cases[286, 351].The number of arterial feeders was mentioned in 61 cases, while the pattern of venous drainage and the number of draining veins were mentioned in 36 and 53 cases respectively. In four cases it remained unknown whether regression was preceded by a clinical event.

The mean age at diagnosis of complete regression of the bAVM of all 68 patients is 37.4 years (range: 1–81).The male to female ratio was 1.2. The clinical presentation that led to diagnosis of the bAVM is presented in Table 2.1. In 57% a hemorrhage (intracerebral, intraventricular, subarachnoid or a combination) led to the diagnosis of an bAVM. The presentation was atypical in five cases: in one patient the bAVM was discovered when a scan was performed

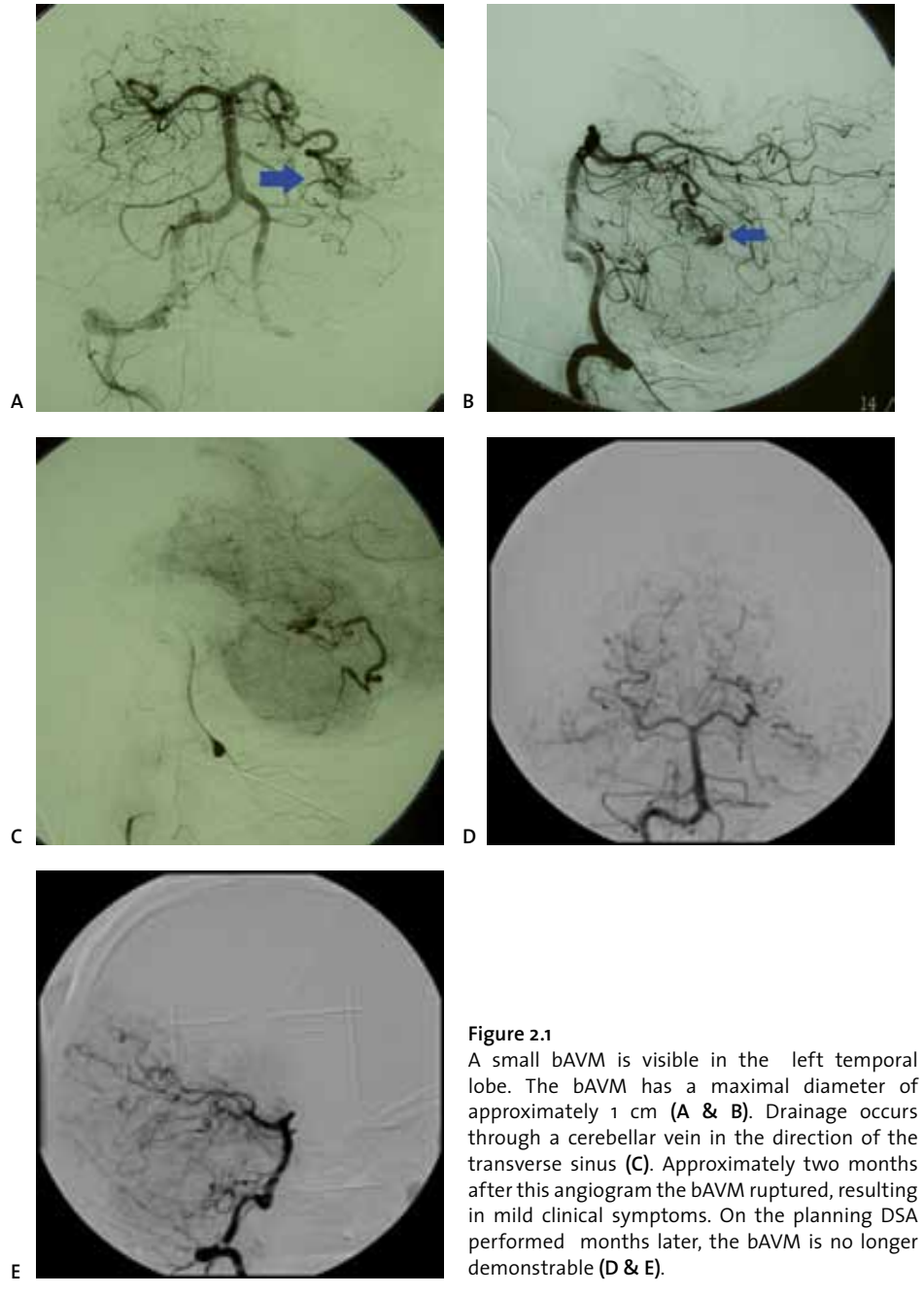

Figure 2.1
A small bAVM is visible in the left temporal lobe. The bAVM has a maximal diameter of approximately 1 cm **(A & B)**. Drainage occurs through a cerebellar vein in the direction of the transverse sinus **(C)**. Approximately two months after this angiogram the bAVM ruptured, resulting in mild clinical symptoms. On the planning DSA performed months later, the bAVM is no longer demonstrable **(D & E)**.

to evaluate head trauma[163], three other patients suffered from a mass lesion with the MRI or CT appearance of an intrinsic cerebral neoplasm[155, 338] or an avascular mass on cerebral angiography[106]. On pathological examination, these masses proved to be completely thrombosed bAVMs. A fifth patient presented with seizures, but neither EEG, nor three cerebral angiographies showed abnormalities. When a fourth cerebral angiogram showed a bAVM of the anterior circulation, an operative resection was performed. Pathological analysis demonstrated recanalization of a previously thrombosed bAVM[63]. The median diameter of the nidus was 2 cm (range 1–7). There were 38 left-sided, 23 right-sided, and three midline bAVMs. For four patients the lateralisation could not be retrieved. According to the Spetzler-Martin classification[423] one case was graded as I (patient 5, Table 2.1), three cases as II (patients 1,4 & 8, Table 2.1), two cases as III (patients 6 & 7, Table 2.1), one case as IV (patient 9, Table 2.1) and two cases as VI (patients 60 & 61, Table 2.1). There was a single arterial feeder in 31 cases (46 %). The number of arterial feeders remained unknown in seven cases. In 40 patients there was a single draining vein (59 %). The number of draining veins was not noted in fifteen patients. The pattern of venous drainage was deep in fifteen and superficial in seventeen patients. In four patients there was a combination of deep and superficial drainage. The pattern of drainage remained unknown in 32 patients.

Regression of the bAVM was accompanied by a neurological deficit (including hemiparesis) in eight patients (12 %), a preceding hemorrhage in three patients (4 %), headache in four patients (6 %), and seizures in four patients (6 %).

In all other patients (72 %) regression occurred without new neurological morbidity. The mean time between diagnosis of the bAVM and the diagnosis of complete spontaneous regression was 54 months (range: 3 days – 21 years). In the, previously mentioned, four patients whose regressed bAVMs were discovered intra-operatively the time span remained unknown. Partial[63, 334] and complete[306] recanalization was seen in three patients (patients 34, 52 & 66,Table 2.1) after 33, 12 and 39 months respectively.

Table 2.1: Review of literature

Nr.	First Author & Year of Publication	Age & Gender		Localization & Lateralisation		Presentation	Nidus Size (cm)	Number of Arterial Feeders	Venous drainage & Number of Draining Veins		Event that Preceded Regression	Timespan between Diagnosis and Occlusion (Months)
1	Buis, 2004	51	M	Temporal	L	Seizure	1	S	Sup,	S	ICH	6
2	Schwartz, 2002	33	M	Occipital	R	Seizure	U	S	U,	U	None	1
3	Cloft, 2002	20	M	Cerebellum	L	ICH	1	S	U,	U	None	60
4	Lee, 2002	36	M	Basal Ganglia	L	ICH	<3	M	Sup,	S	None	30
5		28	F	Occipital	U	ICH	<3	S	Sup,	S	None	27
6		55	M	Basal Ganglia	U	ICH, IVH	<3	M	D,	S	None	3
7		43	M	Parietal	U	HA	3-6	M	B,	M	None	84
8	Krapf, 2001	62	M	Parietal	R	Seizure	2	M	Sup,	M	None	3
9	Carter, 2001	67	M	Temporal	L	Seizure	3.5	M	B,	U	ICH	252
10	Patel, 2001	42	F	Corpus Callosum	M	ICH, IVH, SAH	<1	S	U,	S	None	13
11		55	F	Corpus Callosum	M	SAH	1.5	S	U,	S	None	23
12		18	F	Monro	L	IVH	<1	M	U,	S	None	10
13		44	M	Midbrain	L	ICH	<1	M	U,	S	None	4
14		41	M	Occipital	R	ICH	<1	S	U,	S	None	4
15		30	F	Thalamus	L	IVH	<1	M	U,	S	None	7
16		30	F	Frontal	L	IVH	<1	S	U,	S	None	7
17		43	M	Internal Capsule	L	IVH	<1	S	U,	U	None	4
18		42	M	Parietal	R	Seizure	2.5	S	U,	S	None	28
19		52	F	Central White	L	ICH, IVH	1.5	M	U,	S	None	8
20		13	M	Thalamus	L	ICH, IVH	<1	M	U,	S	None	4
21		51	F	Temporal	L	IVH	1.5	M	U,	S	None	3
22		52	F	Cerebellum	L	ICH	<1	M	U,	S	None	7
23		54	M	Perisylvian	R	Asymptomatic	<1	S	U,	S	None	9
24		19	F	Frontal	R	ICH	<1	M	U,	S	None	6
25		48	M	Suprasellar	M	ICH	1.5	U	U,	S	None	12
26		10	F	Frontal	R	SAH	<1	S	U,	S	None	18
27		42	F	Thalamus	R	IVH	<1	M	U,	S	None	6
28	Abdulrauf, 1999	28	M	Cerebellum	R	IVH	<3	M	Sup,	S	None	2
29		35	M	Parietal	L	IVH	3	U	Sup,	S	None	3
30		37	F	Thalamus	R	ICH	2	S	U,	S	None	2
31		56	F	Occipital	R	HA	3.5	M	U,	S	None	3
32	Auzou, 1997	46	M	Frontal	L	Seizure	2.5	M	Sup,	M	Seizure	120
33	Watanabe, 1995	81	M	Frontal	L	Seizure	U	M	Sup,	M	HP	60
34	Mizutani, 1995	59	M	Frontal	L	SAH	2	M	Sup,	S	None	1.5
35	Guazzo, 1994	34	M	Temporal	L	Seizure	4	U	U,	U	None	N/A
36	Hamada, 1994	14	F	Thalamus	L	Asymptomatic	3.5	M	Sup,	S	None	72
37	Marconi, 1993	36	M	Rolandic	L	Seizure	3	S	U,	U	Seizure	248
38	Barker, 1990	23	F	Parietal	R	IVH	U	S	Sup,	M	None	1,5
39	Megison, 1989	25	M	Temporal	L	Seizure	1.5 - 2	S	Sup,	U	None	120
40	Minakawa, 1989	30	M	Basal Ganglia	L	U	2-4	S	U,	U	U	204
41		35	M	Parietal	L	U	<2	S	U,	U	U	216
42	Salpietro, 1989	35	F	Parietal	L	SAH	U	S	D,	S	HA	36
43	Gibb, 1988	15	F	Basal Ganglia	R	SAH	U	M	B,	M	None	84
44	Leramo, 1987	23	M	Temporal	L	Seizure	U	M	D,	S	None	6
45	Takano, 1987	65	M	Parietal	R	ICH	2	S	D,	S	None	0,1
46	Pasqualin, 1985	48	M	Rolandic	L	ND	>5	M	D,	M	None	84
47		65	M	Rolandic	L	ND	3-5	M	Sup,	U	ICH	111
48		16	M	Rolandic	R	ICH	<2	S	D,	U	None	12
49		40	F	Parietal	R	Seizure	<2	M	D,	U	Seizure	195
50	Wakai, 1983	17	M	Frontal	R	SAH	4	M	D,	M	None	18
51	Nehls, 1982	59	M	Parietal	R	HA	2	S	Sup,	S	HA	156
52	Nukui, 1982	54	M	Occipital	L	SAH	1.4	S	D,	S	HP	120
53		26	M	Parietal	R	ICH	7	S	Sup,	S	None	3
54	Ohara, 1982	24	F	Occipital	L	HA	U	U	U,	U	None	N/A
55	Omojola, 1982	40	F	Parietal	R	ICH	U	S	Sup,	S	ND	60
56		18	F	Temporal	L	ND	U	S	D,	S	ND	36
57	Miyazaki, 1978	46	M	Parietal	R	SAH	3.5	S	Sup,	M	None	47
58	Sartor, 1978	22	F	P-ventricular	L	ICH	U	S	U,	U	None	132
59	Dyck, 1977	6	F	Parietal	L	Seizure	5	M	U,	M	Seizure	N/A
60	Mabe, 1977	1	F	Posterior Fossa	U	HC	>6	M	D,	M	None	8
61	Pascual, 1977	3	F	Entire Hemisphere	R	HP	U	M	D,	M	None	34
62	Heeres, 1976	34	M	Frontal	L	SAH	U	U	D,	S	HA	108
63	Eisenman, 1972	34	F	Parietal	R	SAH	U	U	D,	S	ND	48
64	Conforti, 1971	37	F	Frontal	L	SAH	U	S	D,	S	HA	36
65	Fisher, 1969	48	F	Temporal	L	ND	1	S	U,	S	HP	44
66	Castaigne, 1961	31	F	Frontal	L	Seizure	U	U	U,	U	U	N/A
67	Hook, 1958	54	M	Frontal	L	HC	U	M	B,	M	HP	252
68	De Lange, 1955	64	F	Occipital	L	SAH	3.5	S	U,	S	ND	48

ICH=Intracerebral Hematoma, SAH=Subarachnoid Hemorrhage, HC=Hydrocephalus, IVH-Intraventricular Hemorrhage, M=Multiple, S=Single, D=Deep, Sup=Superficial, HP=Hemiparesis, ND=Neurological Deficit, P-Ventricular=Paraventricular, U=Unknown, B=Both

Discussion

The prevalence of spontaneous, complete regression of a bAVM is not exactly known, but it appears to be a rare event, with only 68 cases reported in the literature since 1955. A prevalence of regression of up to 20% percent has been reported[302],which is high, compared with the 0.3% observed in our center. Abdelrauf *et al.* found an incidence of 0.8 %[1].

Worldwide a large number of bAVMs have been treated by surgery, LINAC or Gamma knife-radiosurgery or endovascular embolization. Retrievable data show that Gamma knife-radiosurgery has been used in 57.130 patients with a bAVM up to December 2008 (http://www.elekta.com/assets/gamma_knife_surgery/pdfs/ww308.pdf). If the real prevalence is 1%, this would mean a minimum number of 570 cases of spontaneous regression encountered in Gamma knife-radiosurgery only. As we found only 68 cases until 2004, the number of spontaneous regressions is likely to be either underrepresented in the literature, or the real prevalence is much lower than 1%.

Spontaneous thrombosis or regression is generally considered a favourable event, as it prevents the bAVM from rupturing[471]. Multiple factors have been proposed as causes or as associations with regression of a bAVM. These factors include hemodynamic alterations caused by a subarachnoid hemorrhage[462], subdural hematoma, intracerebral hematoma[110, 334, 352, 395, 443], the presence of a brain tumor[339], surgery[302],and endovascular and radiation therapy. Other factors are the presence of a single arterial feeder[302, 324, 339], a small nidus-size[83, 352], the number[163, 339, 352] and architecture[106, 163, 298] of draining veins, hypercoagulability[412], embolization from an associated thrombosed aneurysm[339], the presence of atherosclerosis[249, 302, 396] and the use of oral contraceptives[70, 83, 106, 150, 272, 286, 298, 302, 324, 334, 339, 352, 395].However, all of these factors also occur in bAVMs that do not, or only partially, regress. Unfortunately, there are no case-control studies or other studies that have convincingly associated a single factor to spontaneous regression. The frequencies of occurrence mentioned in the present paper are mainly based on case-reports and are therefore probably not representative of real frequencies. Based on the evidence available to date, each factor by itself does not seem sufficient for complete regression to occur.

Associated factors

The most important factor in explaining complete regression of a bAVM is very likely to be hemodynamic changes caused by bleeding or by treatment. Mass effect, caused by an intracranial hematoma with accompanying brain edema and secondary vasospasm, may decrease the blood flow in the bAVM to an extent that complete thrombosis occurs in its vessels. Gliosis, resulting in kinking of vessels may cause a change in bAVM hemodynamics, as a consequence of gradually tapering of the arterial supply and the venous drainage, thereby increasing the likelihood of bAVM thrombosis[241]. In most cases complete regression was diagnosed months or even years after the allegedly causative event, but in the absence of imaging in the intervening period this does not inform us of the real time interval in which spontaneous regression occurs.

Arterial feeders and nidus size

Several case reports conclude that bAVMs regressing spontaneously are of small size and have a single arterial feeder[83, 302, 324, 339, 462]. Minakawa *et al.* Suggested that superficially located bAVMs also had a greater tendency toward regression than did deep bAVMs[302]. In the 68 cases with spontaneous regression we found a median nidus size of 2 cm, which can be considered small, but a single arterial feeder in only 46%. Only in four cases (patients 40, 53, 57 & 68, Table 2.1) was a single arterial feeder associated with a nidus size larger than 3 cm. Therefore the presence of a single arterial feeder may just be a feature of a small nidus size.

Number and architecture of draining veins

The number and the architecture of the draining veins is possibly another important factor in explaining regression of bAVMs. A single draining vein facilitates the occurrence of spontaneous thrombosis, as obstruction of this single vein would more easily result in stasis of blood and thrombosis, caused by a total venous outflow obstruction. A single draining vein was present in 59%. Abdulrauf *et al.* argued that venous obstruction could also be caused by external compression, such as parenchymal hemorrhage, a pathologic venous abnormality or by host related factors, such as a hypercoagulable state. In the presence of one of these factors, obstruction of one single vein is more likely to occur than obstruction of multiple draining veins and likewise, obstruction of a single vein is more likely to cause complete thrombosis of a bAVM[1]. As sudden venous obstruction often results in rupture of an intranidal vessel[130, 159], and a preceding hemorrhage is present in only a small percentage of cases, it is likely that the process of spontaneous regression or thrombosis takes place slowly over the course of months or years, rather than suddenly due to compression from a parenchymal hemorrhage.

Hypercoagulability and oral contraceptive use

Spontaneous thrombosis of the draining veins related to a hypercoagulable state has been described in children and in women taking high-dose oral contraceptive drugs[275, 276, 286]. However, adequate case-control studies demonstrate that hypercoagulability associated with the use of oral contraceptive drugs is common in the general female population, therefore these factors may have been unrelated to regression.

Atherosclerosis and regressive changes of vessel walls

Brain arteriovenous malformations typically present before the age of 40 years. The mean age at discovery of bAVM regression in our review was 37 years, with 31% younger than 30 years. Nevertheless, as fibrous or atheromatous plaques start appearing in the third and fourth decade of life[381], it is possible that atherosclerosis is a contributing factor in spontaneous regression. Ezura and Kagawa found fibrous intimal thickening in the pathological specimen of a completely regressed bAVM and attributed this to atherosclerosis[112]. In addition, tortuosity and the altered mechanical properties of the feeding arteries can cause stasis, eddy currents and turbulent flow[106, 163, 483], leading to compensatory arterial wall changes, such as hypertrophy, endothelial alterations and intima dissection with subsequent stenosis and vessel obstruction, possibly contributing to the formation of thrombi. The role of atherosclerosis remains unproven as most of these factors also take place in bAVMs which do not obliterate completely or even remain patent.

Recanalization

In rare cases bAVMs may reappear, even after treatment[10, 280, 421]. In our review three cases of recanalization of a previously completely regressed bAVM were observed[63, 306, 334]. As all recanalizations took place after a period of at least one year, MR-angiographic follow-up in patients diagnosed with a spontaneously regressed bAVM is recommended.

Conclusion

BAVMs can regress spontaneously under some circumstances. The true prevalence of spontaneous regression remains unknown, but is either less than 1%, or seriously underreported in the literature. Several factors appear to play a role in this process. Intracranial hemorrhage, and the presence of a single draining vein seem to play a larger role than others. We were, however, not able to identify a particular type of bAVM likely to undergo spontaneous obliteration. Given the lack of adequate case-control and sufficiently sized studies on the natural course of bAVMs, to associate one single factor to spontaneous regression remains speculative.

Chapter 3

Target Delineation on DigitalSubtraction Angiography

D.R. Buis
F.J. Lagerwaard
F.D.R.K. Barkhof
C.M.F. Dirven
G.J. Lycklama à Nijeholt
O.W.M. Meijer
R. van den Berg
H.A .Langendijk
B.J.Slotman
W.P. Vandertop

Adapted from: Buis DR, Lagerwaard FJ, Barkhof F, Dirven CM, Lycklama GJ, Meijer OW, Berg van den R, Langendijk HA, Slotman BJ, Vandertop WP. Stereotactic radiosurgery for brain AVMs: role of interobserver variation in target definition on digital subtraction angiography. Int J Radiat Oncol Biol Phys. 2005 May 1;62(1):246-52.

Abstract

Purpose

We evaluated the extent of interobserver variation in contouring brain arteriovenous malformations (bAVMs) on digital subtraction angiography (DSA) with respect to volume, spatial localization, and dosimetry and correlated our findings with the clinical outcome.

Methods

Thirty-one patients who had undergone radiosurgery for bAVMs were studied. Six clinicians independently contoured the nidus on the original DSA. As a measure of variation, the ratio between the volumes of agreement and the corresponding encompassing volumes, as well as the absolute positional shift between the individual target volumes were derived. Using the original treatment plan, the dosimetric coverage of the individually contoured volumes with standard collimators was compared with a similar plan using dynamic conformal arcs.

Results

The mean contoured nidus volume was 3.6 ± 5.6 cm^3. The mean agreement ratio was 0.45 ± 0.18 for all possible pairs of observers. The mean absolute positional shift between individually contoured volumes was 2.8 ± 2.6 mm. These differences were more marked in previously treated groups and tended to be more pronounced in those with treatment failure. The mean coverage of the individual volumes by the 80% prescription isodose was 88.1% ± 3.2% using conventional collimators and 78.9% ± 4.4% using dynamic conformal arcs ($p \leq 0.001$).

Conclusion

Substantial interobserver variations exist when contouring bAVMs on DSA for the purpose of radiosurgical planning. Such variations may result in underdosage to the bAVM and, thereby, contribute to treatment failure. The consequences of contouring variations may increase with the use of more conformal radiosurgical techniques.

Key words

Angiography, Digital subtraction • Cerebral angiography • Intracranial arteriovenous malformations • Radiosurgery.

Introduction

Stereotactic radiosurgery is an established modality for the treatment of brain arteriovenous malformations (bAVM). Because the annual risk of hemorrhage after presentation is 3–4%[21, 216] and remains between 1.8% and 3.1% during the latency period before obliteration[215, 321], the goal of radiosurgery should be to obtain angiographically confirmed complete obliteration of the nidus. This is usually observed at three to four years after treatment, and obliteration rates after radiosurgery between 73% and 95% have been reported in several large series[200, 372, 399, 410]. Nidus obliteration after radiosurgery depends mainly on the size of the bAVM and on the marginal treatment dose[132, 217, 452].

The target delineation for radiosurgery of bAVMs is commonly performed using digital subtraction angiography (DSA)[331], co-registered with stereotactic CT scans. However, determining the nidus on DSA may be difficult because of observer-, imaging-, and bAVM-related factors. Observer related factors are mainly the consequence of the absence of a common definition of the nidus[132, 138, 250, 371, 399]. Imaging related factors reflect the quality of the DSA and the angiographic phase in which the nidus is determined[43, 288]. BAVM-related factors include the presence of a high-flow bAVM with almost simultaneous filling and overlap of feeding arteries, nidus, and draining veins or a history of prior embolization[121]. These factors may result in ambiguity when determining the nidus for the purpose of radiosurgery.

Contouring variations can lead to a suboptimal target definition and, as such, in combination with the steep dose gradients that are characteristic of radiosurgery, may result in treatment failure[121, 138, 371]. To date, only sparse data exist on the magnitude and clinical impact of interobserver variations in contouring bAVMs on DSA. In this study, we evaluated the extent of interobserver variations with respect to volume, spatial localization, and dosimetry in a cohort of patients with bAVMs treated by radiosurgery and correlated our findings with the clinical outcome.

Methods and materials

Between 1991 and 2003, 225 patients have been treated with radiosurgery for a bAVM at the VU University Medical Center. Included in this study were patients whose treatment plans had been stored on CD-ROM (after May 1998) and with a minimal follow-up of 3 years after radiosurgery, except when angiographically confirmed complete obliteration was shown earlier. These criteria resulted in the inclusion of 31 patients for this study of contouring variations, treated between May 1998 and May 2001. The patient and treatment characteristics are shown in Table 3.1 The mean age was 34 years (range, 6 – 68 years). Radiosurgery treatment planning in our center is a multidisciplinary effort, performed by the neurosurgeon, radiation-oncologist, neuroradiologist, and medical physicist. The mean volume of the bAVM nidus, as contoured in the original treatment plan, was 3.4 cm^3 (range, 0.02–32.5 cm^3). Ten patients (32%) had undergone prior, unsuccessful, treatment for their bAVM, including incomplete endovascular embolization (n = 4), incomplete surgical resection (n = 3), or a combination of partial embolization and surgery (n = 3). The original treatment plans were recovered from CD-ROM and loaded into the stereotactic planning system (Brainscan, version 5.2, BrainLAB AG, Feldkirchen, Germany).

The original treatment was performed in a single fraction with a median collimator size of 18 mm (range, 10 – 40 mm) using a standard configuration, usually of five stereotactic arcs. Conformal (dynamic) multileaf collimation was not clinically available during the period reported. Of the 31 patients, 28 had undergone radiosurgery using a single collimator, 2 using two collimators, and 1 using three collimators. The clinically used prescription dose was dependent on the volume of the bAVM with an 80% prescription dose of 21, 18, and 15 Gy for a volume of ≤ 7, 7 – 14, and > 14 cm^3, respectively. The mean prescribed dose was 19 Gy at the 80% isodose.

Six observers (two radiation oncologists, two neurosurgeons, and two neuroradiologists), all actively involved in routine radiosurgical treatment of bAVMs, contoured the nidus on DSA (target volume), co-registered with the stereotactic CT scan. They were unaware of either the original treatment plan or the contours drawn by other investigators. DSA had been performed at a frame rate of 3 – 6 s^{-1}, depending on the flow rate of the bAVM. The commonly used nidus definition was a network of abnormal vessels between arterial feeders and the pathologically early draining veins[32].

Interobserver variation

Because all DSAs were co-registered with the stereotactic planning CT scans, all contours were automatically projected onto the CT images. Additional analysis was performed using the CT data sets (Figure 3.1). An analysis of both spatial invariant and spatial variant parameters was performed. A two-tailed *p* value of < 0.05 was chosen as the threshold for statistical significance. All statistics were performed using Statistical Package for Social Sciences, version 9.0 (SPSS, Chicago, IL).

Spatial invariant parameters

Spatial invariant parameters studied were the mean contoured volume of all six clinicians and the mean volume of each possible pair of observers. A Kruskal-Wallis test was used to identify differences between the target volumes from different observers, as well as between different specialties (i.e., neurosurgery, neuroradiology, and radiation oncology).

Table 3.1: Patient characteristics

Nr.	Gender/Age	Pre-SRS Treatment	Treated Nidus Volume (ml)	Dose* (cGy)	Period of FU (Months)	Complete Obliteration
1	F/33	PE	3,42	1800	44	Y
2	F/41	N/A	12,15	1500	42	N
3	M/6	PSR	0,16	2100	29	Y
4	M/14	N/A	1,96	1800	28	Y
5	F/36	PE	2,57	1800	59	N
6	F/57	N/A	0,08	2100	26	Y
7	M/53	PE	2,95	2100	37	Y
8	M/25	N/A	0,32	2100	38	Y
9	M/41	N/A	1,30	2100	40	N
10	M/14	N/A	0,26	2100	38	Y
11	M/17	PSR	3,91	1800	20	Y
12	M/31	PSR, PE	0,34	2100	26	Y
13	F/19	N/A	0,70	2100	57	N
14	M/14	PE	2,80	1800	46	Y
15	M/34	PE	32,51	1500	52	Y
16	M/40	PSR	0,14	2100	27	Y
17	M/29	PE	2,97	1800	49	N
18	F/38	N/A	5,71	1500	53	Y
19	M/21	N/A	1,16	2100	31	Y
20	F/39	N/A	0,52	2100	26	Y
21	F/30	N/A	0,02	2100	29	Y
22	M/44	N/A	0,14	2100	13	Y
23	M/39	N/A	2,35	2100	32	Y
24	F/43	N/A	3,62	1800	28	Y
25	M/23	N/A	0,08	2100	36	Y
26	M/68	N/A	2,50	1800	39	N
27	M/33	N/A	0,04	2100	30	Y
28	M/49	N/A	1,07	2100	24	Y
29	M/26	N/A	1,36	1800	38	Y
30	F/52	N/A	12,78	1500	55	N
31	M/44	N/A	4,68	1800	29	Y

*Dose administered to the 80%-isodose line; PE = Partial embolization; PSR = Partial Surgical Resection; N/A = Not Applicable

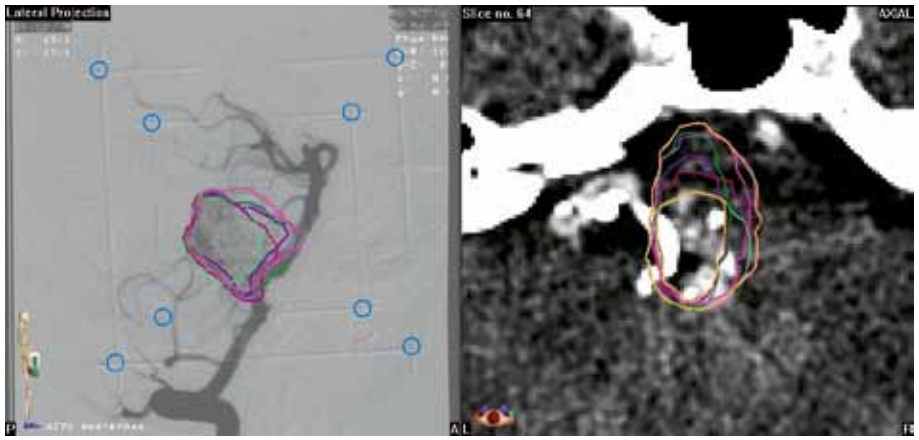

Figure 3.1
Contouring variations in a patient with a brainstem AVM. Target volume are presented as different colors (left image). All contours were automatically projected on CT-images, which were used for further analysis (right image).

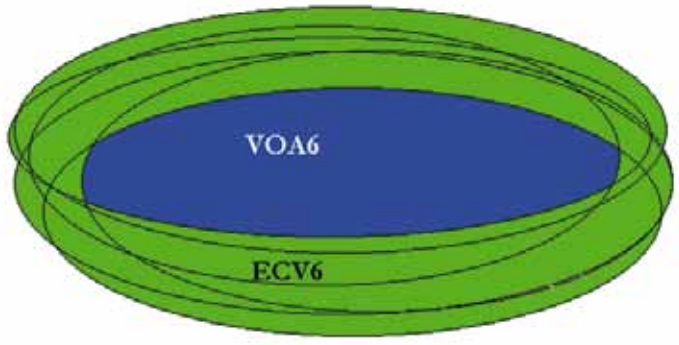

Figure 3.2
Each ellipse represents a target volume. VOA_6 was defined as the common overlapping volume of all target volumes and is illustrated in blue. ECV_6 was defined as the enveloping volume of all six target volumes and is illustrated in green. VOA_2 and ECV_2 are comparable volumes, but derived from a combination of two target volumes.

Spatial variant parameters

The following spatial variant parameters were determined: VOA_6, defined as the common overlapping volume of all six target volumes, and ECV_6, defined as the encompassing volume of all six target volumes (Figure 3.2). The ratio between the VOA and the ECV, that is, the agreement ratio (AR), was taken as a measure of the interobserver agreement. An AR of 1 represents complete agreement, and an AR of 0 represents no agreement. This ratio was determined for all six target volumes (i.e., $AR_6 = VOA_6/ECV_6$), as well as for all possible pairs of observers (i.e., AR_2 = mean VOA_2/ECV_2), because this ratio tends to decrease with an increasing number of observers. To study the absolute positional shift, between individual contours, the three-dimensional distance between the respective centers of mass was computed from the *X* (AP), *Y* (mediolateral), and *Z* (craniocaudal) coordinates, as determined by the Brainscan software using the Pythagoras algorithm. Similarly, the shift between each target volume, and the originally treated volume was determined. Additionally, the positional shift was analyzed as a dichotomized variable comparing an original treatment volume of ≤ 7 cm^3 to those > 7 cm^3 using a Mann-Whitney *U* test.

Previous unsuccessful or partial treatment

The aforementioned parameters in the previously unsuccessfully or partially treated group were compared with those without prior treatment using a Mann-Whitney *U* test or a Student's *t* test, as appropriate.

Clinical outcome

Although the number of patients was insufficient for a detailed failure analysis, we did correlate our parameters with the clinical outcome. Treatment results were analyzed for correlation with the originally treated volume and the marginal dose, using a Mann-Whitney *U* test. The agreement ratios, mean positional shift, individual target volume, and treatment dose were analyzed for correlation with obliteration, using a Student's *t* test and Mann-Whitney *U* test, respectively.

Dosimetry

To correlate the observed contouring variations with dosimetry, treatment planning was performed using the original treatment plan. Dose–volume histograms were used to evaluate the dosimetric consequences of contouring variations. The coverage of the originally treated volume, all individual target volumes, and the VOA_6 were determined using treatment planning with both standard conventional collimators and dynamic conformal arcs. A Mann-Whitney *U* test was used to identify differences in dosimetric coverage when using conventional collimators or dynamic conformal arcs.

Results

Interobserver variation

Spatial invariant parameters.

The mean contoured volume of all six clinicians was 3.6 ± 5.6 cm^3 and the mean contoured volume of each possible pair of observers was 3.6 ± 5.3 cm^3. Both results corresponded well with a mean originally treated volume of 3.4 ± 6.2 cm^3. No significant differences in the size of contoured target volumes were found among the observers (p = 0.557), or among the neurosurgeons, neuroradiologists, or radiation oncologists (*p* = 0.855).

Spatial variant parameters.

The mean AR_6 was 0.19 ± 0.14 and the mean AR_2 was 0.45 ± 0.18 (Figure 3.3A and B). The mean absolute positional shift between the center mass of the individual target volumes was 2.8 ± 2.6 mm (Figure 3.3C). In bAVMs with an originally treated volume of ≤ 7 cm^3 and > 7 cm^3, the corresponding values were 2.8 ± 2.7 mm and 3.1 ± 2.0 mm. Similarly, the mean positional shift between the center mass of the individual target volumes and the center mass of the originally treated volume was 2.5 ± 2.5 mm (Figure 3.3D). In bAVMs with an originally treated volume of ≤ 7 cm^3 and > 7 cm^3, the corresponding values were 2.4 ± 2.5 mm and 3.8 ± 2.1 mm.

Previous unsuccessful or partial treatment

The target volumes in the previously treated group (mean 5.5 ± 7.6 cm^3) were significantly (*p* <0.001) larger than in the group not previously treated (2.6 ± 3.9 cm^3). No significant differences were found in the AR_6 (p = 0.27) between the previously treated group and untreated group; however, the AR_2 was significantly (p = 0.012) smaller for the previously treated group (mean 0.42 vs. 0.47). Both the mean shift between pairs of two observers, as well as the mean shift between individual target volumes and the originally treated volume, were significantly larger in the previously treated group (3.2 vs. 2.5 mm, p = 0.007; 4.3 vs. 1.8 mm, p ≤ 0.001).

Clinical outcome

Complete, angiographically confirmed obliteration was obtained in 24 (77%) of 31 patients at a mean interval of 33 months (range, 13 – 53 months). Failure to obliterate was only marginally affected by the treated nidus volume (p = 0.09) or the marginal dose (p = 0.09); patients with a larger bAVM or lower marginal dose tended to respond less well. With respect to interobserver variation, there appeared to be no correlation between obliteration of the treated bAVMs and the AR_6 (p = 0.70) or the AR_2 (p = 0.09). However, failure to obliterate correlated with a larger mean positional shift between individual target volumes (mean, 3.3

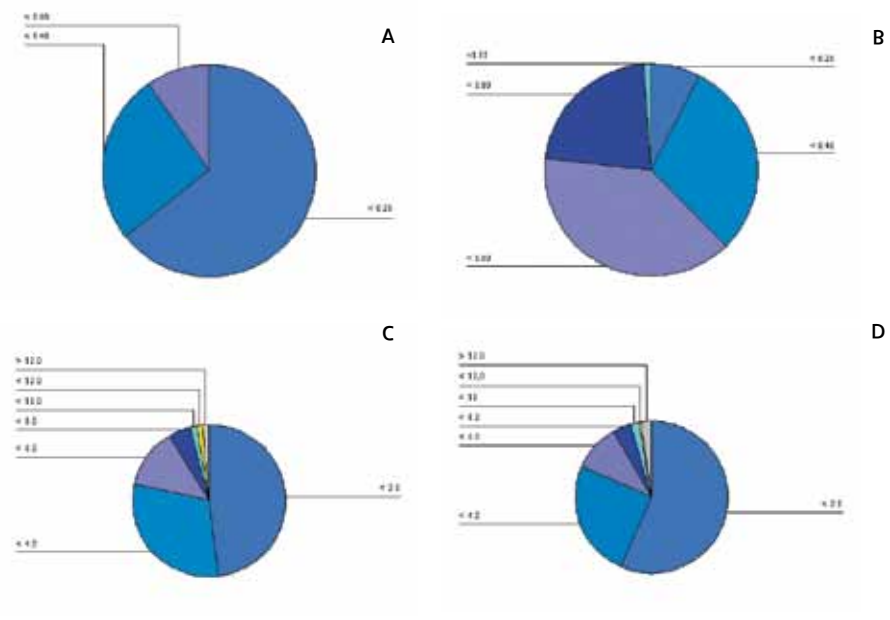

Figure 3.3
The agreement ratio, defined as VOA/ECV for all six observers (AR_6) was < 60% in all cases **(A)**. This ratio improved when all possible pairs of observers were compared **(B)**; however, 76% remained at < 60% of agreement **(C)**. In about 50%, absolute positional shift was < 2 mm between mutual individually contoured target volumes (TV) and between target volumes and the center of mass of the originally treated volume (OTV) **(D)**. However, this shift may increase up to 12 mm.

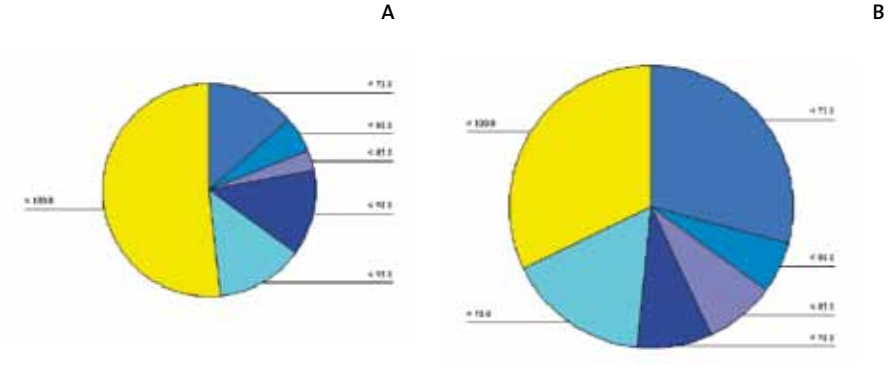

Figure 3.4
Despite a relatively low agreement ratio, use of circular collimators resulted in adequate coverage in most patients **(A)**.This coverage decreased with use of dynamic multileaf collimators **(B)**.

vs. 2.6 mm; p = 0.012), as well as with the shift between individual target volumes and the center of the mass of the originally treated volume (mean, 4.2 vs. 2.0 mm; p ≤ 0.001).

Dosimetry

The mean coverage of the originally treated volume by the 80%-isodose line using standardized treatment with conventional collimators was 96.8% ± 4.0%. The corresponding coverage of the VOA_6 was 95.9% ± 13.5%. In contrast, the mean coverage of the individual target volumes was only 88.1% ± 3.2% (Figure. 3.4). Using a simulated treatment plan with dynamic conformal arcs instead of conventional collimators, the coverage of the originally treated volume and VOA_6 was similar (99.2% ± 1.3% and 95.4% ± 11.9%, respectively). However, the mean coverage of the individual target volumes by the prescription isodose decreased to 78.9% ± 4.4%, significantly lower than with conventional collimators (p ≤ 0.001; Figure 3. 5).

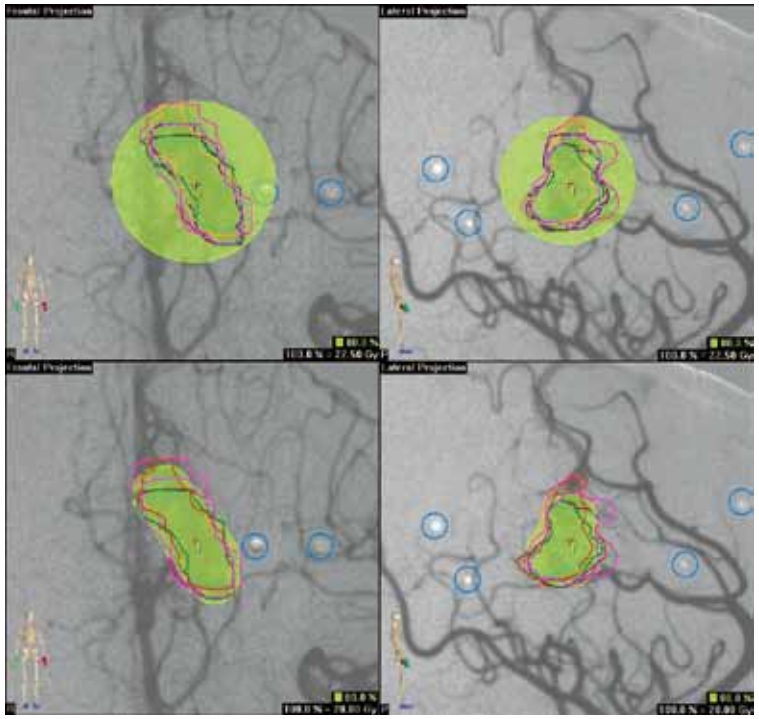

Figure 3.5
Individual target volumes, each in a different color, as contoured by six observers **(upper image)**. When using a treatment plan with circular collimators, the mean dosimetric coverage (yellow area) in this patient was 98.1% ± 1.9%. Using a similar treatment plan with dynamic conformal arcs **(lower image)**, mean dosimetric coverage decreased to 95.2% ± 6.4%. In this patient, complete angiographic obliteration was reached within 28 months.

Discussion

Interobserver variation in contouring target volumes is a well-recognized problem in radiotherapy. It can result in geometric errors and, thereby, treatment failure. Although differences in interpretation of the nidus have been reported extensively, most of these studies have been descriptive[7, 199, 419], and to our knowledge, this is the first analysis to link interobserver variation to both dosimetry and the clinical results of radiosurgery.

The results of the present study revealed a substantial interobserver variation, although our obliteration rate is comparable with that of other centers. Although the mean reported absolute positional shift seems rather small, this may have a profound dosimetric and clinical impact, in view of the steep dose gradients achieved with radiosurgery. In our study, despite a substantial interobserver variation, no significant differences were found among observers from different disciplines.

The drawbacks of stereotactic DSA as the main imaging modality for radiosurgical planning have been described extensively[40, 43, 427]. The main limitation of DSA is that it presents only two-dimensional information on the nidus, but radiosurgical treatment planning requires accurate three-dimensional (3D) target definition. Even with high-quality DSA, its two-dimensional character can lead to under- or overestimation of the actual nidus size owing to superimposition of feeding arteries and draining veins and difficulties in determining complex 3D variations on nidus geometry. However, because of its superior spatial resolution and dynamic demonstration, DSA performed under stereotactic conditions is still the reference standard for defining the nidus for the purpose of radiosurgery[331]. Also, it often is the only means available for making a distinction between the nidus and the surrounding normal vasculature. MRI and, occasionally, CT are used increasingly to portray the true 3D shape of the nidus. Target definition for radiosurgery treatment planning has been demonstrated to be improved by the integration of a 3D imaging modality in the information obtained by DSA, correcting the shortcomings of each imaging modality[29, 82, 237, 454]. Guo *et al.* found that it was possible to delineate medium- and large-size bAVM nidi on stereotactic MRI and that the estimated nidus volumes on MRI tended to be smaller[158]. St. George *et al.* concluded that bAVM nidi, delineated on MRI by different observers, correlated well in terms of size, with little interobserver variability[147]. The targets, however, appeared randomly displaced from volumes obtained using both MRI and DSA, precluding the safe use of MRI as the sole imaging modality for radiosurgical planning[147]. Additionally, when using magnetic resonance angiography, early venous filling is often difficult to reveal because it lacks the temporal information of DSA[18, 441]. Yu *et al.* concluded that MRI-based bAVM delineation without conventional angiography may be feasible only for selected patients, such as those

with nondiffuse bAVMs or large nonembolized bAVMs[486]. Similar problems occur when using 3D DSA in which the phase of the bAVM filling is different for each projection, leading to spatiotemporal uncertainty. Furthermore, magnetic resonance angiography could fail in the detection of small bAVMs owing to an insufficient spatial resolution and disturbances caused by structures with short T_1-times, such as methemoglobin in subacute hemorrhage[314]. Flickinger *et al*. found that the addition of stereotactic MRI to angiography for stereotactic targeting did not significantly decrease out-of-field nidus persistence or decrease overall obliteration, nor did it significantly reduce complications[120, 121]. Although CT was mainly used for dosimetrie computations, the advent of CT angiography (CTA) has made this form of imaging very useful for radiosurgical planning. CTA provides a reliable demonstration of large draining veins but visualizes a lower number of small feeding arteries than magnetic resonance angiography[445]. However, the use of dynamic intra-arterial CTA, demonstrating a relatively high sensitivity of separation of veins from other vascular components, has been described[246]. The development of these dynamic CTA techniques may improve the adequate hemodynamic imaging of the nidus.

In our study, 7 of the 10 previously treated patients had undergone endovascular embolization. Other studies have demonstrated different treatment results after prior endovascular embolization. Bollet *et al*. found a 5-year actuarial rate of obliteration of 77% in a group of 112 patients, of whom 88% had undergone previous embolization[42]. Gobin *et al*. concluded that the residual nidus can be irradiated with results almost as good as for a native bAVM of the same size[151]. These findings are in contrast to those of Miyawaki *et al*., who found the obliteration rate to be negatively associated with a history of prior embolization[304]. Schlienger *et al*. found a greater obliteration rate to be associated with the absence of prior embolization[399]. Prior endovascular treatment complicates nidus identification, because suboptimal subtraction may lead to the embolic agent overlapping the nidus. This fact is illustrated by the significantly larger contouring variation seen in the present study, with respect to both the AR_2 and the positional shift of the target volume. In addition, our results showed significantly larger contoured target volumes in the previously treated group, which may have been caused by the overprojection of embolization material and/or the presence of collateral feeding vessels, although it has been common practice to treat larger bAVMs initially with endovascular treatment. Recently, we started using plain CT scans for radiosurgical planning of bAVMs in embolized patients. A large advantage of CT is its sensitivity to embolization materials, which appear hyperdense in precontrast imaging[385]. We contour the embolization material in the stereotactic CT images and project these onto the stereotactic angiographic images to restrict the radiation field to the persistent nidus.

Conclusion

The results of our study have demonstrated that interobserver variation in contouring can have a significant impact on the dosimetry of radiosurgery for bAVMs. The mean coverage of individually contoured volumes was only 88% using conventional collimators and decreased to 78% when more conformal radiosurgical treatment planning with dynamic conformal arcs were simulated. This finding is particularly important because failure to cover the entire nidus with a therapeutic dose can lead to treatment failure. Therefore, the clinical implementation of more conformal radiosurgical techniques warrants increased attention to accurate and consistent delineation of the nidus in three dimensions. The use of more conformal radiosurgical techniques requires imaging equipment that is able to provide an adequate 3D image of the nidus. Additional research and the development of 3D imaging techniques with a high temporal resolution, resulting in true hemodynamic information, such as dynamic intra-arterial CTA is necessary. To minimize the impact of interobserver variation, radiosurgical treatment of bAVMs should preferably be performed in a multidisciplinary setting by an experienced and dedicated group of specialists.

Chapter 4

Target Delineation on Magnetic Resonance Angiography

D.R. Buis
F.J. Lagerwaard
C.M. Dirven
F.D.R.K. Barkhof
D.L. Knol
R. van den Berg
B.J.Slotman
W.P. Vandertop

Adapted from: Buis DR, Lagerwaard FJ, Dirven CM, Barkhof F, Knol DL, van den Berg R, Slotman BJ, Vandertop WP. Delineation of brain AVMs on MR-Angiography for the purpose of stereotactic radiosurgery. Int J Radiat Oncol Biol Phys. 2007 Jan 1;67(1):308-16.

Abstract

Purpose

To assess the dosimetric consequences of brain arteriovenous malformation (bAVM) delineation on magnetic resonance angiography (MRA) for the purpose of stereotactic radiosurgery.

Methods

Three observers contoured a bAVM in 20 patients, using digital subtraction angiography (V_{DSA}) and three-dimensional time-of-flight MRA (V_{MRA}). Displacement between contours was calculated. Agreement and differences between observers and imaging modalities were assessed. A standardized treatment plan with dynamic conformal arcs was generated and dosimetric coverage of all contours and the volume of normal brain tissue within the high dose region was determined.

Results

The generalized reliability coefficient was "fair" for target volume (0.79), but "poor" for displacement (0.35). V_{MRA} was larger than V_{DSA} (5.0 vs. 4.0 ml, p = 0.001). No difference in displacement was found (2.8 vs. 2.5 mm, p = 0.156). Dosimetric coverage of V_{MRA} was 62.9% (95% CI, 56.9 – 68.8) when V_{DSA} was used as planning target volume, and coverage of V_{DSA} was 83.5% (95% CI, 78.1 – 88.8) when V_{MRA} was used for planning (p < 0.001). The mean volume of normal brain within the 80% isodose was larger when the bAVM was delineated on MRA (0.7 vs. 1.0 ml (p = 0.02) for targets <3 ml, and 3.7 vs. 7.0 ml (p = 0.01) for targets >3 ml).

Conclusion

Brain arteriovenous malformations delineated on MRA are larger and more randomly displaced. However, for bAVMs <3 ml, the difference in volume of normal brain tissue within the high-dose region does not seem to be clinically relevant. Therefore, MRA-images might be used as the sole imaging modality for the radiosurgical treatment of bAVMs ≤ 3 ml when the bAVM is located in a noneloquent position.

Key words

Intracranial arteriovenous malformations • Magnetic resonance angiography, Observer variation • Radiosurgery • Stereotaxic techniques.

Introduction

Stereotactic radiosurgery is an established treatment modality for small brain arteriovenous malformations (bAVM) in eloquent locations. Target definition for radiosurgery of bAVMs requires three-dimensional (3D) imaging of the nidus for which several imaging modalities such as digital subtraction angiography (DSA), computerized tomography angiography (CTA), magnetic resonance angiography (MRA), or combinations of these are being used. These imaging modalities all have their own advantages and disadvantages. Digital subtraction angiography (DSA) is relatively invasive and has been associated with neurologic complications in 1.3–2.3%[266, 474]. Despite the major disadvantage of being a two-dimensional imaging technique with related problems of overprojection of feeding arteries, draining veins, or bone and embolization material in case of incomplete subtraction, DSA remains the gold standard for imaging of bAVMs because it provides unique temporal information[260, 331]. Computerized tomography angiography and MRA both provide 3D visualization of the bAVM nidus; however, the temporal aspect of these techniques is, at present, even for time-resolved MRA, still inferior to DSA[420].

In our institute, treatment planning for radiosurgery of bAVMs is performed using a combination of stereotactic CTA, DSA, and MRA; however, a selected early phase of the DSA study remains the principle imaging modality used for target definition. In the present study, we aimed to compare delineation of the bAVM nidus on either DSA or MRA, to evaluate whether it is possible to perform stereotactic treatment planning without the invasive technique of DSA. We evaluated the extent of interclinician agreement in bAVM contouring with respect to target volume, spatial localization, and finally, the dosimetric consequences of using either DSA or MRA.

Methods

Between 1991 and 2004, 233 patients with a bAVM were treated with linear accelerator radiosurgery at the VU University medical center, Amsterdam. Included in this study were 20 randomly selected patients with a single bAVM that was visible on DSA, CTA, and MRA studies. The mean treated bAVM volume was 4.6 ml (95% CI, 1.1 – 8.1). Previous partial treatment of the bAVM consisted of endovascular embolization (n = 8) or neurosurgery (n = 1), and complete angiographic obliteration during follow-up was reached in 14 patients (70%).

The MRA study was performed on the day before radiosurgery, using a 1.5T whole-body scanner with a standard polarized head coil (Magnetom Vision, Magnetom Sonata;

Siemens, Erlangen, Germany). For each patient, T_2-weighted magnetic resonance images (MRIs) (repetition time = 3000 ms; echo time = 20 ms) with a slice thickness of 3 mm, as well as 3D time-of-flight (TOF) MRA images (repetition time = 39 ms; echo time = 6.5 ms; flip-angle = 20°) with a slice thickness of 1 mm and an in-plane resolution of 0.4 mm were available. These sequences are thought to be optimized for depicting bAVMs. On the day of treatment, an invasive stereotactic frame (BrainLAB AG, Feldkirchen, Germany) was rigidly attached to the patients' skull, after which stereotactic DSA and a 2-mm sliced, contrast-enhanced computed tomography (CT) scan were performed with the frame in place. DSA was performed with a frame rate of 3–6 s^{-1}, depending on the flow rate of the bAVM. From this series, the radiologist who performed the DSA selected two orthogonal images, which were optimized for radiosurgery. The radiologist who selected these images was not eligible for contouring studies (RvdB). All images were digitally transferred to the radiosurgery treatment planning system (Brainscan v. 5.2, BrainLAB AG, Feldkirchen, Germany). The DSA images were co-registered with the CT images using the stereotactic localizer box. Finally, the MRA study was digitally fused with the CT study using the automatic image fusion software of the Brainscan stereotactic planning system.

We used the following, commonly used nidus-definition: a network of abnormal vessels between the arterial feeder(s) and the pathologically early draining vein(s)[32]. Three clinicians (one radiation-oncologist [FJL], neurosurgeon [CMFD], and neuroradiologist [FB]), all actively involved in routine radiosurgery for bAVMs, individually contoured the nidus on DSA (V_{DSA}) and on MRA (V_{MRA}). In our institute, the radiation oncologists takes part in both target delineation of bAVMs and dosimetry. The delineations were performed blinded to both the data from the other imaging modality and the contours drawn by other investigators. As all images were co-registered with the stereotactic CT scan, all contours were automatically projected onto the CT images, which were used for further analysis (Figure 4.1).

The absolute volumes of V_{DSA} and V_{MRA}, as well as the coordinates of the center of each target volume, were derived from the Brainscan planning system. The coordinates of the collective center of mass of all three target volumes ("centroid") was calculated for each modality for each patient. To determine positional shifts between individual contours, the 3D distance (X_{DSA} and X_{MRA}) between the center of each individual target volume and the centroid was calculated from the X (anteroposterior), Y (mediolateral), and Z (craniocaudal) coordinates using Pythagoras' algorithm (Figure 4.2).

To assess the dosimetric consequences of differences in target delineation on either DSA or MRA, a standardized treatment plan using five dynamic conformal arcs (DMLC, which is also used for clinical treatment of bAVMs) was generated for each individual target volume.

Dose–volume histograms were used to determine the coverage of each individual V_{MRA} by the 80% prescription isodose when planning was performed using V_{DSA}. Alternatively, the coverage of V_{DSA} was determined when planning was performed on each V_{MRA}(Figure 4.3). To determine the conformity of the treatment plan, the volume of the prescription 80% isodose surface divided by the target volume was calculated (PITV ratio)[407]. The volume of normal brain tissue within the 80% isodose was determined for each target volume using dose–volume histograms of the normal brain.

Statistical analysis

To perform statistical analysis, all data except dosimetric coverage were log transformed. The dosimetric coverage was assessed using a log transformation of 101 minus the individual dosimetric coverage, to correct for the deviation to the left on a normal distribution histogram.

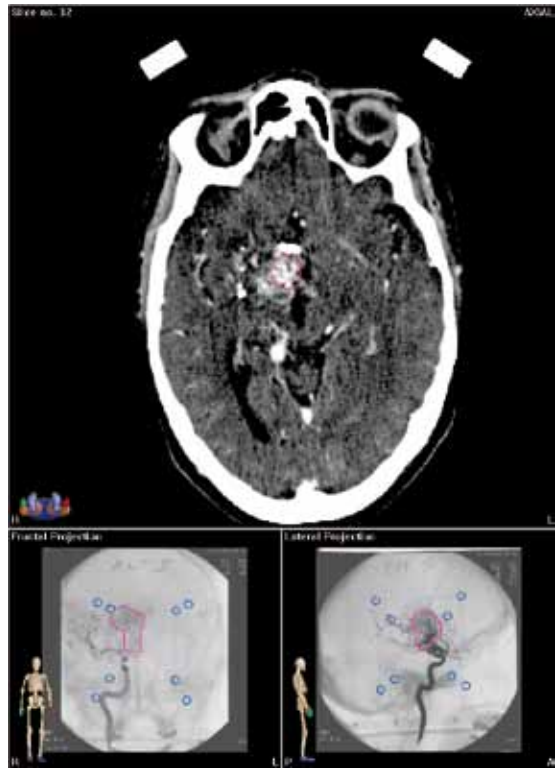

Figure 4.1
Each target volume is presented in a different color. In this case a thalamic bAVM has been contoured on DSA (pink). All contours were automatically projected on CT-images, which were used for further analysis.

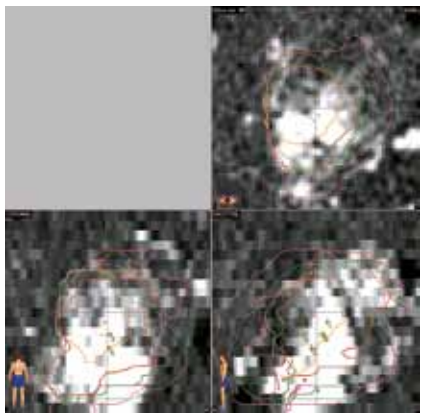

Figure 4.2
Each target volume is represented as a contour in a different color. The location of the isocenter is represented as a yellow dot. The coordinates of each isocenter are calculated by the planning software. The mean of these coordinates was calculated, resulting in the coordinates of a centroid. The distance from each individual contour to the centroid was calculated using Pythagoras' algorithm.

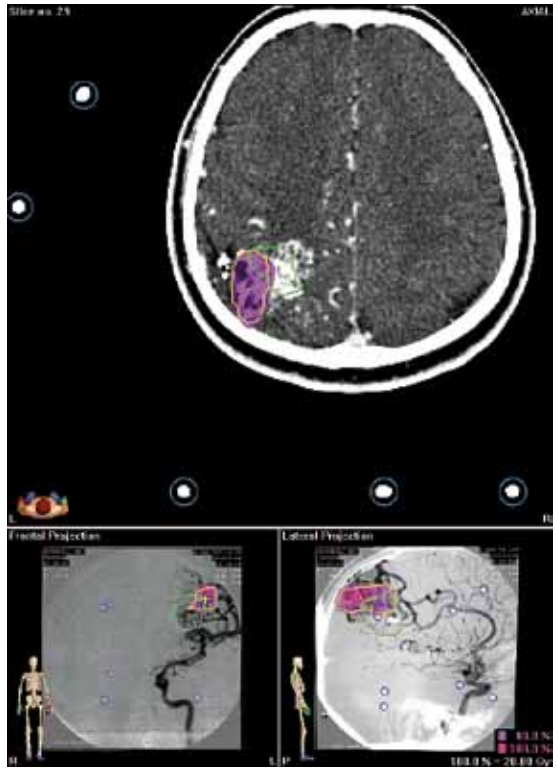

Figure 4.3
A parieto-occipital bAVM has been outlined on DSA (orange contour) and on MRA (green contour). The coverage of V_{DSA} by the 80%-isodose-line was 98% (shaded purple area). However, the dosimetric coverage of V_{MRA} was only 25%.

Interobserver agreement in volume (V_{DSA} and V_{MRA}) and positional shift (X_{DSA} and X_{MRA}) were assessed by calculating the concordance correlation coefficient (CCC), using random effects analysis of variance[60, 278].
Agreement in volume and positional shift, generalized over observers and images, was assessed by the generalizability coefficient ø, using a random effects analysis of variance[45, 406]. Agreement was considered 'poor' with ø values ≤ 0.70, 'fair'with ø values between 0.71 and 0.85, and 'excellent' with ø values ≥ 0.86.

Differences in volume, positional shift, dosimetric coverage, and volume of normal brain tissue within the high-dose region between DSA and MRA were compared using a linear mixed model with observers and imaging techniques as factors. Observer by image interaction was taken into account in this model. A two-tailed *p* value < 0.05 was chosen as the threshold for statistical significance. All statistics were performed using Statistical Package for Social Sciences version 12.0 (SPSS Inc., Chicago, IL).

Results

In general, there was a 'fair' to 'excellent' agreement among the three clinicians with respect to the contoured volume of the bAVMs, resulting in a generalized reliability coefficient ø of 0.79, and a CCC of 0.86 and 0.82 for V_{DSA} and V_{MRA}, respectively. Contouring on MRA tended to overestimate the target volume in comparison to DSA (Figure 4.4). The mean V_{MRA} was larger than the mean V_{DSA} in 17 patients (85%). Overall, the mean V_{MRA} of all twenty patients was 5.0 ml (95% CI: 3.5 – 6.6), which was significantly larger (p = 0.001) than the mean V_{DSA} of 4.0 ml (95% CI: 2.8 – 5.2).

In contrast to the volumetric analysis, there was a 'poor' agreement with respect to spatial localization of the target volumes (Figures 4.4 and 4.5). The generalized reliability coefficient ø was 0.35, with a CCC of 0.62 and 0.30 for X_{DSA} and X_{MRA}, respectively. The mean positional shift between the centroid of the MRA and that of DSA contours was 3.7 mm (95% CI: 2.6 – 4.8). The mean coverage of the V_{DSA} (when planned on V_{DSA}) and V_{MRA} (when planned on V_{MRA}) by the 80% prescription isodose was 98.4% (95% CI: 98.0 – 98.7) and 98.1% (95% CI: 97.7 – 98.6), respectively, using a standard five stereotactic arcs with dynamic multileaf collimation (Table 4.1).

The dynamic conformal arc technique resulted in a mean PITV-ratio of 1.7 for DSA and 1.8 for MRA. The interclinician variability in contouring resulted in a mean coverage of only 62.9% (95% CI: 56.9 – 68.8) of V_{MRA} by the 80% isodose when treatment planning was performed

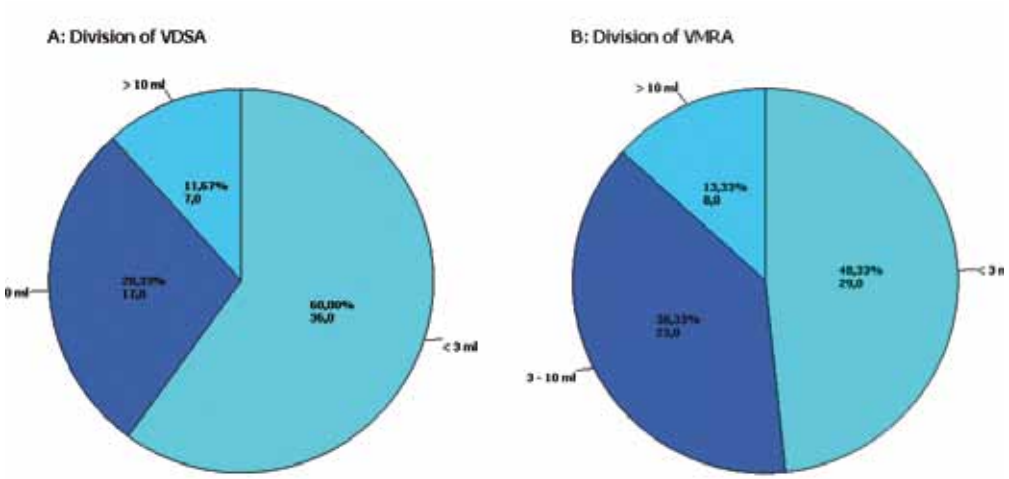

Figure 4.4
Contouring on MRA **(B and D)** tended to overestimate the target volume in comparison to DSA, **(A and C)** with 52% of the target volumes > 3ml, in comparison to 40% of V_{DSA} > 3ml.

on V_{DSA}. Alternatively, for treatment planning using V_{MRA}, the coverage of the V_{DSA} by the 80% isodose was 83.5% (95% CI: 78.1 – 88.8, $p < 0.001$) (Figure 4.3).

The larger target volumes that were derived from contouring on MRA resulted in a significantly larger volume of normal brain within the 80% dose region ($p < 0.001$). The volume of normal brain receiving the prescription dose was 4.1 ml (95% CI: 2.8 – 5.5) for contouring on V_{MRA} vs. 2.0 ml (95% CI: 1.4 – 2.5) for contouring on V_{DSA}. The mean volume of normal brain within the high dose region was 0.7 ml vs. 1.0 ml for contouring on DSA and MRA, respectively, for target volumes ≤ 3 ml ($p < 0.001$). The corresponding figures for target volumes > 3 ml were 3.7 ml vs. 7.0 ml ($p < 0.001$).

In seven measurements V_{MRA} was ≤ 3 ml, and V_{DSA} > 3 ml (Figures 4.4A and B). To correct for this inconsistency, the same statistical analysis was performed again for V_{DSA}, in which all cases with $V_{MRA} \leq 3$ ml, and V_{DSA} >3 ml were considered to be smaller than 3 ml. This was also performed for V_{MRA} in which all cases with $V_{MRA} \leq 3$ ml, and V_{DSA} > 3 ml were considered to be larger than 3 ml. Although this resulted in small changes in the mean volume of normal brain within the high-dose region, the differences remained significant ($p \leq 0.001$).

Table4.1: Coverage of Target Volumes

	Isocenter placed on: VDSA		VMRA	
	Results in mean marginal coverage of:			
Patient-nr.	VDSA (%)	VMRA (%)	VDSA (%)	VMRA (%)
1	97.7	39.3	98.1	99.2
2	97.4	67.1	92.9	88.1
3	99.2	82.9	99.2	97.7
4	98.6	71.1	99.3	84.5
5	99.1	93.9	99.3	88.0
6	95.5	39.5	96.0	79.8
7	99.4	81.6	99.1	65.9
8	99.8	78.2	99.7	68.2
9	97.3	58.5	97.5	91.0
10	96.8	35.2	95.8	37.6
11	98.5	47.9	98.2	95.2
12	99.4	61.8	99.8	95.7
13	98.1	70.8	97.8	91.8
14	99.7	48.9	99.6	64.0
15	98.2	87.4	98.0	82.9
16	98.5	53.3	99.2	99.6
17	99.9	74.5	99.5	78.1
18	99.7	72.0	99.5	90.3
19	96.9	41.9	97.4	81.8
20	97.5	51.3	97.0	89.8

Abbreviations: VDSA: nidus volume as contoured on DSA,
VMRA: nidus volume as contoured on MRA

A B

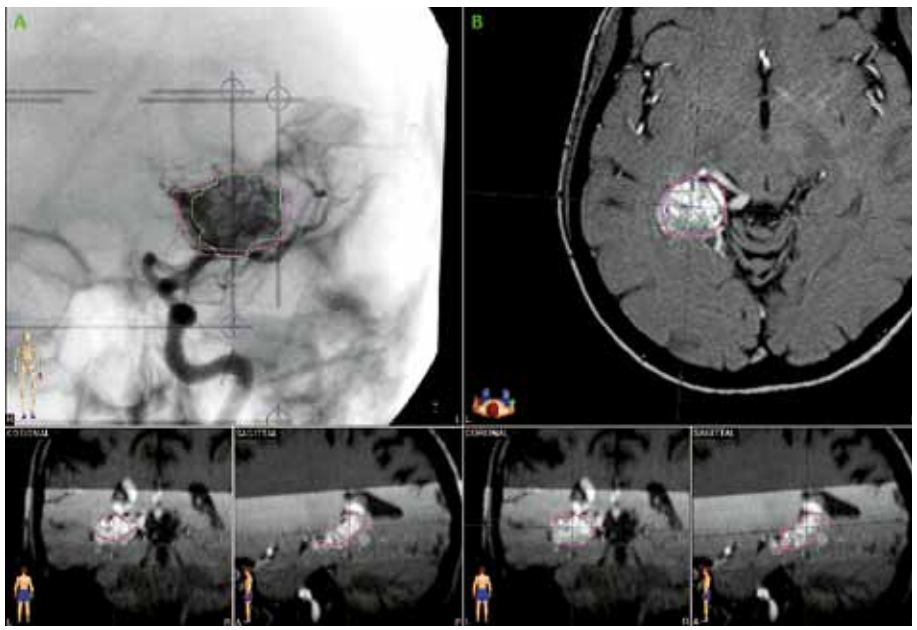

Figure 4.5
'poor' agreement with respect to spatial localization of the target volumes was found.
In this patient the mean positional shift was 1.1 mm for V_{DSA} (4.5A) and 1.3 mm for V_{MRA} (4.5B).

Discussion

Target delineation on MRI/MRA has been studied by several authors[19, 29, 147, 158, 237, 486]. Although the exact MRA sequences used do not become clear in one study[486], in other studies contrast-enhanced, T_1-sequences[147], or both contrast-enhanced TOF and phase-contrast MRA sequences were obtained[237]. In the remaining studies, contrast-enhanced TOF MRA sequences were used[19, 29, 158]. The study design and patient population among these studies differ. Although in five studies, targets were delineated on MRA alone[19, 147, 158, 237, 486], in one study the additional value of MRA was evaluated[29]. Embolized patients are included in four studies[29, 147, 237, 486], and comprise 37% and 64% of the entire patient population in two studies[147, 237]. No mention of prior embolization was made in the studies by Guo *et al*. and Aoyama et al[19, 158]. In none of the previously mentioned studies were possible dosimetric consequences assessed.

Although our study is based on a small sample only, and should, therefore, be interpreted cautiously, our data demonstrate that bAVMs contoured on 3D-TOF-MRA and T_2-MR

sequences without using the additional information of stereotactic DSA are significantly larger and increase the interclinician contouring variability with respect to spatial position. The larger volumes that were contoured on MRA resulted in a reasonable coverage of V_{DSA} (83.5%), but also in a larger volume of irradiated normal brain (4.1 vs. 2.0 ml). These findings are in accordance with Yu *et al*.[486], who reported that the MRI–based volume overestimated the actual treatment volume by a mean of 57% for bAVMs larger than 2 cm^3 and by a mean of 25% for bAVMs smaller than 2 cm^3. Other studies report a comparable or smaller volume for target delineation on MRA[19, 147, 158]. The MRA sequences provide poor hemodynamic information in comparison with contrast-enhanced, time-resolved MRA or DSA, resulting in a poor discrimination of arteries, nidus, and veins[242]. This lack of discrimination between the nidus and surrounding vessels may result in the contouring of larger and less reproducible volumes, particularly in larger bAVMs with more prominent feeding arteries and draining veins. In this respect, other studies may be positively biased by a small bAVM population[158] or by adding hemodynamic information from CTA to the MRA images[19]. Because the mean V_{MRA} was larger in only 5 of 8 embolized patients, it is unlikely that previous embolization is the cause of the increase in volumes with MRA contouring.

One of the objectives of our study was to evaluate the dosimetric consequences of contouring bAVMs using MRA only. We found that this would result in a reasonably adequate coverage of V_{DSA} (83.5%). However, it would also lead to a significantly larger volume of irradiated normal brain tissue (4.1 vs. 2.0 ml). Two factors are responsible for this finding. First, because of the larger V_{MRA}, the 80% isodose shell surrounding V_{MRA} will be more voluminous. As a volume expands exponentially by a factor of $^4/_3\pi R^3$, a small increase in radius will result in a relatively large increase in volume. This theory also explains our finding that the volume of normal brain tissue within the high-dose region is significantly larger when the target volume is > 3 ml. Second, V_{MRA} is often complex and more irregularly shaped. Because the optimal target for radiosurgery is a sphere, the volume of irradiated normal brain tissue will increase with more irregularity of the target. Kubo *et al*. found a PITV ratio (*i.e*., the volume encompassed by the prescription isodose surface divided by the clinical target volume) of 2.3 – 2.5 in very irregular shaped intracranial lesions, when micromultileaf collimators were used[245]. According to the Radiation Therapy Oncology Group guidelines for radiosurgery, a PITV ratio of 1.0 –2.0 is desirable[407]. In our study design, we only evaluated the use of dynamic conformal arcs, because these are also used in clinical practice. This resulted in a highly conformal treatment planning with a mean PITV ratio of 1.7 for DSA, and 1.8 for MRA. Because of the highly conformal properties of dynamic conformal arc treatment, the discrepancy in dosimetric coverage will increase in comparison to treatment planning using conventional collimators[58].

Although the volume of normal brain tissue within the high-dose region was found to be significantly larger when contouring on MRA, the clinical consequences of such an approach remain to be determined. In this study, we did not correct the normal brain tissue dosimetry for noneloquent brain tissue such as the ventricle, adjacent vessels, or surrounding embolization material. For target volumes ≤ 3 ml, the mean volume of normal brain tissue within the high-dose region was increased from 0.7 ml to 1.0 ml with MRA-based target definition, which may not be clinically relevant, when the bAVM is located in a noncritical region.

Magnetic resonance imaging/MRA additionally provides information regarding tissue surrounding the bAVM. Target delineation using MRA can be improved by adding hemodynamic information. Time-resolved contrast-enhanced 3D-MRA, which demonstrates blood directly and irrespectively of flow because of the administration of gadolium chelate[378], seems especially promising, as it results in a high temporal and an adequate spatial resolution. Duran *et al.*, found no differences in delineating feeding arteries and the nidus between TOF-MRA and ultrashort contrast-enhanced 3D-MRA[105]. Contrast-enhanced 3D-MRA was able to detect and delineate the venous drainage patterns in correlation with DSA. However, in a preliminary study, Gauvrit *et al*. reported moderate interobserver agreement for the visualization of the venous drainage, using 3D dynamic MR-DSA[144].

Conclusion

We found that bAVMs contoured on 3D-TOF-MRA are significantly larger and more subject to interclinician variations in contouring in comparison to bAVMs delineated on DSA. This results in a reasonable dosimetric coverage of V_{DSA}, but also in a larger volume of irradiated normal brain tissue. However, for the subgroup of bAVMs ≤ 3 ml, the volume of normal brain tissue within the high-dose region is that small (1 ml) that it does not seem to be clinically relevant, especially when the bAVM is located in a noneloquent region. Therefore MRA images might be used as the sole imaging modality for the radiosurgical treatment of bAVMs ≤ 3 ml in noneloquent regions of the brain. Incorporation of hemodynamic information in magnetic resonance images is the first step to improve bAVM delineation on magnetic resonance imaging.

Chapter 5

Radiosurgery of Brain Arteriovenous Malformations in Children

D.R .Buis
C.M.F. Dirven
F.J. Lagerwaard
E.S. Mandl
G.J. Lycklama à Nijeholt
D.S .Eshghi
R. van den Berg
J.C .Baayen
O.W.M. Meijer
B.J .Slotman
W.P. Vandertop

Adapted from: Buis DR, Dirven CM, Lagerwaard FJ, Mandl ES, Lycklama A Nijeholt GJ, Eshghi DS, van den Berg R, Baayen JC, Meijer OW, Slotman BJ, Vandertop WP. Radiosurgery of brain arteriovenous malformations in children. J Neurol. 2008: 255: 251 – 60.

Abstract

Purpose
The authors describe their experience in treating 22 children with a single brain arteriovenous malformation (bAVM) using a dedicated LINAC stereotactic radiosurgery unit.

Methods
The findings of 22 consecutive patients ≤ 18 years of age who underwent radiosurgery for a single bAVM and with at least 24 months of follow-up, or earlier proven obliteration, were reviewed. The median age at radiosurgery was 13.8 years, with a hemorrhagic presentation in 86%.Median bAVM-volume was 1.8 ml, with a median prescribed marginal dose of 19.0 Gy.

Results
The crude complete obliteration-rate was 68% (n=15) after a median follow-up of 24 months. The actuarial obliteration-rate was 45 % after two years and 64 % after three years. Patients with a radiosurgery-based AVM score ≤ 1 more frequently had an excellent outcome than patients with a bAVM score > 1 (71% vs. 20%, P=0.12), as well as an increased obliteration rate (P=0.03) One patient died from a bAVM-related hemorrhage 27 months after radiosurgery, representing a postradiosurgery hemorrhage rate of 1.3%/year for the complete follow-up interval. Overall outcome was good to excellent in 68% (n=15). Radiation-induced changes on MR-imaging were seen in 36% (n=8) after a median interval of 12.5 months, resulting in deterioration of pre-existing neurological symptoms in one patient.

Conclusion
Radiosurgery is a relatively effective, minimally invasive treatment for small bAVMs in children. The rebleeding rate is low, provided that known predilection places for bleeding had been endovascularly eliminated. Our overall results compare unfavourably to recent pediatric microsurgical series, although comparison between series remains imprecise. Nevertheless, when treatment is indicated in a child with a bAVM that is amenable to both microsurgery or radiosurgery, microsurgery should carefully be advocated over radiosurgery, because of its immediate risk reduction.

Key words
cerebrovascular disorders • intracranial arteriovenous malformations • pediatrics • radiosurgery • stereotaxic techniques

Introduction

Brain arteriovenous malformations (bAVM) in children are reported to have a less favourable prognosis than bAVMs in adults, with a mortality rate after hemorrhage above 20 %[236]. Children (< 20 years) with a bAVM were found to present significantly more often with a hemorrhage (56 %) in comparison to adults (43 %), but they were not found to be at an increased risk for a subsequent hemorrhage[133]. In general, bAVMs should be treated when the cumulative risk of treatment is estimated to be smaller than the cumulative risk of conservative treatment, especially as rebleeding has been associated with a 25% mortality rate[403]. Because the cumulative mortality and morbidity is obviously larger in children than in adults as they are at risk for a prolonged period of time, the necessity for treatment is often more compelling.

In contrast to adult bAVMs, pediatric bAVMs are more often located in deep or eloquent locations[328], making surgical resection less attractive as a treatment option[423]. For these bAVMs stereotactic radiosurgery is the first choice of treatment.

In children, radiosurgery alone or in combination with other modalities has been reported to result in a complete angiographic obliteration varying between 54% three years after radiosurgery and 65 % five years after radiosurgery[488]. Complications after radiosurgery include hemorrhage in the interval until obliteration and radiation-induced morbidity. The actuarial rate of hemorrhage after radiosurgery, before obliteration has been obtained varies between 2.7 and 4.3%/patient/year[323, 417]. In children no adverse effects of radiosurgery on cognitive and neuropsychological functions have been found after long-term follow-up[386]. These findings suggest that radiosurgery is an equally successful, but less invasive alternative to surgery of a small pediatric bAVM. Therefore in our institute it has been the policy to treat small bAVMs with radiosurgery, regardless of its intracranial location. We present our experience in the radiosurgery of bAVMs in 22 children using a dedicated linear accelerator (LINAC) radiosurgery unit.

Materials and methods

Patients

Between June 1992 and September 2005, 244 patients with one or more angiographically visible bAVMs were radiosurgically treated at the VU University Medical Center, Amsterdam. Among these were 25 children (≤18 years-old at time of radiosurgery). In our institute bAVMs <3.5 cm are treated by radiosurgery. Larger bAVMs undergo endovascular embolization, and if this results in a residual nidus smaller than 3.5 cm, radiosurgery follows. Intranidal aneurysms or bAVMs that demonstrate angiographic characteristics suggestive of an increased (re-)bleeding rate are always treated endovascularly first. Excluded from analysis were patients with a follow-up shorter than two years (n=3), except when angiographically confirmed complete obliteration or (re-)bleeding occurred earlier. This resulted in a study cohort of 22 patients. There were 15 males (68 %) and 7 females (32 %).Median age at radiosurgery was 13.8 years (mean 13.0,95% CI: 11.6–14.5).

Presenting symptoms and previous treatment

Presenting symptoms were hemorrhage in 19 patients (86.4 %) (intracerebral hematoma: n=10, intraventricular hematoma: n=6,combined intracerebral and intraventricular hematoma: n=3) and epilepsy in three patients (13.6%). The median interval between presentation and radiosurgery was 13.3 months (mean 25.6, 95% CI: 12.0–39.2).Previous unsuccessful or partial treatment was performed in 14 patients (64%) and consisted of endovascular embolization (n=11) or microsurgery (n=3).

BAVM characteristics

All patients had a single bAVM (Table 5.1). Thirteen were left- and nine were right-sided. Median bAVM-volume was 1.8 ml (mean: 2.9, 95% CI: 1.5–4.2). Grading according to Spetzler-Martin[423] was I (n=6), II (n=9), III (n=5) and IV (n=2).Median bAVM-score[368] (Table 5.2) was 0.76 (mean: 0.82, 95% CI: 0.63–1). The bAVM-score was greater than 1 in five patients.

Imaging, target delineation and treatment

Patients underwent MR imaging of the brain using a 1.5T whole-body scanner, with a standard polarized head coil (Magnetom Vision, Magnetom Sonata; Siemens, Erlangen, Germany). T_2-weighted MR images with a slice thickness of 3mm,as well as Time-of-Flight MRA images with a slice thickness of 2mm were made. In all but five patients, treated before August 1997,MR imaging was performed one day prior to radiosurgery. In the remaining 17 patients the nidus was visible on T_2-sequences only (n=3), or on both T_2- and MRA sequences (n=14).

Table 5.1 Intracranial location of 22 pediatric brain AVMs

	Location	n (%)
Supratentorial (n=14)	Frontal	5 (22.7)
	Temporal	1 (4.5)
	Parietal	7 (31.8)
	Occipital	1 (4.5)
Deep (n=5)	Basal Ganglia	1 (4.5)
	Thalamus	3 (13.6)
	Corpus Callosum	1 (4.5)
Infratentorial (n=2)	Cerebellum	2 (9.1)
Ventricular (n=1)	Left lateral ventricle	1 (4.5)

Table 5.2 bAVM score and Spetzler-Martin bAVM grading system

bAVM score according to Pollock[368]
bAVM score = (0.1)(bAVM volume) + (0.02)(patient age) + (0.3)(bAVM location†)

† bAVM location:	Points
Frontal or temporal	0
Parietal, occipital, intraventricular, corpus callosum or cerebellar	1
Basal ganglia, thalamic, or brainstem	2

Spetzler-Martin bAVM grading system[423]

Size	Points
Small (< 3 cm)	1
Medium (3-6 cm)	2
Large (> 6 cm)	3
Eloquence of adjacent brain‡	
non-eloquent	0
eloquent	1
Pattern of venous drainage!!	
Superficial only	0
Deep	1

‡ Eloquent brain: sensorimotor; language and visual cortex; hypothalamus and thalamus, internal capsule; brainstem; cerebellar peduncles; deep cerebellar nuclei

!! Venous drainage is considered superficial if all drainage is through the cortical venous system; it is considered deep if any or all is through internal cerebral veins, basal veins, or precentral cerebellar vein

On the day of radiosurgery a stereotactic base ring (BrainLAB AG, Feldkirchen, Germany) was attached to the patient's head under local anesthesia (n=10) or under general endotracheal anesthesia (n=12), depending on the child's age and clinical condition. Stereotactic digital subtraction angiography (DSA) and 2mm sliced planning CT angiography scans (CTA) were made with the stereotactic frame in place. The bAVM was visible on DSA in all cases. The DSA images were co-registered with the CT images using the stereotactic localizer box. Finally, the MRA study was digitally fused with the CT study using the automatic image fusion software of the radiosurgery planning system (BrainScan v. 5.1, BrainLAB AG,). For the purpose of target delineation the angiographic nidus was defined as the network of abnormal vessels between arterial feeder(s) and the pathologically early draining vein(s).

Radiosurgery was performed using a 6-MV linear accelerator (Clinac 600C, Varian Medical Systems Inc., Palo Alto, CA, USA) that was especially adapted for radiosurgery (n=17). After installation of the Novalis shaped beam device (BrainLAB AG) in August 2002 only dynamic conformal arcs, producing a more conformal distribution of irradiation, were used (n=5). All patients were treated with five noncoplanar arcs of 140° each, and identical beam weighting for all arcs. Treatment was planned using a circular collimator and a single (n=18) isocenter resulting in a typical spheroid dose distribution. Multiple isocenters were used in four cases. After August 2002 dynamic multileaf collimators were used. The dose was normalized to 100 % and prescribed to the 80 %-isodose line encompassing the bAVM. The clinically used prescription dose was dependent on the volume of the bAVM (normal tissue within 80 % isodose) with an 80% prescription dose of 21, 18, and 15 Gy for a volume of <7, 7–14, and ≥ 14ml, respectively. The median prescribed dose, administered to the 80 %-isodoseline was 19.0 Gy (mean: 18.8, 95% CI: 17.7–19.9 Gy).

Follow-up

Follow-up consisted of an annual neurological examination and MR-imaging of the brain. A DSA was performed after complete obliteration was diagnosed on MR imaging or after an interval of three years after radiosurgery. The angiographic obliteration of the bAVM was defined as the complete absence of abnormal vessels in the former nidus of the malformation, with disappearance or normalization of draining veins from the area, and a normal circulation time on angiography.

Study parameters

Pre-treatment MR images were independently reviewed by two neuroradiologists (GJLàN and OE) for visibility of the nidus. Follow-up MR-images were reviewed for the presence of complete obliteration, a new hemorrhage or radiological complications, which were graded as 1) no radiological abnormalities, 2) T_2-hyperintensity, 3) T_2-hyperintensity with cyst formation, or 4) necrosis. The diagnosis of complete obliteration on DSA images was retrospectively reviewed. The clinical outcome and the bAVM-score were calculated[368]. The patients' clinical condition at time of radiosurgery and at follow-up was retrospectively reviewed and classified according to the Modified Rankin Scale (MRS). Time to obliteration was analysed using Kaplan-Meier curves. Statistical significance was determined using Student's T-test, χ^2-test, or log rank-test when this was appropriate. A two-tailed P-value < 0.05 was chosen as the threshold for statistical significance. All statistics were performed using Statistical Package for Social Sciences v. 12.0.1 (SPSS Inc., Chicago, IL, USA).

Results

Obliteration rate and clinical outcome

The median clinical follow-up was 29 months (mean: 41.0, 95 % CI: 28.9–53.1). The crude complete obliteration rate was 68% (n=15) after a median follow-up of 24 months (mean: 22.9, 95% CI: 14.5–31.4). Obliteration was diagnosed on MRA (n=3), DSA (n=3) or both (n=9) (Figure 5.1). The actuarial obliteration rate was 45% after two years, and 64 % after three years (Figures 5.1 and 5.2). Median interval to obliteration was 25 months (mean 37.5, 95 % CI: 22.8–26.8). None of the grade IV bAVMs obliterated, although one was treated with a high marginal dose of 21 Gy. Two grade III bAVMs did not obliterate, although one of these was treated with a marginal dose of 21 Gy. Among the Spetzler-Martin grade I and II bAVMs complete obliteration was reached in 80%, vs. 43% among the grade III and IV bAVMs. Log-rank tests demonstrated no significant differences for obliteration between different age-groups, Spetzler-Martin gradation, volume or marginal dose (Table 5.3). The overall outcome was scored as 'excellent' or 'good' in 15 patients (68%) (Table 5.4). Patients with a radiosurgery based AVM score ≤ 1 had an excellent outcome more frequently than patients with a bAVM-score > 1 (71% vs. 20%, P=0.12), as well as an increased obliteration rate (P=0.03) (Table 5.3). The MRS deteriorated in one patient (Table 5.5).

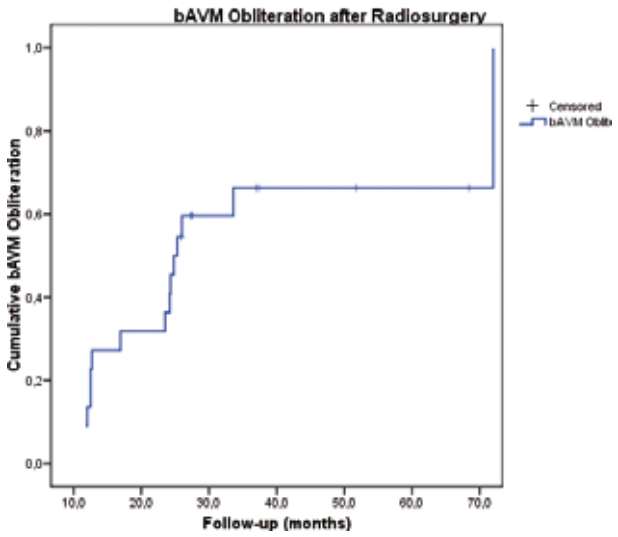

Figure 5.1
Kaplan-Meier plot demonstrating bAVM-obliteration in months after radiosurgery.

A B

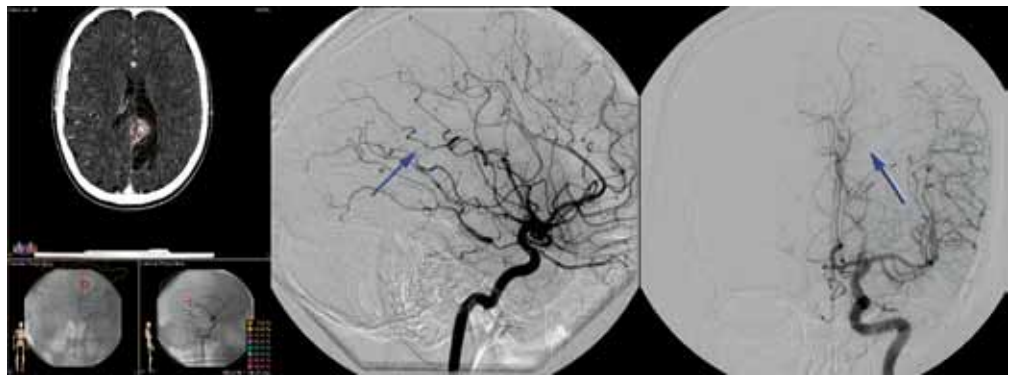

Figure 5.2
Target delineation in a 16 year old girl with a left callosal, Spetzler-Martin grade II bAVM (A). The volume is 1.58 ml, with a bAVM score of 0.78. Dynamic Multileaf collimators and a single isocenter were used to administer 2100 cGy to the 80%-isodose-line. After 12.5 months no more abnormal vessels are visible and there is normalization of circulation time (B). Note that the stereotactic planning software rotates the images horizontally. The markers on the stereotactic localizer box are represented as blue circles.

A B

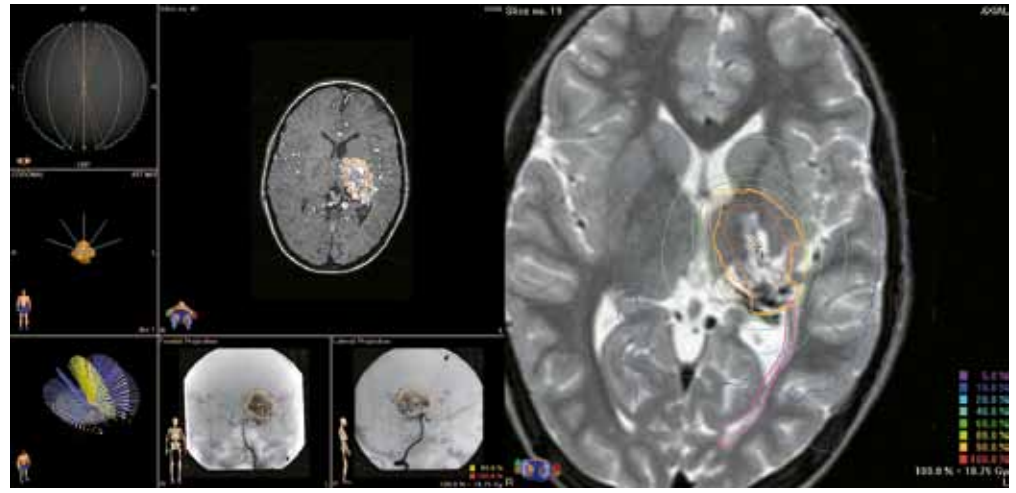

Figure 5.3
Target delineation in a 10 year old girl, with a left thalamic, Spetzler-Martin grade IV bAVM. The volume is 14.05 ml, with a bAVM-score of 2.22. A single collimator and dynamic circular arcs were used to administer 1500 cGy on the 80%-isodose-line (A). After 5 months she noted a deterioration in the function of her right hand. On follow-up MR-imaging, made 12 months after radiosurgery T_2-hyperintensity is visible in the internal capsule (B, contoured in pink). The original treatment plan has been projected over the follow-up MR-images.

Table 5.3 Log rank tests (n=22)

	Number of patients		P-value
Threshold-factor	≤	>	
3 ml	15 (11)	7 (4)	0.45
21 Gy Dose	12 (8)	10 (7)	0.63
SM I & II vs. III & IV	15 (12)	7 (3)	0.16
bAVM-score ffi 1 vs. >1	17 (14)	5 (1)	0.03
16 year of age	16 (10)	6 (5)	0.22
Previous treatment	9 (7)	13 (8)	0.53

The number in parentheses referes to the actual number of obliterations in each group

Table 5.4 Outcome according to Pollock et al.[368] (n=22)

	n (%)
Excellent (complete obliteration and no new deficit)	13 (59%)
Good (complete obliteration, but a minor deficit)	2 (9%)
Fair (complete obliteration, but a major deficit)	0 (0%)
Unchanged (residual AVM and no deficit)	5 (23%)
Poor (persistent AVM and any new deficit)	1 (4.5%)
Dead	1 (4.5%)

Table 5.5 Clinical outcome (n=22)

Modified Rankin Score	Pre-radiosurgery n (%)	Follow-up n (%)
0 No symptoms	13 (59.1)	13 (59.1)
1 No significant disability	4 (18.2)	4 (18.2)
2 Slight disability	4 (18.2)	3 (13.6)
3 Moderate disability		
4 Moderately severe disability	1 (4.5)	1 (4.5)
5 Severe disability		
6 Dead		1 (4.5)

Treatment failure

In seven patients (32%) the bAVM failed to obliterate after a median follow-up of 37 months (mean: 39.3, 95% CI: 24.8–53.8). Partial obliteration was reached in four. Two patients withdrew from further follow-up, and two more patients are scheduled for further imaging next year. In two patients the bAVM did not show any changes. One of these was scheduled for repeated radiosurgery and the other patient underwent surgery. One patient suffered a fatal hemorrhage from a left parietal bAVM 27 months after radiosurgery, representing a post-radiosurgery hemorrhage rate of 1.3%/year for the complete follow-up (one patient with a bleeding for a follow-up of 75 patient-years).His bAVM volume at the time of radiosurgery was 4.2 ml, with a Spetzler-Martin grade II and no earlier hemorrhage. Previous MR-images had demonstrated near total obliteration less than one month before this hemorrhage occurred.

Toxicity

Radiation-induced changes on follow-up MR imaging were seen in eight patients (36 %) after a median interval of 13 months (mean: 13.8, 95% CI: 10.4–17.3), and consisted of T_2-hyperintensity in seven patients (32 %), and cyst formation in one (4.5 %). These changes resulted in a delayed persisting neurological deficit in one patient (4.5%) with a left thalamic, Spetzler-Martin Grade IV, bAVM-score 2.22, bAVM, which had bled previously and was partially embolized. She presented with a partial right-sided weakness. Her bAVM had a volume of 14.1 ml and was treated with 1500 cGy on the 80-%-isodose-line (Fig. 3). Starting at 5 months after radiosurgery there was deterioration of the function of her right hand. Follow-up MR images demonstrated perinidal gliosis, T_2-hyperintensity and partial obliteration at an interval of 25 months after radiosurgery.

Tables.6 Stereotactic radiosurgery for bAVMs in pediatric patients ∫

First Author	Year of Publication	n	GK/LINAC †	Mean/ Median age at SRS (Range) (year)	Mean/Median Marginal Dose* (Range) (Gy) ‡	FU Available § n (%)	Mean/ Median FU (Range) (months)	Obliteration n (%)	ICH n	Complications or Treatment Failure Transient n	Permanent n	Death n
Buis	present study	22	LINAC	14.6/14.1 (6.1 - 20.9)	19/ 18 (15 - 21)	22 (100)	41.0/ 29.1 (17.5 - 135)	15 (68)	1	0	1	1
Reyns[384]	2007	100	LINAC	NR/ 12 (2 -16)	23/ NR (15 - 25)	100 (100)	NR/ 26 (11-126)	72 (70)*	2	1	8	1
Nicolato[328]	2006	62	GK	NR/ 14 (5 -20) ∞	NR/ 22.6 (14 - 26.4)	63 (100)	NR/ 29 (6.2 -77.2)	53 (85.5)	1 ≈	1 ≈	1 ≈	NR
Zabel-du Bois[488]	2006	22	LINAC	NR/ 11.8 (4.4 - 16.4)	NR/ 18 (15 - 20)	22 (100)	NR/ 37.2 (20.4 - 87.6)	14 (64)	5	0	0	0
Cohen-Gadol[80]	2006	38	GK	NR/15 (7 -18)	NR/20 (16 - 25)	38 (100)	NR/42 (12 - 131)	23 (66)**	1	1	0	0
Fuss[135]	2005	7	IMRS	13.1/13 (7 - 18)	18.2/ 18 (17.5 - 20)	6 (86)	26.9/ 32 (5 - 49)	2 (33)	0	0	0	0
Nicolato[326]	2005	63	GK	11.7/NR (5 - 16)	21.6/NR (16 - 26)	47 (74)	NR/ 32.8 (1.2 - 77.2)	31 (79)***	0	1	1	0
Maity[287]	2004	17	LINAC	11.6/ 12 (5 - 18)	17.6/ 18 (16 - 18)	17 (100)	28.0/ 29.6 (9.4 - 63.1)	9 (53)	0	1	3	0
Nataf[323]	2003	57	LINAC	11/12 (7 - 15)	23.8/ 25 (18 - 28)	49 (86)	40/34 (7 - 172)	30 (61)	4	0	0	1
Shin[410]	2002	100	GK	NR/15 (4 - 19)	NR/20 (17 - 28)	82 (82)	NR/71 (6 - 124)	71 (87)	5	2	3	1
Smyth[417]	2002	31	GK	11.3/ 11.2 (3.4 - 17.5)	NR/11.2 ((3.4 - 17.5)	31 (100)	61.9/ 60 (6 - 99)	11 (35)	5	0	2	0
Amendola[12]	2000	31	GK	13.3/ 12.5 (7 - 19)	23/ 23 (20 - 25)	31 (100)	NR	22 (71)	0	0	0	0
Hoh[191]	2000	15	BP	11.1/13 (1 - 18)	15.9/16 (8 - 26)	9 (60)	NR	7 (47)	2	0	1	1
Levy[273]	2000	53	GK	NR/12 (2 -17)	NR/ 20 (15 - 25)	53 (100)	NR/36 (6 - 103)	39 (74)	4	0	4	2
Nicolato[327]	1997	7	GK	12.3/NR (5 - 16)	24.7/NR (23.6 - 25.8)	6 (85%)	NR/ 18.8 (4 - 29)	2 (33)	0	1	0	0
Gertszen[148]	1996	15	GK	NR/ 16 (2 - 17)	20/ NR (15 - 25)	15 (100)	NR	6 (40)	0	0	0	0
Tanaka[447]	1996	23	GK	11.5 / NR (2 - 15)	20.5/ NR (NR)	21 (91)	>24	20 (95)	0	0	0	0
Yamamoto[480]	1992	9	GK	12/13 (9 -16)	23/NR (15 - 30)	9 (100)	66/54 (37 - 137)	6 (67)	0	0	0	0
Loeffler[284]	1990	8	LINAC	13.9/ 14.5 (6 - 20)	17.8/ 17.5 (16.5 - 20.0)	8 (100)	22.9/ 19 (8 - 37)	5 (63)	0	0	0	0
Altschuler[11]	1989	18	GK	12.3/NR (2.8 - 18)	NR/NR (17.5 - 25)	15 (83)	9.5/12 (4-14)	3 (20)	0	1	0	0

∫ All studies were of retrospective design
† BP Bragg Peak Proton Beam; GK Gamma-Knife, IMRS Intensity-Modulated Radiosurgery; LINAC Linear Accelerator
‡ Gy Gray
∞ Out of 92 patients
≈ Out of 75 patients (1.3%)
§ FU Follow-up, n refers to the number of patients, NR Not reported
* 103 bAVMs were treated in 119 radiosurgical procedures; 72 obliterated
** Out of 35 patients after single session radiosurgery
*** Out of 39 patients with a FU > 36 months

Discussion

LINAC radiosurgery has demonstrated good results in the treatment of bAVMs in adults with documented obliteration rates varying between 50 and 65 %[490]. In children the obliteration rate varies between 27 % three years after radiosurgery and 95 % five years after radiosurgery (Table 5.6)[11, 12, 80, 135, 148, 191, 273, 284, 287, 323, 326, 327, 329, 384, 410, 417, 447, 480, 488]. In this study of 22 patients ≤ 18 years old we found 68% complete obliteration after a median follow-up of 24 months with a good or excellent outcome in 68% (Table 5.3). Only the radiosurgery-based AVM-score was found to be significantly related with obliteration. Clinical complications occurred in two children (9%): one died due to a bleeding before complete obliteration occurred and one demonstrated deterioration of pre-existing neurological symptoms due to radiation toxicity. Asymptomatic radiological changes were observed in seven patients (32 %).

Obliteration rate

Overall the risk of hemorrhage from a bAVM has been found to decrease by 54% during the latency period after radiosurgery[291]. The annual bleeding risk after obliteration has been reported to be 0.3 % and 2.2 % for a cumulative risk over 10 years[409]. Partial, or even complete obliteration therefore does not protect completely from a future (re-)bleeding. Nevertheless, the goal of treatment should be complete angiographic obliteration, without inducing new neurological deficits. An increased obliteration-rate after radiosurgery has been associated with a smaller treatment volume and subsequently a higher marginal dose[273]. Although in children the time-to-obliteration was found to be significantly shorter[329], and younger age has been reported to be a predictive factor for obliteration[384, 410], only seven studies report an obliteration-rate larger than 70% (Table 5.6)[12, 273, 326, 328, 384, 410, 447]. The more complete follow-up varying between 60 and 100 % in pediatric series in comparison to those in adults, is a likely explanation (Table 5.6). If data analysis is limited to patients who undergo follow-up DSA the obliteration-rate has been shown to be overestimated, with an actual 2-year obliteration rate in the range of 40% rather than the usually reported 80%, if all data are considered[180]. As the reason for incomplete follow-up of bAVM patients is often linked to important prognostic outcome, incomplete follow-up may jeopardize study results. In our study no patients were lost to follow-up and we did exclude patients with a follow-up ≤ 24 months, unless complete angiographic obliteration or (re)-bleeding occurred earlier. Therefore our results are representative for the whole population we have treated and accurately reflect our overall treatment results.

The importance of adequate assessment of obliteration, preferably using DSA, has been stressed[323, 384]. The sensitivity and specificity of 3D dynamic MRA for remaining nidus was found to be 81 and 100%, respectively. Therefore, the authors concluded that DSA investigation remains necessary to rule out small bAVM remnants[145]. In three of our patients obliteration was diagnosed on MRA only, as they refused further angiographic follow-up. We included these patients nevertheless, as all images were independently reviewed by an experienced neuroradiologist. Moreover, although MRA is not the gold standard, exclusion of patients with an adequate follow-up and negative MRA images, could lead to underestimation of the obliteration rate. In order to adequately assess obliteration, without exposing the patient to the risk of serial angiographies, an optimal follow-up should consist of MRA imaging followed shortly by a DSA investigation, when complete obliteration has been diagnosed on MRA.

In children recurrence of a bAVM after microsurgery or radiosurgery has been documented in up to 5.6 %[49]. Recanalization of thrombosed vessels after radiosurgery[280], or 'regrowth' and subsequent recanalization of immature, angiographically undetectable vessels, located in the periphery of the bAVM[389] are thought to be the mainstay in this process. Therefore follow-up angiography at 3 and 10 years[49] or after reaching adulthood has been advised[80]. Rapid investigation of neurological changes is also imperative[49]. Although we recommend MR angiography at 5 years after complete obliteration, we have not encountered recurrence of a bAVM yet.

Complications: radiation-induced neurological deficits and rebleeding

A recent study consisting of 100 pediatric patients with ≥ 36 months follow-up demonstrated a 5% permanent neurological deficit rate[384]. We found deterioration of pre-existing neurological symptoms due to radiation toxicity in a single patient (4.5 %). However, radiation induced changes were seen on follow-up MR images in 32%. This is comparable to other reported rates of symptomatic and asymptomatic parenchymal changes on follow-up MR images after radiosurgery[323, 410, 460, 490], suggesting that only in a small percentage these radiological changes result in neurological signs or symptoms, although long term data are to be awaited. It has been suggested that delayed cyst formation is associated with a higher maximal treatment dose, a larger bAVM volume, complete nidus obliteration, and a lobar location of the bAVM[204].While our series is too small to investigate long-term radiation-induced toxicity, it is interesting to note that in the case in which neurological damage due to radiation toxicity was seen, the bAVM volume was relatively large, with a deep, non-cortical location, and therefore a bAVM-score larger than 2. These findings support those of Ganz *et al.*, who described that a larger bAVM-volume was significantly related to adverse radiation effects[140]. Furthermore, Friedman *et al.* reported that the 12 Gy-volume was predictive of persistent neurological complications, while both 12 Gy-volume and an eloquent bAVM location were predictive of transient neurological deterioration[131]. Therefore, a careful analysis of large bAVMs in an eloquent location that are not suitable for

endovascular or surgical treatment, should be performed before radiosurgery is undertaken, especially in bAVMs that have not bled before.

Patients with a radiosurgery-based AVM score ≤ 1 more frequently had an excellent outcome, as well as an increased obliteration rate (P=0.03), therefore our data support the use of Pollock's bAVM-score in children[368]. In children the risk of hemorrhage in the interval period until complete obliteration was found to be smaller than in adults, although the difference was not significant[329]. However, one of our patients died after nearly complete obliteration was diagnosed on MRA-images, representing a relatively low annual (re-)bleeding rate of 1.3%. In a comparable study of 22 children treated with LINAC radiosurgery bleeding occurred in five patients[488]. In this series radiosurgery was preceded by embolization in 31%, compared to 50 % in our series. Although prior endovascular treatment complicates nidus identification, due to embolic agents overlapping the nidus, it also leads to a flow reduction which has been associated with a decreased time to obliteration[361], as well as a decreased hemorrhage risk one to two years after treatment[300]. Therefore, it has been the practice in our institute to eliminate known predilection places for bleeding, such as intranidal aneurysms or fistulae by endovascular embolization. For the radiosurgical planning of bAVMs in embolized patients we use plain CT images in addition to CT angiography. In such images the embolization material appears hyperdense. We contour the embolization material in the stereotactic CT images and project these onto the stereotactic angiographic images in order to restrict the radiation field to the persistent nidus.

Whether the incidence of intracranial tumors after radiosurgery in childhood increases remains unanswered. So far four cases of radiosurgery-associated brain tumors have been published, including one case of glioblastoma multiforme, presenting 6.5 years after radiosurgery of a right parietal bAVM at the age of 14[297]. However, the overall age-adjusted incidence of brain tumors is 6.1 cases per 100,000 person-years[96]. Given that in between 1991 and December 2005, 44,185 bAVMs have been treated using a gamma-knife alone (http://www.elekta.com/assets/gammaknife/treat_stats/ww05.pdf), this seems to be a very rare, although serious, complication. Parents and patients should be informed that although radiation therapy to the brain induces a long lasting biological tissue reaction, and in general radiation therapy has been known to induce tumors, there is no current compelling evidence to suggest that radiosurgery induces brain tumors.

Implications for treatment

In adults no evidence from randomised trials with clear clinical outcomes, comparing different interventional treatments for bAVMs against each other or against usual medical therapy, to guide the interventional treatment of bAVMs was found[8]. The decision regarding optimal treatment in children is no less difficult. We chose radiosurgery as the primary treatment of bAVMs, after known predilection places for bleeding were endovascularly eliminated and found representative obliteration rates, with clinical complications in 9%.

Different treatment modalities have their own advantages and disadvantages: endovascular treatment has been associated with a periprocedural morbidity and mortality rate of 11.8 %[228], but seldom leads to complete obliteration, and is often followed by either microsurgery or radiosurgery. For non-eloquent bAVMs in children microsurgery is advantageous because of its immediate risk reduction, with a good or excellent clinical outcome in around 80%, and a post-operative mortality of approximately 3.7 %[49]. In our series the best obliteration rate was found to approach 82% among the Spetzler-Martin grade I and II bAVMs, which might have been treated microsurgically. Based on our findings, especially, when considering that even in this sub cohort the median interval to obliteration took 21 months, and that one bAVM bled within this interval, resulting in the death of a patient, we now carefully advocate elective microsurgery more often.

Our findings should be interpreted cautiously as they are based on a retrospective, non-randomized study, in which a selection bias may have been introduced. Although in our institute all bAVMs are treated radiosurgically, the present series include five patients with a deep bAVM which would not have been suitable for microsurgery. Furthermore a direct comparison between data is difficult, as most studies present results from tertiary referral centers in which patients have undergone different treatment modalities subsequently. Nevertheless our findings may have two consequences. First, when a treatment decision is taken, parents should be informed that in children the obliteration rate probably compares unfavourably to the obliteration rate found in adults, and the overall outcome after radiosurgery compares unfavourably to those in recent pediatric microsurgical series. Therefore in a child with a bAVM that is amenable to both microsurgery or radiosurgery, microsurgical resection may carefully be advocated over radiosurgery, because of its immediate risk reduction. Second, although radiosurgery is a relatively low-invasive treatment, there is a small, but long-term risk of neurological deterioration due to radiation toxicity, especially when the bAVM is in a highly eloquent or deep location. This risk is, however, much lower than the risk of a neurological devastating hemorrhage in the long term, when no treatment is given at all. Therefore, in order to reduce the chance of (re-) bleeding, when a bAVM is in a deep or eloquent location, radiosurgery is the first choice of treatment.

Chapter 6

White Matter Changes after Radiosurgery for Brain Arteriovenous Malformations

R. van den Berg
D.R. Buis
F.J. Lagerwaard
G.J. Lycklama à Nijeholt
W.P. Vandertop

Adapted from: Berg van den R, Buis DR, Lagerwaard FJ, Lycklama à Nijeholt GJ, Vandertop WP. Extensive white matter changes after stereotactic radiosurgery for brain arteriovenous malformations: a prognostic sign for obliteration? Neurosurgery. 2008 Dec;63(6):1064-9.

Abstract

Purpose

Perinidal high-signal-intensity changes on T_2-weighted magnetic resonance imaging can be seen surrounding radiosurgically treated brain arteriovenous malformations (bAVM). Occasionally, these signal intensity changes develop far beyond the irradiated volume. A retrospective analysis of both the pre- and postradiosurgery magnetic resonance imaging and angiographic studies was performed to analyze the cause of these extensive perinidal white matter changes.

Methods

The pre- and postradiosurgical magnetic resonance imaging and angiographic studies of 30 patients with T_2-high-signal-intensity changes surrounding a bAVM were analyzed retrospectively. Patients were divided into 2 groups on the basis of the extension of the signal intensity changes within or beyond the 10-Gy isodose area. The angiographic analysis was focused on the venous drainage pattern (deep versus superficial), venous stenosis, and the number of draining veins before and after radiosurgery. In addition, the obliteration rate was determined for the 2 subgroups.

Results

Fourteen patients (47%) showed high-signal-intensity changes far beyond the 10-Gy isodose area. A single draining vein was more often present in these patients with extensive T_2-hyperintensity signal changes than in the other group. Obliteration was achieved in 12 (88%) of 14 patients with extensive signal intensity changes, as opposed to 8 (50%) of 16 patients in the other group.

Conclusion

High-signal-intensity changes after radiosurgery for bAVMs, far beyond the 10-Gy isodose area on T_2-weighted images, are especially seen in bAVMs draining through a single vein. The higher occlusion rate of bAVMs under these circumstances is well appreciated.

Key words

Angiography • Brain arteriovenous malformations • Complications • Magnetic resonance imaging • Radiosurgery • Stereotactic techniques

Introduction

Stereotactic radiosurgery is an established modality for the treatment of brain arteriovenous malformations (bAVM), with reported obliteration rates at 3 years varying from 65 to 80%[121, 132, 335, 372, 375]. Complications of radiosurgery may be related to the adverse effects of the radiation itself, usually resulting in circumscribed perinidal gliosis[72, 131, 364]. In some cases, however, more extensive magnetic resonance signal intensity changes occur in the white matter far beyond the target area, and these may be associated with new neurological symptoms. In a report of two such cases, obstruction of the venous outflow of the bAVM was held responsible for these magnetic resonance signal intensity changes[69, 366], and the term 'occlusive hyperemia' was proposed, in analogy with changes seen after surgical resection of bAVMs, in which hyperemia caused by acute thrombosis of the draining vein was found to be responsible for the clinical deterioration and the magnetic resonance signal intensity changes. However, in these two publications, the authors were unable to demonstrate these venous occlusive changes in other patients with neurological deficits and T_2-hyperintensity changes. We performed a retrospective study of both the pre- and postradiosurgery magnetic resonance imaging (MRI) and angiographic studies in our own patient cohort to analyze these perinidal white matter changes.

Methods

Between May 1998 and January 2006, 203 patients with bAVMs were treated with linear accelerator-based radiosurgery at the VU University Medical Center, Amsterdam, The Netherlands. They underwent MRI of the brain using a 1.5-T whole-body scanner, with a standard polarized head coil (Magnetom Vision, Magnetom Sonata; Siemens, Erlangen, Germany). T_2-weighted MRI scans with a slice thickness of 3 mm and time-of-flight magnetic resonance angiographic images with a slice thickness of 2 mm were obtained one day before radiosurgery. Digital subtraction angiography (DSA) of the brain was performed with the stereotactic localizer frame in place. Radiosurgery was performed using a 6-MV linear accelerator (Clinac 600C; Varian Medical Systems, Inc., Palo Alto, CA) that was especially adapted for radiosurgery. The dose was normalized to 100% and prescribed to the 80% isodose line encompassing the bAVM. The clinically used prescription dose was dependent on the volume of the bAVM (normal tissue within 80% isodose) with an 80% prescription dose of 21, 18, and 15 Gy for a volume of less than 7, 7 to 14, and ≥ 14 cm^3, respectively. The median prescribed dose, administered to the 80% isodose line, was 19.0 Gy.

Follow-up consisted of an annual neurological examination and MRI of the brain, using the previously mentioned sequences. Patients were followed with annual MRI for three years after radiosurgery, unless complete obliteration was diagnosed earlier. DSA was performed when MRI suggested complete obliteration. Alternatively, when no complete obliteration was obtained at 4 years after radiosurgery, DSA was performed to assess the need for salvage treatment. Angiographic obliteration of the bAVM was defined as the complete absence of abnormal vessels in the former nidus of the malformation, with disappearance or normalization of early draining veins from the area and a normal circulation time on angiography[279, 440].

Included in this study were all patients who underwent radiosurgery for a single bAVM and in whom one or more follow-up MRI studies and DSA were performed. All available pre-treatment and follow-up MRI studies were reviewed by an experienced neuroradiologist (GJLàN) for the presence of hyperintensity on T_2-weighted images. If T_2-hyperintensity was diagnosed, the appropriate MRI series were digitally transferred to the BrainLAB planning system (BrainScan, Version 5.3; BrainLAB, Inc., Feldkirchen, Germany), and image registration with the original treatment plan was performed using the automated fusion software of the planning system. This allowed exact comparison of the observed T_2-hyperintensity changes in relation to the radiosurgical target area. We divided the entire irradiated volume in two by defining a low-dose area receiving less than 10 Gy and a high-dose area receiving more than 10 Gy. This division was made cautiously, based on findings in a study analyzing predictors of complications in which 12 Gy was determined to be a 'cutoff-point' beyond which radiation-induced changes were unlikely to develop[131]. In the subsequent analysis, we compared patients with high-signal-intensity changes (HSIC) within the 10-Gy isodose area (HSIC < 10-Gy area) versus those outside the 10-Gy isodose area (HSIC > 10-Gy area). Both the Spetzler-Martin and Pollock-Flickinger AVM grading systems were applied to allow comparison of bAVM characteristics for both patient groups[368, 423]. In addition, the applied radiation dose and whether or not embolization was performed before radiosurgery were determined.

Pre- and posttreatment DSA images were reviewed independently by an experienced interventional neuroradiologist (RvdB), who was blinded to the pattern of hyperintensity on follow-up MRI scans, for the following parameters: deep versus superficial venous drainage, number of draining veins, venous stenosis and posttreatment changes in the venous drainage pattern, including obliteration of the original draining veins. The patients' clinical records were reviewed during follow-up, which was performed 6 months after radiosurgery and subsequently each year to assess changes in the neurological status.

Statistical analysis

Data for both groups of patients were compared using the χ^2 test. Depending on the distribution of the data in the cross-tables, Pearson's χ^2 test, Fisher's exact test, or a linear-by-linear association was performed. In addition, Student's *t* test was used to compare bAVM volume and radiation dose for both groups. Differences between data were considered statistically significant for values of *P* less than 0.05. Analysis was performed using SPSS software (Version 14.0; SPSS, Inc., Chicago, IL).

Results

Multiple follow-up MRI studies were available for 85 patients. Hyperintensity changes on T_2-weighted images were demonstrated in 45 (53%) of these 85 patients. In 30 of these patients, both pretreatment and follow-up DSA studies were available. Of the 30 patients, white matter signal intensity changes developed after treatment in 24 patients. Based on the extension of HSICs on the MRI scans within or beyond the 10-Gy isodose line, these 24 patients were divided into two groups. The first group consisted of 14 patients with hyperintensity changes extending well beyond the 10-Gy isodose line. The second group consisted of 10 patients with a rim of HSICs in close proximity to the nidus of the bAVM (thus, well within the 10-Gy isodose area). The remaining 6 patients were characterized as having HSICs before radiosurgical treatment that were mostly attributable to previous embolization (n = 3) or hemorrhage (n = 3). These white matter changes were stable over time in two patients and showed a slight increase in 4 patients but were all located within the 10-Gy isodose area.

The 16 patients with HSICs within the 10-Gy isodose area (HSIC < 10-Gy area) were compared with the 14 patients with changes outside the 10-Gy isodose area (HSIC > 10-Gy area). Characteristics of both groups are summarized in Table 6.1. Age and sex were comparable for the two groups. bAVMs were distributed equally for both groups and were especially localized in the parietal, frontal, and temporal lobes. The average volume of T_2-high signal intensity measured 40.63 cm^3 (range, 3–139 cm^3) in the HSIC > 10-Gy-area group of patients and 3.29 cm^3 (range, 0.11–12.5 cm^3) in the HSIC < 10-Gy-area patients. Over time, T_2-hyperintensity changes were reversible (partially or completely) in 12 of 14 patients with extensive hyperintensity changes diminishing from 40.63 to 9.67 cm^3. In the other group (HSIC < 10-Gy area), the T_2-hyperintensity volume diminished from 3.29 cm^3 to 2.2 cm^3.

The mean bAVM volume was 4.0 cm^3, and the volume was not different for either group (Student's *t* test, *P* = 0.159), although it was slightly larger for patients with extensive

hyperintensity changes (mean, 5.17 cm^3; range, 0.5–16.7 cm^3) compared with the other group (mean, 3.04 cm^3; range, 0.02–14.1 cm^3). The Spetzler-Martin grade for both groups (Table 6.1) and the Pollock-Flickinger grade were also comparable for both subgroups. The latter was 1.21 for the HSIC < 10-Gy-area group (range, 0.43–2.2) and 1.51 for the HSIC >10-Gy-area group. The mean radiation dose was 1864 Gy for the HSIC > 10-Gy-area group and 1937 Gy for the HSIC < 10-Gy-area group (Student's *t* test, *P* = 0.134). Twelve (86%) of 14 patients with extensive T_2-hyperintensity changes showed complete obliteration, as opposed to 8 (50%) of 16 in the other group; however, statistical significance was not reached (Fisher's exact test, *P* = 0.058). BAVM obliteration for the total study group was 70%.

Table 6.1: Characteristics of both groups[a]

	HSIC < 10-Gy area (n = 16)	HSIC > 10-Gy area (n = 14)
Male/Female	5/11	6/8
Age (years)	37	38.3
Volume of bAVM (cm^3)	3.04	5.17
Spetzler-Martin Grade (no)		
1	4	4
2	6	8
3	5	2
4	1	0
Embolization before radiosurgery (no)	9	4
Volume of T2 HSIC (cm^3)	3.29	40.6
Time to Obliteration (months)	31	36
Obliteration-rate (%)	56%	86%[b]

[a] HSCI: High Signal Intensity Change
[b] χ^2-test: p = 0.058

Table 6.2: Pattern of venous drainage[a]

	HSIC < 10-Gy area (n = 16)	HSIC > 10-Gy area (n = 14)
Venous Drainage		
Superficial	9	9
Deep	4	4
Mixed	3	1
Venous Stenosis	3	4
No. Of Draining Veins		
1	6	11
2	6	2
3	4	1
Occlusion of Draining Vein after Radiosurgery	3	9
Resolution of T2-HSIC	3	12[b]

[a] HSCI: High Signal Intensity Change
[b] χ^2-test: p = 0.05

Data on the pattern of venous drainage are presented in Table 6.2. A single draining vein was more often present in patients with extensive T_2-hyperintensity changes than in the other group (Figure 6.1). In this selected population, no correlation was found between bAVM size and the number of draining veins. In the HSIC > 10-Gy-area group, drainage was through a single draining vein in 11 of 14 cases. In the HSIC < 10-Gy-area group, drainage was mostly through multiple veins. A relation with nidus size could not be established for either group.

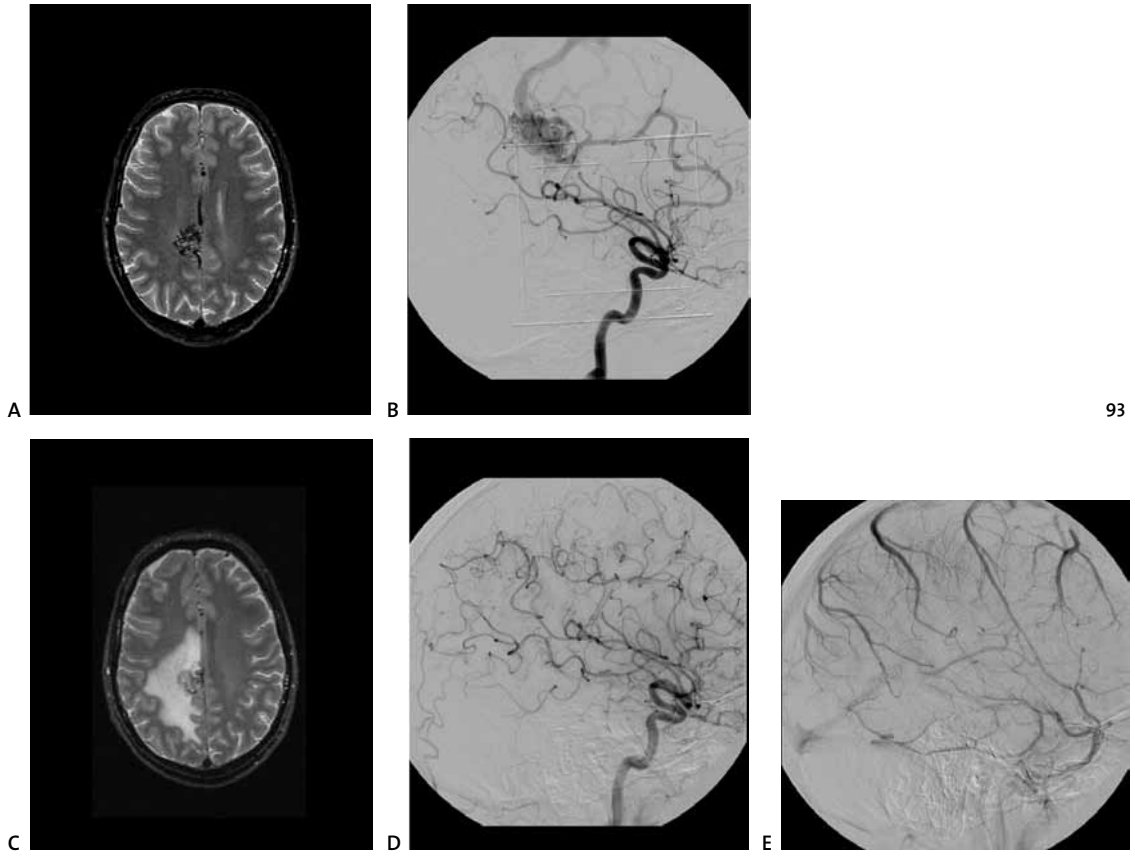

Figure 6.1
Images of a 36-year-old man initially presenting with a subarachnoid hemorrhage caused by a ruptured arteriovenous malformation (bAVM), from which he recovered completely. The bAVM was treated with radiosurgery in September 2004. **A**, magnetic resonance imaging (MRI) scan depicting the intranidal flow void of the AVM. **B**, digital subtraction angiogram showing early and late venous drainage. **C**, follow-up MRI scan obtained 1 year later showing complete obliteration and perinidal edema well outside the target area. **D** and **E**, control angiograms showing occlusion of both the bAVM and the single draining vein on the arterial **(D)** and late venous phase **(E)**.

Extensive T_2-changes diminished over time in 12 of 14 patients. Corticosteroids were administered in only four patients, with no evident radiological effect in the short term. New neurological symptoms were seen in six patients with extensive T_2-changes. One patient developed cognitive disorders in combination with balance disturbances, one patient had increased seizure activity, and 4 had both an increase of seizure activity and either sensory or motor deficits. Again, no evident clinical improvement was noticed on corticosteroid administration; however, seizure activity was controlled by changing medication.

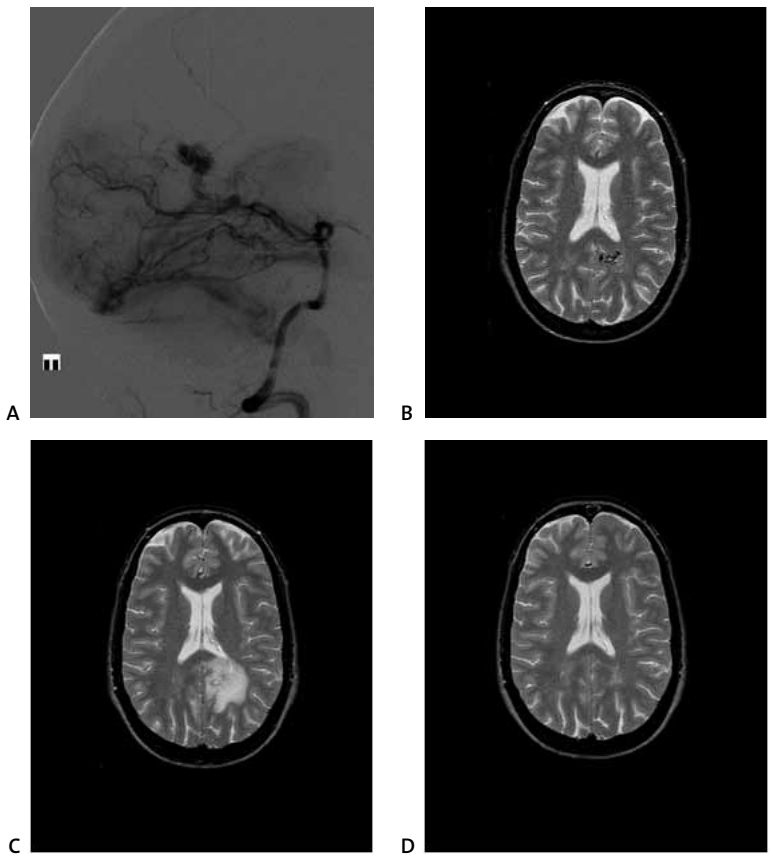

Figure 6.2
Angiogram **(A)** and MRI scan **(B)** of a 39-year-old woman treated with radiosurgery in January 1999 for a left-sided occipital bAVM. **C**, follow-up MRI scan, obtained in January 2000, showing severe perinidal edema. The patient exhibited no neurological symptoms. **D**, control MRI scan, obtained in January 2001, showing complete obliteration of the nidus and resolution of perinidal edema.

Comparing drainage through 1 versus 2 versus 3 or more veins resulted in a *P* value of 0.037 (χ^2 test, linear-by-linear association). Obliteration of the venous drainage, including the normal parenchymal drainage, was present in 9 (64%) of 14 cases in patients with extensive T_2-hyperintensity changes as compared with 3 (19%) of 16 patients in the control group (χ^2 test, *P*= 0.024). These results suggest that patients developing extensive T_2-hyperintensity are more likely to have drainage through a single vein and show a higher obliteration rate of the nidus.

In five patients, these symptoms diminished over time, with complete resolution of symptoms in two, in concordance with the T_2-hyperintensity changes (Figure 6.2). In two other patients, both symptoms and T_2-hyperintensity changes persisted. In one patient, seizure activity was increased permanently.

Discussion

Effectiveness of bAVM radiosurgery

Stereotactic radiosurgery is an effective modality for treating patients with bAVMs[129, 449]. The main determinants of successful obliteration are directly related to bAVM characteristics such as bAVM size, hemispheric localization, and number of draining veins[131, 371]. In addition, treatment-related factors such as lower Spetzler-Martin grades, higher doses, and steeper dose gradients influence treatment results[131]. The obliteration rate after radiosurgery for bAVMs has been reported to be 65 to 80%[121, 132, 335, 372, 375]. The overall obliteration rate observed in our group of 30 patients falls within this range. However, for the two subsets of patients, striking differences in occlusion rates were found, despite the fact that bAVM nidus size and radiation dose were comparable for both groups. Patients developing severe T_2-hyperintensity changes showed a higher occlusion rate (although it was not statistically significant) compared with patients who did not have these changes. These signal changes were more frequently present in patients with bAVMs draining through a single vein. In previous reports, such a better response for bAVMs draining through a single vein had already been noticed and attributed to easier delineation of the nidus in a time when MRI had not yet been used for treatment planning[371]. This, however, is not applicable to our study population, as treatment planning was performed using MRI, magnetic resonance angiography, computed tomography, and DSA in all cases.

White matter changes in relation to bAVMs

Perinidal high-signal-intensity changes on T_2-weighted MRI scans can be present in treated and untreated bAVMs, as a result of ischemia resulting from arterial steal, in relation to an

intracranial hematoma, or after embolization[262, 457]. High signal intensity of the intervening or surrounding parenchyma on T_2-weighted images might also indicate gliosis[457]. Pre-existing hyperintensity changes were frequently present in our patient population and show the importance of pre- and posttreatment magnetic resonance studies to better judge the time course of white matter changes in relation to radiosurgery.

White matter changes in the direct vicinity of the nidus can develop as the direct consequence of the radiation itself. Although radiosurgery can be considered to be a well-tolerated, minimally invasive treatment modality, complications can occur early (e.g., related to the placement of the stereotactic frame, the DSA procedure, or early radiation damage) or late, with the latter usually being radiation related[157, 270]. Radiation-induced gliosis has been reported to occur frequently after high-dose conventional fractionated radiotherapy; however, because of the steep dose gradient and the lower treatment dose, this is a very rare complication in radiosurgery[271]. In an analysis of factors useful for predicting complications in bAVM radiosurgery, the 12-Gy volume was found to be correlated with the occurrence of radiation-induced complications[131]. The wide extension of the white matter changes, far beyond the 10-Gy volume, that we chose as an even stricter safety zone, makes it highly unlikely that the cause of these abnormalities is directly related to radiation-induced changes. Therefore, a different causative mechanism seems plausible.

Venous drainage pattern of bAVMs

T_2-hyperintensity changes in relation to treatment or occlusion of bAVMs have been described previously[157]; however, the angiographic patterns and changes have never been studied in detail. Pollock held a venous occlusive cause responsible for severe radiation-induced changes in two patients[366].

Data in our study seem to indicate that the venous drainage of the bAVM through a single vein affects the development of white matter hyperintensity changes and has a positive effect on the obliteration rate (Figure 6.1). A possible mechanism leading to these changes might be that the intranidal flow reduction in the course of the slow process of obliteration will lead to diminished flow in the dilated (single) venous outlet and subsequent progressive thrombosis of the draining vein. These effects augment each other, resulting in progressive occlusion of the nidus. Thrombosis of the draining vein will impair the drainage of the surrounding white matter through the small venules. These effects will be depicted as T_2 HSICs in the brain parenchyma adjacent to the bAVM and draining vein. Venous outflow through a single (dilated) vein is probably more susceptible to these phenomena than when multiple draining veins are present[56]. In the majority of our patients, both the signal intensity changes and the neurological symptoms were reversible. Over time, collateral venous drainage probably develops and is capable of restoring the venous flow.

Impairment of intranidal flow and venous drainage plays an important role in the development of treatment-related complications of bAVMs[159]. This has been described as the 'normal pressure perfusion breakthrough'" after surgical resection[426]. Patients will develop either bleeding or progressive neurological deficits related to edema formation because of the improper autoregulation of the dilated vessels or because of a venous outflow restriction. Edematous changes after surgical resection of bAVMs have also been described by Morgan *et al.*[313]. Computed tomographic scanning demonstrated hyperdense superficial venous drainage, suggesting propagated venous thrombosis. Similar changes have been reported after embolization of bAVMs[89]. Extensive thrombosis involving the feeding artery, the nidus and, in particular, the draining vein resulted in vasogenic edema in the white matter. The development of 'congestive brain edema' in association with impaired venous drainage has even been described in patients with untreated bAVMs[248]. All of these factors point to a venous occlusive cause and not to radionecrosis per se to explain the extensive HSICs.

Incidence of T_2 HSICs after radiosurgery

In the report by Pollock[366], only two cases of what he describes as 'occlusive hyperemia' were identified in a group of 287 patients (< 1%). The assumption was made that this may have underestimated the incidence because follow-up examinations were incomplete. We were able to identify a much higher incidence because of a more meticulous follow-up protocol with annual MRI scans. Hyperintensity changes well beyond the borders of the high-dose region were present in 53% of patients with multiple follow-up magnetic resonance studies, confirming that the described pattern of obliteration is more frequent[157]. We should, however, be careful with the interpretation of our data because of the limited size of the studied sample, from which we were unable to determine a statistically significant difference. Moreover, we might have introduced a bias in favor of occlusion, as a control angiogram was necessary for inclusion. However, the group of patients with less extensive HSICs was selected under similar inclusion criteria (multiple MRI scans and pre- and postradiosurgical DSA), was irradiated with the same protocol and radiation dose for comparably sized bAVMs, showed comparable Pollock-Flickinger and Spetzler-Martin AVM grades, but failed to show the same occlusion rate as the patients with extensive signal intensity changes. Therefore, we propose that the extensive signal intensity changes are not related to the direct effect of radiosurgery, but rather is related to a secondary (most likely) venous occlusive response of the nidus and the surrounding perimedullary veins.

As opposed to the patients in the publication by Guo *et al.*[157], in which 7 of 9 patients were symptomatic, most of our patients did not present with acute neurological symptoms. Only

3 had neurological symptoms at the time of maximum T_2-hyperintensity. The other patients were either asymptomatic or had very minor symptoms. Those with symptoms showed at least partial improvement over time. When symptoms persisted, the HSICs also persisted. Both magnetic resonance changes and neurological symptoms were reversible in 12 of 14 patients, again strongly pointing in the direction of a transitory venous congestive process.

Conclusion

Although uncommon, a progressive venous occlusion leading to congestion should be proposed when HSICs on T_2-weighted images extend far beyond the high-dose region. The changes are most likely related to thrombosis of draining veins at the time of bAVM obliteration. These HSICs are occasionally the cause of neurological symptoms and, when present, are mostly reversible. The higher occlusion rate of bAVMs under these circumstances is well appreciated.

Chapter 7

The Clinical Outcome after Repeated Radiosurgery for Brain Arteriovenous Malformations

D.R. Buis
O.W.M. Meijer
R. van den Berg
F.J. Lagerwaard
J. Bot
B.J. Slotman
W.P. Vandertop

Adapted from: Buis DR, Meijer OWM, Berg van den R, Lagerwaard FJ, Bot J, Slotman BJ, Vandertop WP. Clinical outcome after repeated radiosurgery for brain arteriovenous malformations. Radiotherapy and Oncology. 2010: 95(2):250-6.

Abstract

Purpose

We assessed the clinical and radiological outcome after repeated radiosurgery for brain arteriovenous malformations (bAVMs) after failure of initial radiosurgery.

Methods

Fifteen patients underwent repeated radiosurgery. The mean bAVM volume at first radiosurgery (S1) was 4.6 ± 4.3 ml and that at second radiosurgery (S2) was 2.1 ± 2.5 ml. The median marginal dose was 18 Gy at S1, and 21 Gy at S2. Modified Rankin Scale (MRS) score was determined in all patients at last follow-up (FU).

Results

Complete obliteration was reached in nine patients (60%). Median time to obliteration was 50 months after S2. An excellent outcome (no new neurologic deficiencies, complete obliteration) was reached in seven patients (47%). Eleven patients (73%) showed a MRS 6 1. Radiation-induced complications occurred in 20%, of which 13% occurred after S2. Radiological complications included cyst formation (n = 1), radiation-related edema (n = 4), and radiation necrosis (n = 1), resulting in an increasing mean MRS of 0.5 at S1, 0.6 at S2, to 0.8 at FU. No (re-)bleedings were encountered during 137-patient years at risk.

Conclusion

Repeated radiosurgery is a viable option for the treatment of small remnant bAVMs. We report 20% permanent radiation-induced complications. Such complications were mainly seen in relatively large, and therefore difficult to treat, bAVMs.

Key words

Intracranial arteriovenous malformations • Nervous system diseases • Radiosurgery • Surgical procedures, operative • Therapeutics

Introduction

The goal in the treatment of brain arteriovenous malformations (bAVMs) is complete obliteration or resection without inducing new neurological deficits[336]. Using radiosurgery this goal is reached in 67–81% after 4 years and in 87–91% after 5–6 years[291, 411, 487, 489]. Although failure analyses report several causes for treatment failure, i.e.: inadequate nidus definition, intentional partial irradiation, large nidus volume, suboptimal radiation dose, recanalization or re-expansion of the nidus, and radioresistance associated with an intranidal fistula[138, 139, 250, 375], the appropriate treatment after incomplete obliteration has not been addressed extensively.

Previous studies have demonstrated that the chance of successful obliteration after repeated radiosurgery, in case of failure of initial radiosurgery, may be comparable to that of the initial radiosurgery, with reported obliteration rates varying between 35% and 86%[125, 213, 372, 382, 400]. However, as the complication rate increases with the amount of radiation previously given[213], we have evaluated our performance and the clinical outcome in 15 patients with a bAVM who were submitted to repeated radiosurgery after failure of the initial radiosurgical procedure.

Methods

Between January 1991 and December 2007, 312 radiosurgical procedures for the treatment of one or more angiographically visible bAVMs were carried out in the VU University Medical Center (Amsterdam, The Netherlands). Seventeen of these procedures were salvage treatment for previously unsuccessfully radiosurgically treated bAVMs.

Our treatment regimen has been published previously[57]. In summary, unruptured bAVMs ≤ 3.5 cm are treated by radiosurgery. Larger bAVMs undergo endovascular embolization, and if this results in a residual nidus 63.5 cm, radiosurgery may follow. Ruptured bAVMs, or bAVMs that demonstrate angiographic characteristics suggestive of an increased (re-)bleeding rate, such as intranidal aneurysms[91], are always treated endovascularly first.

Patients were examined with MR imaging of the brain using a 1.5 T whole-body scanner, with a standard polarized head coil (Magnetom Vision, Magnetom Sonata; Siemens, Erlangen, Germany). T_2-weighted MR images with a slice thickness of 3 mm, as well as Time-of-Flight MRA images with a slice thickness of 2 mm were acquired. MR imaging was usually performed 1 day prior to radiosurgery. On the day of radiosurgery, a stereotactic

base ring (BrainLAB AG, Feldkirchen, Germany) was placed on the patient's head under local anesthesia. Digital subtraction angiography (DSA) and 2 mm sliced planning CT angiography scans were made with the stereotactic frame in situ. The DSA images were co-registered with the CT images using the stereotactic localizer box. Finally, the MRA study was digitally fused with the CT study using the automatic image fusion software of the radiosurgery planning system (BrainLAB AG). For the purpose of target delineation, the angiographic nidus was defined as the network of abnormal vessels between arterial feeder(s) and the pathologically early draining vein(s)[32].

Radiosurgery was performed using a 6-MV linear accelerator (Clinac 600 C, Varian Medical Systems Inc., Palo Alto, CA, USA) that was especially adapted for radiosurgery. Usually patients were treated with five noncoplanar arcs of 140° each, with identical beam weighting for all arcs, and a single circular collimator resulting in a typical spheroid dose distribution. After installation of the Novalis-shaped beam device (BrainLAB AG) in June 2002, only dynamic conformal arcs with dynamic multileaf collimators, producing a more conformal distribution of irradiation, were used. The dose was normalized to 100% and prescribed to the 80%-isodose line encompassing the bAVM. The clinically used prescription dose was dependent on the volume of the bAVM (normal tissue within 80%-isodose) with an 80% prescription dose of 21, 18, and 15 Gy for a volume of 67, 7–14, and P14 ml, respectively.

Follow-up consisted of an annual neurological examination and MR imaging of the brain, using the previously mentioned imaging protocol. Patients were followed annually with MRI until 3 years after radiosurgery, unless complete obliteration was diagnosed earlier. DSA was performed when MR imaging suggested complete obliteration. Alternatively, when MR imaging failed to show obliteration at 4 years after radiosurgery, DSA was performed to assess the need for repeat treatment. Angiographic obliteration of the bAVM was defined as the complete absence of abnormal vessels in the former nidus of the malformation, with disappearance or normalization of early draining veins from the area, and a normal circulation time on angiography[279, 440].

Included in this study were all patients who underwent repeated radiosurgery of the same bAVM for the purpose of complete obliteration. Excluded from analysis were patients with a follow-up shorter than 2 years after the second radiosurgical procedure, except when angiographically confirmed complete obliteration or (re-)bleeding occurred earlier. The follow-up interval was considered complete when complete obliteration was reached, a (re-) bleeding occurred, or when new treatment, directed at bAVM obliteration, was initiated.

The patients' demographic data at the time of first (S1) and second (S2) radiosurgery, and at last follow-up (FU) were reviewed retrospectively. Their clinical condition at S1, S2, and FU was classified according to the Modified Rankin Score (MRS). Pollock's modified bAVM-score, as well as the Spetzler–Martin gradation (SM) at S1 and S2 was determined[369, 423]. A bAVM-related bleeding was defined as the sudden onset of neurological symptoms of decrease of consciousness with radiological confirmed presence of new hemorrhage in the surroundings of the bAVM. MR images were independently reviewed by two experienced neuroradiologists (JB and RvdB) for the presence of complete obliteration, a new hemorrhage or radiological complications. The latter were graded as (1) no radiological abnormalities, (2) T_2-hyperintensity, (3) T_2-hyperintensity with cyst formation, or (4) necrosis[57]. The diagnosis of complete obliteration on DSA images was retrospectively reviewed.

Cumulative incidence of bAVM-related (re-)bleeding was calculated by dividing the number of bAVM-related hemorrhages after S1, and before obliteration by the number of people at risk in the cohort at S1. Time to obliteration was calculated using Kaplan–Meier curves. Statistical significance was determined using Student's T-test, χ^2-test, or log rank-test when this was appropriate. The results are reported as mean and 95% confidence interval (95% CI), unless otherwise stated. A two-tailed P-value <0.05 was chosen as the threshold for statistical significance. All statistics were performed using Statistical Package for Social Sciences v. 15.0 (SPSS Inc., Chicago, IL, USA).

Results

From a series of seventeen patients, fifteen, nine females and six males, were included in this study. Two patients were excluded from further analysis: one was lost to follow-up after he returned to his native country. In another the bAVM was contoured incompletely during the second radiosurgery planning in order to decrease the treatment dose on the optic nerve below 10 Gy.

Mean age at diagnosis of the bAVM was 31.3 years (95% CI: 23.1–39.5). There were eight left- and six right-sided bAVM; one bAVM was located in the vermis (Table 7.1). One patient was diagnosed with Hereditary Hemorrhagic Teleangiectasias: three small bAVMs were present; one left occipital and two right temporal. One of the right temporal bAVMs failed to obliterate, and only this bAVM was analyzed in this study.

In one patient partial surgical resection was performed before first radiosurgery (Table 7.1). In seven patients up to four embolization sessions were performed before S1. Median age at

Table 7.1: Treatment parameters & Initial presentation of 15 bAVMs

					S1				S2		
Patient	Location	Presentation‡	Previous partial treatment*	Volume (ml)	SM†	bAVM-score§	Treatment-dose (cGy)	Volume (ml)	SM†	bAVM-score§	Treatment-dose (cGy)
1	Temporal	Headache	N/A	0,7	1	0,43	2100	2,0	1	0,66	2100
2	Temporal	Epilepsy	Endovascular embolisation (3)	2,8	1	0,90	2100	0,3	1	0,73	2100
3	Parietal	ICH	Resection	1,8	2	0,42	1800	4,0	2	0,72	1500
4	Cerebellum	FND	Endovascular embolisation (2)	14,1	1	2,13	1500	0,1	1	0,83	2100
5	Frontal	Epilepsy	Endovascular embolisation (2)	5,0	3	1,57	2100	9,4	3	2,08	1800
6	Occipital	ICH	N/A	4,2	3	1,38	1500	1,8	2	1,22	1500
7	Cerebellum	ICH	Endovascular embolisation (4)	8,7	4	1,47	1500	0,4	4	0,74	2100
8	Temporal	Screening	N/A	4,8	3	1,20	1800	4,2	2	1,22	2100
9	Cerebellum	ICH	Endovascular embolisation (1)	0,7	3	0,32	2100	4,8	1	0,84	1800
10	Temporal	Screening	N/A	0,6	1	0,92	2100	0,2	1	0,98	2100
11	Cerebellum	SAH	N/A	0,5	1	1,07	1500	0,5	1	1,15	2100
12	Temporal	Epilepsy	Endovascular embolisation (2)	6,4	4	1,00	1800	0,8	2	0,52	2100
13	Parietal	Screening	N/A	0,9	1	1,31	2100	1,2	1	1,44	2100
14	Basal ganglia	FND	N/A	12,2	4	2,34	1500	1,9	3	1,37	1500
15	Temporal	Epilepsy	Endovascular embolisation (2)	6,0	4	1,56	1420	0,2	3	1,08	2100

‡ ICH: Intracranial hemorrhage, FND: Focal Neurological Deficit: SAH: Subarachnoid Hemorrhage
* The number between brackets refers to the number of embolisation sessions
† SM: Spetzler-Martin grade[423]
§ The bAVM-score refers to the modified score developed by Pollock et al. in order to predict the outcome after radiosurgery of bAVMs[369]

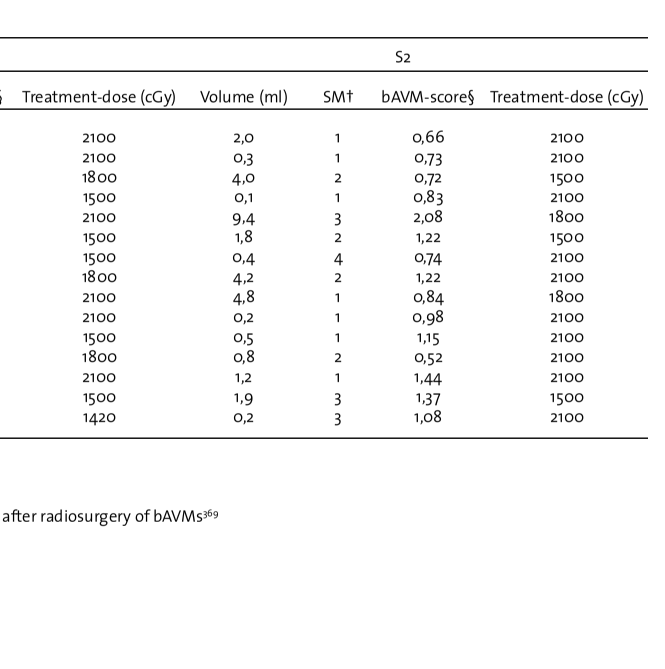

Figure 7.1
The original treatment plan shows a 0.63 ml bAVM, mainly fed from the left superior cerebellar artery with superficial drainage (left). At the second radiosurgical planning, when the external carotid artery was depicted, a significant contribution from the left occipital artery was found (right). The bAVM volume was 4.76 ml.

Figure 7.2
In 15 patients who underwent repeated radiosurgery a Kaplan–Meier survival analysis demonstrates a median time to obliteration of 99 months after S1, and 50 months after S2.

Table 7.2: Follow-up of 15 patients who underwent repeated radiosurgery for a bAVM

		Complications occurring during the entire follow-up interval		
Patient	Obliteration‡	Clinical	Radiological	Subsequent Therapy
1	P	N/A	Cyst formation	Resection of cyst with residual bAVM
2	Y	N/A	N/A	N/A
3	Y	N/A	N/A	N/A
4	Y	N/A	N/A	N/A
5	P	Hemiparesis	Severe radiation edema	Dexamethason
6	Y	N/A	N/A	N/A
7	N	N/A	N/A	Three endovascular embolisations
8	P	N/A	Radiation edema	N/A
9	P	N/A	N/A	N/A
10	Y	N/A	Minor radiation edema	N/A
11	Y	N/A	N/A	N/A
12	Y	Central n. VII palsy, hemiparesis	Severe radiation edema	Dexamethason
13	Y	N/A	N/A	N/A
14	Y	Hemiparesis	Radiation necrosis	N/A
15	N	N/A	N/A	N/A

‡ Y: Yes, P: Partial, N: No

S1 and S2 was 36.0 and 41.0 years, respectively. The mean interval between S1 and S2 was 52 months. The mean bAVM volume was 4.6 ± 4.3 ml at S1 and 2.1 ± 2.5 ml at S2, representing a mean reduction in volume of 54%. Mean Spetzler–Martin gradation and modified bAVM-score were 2.5 (1.7–3.3) and 1.20 at S1 and 1.9 (1.3–2.4) and 1.04 at S2, respectively. The median marginal dose was 1800 cGy at S1 and 2100 cGy at S2. In two patients the external carotid artery was inadequately depicted at S1, but was found to be a major feeder of the bAVM at S2 (Figure 7.1).

Median follow-up was 103 months (range 71–135) after S1 and 49 months (range 19–79) after S2. Complete angiographic obliteration was reached in nine patients (60%) (Table 7.2). Median time to obliteration was 99 months after S1 and 50 months after S2 (Figure 7.2). No hemorrhagic events were encountered after S1. No significant differences in rate of obliteration (P = 0.12) nor between bAVM-score at S1 or S2 was found (P = 0.65 and P = 0.73, respectively) between patients who had, or had not undergone previous partial embolisation.

Repeated radiosurgery failed to induce complete obliteration in six patients (40%), despite a mean interval of 56 months (range 35 – 75) after S2. Further therapy consisted of complete resection (n = 1, see below) and complete endovascular obliteration (n = 1). In one patient reduction of the nidus was diagnosed, but he refused further follow-up (see below). Further reduction of the nidus was diagnosed in one patient who is currently scheduled for further follow-up. In another no reduction of the nidus was seen and no further treatment was carried out. In the sixth patient progressive obliteration was diagnosed more than 4 years after S2. As the bAVM had not bled before and was diagnosed only during a screening for infertility, no further treatment was carried out.

According to Pollock's bAVM-score an excellent outcome (no new neurologic deficiencies, complete obliteration) was reached in seven patients (47%, Table 7.3). A good outcome (MRS ≤ 1) occurred in 11 of 15 patients (73%, Table 7.4). During the entire follow-up radiation-induced complications occurred in three patients (20%): before S2 (n = 1, 7%) and after S2 (n = 2, 13%). These complications resulted in a mean MRS which increased from 0.5 at S1, 0.6 at S2, to 0.8 at FU. Radiological complications occurred in 40% and included cyst formation (n = 1), radiation-related edema (n = 4), and radiation necrosis (n = 1) (Table 7.2).

In one patient (nr. 12) progression of epileptic seizures occurred, with a spastic hemiparesis and a central facial nerve palsy 15 months after S1. MR images demonstrated radiation-induced T_2-hyperintensity from 13 months after S1. Fourteen months later, the volume of T_2-hyperintensity had decreased, and 50 months after S1 she again underwent radiosurgery on the remnant of her bAVM. At FU the bAVM had obliterated completely, but there was a remaining spastic hemiparesis, with which she was able to walk, using a cane. Although she was still using anti-epileptic drugs, she had had no further seizures for over 30 months. New clinical deterioration after S2 occurred in two patients (Tables 7.2–7.4).

Table 7.3: Outcome according to Pollock et al.[369] after repeated radiosurgery (n=15)

	n (%)
Excellent (complete obliteration and no new deficit)	7 (46.7)
Good (complete obliteration, but a minor deficit)	0
Fair (complete obliteration, but a major deficit)	2 (13.3)
Unchanged (residual AVM and no deficit)	5 (33.3)
Poor (persistent AVM and any new deficit)	1 (6.7)
Dead	0
	15 (100)

Table 7.4: Clinical outcome (n=15)

Modified Rankin Score	S1 n (%)	S2 n (%)	S3 n (%)
0 No symptoms	9 (60.0)	9 (60.0)	9 (56.3)
1 No significant disability	5 (33.3)	4 (26.7)	2 (13.3)
2 Slight disability	1 (6.7)	1 (6.7)	2 (13.3)
3 Moderate disability		1 (6.7)	2 (13.3)
4 Moderately severe disability			
5 Severe disability			
6 Dead			

One patient (nr. 5, Figure 7.3), who initially presented with an epileptic fit every 6 months, demonstrated progressive seizures and a spastic hemiparesis from 16 months after S2. An MRI obtained shortly before S2 had already demonstrated minor perifocal hyperintensity on T_2-sequences (Figure 7.4, left column, middle picture), although without clinical complaints. The second radiosurgical planning was more difficult due to the presence of new collateral vessels or a dysplastic angiopathy, resulting in an ill defined and relatively large nidus which may have included surrounding brain (Figure 7.3, right column). MRI at 25 months after S2 showed an increase in the volume of hyperintensity around the central sulcus (Figure 7.4, right column). He was treated with dexamethasone, but his hemiparesis did not improve. At last by MRI examination, his bAVM was not obliterated, and the patient refuses further follow-up.

Another patient (nr. 14) with a bAVM in the left basal ganglia originally presented right-sided hypesthesia and hemianopia, without a preceding hemorrhage.

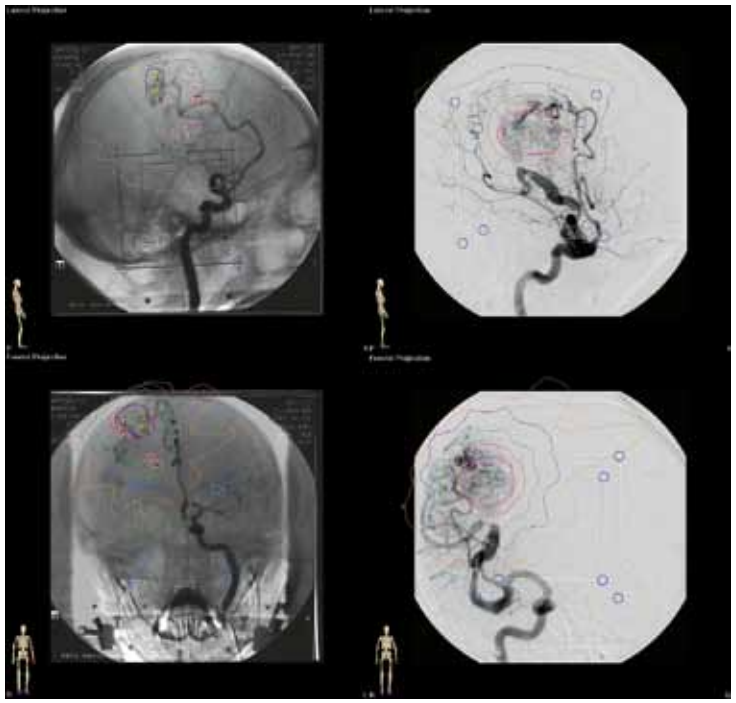

Figure 7.3
DSA images demonstrate a 4.93 ml bAVM fed from the middle cerebral (not depicted), as well as the anterior cerebral artery (left). On repeated radiosurgery 41 months later there was a massive collateralization (right), resulting in a volume of 9.35 ml. On all images the isodose lines (narrow contours in several colors) are imaged around the contoured bAVM (fat pink contour).

An MRI made at S2 already demonstrated minor hyperintensity on T_2-sequences, but without clinical complaints. From 23 months after S2 a progressive spastic hemiparesis emerged.

One patient (nr. 1) with a right temporal bAVM demonstrated the formation of a radiation-induced cyst 47 months after S2, without obliteration of the bAVM. There were no signs or symptoms. She underwent uncomplicated neurosurgical resection of the cyst and the remnant bAVM.

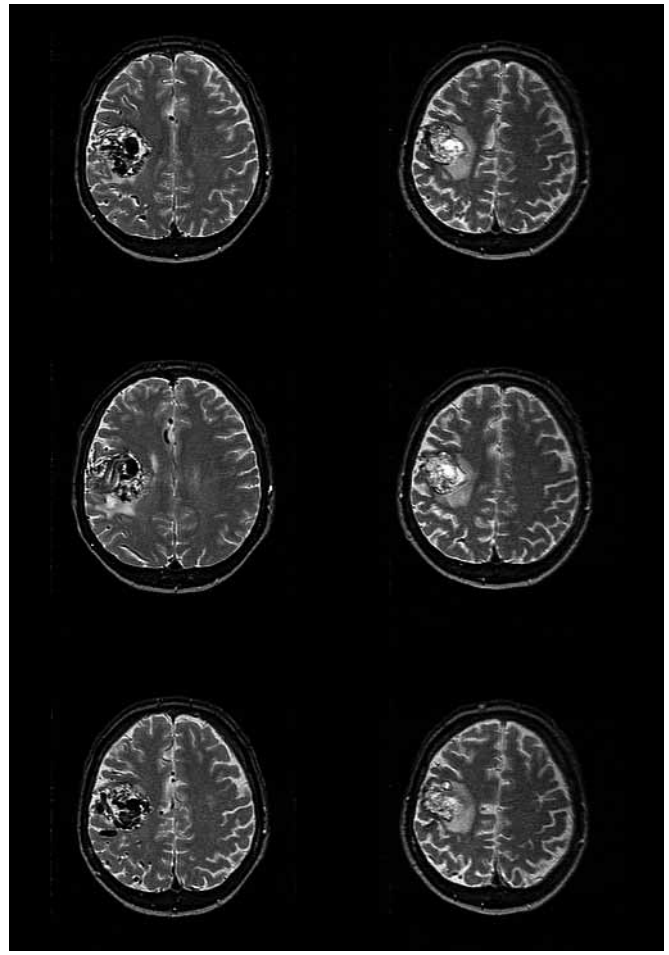

Figure 7.4
One patient with 9.35 ml bAVM at S2 demonstrated progressive seizures and a spastic hemiparesis from 16 months after S2. An MRI made 1 day before S2 already demonstrated minor hyperintensity on T2 sequences (left column, middle picture). At that moment there were no clinical complaints. However, an MRI made 25 months after S2 showed a major increase in volume of hyperintensity around the central sulcus (right column).

Discussion

Successful radiosurgery of a bAVM results in slow, but progressive endothelial proliferation leading finally to complete obliteration of the bAVM[67, 401, 439]. This process succeeds in 67–81% after 4 years, suggesting that 19–33% of the radiosurgical procedures fail[291, 411, 487, 489]. Publications regarding the fate of this substantial group of patients are relatively sparse, especially considering the fact that more than, 48,000 bAVMs (data December 2006) have been treated world-wide using Gamma-Knife alone (http://www.elekta.com/assets/gamma_knife_surgery/pdfs/ww06.pdf)[125, 213, 224, 370, 382, 400].

In this retrospective cohort study we evaluated the clinical and radiological results of repeated radiosurgery for a bAVM, in case of failure of initial radiosurgery and found a complete obliteration rate of 60%, with an excellent outcome in 47% and an MRS ≤ 1 in 73%, respectively. During the entire follow-up duration (i.e., after S1) permanent treatment-induced neurological complications occurred in 20%.

Although our study did not include a formal failure analysis, some findings justify a discussion. Previously reported causes of treatment failure include an inadequate nidus definition, a large nidus volume, suboptimal radiation dose, recanalization or re-expansion of the nidus, and radioresistance associated with an intranidal fistula[250]. In two of our patients a six-vessel DSA, done at S2, revealed feeding of the nidus from the external carotid artery (Figure 7.1). As no earlier six-vessel DSA was done, it remains unknown whether these feeders were new, or already present before the initial radiosurgery. In these patients the second radiosurgical procedure might have been avoided if a complete DSA had been made at S1. In order to prevent such omissions we advocate a recent six-vessel DSA before every bAVM-related radiosurgical procedure.

The rate of obliteration reported in this study (60%) is comparable to the obliteration rate varying between 59% and 86%, reported by other studies after repeated radiosurgery[125, 213, 372, 400].Two of these studies also used LINAC radiosurgery[125, 400]. In both studies, a complete obliteration rate of 59% is reached, albeit in one study lower marginal doses of 12.5 Gy at S1 and 15 Gy at S2 were used[125].However, in this latter study previous treatment is not mentioned. Schlienger et al. used a higher marginal dose of 23 and 22.8 Gy at S1 and S2, but in this series, comparable to ours, 59% had undergone previous endovascular embolization, which was found to be a causative factor in the failure of initial radiosurgery due to overprojection of embolization material[15, 25, 58]. However, in our series, nor in others, previous endovascular treatment was not found to be a significant factor in the failure of repeated radiosurgery, but this may also be explained by a relatively small patient cohort.

After S1 a mean reduction in nidus volume of 54% was reached. Therefore, according to our treatment protocol the marginal dose could be increased, resulting in a median marginal dose of 1800 cGy at S1 and 2100 cGy at S2. Although the obliteration rate after radiosurgery has been found to be associated with a smaller treatment volume, and subsequently an enlarged marginal dose[273], the follow-up factor has been ignored too easily[180]. Among the above-mentioned studies, approximately 10–20% of patients were not included in the final analysis due to loss to follow-up[125, 372, 400], suggesting that the obliteration rate might have been overestimated[180].

Although no (re-)bleeding was encountered after S1, radiological complications occurred in six patients, resulting in permanent neurological deterioration in three patients (20%) during the entire follow-up, and in two (13%) after S2. This is a relatively high rate of complications in comparison to other series which report between 1.9% and 9% permanent, or partially regressive radiation-induced complications after repeated radiosurgery[125, 400]. An increased complication rate was already demonstrated by Karlsson et al. who predicted five, but found 14 complications, among 112 patients who underwent repeated radiosurgery[213]. He concluded that the complication rate after second radiosurgery increases with the amount of radiation previously given. In both our patients who fared worse after S2, some late perinidal hyperintensity was seen on T_2-weighted MRI-sequences before S2 already, suggesting the presence of radiation-related gliosis. After the second radiosurgery the volume of gliosis increased and led to clinical deterioration. These findings therefore suggest that radiosurgery should not be repeated when perinidal hyperintensity on T_2-weighted images is still, or already present.

However, all patients who deteriorated clinically in our series had a relatively large bAVM volume at initial radiosurgery and would have been difficult to treat using other modalities as well.

Conclusions

Repeated radiosurgery can be considered a viable option for the treatment of small remnant bAVMs. No (re-)bleedings were encountered during 137-patient years at risk. During the entire follow-up interval (i.e., after S1) permanent treatment-induced neurological complications occurred in 20%. However, such complications were mainly seen in relatively large, and therefore difficult to treat, bAVMs.

Chapter 8

The Predictive Value of 3D- TOF MR Angiography in Assessment of Brain AVM Obliteration after Stereotactic Radiosurgery

D.R. Buis
J. Bot
F.D.R.K. Barkhof
O.W.M. Meijer
D.L. Knol
F.J. Lagerwaard
B.J. Slotman
W.P. Vandertop
R. van den Berg

Adapted from: Buis DR, Bot J, Barkhof F,Knol DL, Lagerwaard FJ, Slotman BJ, Vandertop WP, Berg van den R. Standard MR-Angiography is insufficient for diagnosing nidus obliteration after radiosurgery. Submitted.

Abstract

Purpose We assessed the diagnostic accuracy of 1.5T T_2-weighted and TOF-MR-Angiography (MRA) images for detecting nidus obliteration after radiosurgery.

Methods The pre- and postradiosurgery MRI and Digital Subtraction Angiography (DSA) images from 120 patients who were radiosurgically treated for a brain arteriovenous malformation (bAVM) were re-evaluated by three observers for patency of the nidus (pre-radiosurgery) and obliteration (post-radiosurgery), using a five point scale of confidence. Consensus reading of the DSA after radiosurgery was considered the gold standard for obliteration. Sensitivity, specificity, positive and negative predictive values, as well as overall diagnostic performance using ROC analysis were determined.

Results
Mean bAVM volume during radiosurgery was 3.4 (95% CI: 2.6 – 4.3) ml. Sixty-six patients (55%) had undergone previous endovascular embolisation. The mean interval between radiosurgery and follow-up MRI, resp. DSA was 35.6 (95% CI: 32.3 – 38.9) and 42.1 (95% CI: 40.3 – 44.0) months. Using ROC analysis an Area under Curve of 0.85 – 0.86 was found. An average false positive rate, meaning overestimation of nidus obliteration, of 0.16, and an average false negative rate of 0.21 was found.

Conclusion
MRA is an insufficient investigation to diagnose obliteration in the follow-up of bAVMs after radiosurgery. However, when MRA is strongly suggestive of obliteration, performing a DSA can be considered to confirm obliteration. When there is doubt about the presence of obliteration on MRA it is probably not useful to perform a DSA yet. Regarding the potential consequences of misdiagnosing a patent nidus we highly recommend follow-up DSA for definitive diagnosis of complete obliteration.

Key words
Cerebral Angiography • Diagnosis • Intracranial Arteriovenous Malformations • Magnetic Resonance Angiography • Magnetic Resonance Imaging • Radiosurgery

Purpose

Radiosurgery is an established modality for the treatment of brain arteriovenous malformations (bAVMs). Its purpose is to completely obliterate the nidus without causing new neurological damage[129]. Its efficacy is high and obliteration may be reached in 81% after four years, and in 91% after six years[291]. The established method to evaluate nidus obliteration is digital subtraction angiography (DSA).

Although the neurological risk of DSA is low with 0.09 - 0.8% permanent neurologic deficits[94, 101, 107, 154, 182, 235], silent embolisms were demonstrated after DSA on diffusion weighted MRI in up to 23% of all cases[31]. Other risks include bleeding, nephrotoxicity, and allergies[94, 223, 310]. Moreover, patients regard DSA as an unpleasant exam due to its invasiveness, pain and post-procedural bed rest [229]. Finally DSA carries inherent ionizing radiation risks, especially in children[380, 442, 451] and it is a costly investigation because it is labour-intensive and requires post-procedural hospitalization of the patient[438].

MRI evaluation may be a sensitive and non-invasive substitute[108, 160, 383, 448]. The risk of complications during an MRI examination of the brain is considerably lower, with no harmful effects reported in 1023 patients[468]. In many institutions MRI alone, or in combination with MR-angiography (MRA) is used for radiological follow-up, and in case of suspected obliteration, or after a maximum follow-up time, patients are referred for a DSA[57, 103, 166, 218, 230]. We performed a retrospective analysis of 1.5T T_2-weighted MRI and Time-of-Flight-MRA (TOF-MRA) to assess its ability to correctly predict nidus obliteration after radiosurgery, using DSA as the gold standard.

Methods

Between January 1998 and June 2007, 251 patients underwent radiosurgery for a bAVM at the VU University Medical Center (Figure 8.1). Our radiosurgical treatment protocol has been described elsewhere[57]. All patients were examined with MR-imaging of the brain using a 1.5T whole-body scanner, with a standard polarized head coil (Magnetom Vision, Magnetom Sonata; Siemens, Erlangen, Germany). The imaging protocol included T_2-weighted MRI images with a slice thickness of 3 mm (repetition time 3000 ms; echo time 20 ms), as well as TOF-MRA images (repetition time 39 ms; echo time 6.5 ms; flip-angle 20°) with a slice thickness of 1 mm and an in-plane resolution of 0.4 mm.
On the day of radiosurgery, a stereotactic base ring (BrainLAB AG, Feldkirchen, Germany) was attached to the patients head under local anesthesia followed by a stereotactic DSA with

a frame rate of 3 – 6 s^{-1}. A CT-Angiography (CTA) with 2 mm slice thickness reconstructions with the stereotactic frame in place was made. The DSA images were co-registered with the CT images using the stereotactic localizer box. Finally, the MRI studies were digitally fused with the CT study using the automatic image fusion software of the radiosurgery planning system (BrainScan v. 5.1, BrainLAB AG). Follow-up included biennial MR-imaging of the brain using the above mentioned sequences. MR-imaging could be moved forward on clinical grounds. DSA was performed when MR-imaging suggested complete obliteration. Alternatively, when no complete obliteration was observed on MRI at four years after radiosurgery, DSA was performed in order to assess the need for salvage treatment. Angiographic obliteration of the bAVM was defined as the complete absence of abnormal vessels in the former nidus of the malformation, with disappearance or normalization of early draining veins from the area, and a normal circulation time on angiography[279, 440].

Patient selection

Included in this study were patients who were radiosurgically treated for a bAVM, in whom the bAVM was reported visible in the radiological reports of MRI- and DSA-images made shortly before radiosurgery (MR_1 and DSA_1), and in whom final follow-up MRI and DSA studies (MRI_2 and DSA_2) were made. BAVMs that were not visible on MRI_1 were excluded from further analysis. These criteria led to the inclusion of 120 patients (Figure 8.1).

All imaging series were independently reviewed by two experienced neuroradiologists (Observers 1 and 2) and a PGY4 neurosurgical resident (Observer 3) on the local PACS system. DSA_1-images were reviewed for visibility of the nidus, size, drainage pattern and eloquence of the bAVM. From these data the Spetzler-Martin gradation was derived[423]. Follow-up MR-images were examined for patency of the bAVM. BAVM obliteration on MRI was assessed using a five point scale: definite obliteration, probable obliteration, indeterminate obliteration, probably patent, and patent. DSA_2-images were reviewed for the presence of partial or complete obliteration. In case of partial obliteration the maximum diameter of the remaining nidus was measured.

Each series of examinations had to be reviewed for each patient in a strict sequence simulating normal clinical practice: MRI_1 – DSA_1 – MRI_2 – DSA_2. All DSA_2 images were re-evaluated in a consensus meeting in order to create a uniform reference standard (DSA_{2C}). Clinical and treatment parameters noted included gender, clinical presentation, age at time of radiosurgery, marginal dose, volume and location of the bAVM (Table 8.1), previous partial or unsuccessful treatment and length of follow-up. Pollock's modified bAVM-score was derived from these data[369].

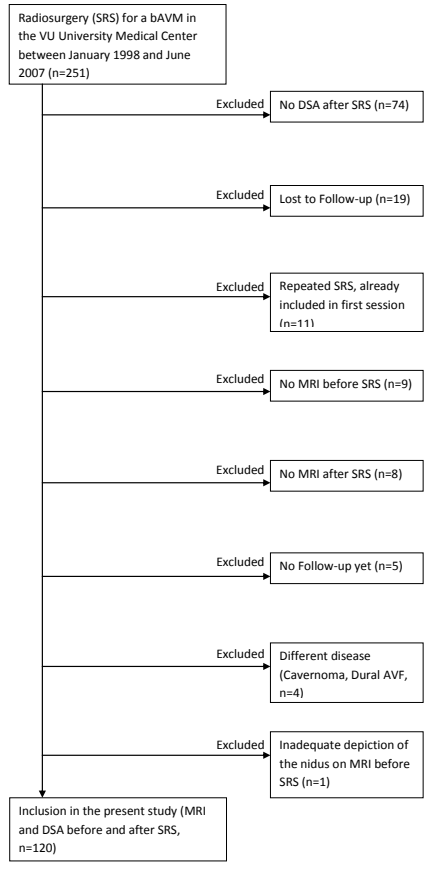

Figure 8.1
Flow-chart demonstrating the selection of patients who were radiosurgically treated in the VU university Medical Center for a bAVM. Included were patients that had a visible bAVM on DSA_1 and MRI_1, and who underwent follow-up MRI and DSA (MRI_2 and DSA_2).

Table 8.1: Presentation and location of 120 bAVMs

Location	n (%)	Presentation	n (%)
Frontal	25 (20.8)	Seizures	40 (33.3)
Temporal	30 (25.0)	Parenchymal Hemorrhage	40 (33.3)
Parietal	22 (18.3)	Subarachnoid Hemorrhage	5 (4.2)
Occipital	14 (11.7)	Intraventricular Hemorrhage	8 (6.7)
Basal Ganglia	1 (0.8)	Focal Neurological Deficit	4 (3.3)
Thalamic	13 (10.8)	Headache	13 (10.8)
Cerebellum	9 (7.5)	Screening	10 (8.3)
Brainstem	1 (0.8)		
Periventricular	1 (0.8)		
Corpus Callosum	4 (3.3)		
Thalamic	13 (10.8)		

Statistics

Sensitivity, specificity, negative (NPV), and positive predictive values (PPV) for obliteration were determined. Sensitivity was defined as the probability of finding obliteration on MRI_2 among those who demonstrated complete obliteration on DSA_{2c}. Specificity was defined as the probability of finding a patent nidus among those who demonstrated no obliteration on DSA_{2c}. NPV was defined as the percentage of patients among whom the nidus was diagnosed patent on MRI_2, and in whom this was confirmed on DSA_{2c}. PPV was defined as the percentage of patients among whom the nidus was diagnosed obliterated on MRI_2, and in whom this was confirmed on DSA_{2c}. Cut-off points for determining obliteration were chosen between 'probable obliteration' and 'indeterminate obliteration'.

For differentiating a patent from an obliterated bAVM on MRI_2 in comparison to DSA_{2c}. Receiver Operator Characteristic (ROC) analysis per observer was performed[301].

A univariate regression analysis was done to asses which factors (Spetzler-Martin Grade, drainage pattern, previous embolisation and interval between MRI_2 and DSA_2) correlated with discrepant findings between MRI_2 and DSA_{2c}. All statistics were done using SPSS 17.0 (SPSS Inc., Chicago, IL, USA)

Results

One hundred twenty series of images from 120 patients were included in this study (Table 8.1). There were 56 females and 64 males. Lateralization was right (n=44), midline (n=5), or left (n=71). Mean bAVM volume during radiosurgery was 3.4 (95% CI: 2.6 – 4.3) ml, with a mean marginal dose administered to the 80%-isodose-line of 1917 (95% CI: 1878 – 1956) cGy. Mean age at radiosurgery was 37.5 years (95% CI: 35.9 – 39.0). Sixty-six patients (55%) had undergone previous endovascular embolisation. Spetzler-Martin Grade was 1 (n=20), 2 (n=39), 3 (n=48) or 4 (n=13). Mean modified bAVM-score was 1.15 (95% CI: 1.1 – 1.2).

All DSA_1 investigations were made on the day of radiosurgery. The mean interval between MRI_1 and radiosurgery was -4.5 (range -211 - 7, median -1) days. The mean interval between Radiosurgery and MRI_2, and DSA_2, respectively was 35.6 (95% CI: 32.3 – 38.9) and 42.1 (95% CI: 40.3 – 44.0) months. The mean interval between MRI_2 and DSA_2 was 6.2 (95% CI: 5.3 – 7.1) months, with a median of 3.6 months. The interval between MRI_2 and DSA_2 was ≤ 3 months (n=48, 40%), between 3 – 6 months (n=39, 32.5%), or > 6 months (n=33, 27.5%).

Each series of images (n=120) was reviewed by three observers (360 patient-series). However, observer 3 determined that the nidus was not patent in one patient on MRI_1, observers 1 and 2 determined the same in three other patients. Therefore 7 patient-series, based on 6 patients were discarded. Further statistical analysis was based on the reviews of MRI_1, MRI_2 and DSA_2 in 353 patient-series: 119 for observer 3, and 117 observations for observers 1 and 2 each (Table 8.2). Observers 1 and 2 were more self-assured in the determination of the presence of nidus obliteration on MRI_2: they diagnosed a definite and probable obliteration in 38 – 45%, and in 14 – 16%, respectively. Observer 3 diagnosed a definite obliteration in 14% and a probable obliteration in 47%.

Positive and negative predictive value for 'true obliteration' varied between 0.89 and 0.93, and 0.63 and 0.70, respectively (Table 8.3). The mean diameter of the remaining nidus (n=119 observations) was 14.7 mm (95% CI: 12.3 – 17.1).

Obliteration was wrongly diagnosed on MRI_2 in 19 observations for an average false positive rate of 0.16 (Figure 8.2A). The remaining nidus was ≤ 10 mm in 16 observations (84%).
Conversely, a patent nidus was wrongly diagnosed on MRI_2 in 50 for an average false negative rate of 0.21 (Figure 8.2B).

Table 8.2: Determination of nidus obliteration on MRI2†

DSA2c	MRI_2 Obs.1 (n=117)		MRI_2 Obs.2 (n=117)		MRI_2 Obs.3 (n=119)	
	Patent	Obliterated	Patent	Obliterated	Patent	Obliterated
Obliterated	15	63	21	56	14	65
Patent	32	7	36	4	32	8
	47	70	57	60	46	73

† On MRI2 the cut-off point for determining obliteration was chosen between 'probable obliteration' and 'indeterminate obliteration'.

Table 8.3: Predictive value of MRI_2 for 'True obliteration' in comparison to DSA_{2c}

	Observer 1 n=117	Observer 2 n=117	Observer 3 n=119
Sensitivity	0.81	0.73	0.82
Specificity	0.82	0.90	0.80
Positive Predictive Value	0.90	0.93	0.89
Negative Predictive Value	0.68	0.63	0.70
Prevalence	0.67	0.66	0.66
False Positive Rate	0.18	0.10	0.20
False Negative Rate	0.19	0.27	0.18

For differentiating a patent from an obliterated bAVM on MRI_2 in comparison to DSA_{2c} Receiver Operator Characteristic (ROC) analysis demonstrated an area under the ROC-curve for predicting obliteration varying between 0.85 – 0.86 (Figure 8.3).

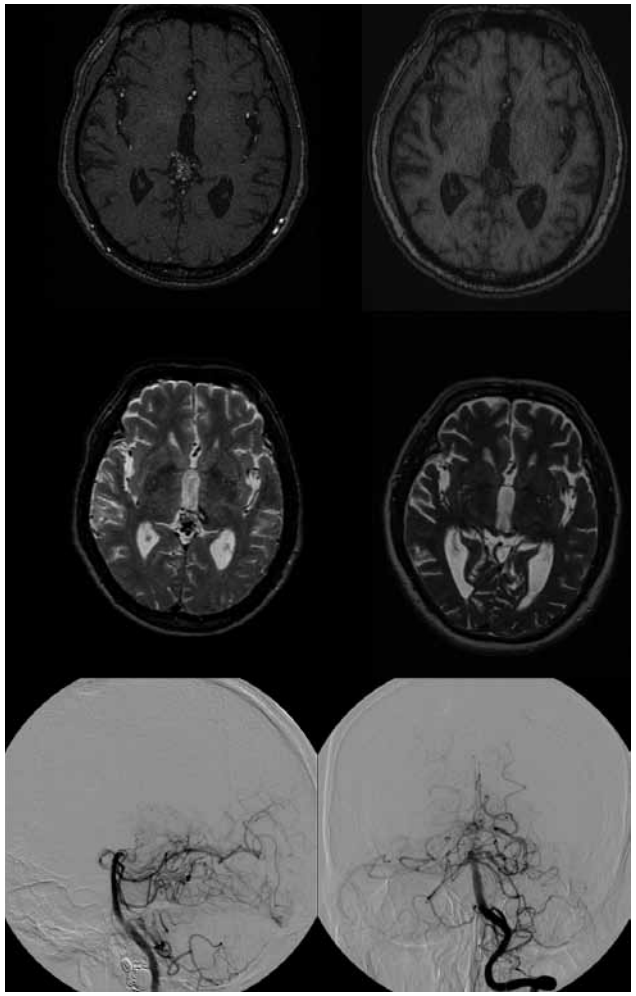

Figure 8.2A
A 0.90 ml tectal bAVM, which was clearly visible on MRI_1 (TOF-MRA and T2-weighted images, left column). Two out of three observers determined this bAVM obliterated on MRI_2 (right column), almost three years later. However DSA_2, made six weeks after MRI_2 still demonstrates early venous drainage towards the lateral sinus (DSA lowest row).

In a univariate regression analysis bAVM-volume, Spetzler-Martin Grade, drainage pattern, previous embolisation and interval between MRI_2 and DSA_2 were found to be not significant factors for determination of obliteration on MRI_2.

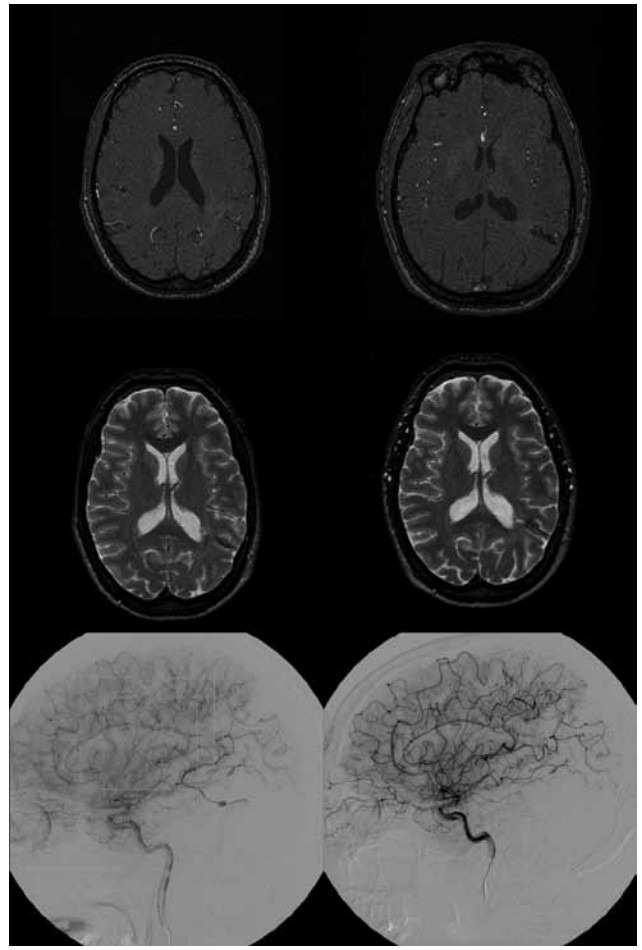

Figure 8.2B
A 0.17 ml central bAVM that was previously partially treated by endovascular embolization (left column). Two out of three observers determined this bAVM patent on MRI_2, one year after radiosurgery (right column). However DSA_2, made two months after MRI_2 demonstrates absence of early venous drainage (DSA, right column).

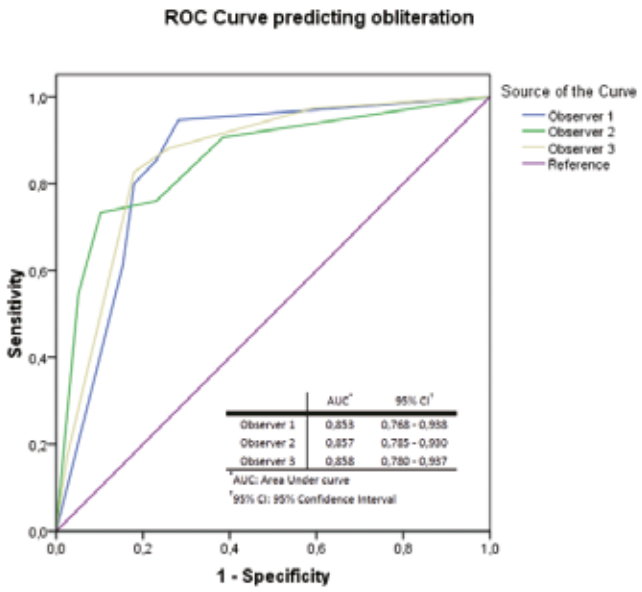

Figure 8.3
Receiver Operator Characteristic (ROC) analysis demonstrated an area under the ROC-curve for predicting obliteration of 0.85 – 0.86 for for each individual observer.

Discussion

The endpoint in radiosurgery of bAVM's is complete obliteration of the nidus a few years after radiosurgery. Due to its high spatial and temporal resolution DSA is the reference technique, for judging obliteration[279, 342, 440]. Although the clinical risks of being subjected to a DSA remain low[94, 101, 107, 154, 182, 235], this risk increases when multiple consecutive cerebral angiographies are performed, such as in bAVM patients. MRI has practically no risk[468]. In a previous study we demonstrated that MRA-based images might be used as the sole imaging modality for radiosurgery of bAVMs smaller than 3 ml, when in a noneloquent location[59].

In this study we aim to answer two questions. First: can MRA be used to predict obliteration reliably? Second: can MRA replace DSA in the follow-up of bAVMs after radiosurgery? We found an average false positive rate of 0.16 for three observers, which is comparable to other studies[145, 374]. A false negative rate of 0.21 was found.
These findings may have serious consequences. As partial nidus obliteration does not offer protection[291] overestimation of the 'true obliteration-rate' may result in insufficient additional therapy, or an increased fraction of patients suffering from intracranial hemorrhage after complete obliteration was falsely diagnosed. Based on our data a small remaining nidus seems to be the major cause for overestimation of nidus obliteration. Similarly, Mukherji et al. demonstrated at least 95% sensitivity and 100% specificity for depicting a residual nidus, provided that an arteriovenous shunt and a residual nidus > 1 cm remains. Using gradient echo imaging the sensitivity did not become less than 100% until the nidus diameter was less than 0.36 cm[317]. Recently more sophisticated MRI techniques were developed that have demonstrated improved depiction of bAVMs in small series, but cutoff points for diagnosing obliteration were not given[108, 247, 362, 391, 392, 448].

Conversely, misdiagnosing an obliterated nidus for a patent one means the patient suffers from his disease for a longer interval, and may be subjected to additional, and unnecessary therapy. The cause for the poor negative predictive value might be the absence of a regular T_1-sequence in our follow-up protocol. T_1-sequences have very short repetition times, which results in saturation of all static tissues, except for tissues with a very short T_1-relaxation time, such as hematoma or coagulated blood. As 3D-TOF MR Angiography is also a T_1-based technique, coagulated or slow flowing blood might present as hyperintense signal as well. The combination of T_1- and 3D-TOF-MRA might overcome misinterpreting stagnation of nidal blood flow as persistent flow. The drawback of our follow-up protocol is the unability to make this differentiation. This may have resulted in underestimation of nidus obliteration, as some 3D-TOF-MRA sequences may demonstrate hyperintensity due to the presence of coagulated blood. Other factors that might have affected the performance of MRI could be the relatively long time interval (> 6 months in 28% of the population) between MRI_2 and DSA_2 when the nidus approaches obliteration and intranidal is slow, although a univariate regression analysis demonstrated that this factor did not contribute significantly in determining obliteration on MRI_2.

There are several limitations to the way the present study was done. There is the obvious exclusion bias due to patients that were not subjected to a follow-up DSA, or had a follow-up DSA in a different hospital.

Furthermore we used non contrast enhanced 1.5T T_2-weighted MRI and TOF-MRA images to determine nidus obliteration, meaning that temporal resolution is limited. This might explain a worse outcome in comparison to other studies which report a sensitivity varying between 80 – 100% for detection of residual nidus[145, 264, 374]. Using these dynamic contrast enhanced MR-angiographic sequences the temporal resolution is one frame per 1.7 seconds, in comparison to six images s^{-1} for DSA. However, the signal to noise ratio for

such dynamic contrast enhanced MR-angiographic sequences is better than that of 3D-TOF-MRA. In addition 3D-TOF-MRA is known to suffer from spin dephasing due to complex or turbulent flow patterns, as well as signal saturation in areas of slow flow[346]. Due to these shortcomings isolating venous drainage, depicting slow flow or a small nidus becomes more difficult[145]. These shortcoming become exaggerated in the absence of gadolinium, as gadolinium confers a high sensitivity to slow flow due to its T_1-shortening effect, with rare saturation effects[455].

Recently other studies using far more sophisticated MRI sequences were published[160, 181, 350, 362, 383, 391, 392, 448]. Currently the most promising technique for depicting a residual nidus may be 4D radial acquisition contrast enhanced MRA (4D rCE-MRA), in which a combination of several MR-techniques, such as radial undersampling, sliding window reconstruction and sliding mask subtraction are used, and which leads to a sufficiently high temporal and spatial resolution, such that all phases of the intracranial circulation can be separated adequately. Using this MR-technique in comparison to DSA three observers were able to correctly identify nidus size, location, and identification of arterial feeders and drainage pattern in 13 bAVM patients. Spetzler-Martin grade was correctly assessed in all but one[108]. However, the spatial resolution of 4D rCE-MRA is in the order of 1 mm[108], therefore even this sophisticated technique may miss a small remnant nidus.

Observers may have been biased by the visible presence of the stereotactic frame when DSA_2 was done for the purpose of re-irradiation. However, as all DSA_2 images were evaluated after MRI_2 this should not have changed the primary outcome of this study.

In our institute decisions regarding radiosurgery of bAVMs are made in a meeting in which all patient data are readily available. Therefore, different from some comparable studies[160, 181, 247, 362, 391], but in order to simulate the actual clinical situation, our observers were not blinded to the patients clinical situation.

As demonstrated in the ROC analyses (Figure 8.3), assessment of nidus patency was comparable for all observers. Although the assessment of nidus patency, as judged by a PGY4 neurosurgical resident (observer 3) was comparable to the assessment of both neuroradiologists, he was less confident in giving an assured judgement. The resident pronounced the nidus definitely obliterated in 14% vs. 38 and 45% for both neuroradiologists. However, as the cut-off point for obliteration was chosen between 'indeterminate obliteration' and 'probable obliteration' this difference in nuance does not reflect in our results.

Getting rid of the DSA?

In our institute we use consecutive MRI investigations to determine whether nidus obliteration has occurred. Our findings, presented in this study, are somewhat disappointing, and demonstrate that, in the absence of new signs and symptoms, and if only for the follow-up of a bAVM after radiosurgery, it is useless to perform a follow-up DSA before an obliterated nidus is diagnosed on MRA.

The bAVMs that are misdiagnosed as obliterated are likely to be either small, or drain into a single vein[374, 485]. Although such a configuration was found in conjunction with an increased obliteration rate, or even spontaneous obliteration[33, 56], the clinical course of a partially obliterated nidus remains unpredictable, with 23 reported hemorrhages before obliteration among 458 patients who were radiosurgically treated for a bAVM[291]. The importance of performing a DSA in order to rule out a persistent nidus after radiosurgery has been stressed before[398]. Reasons for still performing a DSA included the limited diagnostic performance of 3D-TOF-MRA, a lower morbidity rate during cerebral angiographic procedures in young patients[107, 154, 182], as well as the above mentioned consequences of misdiagnosing a patent nidus we agree with this point of view. As the potential consequences of bleeding from a bAVM, and potential morbidity due to cerebral angiography are known, but the odds of bleeding due to a persistent nidus remains unknown, and taking into account that newer MRI modalities demonstrate an improved depiction of the nidus, a large prospective study in which follow-up using dynamic contrast enhanced MRA and DSA, vs. MRI only might be appropriate.

Chapter 9

Final Considerations and a Glance at the Future of Radiosurgery for Brain Arteriovenous Malformations

D.R. Buis

General discussion: from target delineation to obliteration

After diagnosis of a bAVM, a decision should be taken whether it should be treated, or left alone. When treatment is indicated, an individualized treatment plan should be made in a multidisciplinary meeting. In general, this means that the patient is submitted to several diagnostic tests, including at least an MR-Angiogram (MRA) and a digital subtraction angiogram (DSA) in order to visualize the exact location of the bAVM, its relation with surrounding cerebral structures, and identify feeding arteries and draining veins, evaluate the angioarchitecture and other particularities of the nidus, as well as the different manifestations of high-flow angiopathy, any associated parenchymatous lesions, or other incidental and clinically asymptomatic cerebral pathologies. Microsurgery can be considered for Spetzler-Martin grade I and II bAVMs as surgical morbidity for these lesions has shown to be very low[92, 171, 185, 312, 355, 423], but in general for all bAVMs ≤ 3 cm radiosurgery is an excellent alternative. Larger bAVMs, or bAVMs with predilection places for bleeding, such as intranidal aneurysms or high flow fistulas, may be subjected to endovascular embolization first[115, 336, 465]. Although each modality may cure a patient from a bAVM, a multimodality treatment is often used.

When radiosurgery is the chosen treatment option, the patient is scheduled for MR-imaging of the brain. On the day of radiosurgery the stereotactic localizer box is attached to the patients' skull and a stereotactic DSA and CT-Angiography (CTA) are made. Based on this information a treatment plan is made in the next few hours, after which radiosurgery follows. Radiosurgery results in slow, but progressive endothelial proliferation of the nidus vessel walls, and finally in complete obliteration of the bAVM[67, 401, 439]. In recent publications this process succeeds in between 67 – 81 percent after four years and between 87 – 91 percent after five to six years[291, 411, 487, 489]. In order to observe this process MRI scans are made regularly after radiosurgery. When obliteration is diagnosed on MR-angiography one more DSA follows to confirm complete angiographic obliteration.

The first part of this thesis focuses on problems in conjunction with delineating bAVMs for the purpose of radiosurgery. The second part of this thesis aims to identify the clinical and radiological problems that occur in the interval between radiosurgery and complete obliteration of the bAVM.

Spontaneous regression of bAVMs: to treat or to observe?

Like complete obliteration, spontaneous complete regression seems to be a safe, although much rarer, endpoint as it prevents the bAVM from rupturing[471]. Among 337 patients with bAVMs treated in the VU University Medical Center (VUmc) only one regressed spontaneously and completely before treatment could be initiated[56]. The main working mechanisms associated with spontaneous regression seems to be gradual tapering of the blood flow due to intranidal thrombosis, or thrombosis of the single draining vein[347, 402]. A small bAVM rupture may causes local compression and result in permanent occlusion of the bAVM due to fibrosis. Thrombosis of bAVMs during childhood has been postulated to explain a lower frequency of multiple bAVMs in adults[257].

Unfortunately our study did not reveal which bAVMs are likely to occlude spontaneously, therefore it should not be considered a realistic option in the treatment of bAVMs[265]. Although there is a strong tradition of treating any bAVM, nowadays there is doubt regarding if asymptomatic bAVMs should be treated at all[435]. The rationale behind this doubt is the absence of randomized controlled trials to guide the choice of interventional treatment for bAVMs in clinical practice[8]. In the original landmark studies regarding the natural history of bAVMs no clear distinction between symptomatic and asymptomatic bAVMs were made, and its conclusions were often based on older imaging technology through which it was not possible to identify predilection places for bleeding such as intranidal aneurysms[53, 134, 152, 340]. Newer longitudinal or prospectively collected series show that the bleeding risk of unruptured bAVMs is nearly five times lower (1.2% $year^{-1}$) as compared with already ruptured bAVMs (5.6% $year^{-1}$)[161, 433]. Moreover the bleeding risk is especially low (0.9% $year^{-1}$) among the most common type of bAVM: a small and lobar bAVMs with superficial drainage[433]. In a recent prospective, population-based study after interventional or conservative treatment of unruptured bAVMs, only bAVM size and interventional treatment were independent predictors of progression to a poor outcome[466]. When treatment outcome is analyzed separately for ruptured and unruptured bAVMs 27% of patients with an unruptured bAVM experienced treatment related deficits, versus 58% of patients with a previously ruptured bAVM[435]. These observations suggest that interventional treatment may induce symptomatic haemorrhages or neurological deterioration otherwise[435]. Currently a randomized multicenter trial of unruptured bAVMs (ARUBA) takes place to assess whether conservative or interventional management will reduce the risk of death and stroke by at least 40% in a 5-year interval[429]. In order to detect such a difference 800 patients should be included. Although the ARUBA-trial will deliver new information, it also suffers from an inherent selection bias, due to a strong tradition of established treatment patterns, which makes the randomization of an adequate representation of bAVMs with various risk

profiles and multimodality treatment patterns difficult[78, 294]. This bias threatens its external validity and is demonstrated by a lack of included patients. The ARUBA-trial started in October 2006 and is estimated to be complete in July 2011. Only 100 patients were included despite 3.5 years of recruitment and the number of patients to be included has already been downgraded to 400 (http://clinicaltrials.gov/show/NCT00389181, http://arubastudy.org/frameSetBkgrndRation.html and http://www.strokecenter.org/trials/TrialDetail.aspx?tid=683). Therefore it remains particularly doubtful whether the ARUBA-trial will demonstrate any clinical or angiographic characteristics that can predict spontaneous regression.

Target delineation

A radiosurgical treatment plan should offer the highest chance of complete nidus obliteration, and the lowest risk of clinical deterioration or side effects in a patient. This is best achieved by depiction of the actual outer contour of the bAVM in order to ensure full coverage of the nidus, as well as limited radiation exposure to surrounding healthy brain tissue. Angiographically the nidus should be defined in the early arterial phase, when it is completely opacified, and early venous drainage is just visible[34]. Creating the true outer contour is therefore time and space dependent. In a clinical setting this problem is overcome by either reconstructing a fictive 3D outer contour based on the early arterial phases from a lateral and AP angiogram, or by disregarding the temporal information from the DSA and basing the outer contour on 'true' 3D MRI images. Both 'solutions' have drawbacks.

Although 3D DSA for brain aneurysms is feasible, a 'true' 3D DSA of a bAVM is not possible due to constraints on irradiation and iv contrast. As the outer nidus contour is a volume, in many radiosurgical centers it is reconstructed from two angiographic orthogonal stereotactic projections in such a way that the nidus resembles a prolate spheroid whose axes coincide with the three maximum diameters of the nidus. Such reconstructions are less reliable when the nidus shape is irregular. In general these reconstructions lead to larger target volumes[494], and therefore a lower marginal dose must be used, decreasing the odds of obliteration. Additionally, there is an increased chance of the inclusion of normal brain tissue within the target volume, increasing the odds of complications.

Another problem that occurs when angiographic orthogonal stereotactic projections are used is overprojection of bone, embolization material, or arteries and veins over a part of the nidus, as well as the inability to use more than two orthogonal projections simultaneously[43, 121, 288]. Therefore, in clinical practice, detailed examination of numerous consecutive DSA images is needed to study the various components of the nidus because not all shunt areas exhibit the same pace of flow. These circumstances lead to uncertainty regarding the exact 3D shape of the nidus, as defined on 2D DSA.

Meanwhile, MRI can quickly provide detailed images of intracranial vessels, and has therefore a high spatial resolution, but it lacks sufficient temporal resolution, which is crucial when depicting bAVMs either for delineation, or during follow-up, as the crucial event of a too early filling vein may be the only evidence of a residual arteriovenous shunt. This shortcoming has been tried to be solved by using Time-of-Flight MR-Angiography (TOF-MRA) which regards stationary tissues as 'unsaturated' showing it as a low signal intensity. When blood flows into the imaging volume it is 'saturated' and shows bright. However, the imaging time of this technique is still between two and eight minutes, and thus provides only a static image of the nidus. This problem might be overcome using dynamic contrast-enhanced MRA in which gadolinium chelate is introduced to change the T_1-relaxation of blood, such that it is very different from surrounding tissues. It also uses shorter acquisition times per scan, and a higher signal-to-noise ratio, thereby improving image quality, although not yet to the level of DSA[62, 454, 455, 493]. Although MR-techniques are improving very fast, and a frame rate acquisition of six frames s^{-1} has been reached, which might be sufficient for diagnosis and follow-up of bAVMs[108, 160, 392], such techniques have not yet been used for target delineation.

The above mentioned circumstances lead to interpretation differences among treating clinicians, and therefore to interobserver variation[58, 59]. Whether the proposed interobserver variation actually occurs, its amount, and the possible dosimetric consequences are described in **Chapter 3**. Two conclusions may be drawn from these studies: first the outcome after radiosurgery of a bAVM is not entirely predictable, which is partly caused by a substantial amount of variation in target delineation Second, using novel hardware, such as dynamic micro multileaf collimators, the actual drawn contour can be followed more closely, resulting in an improved conformity index[308]. Inevitably the treatment plan is therefore directly dependent on the quality of the contour, and indirectly on how well the treating physicians know to outline a nidus on DSA or MRA. As this situation differs for each physician the influence of randomness will increase, and therefore the predictability of outcome after radiosurgery will decrease. As obliteration rates depend on marginal dose only, and most centres reach 67 – 81% obliteration for three to four years after radiosurgery[291, 411, 487, 489], this means that, with increased use of more conformal techniques, it will be more difficult to predict which seven or eight out of ten bAVMs will obliterate.

Although it is unknown if a learning curve exists in contouring bAVMs some researchers state that observer related factors, such training, specialty and personal bias play an

important role, in addition to the role of imaging modalities[333, 469]. In order to decrease these factors we advised treatment of bAVMs in a multidisciplinary setting[58, 59]. Although the additional value of a team has not been proven, the use of guidelines and simplified rules for delineation did improve the consistency of contouring among radiation oncologists performing target volume delineation for partial breast radiation therapy in some, but not all studies[64, 316, 476]. However, images of breast tissue are not flow related, and therefore not entirely comparable to the dynamic situation that exists in bAVMs. In lung cancer a somewhat comparable dynamic situation exists, as the lung, and therefore the tumor moves during in- and expiration[414]. In such a situation significant interphysician variations persisted when contouring target volumes, despite the use of an institutional contouring protocol[44, 404, 461]. Therefore, the use of guidelines is only appropriate when these guidelines are prospectively evaluated in a clinical trial.

Other solutions include the use of automatic target delineation, which has successfully been used in delineating lung tumors on CT with an accuracy varying between 89 – 94% for CT and a mean classification error of less than 9% on positron emission tomography (PET) images[175, 176, 212]. For bAVMs, automatic target delineation was used during planning for cyberknife treatment[81]. The reconstruction of the nidus is based on 100 frames, made during one 240° turn of the C-arm. Different phases are studied by modifying the time at which the contrast is injected with respect to the position of the C-arm. The 3D reconstruction was based on images corrected for inherent distortion, using a correction algorithm, which resulted in less than 1 mm discrepancy[37, 47, 82]. The reconstructed image was matched with stereotactic CT images. Finally, delineation of the nidus is performed slice by slice on axial sections of the reconstructed images using an automatic contouring function with an appropriate threshold for voxel values. The radiological density of nidus vessels is determined by placing a 'density evaluation cursor' on the nidus volume. Due to the high contrast of angiographic images obtained by direct intra-arterial contrast, contouring of the nidus can be conducted automatically[81]. Using this method complete obliteration was reached in 65 of 80 patients (81%), which is comparable to other studies[81]. No study comparing automatic target delineation with manual target delineation was performed. It is therefore difficult to state that automatic target delineation makes a clinical difference.

In the **Appendix** we present a method, arrival-time color intensity projection (CIP), that combines the information contained in a number of sequential DSA images into a single composite color image[85]. This composite image represents the arrival time of contrast at each pixel with each pixel's hue, brightness, and saturation conveying the intensity and intensity variation, respectively, of the pixel over the DSA component images. Previously CIP permitted immediate visualization of mobility of lung tumors using 4D CT[86]. CIP may enhance the discrimination of the nidus from feeding arteries and draining veins, even when these are projected over the nidus. Therefore, CIP may improve the target definition for radiosurgery of bAVMs. Furthermore, more accurate nidal measurements may facilitate a more accurate bAVM classification by size. No interobserver studies using CIP images have been done yet. However, the concept of visualizing the temporal aspect of transnidal flow through color images was successful, and currently ZEISS has integrated this concept in a software package for their Pentero neurosurgical microscope[379]. In the astronomical sciences, CIP was successfully used in detecting trans-Neptunian objects, as well as a comet plunging into the sun[87].

In order to decrease the amount of interobserver variation the next step may include a study after the integration of CIP in MR-images with a high spatial and temporal resolution, such as 4D radial acquisition contrast enhanced MRA[108], and use a neural network to contour the nidus. A neural network is a mathematical model that simulates the structure or functional aspects of a biological neural network. It is often an adaptive system that changes its structure based on external or internal information that flows through the network during the learning phase. Previously used clinical images and nidus contours can be used to train the network[219]. Such an approach was successfully used in measuring endo- and epicardial boundaries of the left ventricle in time series of short-axis MRI and angiograms[16, 146, 341]. Automatic contour detection was successful in 17 of 20 studies which is comparable to manual contouring using multiple temporal frames in multiple slices from base to apex[146]. Using more images in the training set resulted in a better accuracy of the detected contours[16]. Although these results are encouraging, the situation in a bAVM is much more complex as, unlike in a left ventricle, blood flow occurs in more than one direction simultaneously, and every bAVM has a completely different structure. This means that a potential neural network will very complex, and therefore difficult to train[219].

Towards obliteration

After radiosurgery a process of slow, but progressive endothelial proliferation with hyalin and calcium deposition in the vessel walls sets in[67, 401, 439]. This process may lead to complete obliteration of the bAVM after three to four years. Besides progressive obliteration of the nidus, post-irradiation changes, consisting of T_2- or FLAIR-hyperintensity and T_1-hypo-intensity, with or without contrast enhancement, are seen in one third of all treated patients[38, 124]. Among our own patients we found post-irradiation changes in 53%[33].
In **Chapter 6** we evaluated a subgroup of fourteen patients who demonstrated T_2-hyperintensity far beyond the irradiated area. Obliteration of the venous drainage, including

the normal parenchymal drainage, was significantly more often present in nine (64%) of fourteen patients with extensive T_2-hyperintensity changes as compared with three (19%) of sixteen patients in the control group. Moreover, complete obliteration was reached in 88% in the group with extensive T_2-hyperintensity vs. 50% in the other group[33]. We postulated that the intranidal flow reduction in the course of the slow process of obliteration will lead to turbulence and subsequent progressive thrombosis of the draining vein. When these effects augment each other it leads to both progressive occlusion of the nidus, resulting in an improved probability of obliteration. The mechanism may be comparable to the situation that occurs in spontaneous regression of a bAVM[56], although spontaneous regression is much rarer. When the thrombus propagates, it may impair the drainage of the surrounding white matter through the small venules, leading to venous congestion, which becomes visible as T_2-hyperintensity on follow-up MRI scans. Due to other outflow possibilities in the presence of multiple draining veins this phenomenon may occur more often in bAVMs with a single draining vein. Our patient cohort was probably too small to demonstrate the more dangerous consequences of thrombosis of a single draining vein, as progressive non-hemorrhagic symptoms may be associated with an increased risk of haemorrhage[225].

Based on experience with the treatment of cytotoxic edema after whole brain radiation therapy, radiation edema after radiosurgery for bAVMs is often treated with dexamethasone, although the results are often disappointing. Therefore other treatments such as hyperbaric oxygen or oral Vitamin E have been proposed[285, 472]. The ultimate consequence of our findings is that one may consider performing an angiography in cases of severe clinical deterioration and extensive edema due to refractable venous congestion in order to demonstrate the new absence of a previously present draining vein. Similar to the situation in cerebral venous thrombosis[84] endovascular thrombolysis might then be attempted.

In **Chapter 7** we evaluated the clinical and radiological outcome in fifteen patients who underwent repeated radiosurgery, after failure of the initial radiosurgery. The complication rate after second radiosurgery is known to increase with the amount of radiation previously given[213]. Using LINAC radiosurgery the lower doses (< 5 Gy) are spread through the normal brain in a star like configuration (Figure 9.1). A second radiosurgical treatment will result in a comparable star like pattern of radiation. However, using BrainLAB software it is not possible to determine exactly where the arms of the previous 'star' were located, therefore, and especially when one takes into account the above discussed interobserver variation, the arms of the new and old 'star' might intersect, resulting in elevated doses of radiation to healthy brain tissue. Improved conformality, for example when using Intensity Modulated Radiation Therapy (IMRT)[142], has shown to be correlated with at least a reduced incidence of temporary complications[131]. Using IMRT, target delineation takes place in the regular way, but thereafter treatment prioritization values, and therefore rank, and dose limits are assigned to surrounding normal structures by the radiation-oncologist. Subsequently the beam arrangement is evaluated and a clinically optimized treatment plan that maximizes the radiation dose to the nidus, but minimizes exposure to healthy brain is determined[244, 428]. IMRT is thus especially suited for treatment of large and irregular bAVMs that are closely located to critical structures[201]. Although this does not solve the problems associated with repeated radiosurgery directly, it does decrease the radiation dose on healthy brain, hence decreasing the odds of complications after repeated radiosurgery.

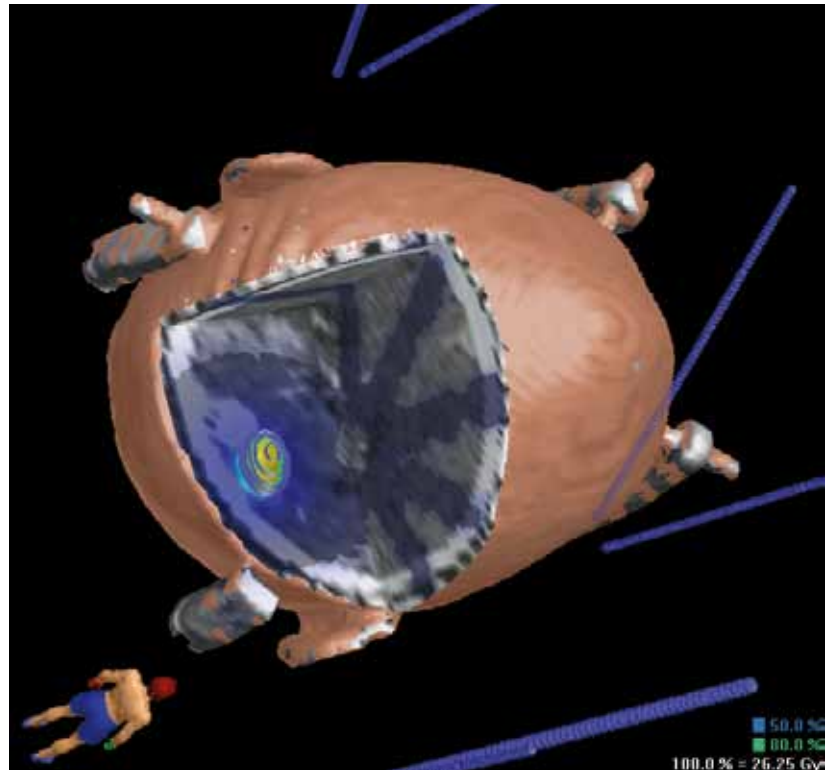

Figure 9.1
A 66 year old male with a 1.17 ml right parieto-occipital bAVM. He was treated with a marginal dose of 21 Gy. The 5% isodose distribution is visible as a star-like pattern.

BAVMs in children, and especially in young children, may not be entirely comparable to those in adults. Multifocal bAVMs, with remote arteriovenous shunts[141, 197], large venous ectasias, brain atrophy and systemic phenomena are more often seen in children[90, 168, 388]. Conversely high flow angiopathic changes or flow related aneurysms are rarely seen[256]. These characteristics may result in a more aggressive behaving bAVM, as they present more often with a hemorrhage and demonstrate an increased mortality in comparison to adults[65, 98, 133, 236, 315, 328]. Taking into account the long life expectancy of a child the necessity for treatment is often more compelling.

The same arguments for making radiosurgery a safer and more effective treatment apply in children as well, but are more essential as the developing brain is more susceptible to radiation injury. Due to the long life expectancy once a patient, and especially a child, is radiosurgically cured from his bAVM there is a risk of secondary neoplastic transformation of surrounding cerebral structures. Although this risk can't be assessed accurately, it is likely to be very low, with six reported patients by 2003[283]. The secondary tumours are often high grade gliomas, and occur close to the target volume from 6 – 20 years after radiosurgery. Among these six, three patients developed complications after radiosurgery, which was a ten-fold increase in comparison to typical radiosurgery series[283]. Although this may be coincidence, it also suggest that problems occurring during delineation, such as inclusion of healthy brain in the irradiated area, may result in secondary tumors later in life. Since this occurrence is very rare, it does not seem that current treatment regimes that should be changed[283, 332].

In children, as in adults, most complications after radiosurgery occur in large and difficult to treat bAVMs, leaving the best outcomes for the smaller bAVMs, which might be treated surgically as well, if located in a surgically accessible location. Therefore, the indication for radiosurgery of bAVMs in children, but also in adults is still defining itself.

Due to radiation exposure in sequential diagnostic tests, children may suffer an overall increased lifetime risk of cancer of approximately one percent[380, 450]. In order to protect bAVM patients from radiation injury and from complications during DSA we investigated whether it was possible to abandon the DSA in our follow-up regime.

The endpoint of nearly all studies regarding treatment of bAVMs is complete obliteration, or complete surgical resection, which is thought to be a new, stable situation, in which the bAVM will no longer hemorrhage and the patient is actually cured. In children, but rarely in adults, bAVMs have been known to reappear[13, 128, 136, 166, 172, 188, 232, 349, 354, 389]. Dysregulation of angiogenesis and the presence of angiographically invisible compartments in the bAVM have been postulated as potential causes of this phenomenon[172]. Although we did not encounter recurrence of a bAVM among our pediatric patients yet, we do advocate repeating an MRA five years after obliteration was diagnosed, as most recurrences reported have occurred within six years[232].

Other bAVMs do not reappear, but bleed despite angiographic evidence of complete obliteration[295, 377, 409]. Clinically such bleedings are very rare, with ten patients reported worldwide[280, 295, 377, 409, 479]. On histological examination of the previous nidus small endothelial cell lined channels containing erythrocytes within the area of hyalinization was found, suggesting that these new lesion might resemble angiographically occult vascular malformations, such as cavernous angiomas[377, 409]. New contrast enhancement on MRI in the area where the obliterated nidus is located, and where contrast enhancement disappeared with obliteration of the nidus may suggest the presence of new vascular channels[295, 377, 409]. From a medical and scientific point-of-view it would be of great interest to follow patients with obliterated bAVMs. But considering that bleeding from an obliterated bAVM is very rare, and shows temporary neurological deficits only[280, 295, 377, 409, 479] radiological follow-up in adult patients should not be performed on a regular basis after complete obliteration has been reached, as such imaging leads to uncertainty with the patient and his treating physicians, and increases the cost of medical practice. This can be different when there are new signs and symptoms, especially when MR-imaging shows new contrast enhancement as well. Surgery might be indicated to differentiate the new lesion between previous nidus and radiation induced tumor, and to reduce mass effect or prevent future bleeding. Adult patients should be informed that after reaching complete obliteration the odds of having a clinically significant bleeding from the previous bAVM reaches zero, and that therefore, in the absence of new signs and symptoms no new imaging should be performed.

Finally there are bAVMs that obliterate subtotally, but do not bleed anymore[2, 485]. Although in some this stadium represents a stage towards complete obliteration, in 27% an early draining vein remains[485]. An insufficient dose targeting a part of the nidus is thought to be responsible for this phenomenon[2]. Among 121 patients with a persistent early draining vein after radiosurgery the bleeding rate was zero, despite a global annual bleeding rate of 3.08% after radiosurgery[2]. A further 53% progressed to obliteration[2]. This situation seems to represent a clinical, but not a radiological cure. Treatment should therefore be only advised cautiously, and then only after waiting for another one or two years, as a remaining early draining vein is likely to progress to complete obliteration.

The future of radiosurgery of bAVMs

Radiosurgery is an established treatment for bAVMs. The above mentioned studies may eventually result in better nidus delineation, and improved follow-up of bAVM patients. When imaging modalities improve and we can get rid of the DSA, radiosurgery for bAVMs may take place on an outpatient basis. As we have seen radiosurgery is especially successful in small bAVMs, regardless of the intracranial location. In a comparison of radiosurgery vs. microsurgery in two cohorts of 39 patients each, the cure rate was similar, although the neurological morbidity was higher in the microsurgery group, but the re-bleeding rate was higher in the radiosurgery group[322]. When the long term outcome in both groups turns out to be equal, radiosurgery may be given preference for reasons of economy and patient satisfaction. Further studies should be performed in order to increase our understanding of the process of progressive obliteration, and whether we can accelerate this process safely by adding radiation sensitizers. As bAVMs are relatively inaccessible to flow studies, hemodynamics and dose response behaviour are currently successfully simulated using computerized electrical, or biomathematical models[26, 156].

The use of radiation sensitizers has been explored in brain tumors[193, 330, 337], where they are used to reduce the amount of radiation needed to kill a given population of tumor cells. Although killing cells is not the purpose in radiosurgery of bAVMs, a substance that increases endothelial proliferation in a bAVM might be added to endovascular embolization material in order to decrease the interval to obliteration. Endothelial cells derived from bAVMs were found to overexpress proangiogenic growth factors, and in experimental models radiosurgery has been found to decrease angiogenic activity[4, 205]. Conversely endovascular embolization increased angiogenic activity, and embolization before radiosurgery decreases the obliteration rate and reduces the radiation dose delivered[4, 14, 15]. Therefore adding an angiogenic growth factor inhibitor to the embolization material may improve outcome in the multimodality treatment of bAVMs.

The delay to obliteration may decrease when the moment of obliteration can be monitored with more certitude. Recently a downregulation of neuropilin-2, protein C inhibitor and cyclin-dependent kinase 6 was found in venous blood samples from patients with progressive obliterating bAVMs after radiosurgery[492]. Such measurements may be used to determine the moment of obliteration more exactly.
Despite improved target delineation and radiation delivery, injury to healthy brain tissue will occur eventually in some patients. Further research after the use of radioprotection agents is needed when aggressive radiosurgery of bAVMs in highly eloquent structures, such as in the brainstem, or around the optic nerve, is indicated. Ideally, a pharmacological radioprotection agent would not impact the treatment delivered to the brain lesion but would protect the surrounding brain in the region of dose falloff[240]. In animal models 21-aminosteroids and metalloporphyrin anti-oxidants were shown to protect healthy brain from radiation injury[35, 55, 239, 240, 359]. Especially 21-aminosteroids seem promising because of their potential selectivity to vascular endothelium. Since bAVM vessels that were subjected to endovascular embolization demonstrate complete disruption of endothelial cells[477], use of a radioprotection agents might be successful in such bAVMs. However, no comparable studies were done in humans so far.

Conclusions

The results presented in this thesis suggest that I) There is a substantial amount of interobserver variation when delineating a bAVM, when either MRA or DSA are used as the main imaging modality. II) The consequences of this variability increase once more conformal radiosurgical techniques are used. III) the presence of a single draining vein in a bAVM is often seen in conjunction with a faster obliteration, either after radiosurgery in conjunction with the presence of T_2-hyperintensity, or before radiosurgery during the process of spontaneous obliteration. IV) In children the obliteration rate after radiosurgery compares unfavorably to the obliteration rate found in adults. Therefore, in a child, when the bAVM is in a surgically reachable location, preference should be given to microsurgery. V) Repeated radiosurgery is a viable option for remnant bAVMs, although this leads to clinical deterioration in 20% of the patient population, especially when the bAVM is large. And VI) MRA is an adequate imaging modality to diagnose obliteration in the follow-up of bAVMs after radiosurgery, however, DSA remains the golden standard to diagnose complete nidus obliteration.

Chapter 10

Summary in Dutch and English

D.R. Buis

**Radiochirurgie voor intracraniële arterioveneuze malformaties:
van doelwit bepaling tot obliteratie**

Samenvatting

Hoofdstuk 1 geeft een algemene inleiding van dit proefschrift. Een intracraniële arterioveneuze malformatie (bAVM) is een netwerk, de nidus, van abnormale bloedvaten tussen de arteriële voeders en de afvoerende venen. Een bAVM wordt waarschijnlijk veroorzaakt door een structureel defect in de vorming van het primitieve arteriolaire-capillaire systeem. BAVMs zijn vrij zeldzaam: jaarlijks zijn er 1,1 tot 1,34 nieuwe patiënten per 100.000 personen. De prevalentie is vermoedelijk 18 per 100.000 personen. Wanneer deze gegevens geëxtrapoleerd worden naar de volwassen Nederlandse bevolking betekent dit dat er zich ca. 180 nieuwe patiënten per jaar presenteren, en dat er in Nederland ca. 3000 patiënten met een bAVM zijn.

De eerste manifestatie van een bAVM is bij 53 – 71% van alle patiënten een intracraniële bloeding. Andere presentaties bestaan uit epileptische insulten (30 – 40%), focale neurologisch uitval (7 – 15%) en hoofdpijn (4 – 16%).

Een bAVM wordt behandeld wanneer verwacht wordt dat het risico van de morbiditeit ten gevolge van het bAVM zelf, gedurende de rest van het leven van iedere specifieke patiënt groter is dan de door de behandeling geïnduceerde morbiditeit. Behandelingsmodaliteiten bestaan uit: microchirurgische resectie, endovasculaire embolisatie, en stereotactische radiochirurgie, of iedere combinatie van deze drie. Bij stereotactische radiochirurgie wordt een grote dosis ioniserende straling (15 – 21 Gy) in één fractie op een van te voren aangegeven stereotactisch gelokaliseerd doelwit, de nidus, toegediend. Het omliggende hersenweefsel wordt hierbij vrijwel gespaard. Door progressieve proliferatie van endotheel, en afzetting van hyaline en calcium in de wanden van de nidus, treedt er progressieve obliteratie van de nidus op. Ten gevolge hiervan is het bAVM na drie tot vier jaar niet meer doorgankelijk en is de patiënt beschermd tegen nieuwe intracraniële bloedingen.
Het eerste deel van dit proefschrift behandelt de problemen die optreden bij het intekenen van de nidus als doelwit voor radiochirurgie. Het tweede deel van dit proefschrift is gericht op de identificatie van de klinische en radiologische problemen die zich voordoen in de periode tussen radiochirurgie en de volledige obliteratie van het bAVM.

Deel I. Van spontane regressie en intekenen van het doelwit...

Spontane regressie van bAVMs is een eerder beschreven, maar zeldzaam verschijnsel. Omdat het bAVM na regressie niet meer doorgankelijk is wordt de patiënt tegen verdere bloedingen beschermd, en daarom wordt spontane regressie beschouwd als een gunstig verschijnsel. In **hoofdstuk 2** beschrijven we de pathologische, klinische en angiografische kenmerken van bAVMs die spontaan in regressie gingen. Bij een zoekactie in Embase en in de National Library of Medicine database of literature werden 38 artikelen gevonden waarin 67 patiënten bij wie zich spontane regressie van een bAVM had voorgedaan, werden beschreven. Tevens werd één van onze eigen patiënten aan deze serie toegevoegd. We toonden aan dat spontane regressie bij 72% van de patiënten optrad zonder nieuwe neurologische uitval. Bij 59% van de bAVMs die spontaan in regressie gingen was er sprake van één drainerende vene. Al met al lijkt spontane regressie het resultaat te zijn van meerdere op elkaar inwerkende factoren, waarbij de aanwezigheid van één drainerende vene een belangrijke rol lijkt te spelen. De daadwerkelijke prevalentie wordt niet geheel duidelijk, maar of deze is kleiner dan 1%, of spontane regressie wordt ernstig ondergerapporteerd.

Het doel van **hoofdstuk 3** is evaluatie van de omvang van de interobserver variatie bij het intekenen van de nidus als doelwit voor radiochirurgie, en dit speciaal met betrekking tot het nidus-volume, de ruimtelijke lokalisatie en dosimetrie. Zes waarnemers (twee radiotherapeuten, twee neurochirurgen, en twee neuroradiologen), tekenden de nidus in op beelden verkregen door middel van digitale subtractie angiografie (DSA) bij 31 patiënten met een bAVM. De DSA-beelden waren gecoregistreerd met stereotactische CT-beelden, waardoor alle contouren automatisch op de CT-beelden werden geprojecteerd. Er werden ruimtelijk afhankelijke en ruimtelijk onafhankelijke parameters bekeken. Ruimtelijke invariante parameters bestonden uit het volume van iedere contour, het gemiddelde nidus volume van alle zes waarnemers en het gemiddelde nidus volume van ieder mogelijk paar van waarnemers. Ruimtelijk variante parameters bestaan uit: VOA_6, gedefinieerd als het gemeenschappelijk overlappende volume van alle zes de intekeningen en ECV_6, gedefinieerd als het omvattende volume van alle intekeningen. De verhouding tussen de VOA en de ECV, de 'agreement-ratio' (AR) werd bepaald om de mate van overeenkomst te beoordelen. Omdat de AR afneemt naarmate het aantal waarnemers toeneemt werd deze ratio bepaald voor zowel alle zes waarnemers (dwz $AR_6 = VOA_6/ECV_6$), als voor alle mogelijke paren van waarnemers (dwz $AR_2 = VOA_2/ECV_2$). De dosimetrische consequenties van de intekeningen werden bepaald aan de hand van dosis-volume histogrammen. Er werden geen significante verschillen per waarnemer aangetoond in het volume van de intekeningen. Evenmin waren er verschillen tussen neurochirurgen, neuroradiologen, of radiotherapeuten. De gemiddelde AR was 0,45 ± 0,18 voor alle mogelijke paren van waarnemers, met een gemiddelde

absolute positie verschuiving tussen de individuele intekeningen van 2,8 ± 2,6 mm. Deze verschillen waren meer uitgesproken bij eerder, gedeeltelijk behandelde, patiënten en hadden de neiging groter te zijn in patiënten bij wie de radiochirurgische behandeling mislukte. De gemiddelde dekking van iedere individuele intekening door de voorgeschreven 80%-isodosislijn bedroeg 88,1% ± 3,2% wanneer conventionele collimatoren en 78,9% ± 4,4% wanneer 'Dynamic Conformal Arcs' werden gebruikt. We concludeerden dat interobserver-variatie bij het intekenen van bAVMs een aanzienlijke invloed kan hebben op de dosimetrie. Bovendien neemt deze invloed toe wanneer meer conforme radiochirurgische technieken worden gebruikt.

In **hoofdstuk 4** bespreken we de dosimetrische consequenties van het intekenen van de nidus op MRA. Drie waarnemers: één radiotherapeut, neurochirurg, en neuroradioloog tekenden de nidus in op MRA (V_{MRA}) en DSA (V_{DSA}). Om verplaatsingen in positie tussen de individuele contouren te kunnen bepalen werd de driedimensionale afstand (X_{DSA} en X_{MRA}) tussen het centrum van ieder volume berekend op basis van de X- (anteroposterieur), Y- (mediolateraal) en Z- (craniocaudaal) coördinaten, volgens de stelling van Pythagoras. Aan de hand van dosis-volume histogrammen werd de dekking van ieder individueel V_{MRA} door de 80%-isodosislijn bepaald. Tevens werd de dekking van V_{DSA} bepaald bij iedere intekening op V_{MRA} en vice versa. We toonden een goede interobserver variatie aan voor volume, maar een slechte interobserver variatie voor verplaatsing. Daarenboven was V_{MRA} gemiddeld groter dan V_{DSA}. De dosimetrische dekking van V_{MRA} was 62,9% wanneer V_{DSA} werd gebruikt als doelwit-volume, andersom was de dosimetrische dekking van V_{DSA} 83,5% wanneer V_{MRA} werd gebruikt als doelwit-volume. Echter, het gemiddelde volume normaal hersenweefsel binnen de 80%-isodosislijn was significant groter wanneer V_{MRA} als doelwit-volume werd gebruikt, bovendien bevonden deze volumina zich meer willekeurig in de ruimte verplaatst. Echter, voor bAVMs <3 ml, lijkt het verschil in nidus volume en het extra volume normaal hersenweefsel binnen het hoge dosisgebied klinisch niet relevant. Derhalve zou MRA voor bAVMs < 3 ml, dienst kunnen doen als primaire bron voor het intekenen van de nidus.

Deel II...naar obliteratie

In **hoofdstuk 5** worden de klinische en radiologische resultaten van radiochirurgie van bAVMs in 22 kinderen besproken. Follow-up MRI- en DSA-beelden werden geanalyseerd voor de aanwezigheid van volledige obliteratie van de nidus, of radiologische complicaties. De klinische toestand van de patiënten ten tijde van radiochirurgie en bij follow-up werd achteraf geëvalueerd en beoordeeld volgens de Modified Rankin Scale (MRS). We toonden 68% obliteratie aan na een mediane follow-up van 24 maanden. Patiënten met een 'bAVM score > 1' bereikten vaker een uitstekend resultaat (volledige obliteratie, zonder nieuwe neurologische uitval), en een volledige obliteratie dan patiënten met een 'bAVM-score > 1'. Bij één patiënt trad echter na radiochirurgie, maar vóór obliteratie een fatale bloeding op. Derhalve was er in dit cohort 1,3% kans op een bAVM gerelateerde bloeding/jaar. Daarnaast werden er bij 36% van de patiënten radiatie-geïnduceerde veranderingen op de follow-up MRI gezien na een mediaan interval van 13 maanden. Bij één patiënt resulteerde dit in late neurologische uitval. Bij kinderen lijkt het beloop na radiochirurgie voor een bAVM dus iets minder gunstig te zijn dan bij volwassenen. Bovendien zijn de uitkomsten na radiochirurgie ongunstig in vergelijking met recente uitkomsten na microchirurgie door ervaren neurochirurgen. Ouders dienen hierover voor de behandeling te worden geïnformeerd. Hoewel radiochirurgie een laag-invasieve behandeling is bestaat er een klein risico op neurologische verslechtering op lange termijn ten gevolge van radiatie-geïnduceerde schade. Dit risico is echter klein in vergelijking met het risico op een intracerebrale bloeding op langere termijn, m.n. wanneer het bAVM zich in een eloquente lokatie bevindt.
Na radiochirurgie wordt bij veel patiënten op MRI-beelden hyperintensiteit op de T_2-sequentie gezien. Soms bevinden deze veranderingen zich ver buiten het eigenlijke doelgebied, waarbij er ook neurologische uitval optreedt

Het doel van **hoofdstuk 6** is de evaluatie van de oorzaak van deze uitgebreide perinidale witte stof afwijkingen. De pre- en postradiochirurgische MRI- en DSA-beelden van 30 patiënten met perinidale hyperintensiteit op de T_2-sequentie werden geanalyseerd. Bij veertien patiënten werd er hyperintensiteit waargenomen ver buiten de 10-Gy isodose-lijn. Bij deze patiënten was er vaker één drainerende vene aanwezig. In deze groep werd bij 88% volledige obliteratie bereikt. Daarentegen werd in de groep met milde afwijkingen op de T_2-sequentie bij slechts 50% volledige obliteratie bereikt. Het lijkt aannemelijk dat de hyperintensiteit op T_2-sequenties welke zich tot ver buiten de hoge dosis regio uitstrekken, worden veroorzaakt door geleidelijke veneuze occlusie van de nidus, voor afsluiting van de arteriële toevoer, hetgeen daarom leidt tot congestie. Zulke veranderingen zijn mogelijk gerelateerd aan trombose van de drainerende vene vóór het moment van arteriële obliteratie.

Het doel van radiochirurgie van bAVMs is het bereiken van volledige obliteratie van de nidus. Dit slaagt bij 70 à 80% van alle patiënten. Er blijft dus een aanzienlijke groep patiënten over bij wie eerdere radiochirurgie mislukte. Deze patiënten worden meestal opnieuw behandeld, bijvoorbeeld door wederom radiochirurgie toe te passen. In **hoofdstuk 7** evalueren we de klinische en radiologische resultaten van herhaalde radiochirurgie bij vijftien patiënten, bij wie een eerdere radiochirurgische behandeling niet tot obliteratie leidde. Naast het klinische beloop in tijd op momenten S1 (eerste radiochirurgie), S2 (tweede

radiochirurgie) en FU (laatste contact) werden de MRI-beelden onafhankelijk beoordeeld op de aanwezigheid van volledige obliteratie, een (recidief) bloeding, of radiologische complicaties. Volledige obliteratie werd bereikt bij negen patiënten, na een mediane tijd van 50 maanden na S2. In 47% werd een optimale situatie bereikt, waarbij het bAVM volledig oblitereerde en zich geen nieuwe neurologische complicaties voordeden. Bij elf van de vijftien patiënten was er een Modified Rankin Score van ≤ 1. Echter bij drie patiënten traden stralings-geïnduceerde complicaties, bestaande uit permanente neurologische uitval, op. Bij twee van de drie patiënten vingen de complicaties aan na S2. Ondanks gezamenlijk 137 risicojaren waarin patiënten waren blootgesteld aan het risico op intracraniële bloedingen deed dit zich niet voor.
De gouden standaard voor het beoordelen van complete obliteratie van de nidus is DSA. Bij het ondergaan van een DSA bestaat er een klein risico op neurologische schade. In hoofdstuk 8 werd geëvalueerd of MRI/MRA betrouwbaar kan worden gebruikt om obliteratie te voorspellen, en of MRI/MRA DSA kan vervangen in de follow-up na radiochirurgie. Hiertoe werden de MRI/MRA beelden vóór en na radiochirurgie met elkaar vergeleken. De doorgankelijkheid van de nidus werd door drie beoordelaars, waaronder twee ervaren neuroradiologen, op een vijfpuntsschaal beoordeeld, en vergeleken met de gouden standaard: de DSA na radiochirurgie. Met een ROC-analyse werd voor alle waarnemers een oppervlakte onder de curve van 0.85 – 0.86 aangetoond. De positieve en negatieve voorspellende waarden voor 'echte obliteratie', gedefinieerd als een niet-doorgankelijke, of een waarschijnlijk niet doorgankelijke nidus varieerden respectievelijk tussen 0.89 – 0,93 en 0,63 – 0,70. Met MRI/MRA werd obliteratie fout gediagnosticeerd in 16%. Omgekeerd werd obliteratie gemist in 21%. Derhalve lijkt MRI/MRA een adequaat onderzoek om obliteratie na radiochirurgie aan te tonen. Wanneer er geen duidelijke obliteratie op MRI/MRA wordt gezien, is het niet zinvol om al een DSA onderzoek te laten verrichten teneinde obliteratie aan te tonen. Met inachtneming van de zeer ernstige consequenties die het fout diagnosticeren van obliteratie kan hebben is het zinvol om uiteindelijk DSA te gebruiken om obliteratie aan te tonen.

In **Hoofdstuk 9** worden nieuwe ontwikkelingen besproken die kunnen worden gebruikt om de mate van interobserver variatie bij het intekenen van bAVMs te verkleinen. Daarnaast worden methoden besproken die het interval tussen radiochirurgie en het bereiken van volledige obliteratie verkorten.
In de **Appendix** wordt een methode gepresenteerd die mogelijk de hierboven genoemde interobserver variatie kan verkleinen. Deze methode maakt gebruik van verschillende kleuren waarmee de tijd dat contrast aankomt op elke locatie in de cerebrale vasculatuur wordt gecodeerd in één afbeelding. Door middel van deze kleur-gecodeerde beelden is het beter mogelijk om arteriën van venen te onderscheiden, zelfs wanneer deze over de nidus heen zijn geprojecteerd. Mogelijk kan gebruik van deze methode leiden tot minder interobserver-variatie bij het intekenen van bAVMs.

Radiosurgery of brain arteriovenous malformations:
from target delineation to obliteration

Summary

Chapter 1 provides a general introduction for this thesis entitled 'Radiosurgery of Brain Arteriovenous Malformations. From target delineation towards obliteration'. A brain arteriovenous malformation (bAVM) is a network, the nidus, of abnormal channels between the arterial feeders and the draining veins. A bAVM is caused by a structural defect in the formation of the primitive arteriolar-capillary system. They are quite rare, with an annual new number of patients presenting with a bAVM varying between 1.1 and 1.34 per 100.000 person-years. The prevalence is thought to be 18 per 100.000 persons. Extrapolating these data to the adult population of the Netherlands, this frequency estimates approximately 180 new patients each year, and 3000 prevalent patients alive with a bAVM at any given day.

An intracerebral hemorrhage is the main mode of presentation for a bAVM[1, 6, 71, 7, 8], with around 53 - 71 percent of all patients presenting with an initial hemorrhage. Seizures are the second most common form of presentation. Approximately 30 – 40 percent of bAVMs presents with epileptic seizures. Headache is the presenting symptom in 4 – 16 percent of patients. Focal neurological deficits are reported in 7 – 15 percent.

Treatment of a bAVM is indicated when the risk incurred during the natural history of a specific bAVM in a specific patient is expected to be higher than the risk of treatment-induced neurological morbidity. Modalities for treatment of a bAVM include microsurgical resection, endovascular embolization, and stereotactic radiosurgery, or any combination of these three. Stereotactic radiosurgery uses stereotactic localization coupled with the delivery of a large, single fraction dose of ionizing radiation onto the bAVM. Its goal is to obliterate the bAVM after an interval of three to four years, while sparing adjacent and distant normal brain tissue.
The first part of this thesis focuses on problems in conjunction with delineating bAVMs for the purpose of radiosurgery. The second part of this thesis aims to identify the clinical and radiological problems that occur in the interval between radiosurgery and complete obliteration of the bAVM.

Part I. From target delineation...

Spontaneous regression of bAVMs is a well recognized, but rare phenomenon, which is considered to have a favourable outcome as it prevents a bAVM from (re)rupturing. In **Chapter 2** we investigated the pathological, clinical and angiographical features of bAVMs that regressed spontaneously in order to identify predictors that a bAVM is likely to regress spontaneously. A search in Embase and the National Library of Medicine database of literature revealed 38 articles since 1955 in which 67 patients were described in whom spontaneous regression of a bAVM had occurred were described since 1955. We added one of our own patients and found that regression occurred in 72% without new neurological deficits, and that regression occurs in bAVMs that have a single draining vein in 59%. Spontaneous regression is the result of multiple interacting factors, in which the presence of a single draining vein may play an important role. We concluded that the true prevalence of spontaneous regression remains unknown, but it is thought either to be less than 1%, or is seriously underreported.

The objective of **Chapter 3** was to evaluate the extent of interobserver variations with respect to volume, spatial localization, and dosimetry in a cohort of patients with a bAVM treated by radiosurgery and correlated our findings with the clinical outcome. Six observers (two radiation oncologists, two neurosurgeons, and two neuroradiologists), contoured the nidus on 31 DSAs, co-registered with the stereotactic CT scan. Because all DSAs were co-registered with the stereotactic planning CT scans, all contours were automatically projected onto the CT images. Spatial invariant parameters studied were the mean contoured volume of all six clinicians and the mean volume of each possible pair of observers. The following spatial variant parameters were determined: VOA_6, defined as the common overlapping volume of all six target volumes, and ECV_6, defined as the encompassing volume of all six target volumes. The ratio between the VOA and the ECV, i.e. the agreement ratio (AR), was taken as a measure of the interobserver agreement. This ratio was determined for all six target volumes (i.e., AR6 = VOA_6/ECV_6), as well as for all possible pairs of observers (i.e., AR2 = mean VOA_2/ECV_2), because this ratio tends to decrease with an increasing number of observers. Dose–volume histograms were used to evaluate the dosimetric consequences of contouring variations. We found no significant differences in the size of contoured target volumes among the observers, or among the neurosurgeons, neuroradiologists, or radiation oncologists. The mean agreement ratio was 0.45 ± 0.18 for all possible pairs of observers. The mean absolute positional shift between individually contoured volumes was 2.8 ± 2.6 mm. These differences were more marked in previously treated groups and tended to be more pronounced in those with treatment failure. The mean coverage of the individual volumes by the 80% prescription isodose was 88.1% ± 3.2% using conventional collimators and 78.9% ± 4.4% using dynamic conformal arcs. We concluded that interobserver variation in contouring can have a significant impact on the dosimetry of radiosurgery for bAVMs. This impact increases when more conformal radiosurgical techniques are used.

In **Chapter 4** we assessed the dosimetric consequences of nidus delineation on MRA for the purpose of stereotactic radiosurgery. Three clinicians, one radiation-oncologist, neurosurgeon, and neuroradiologist, individually contoured the nidus on DSA (V_{DSA}) and on MRA (V_{MRA}). To determine positional shifts between individual contours, the 3D distance (X_{DSA} and X_{MRA}) between the center of each individual target volume and the centroid was calculated from the X (anteroposterior), Y (mediolateral), and Z (craniocaudal) coordinates using Pythagoras' algorithm. Dose–volume histograms were used to determine the coverage of each individual V_{MRA} by the 80% prescription isodose when planning was performed using V_{DSA}. Alternatively, the coverage of V_{DSA} was determined when planning was performed on each V_{MRA}. The interobserver variation was 'fair' for target volume, but 'poor' for displacement. Moreover, V_{MRA} was larger than V_{DSA}. No difference in displacement was found. Dosimetric coverage of V_{MRA} was 62.9% when V_{DSA} was used as planning target volume, and coverage of V_{DSA} was 83.5% when V_{MRA} was used for planning. The mean volume of normal brain within the 80% isodose was larger when the bAVM was delineated on MRA. We concluded that bAVMs delineated on MRA are larger and more randomly displaced. However, for bAVMs <3 ml, the difference in volume of normal brain tissue within the high-dose region does not seem to be clinically relevant.

Part II. ...towards obliteration

In **Chapter 5** we evaluate the clinical and radiological outcome after radiosurgery of bAVMs in 22 pediatric patients. Follow-up MRI and DSA images were reviewed for the presence of complete obliteration, or radiological complications. The patients' clinical condition at time of radiosurgery and at follow-up was retrospectively reviewed and classified according to the Modified Rankin Scale (MRS). The crude complete obliteration-rate was 68% after a median follow-up of 24 months. Patients with a radiosurgery based bAVM score ≤ 1 had an excellent outcome more frequently than patients with a bAVM-score > 1, as well as an increased obliteration-rate. However, one patient suffered a fatal hemorrhage, representing a post-radiosurgery hemorrhage rate of 1.3%/year for the complete follow-up. Radiation-induced changes on follow-up MRI were seen in 36 % after a median interval of 13 months. These changes resulted in a delayed persisting neurological deficit in one patient. We concluded that when a treatment decision is taken, parents should be informed that in children the obliteration rate probably compares unfavourably to the obliteration rate

found in adults, and the overall outcome after radiosurgery compares unfavourably to those in recent pediatric microsurgical series. And that, although radiosurgery is a relatively low-invasive treatment, there is a small, but long-term risk of neurological deterioration due to radiation toxicity, especially when the bAVM is in a highly eloquent or deep location. This risk is however, much lower than the risk of a neurological devastating hemorrhage in the long term, when no treatment is given at all.

After radiosurgery perinidal T_2-hyperintensity on MRI is seen in many patients. However, sometimes such changes occur in the white matter far beyond the target area, and these may be associated with new neurological symptoms. The purpose of **Chapter 6** was to evaluate the cause of these extensive perinidal white matter changes. The pre- and postradiosurgical magnetic resonance imaging and angiographic studies of 30 patients with T_2 high-signal-intensity changes surrounding a bAVM were analyzed retrospectively. We found high-signal-intensity changes far beyond the 10-Gy isodose area in fourteen patients. A single draining vein was more often present in these patients as well. Obliteration was achieved in 88% of these fourteen patients with extensive signal intensity changes, as opposed to eight of sixteen patients in the other group. We concluded that hyperintensity changes that extend far beyond the high-dose region on T_2-sequences are caused by a progressive venous occlusion before arterial obliteration, leading to congestion. Such changes are most likely related to premature thrombosis of draining veins before arterial obliteration.

The purpose in treating bAVMs is complete obliteration of the nidus. Using radiosurgery this succeeds in between 70 – 80%. Therefore a substantial cohort of patients needs retreatment, which may consist of repeated radiosurgery. In **Chapter 7** we evaluate the clinical and radiological outcome in fifteen patients who underwent repeated radiosurgery after failure of initial radiosurgery. The patients' demographic data at the time of first (S1) and second (S2) radiosurgery, and at last follow-up (FU) were reviewed. MR images were independently reviewed for the presence of complete obliteration, a new hemorrhage or radiological complications. Complete obliteration was reached in nine patients (60%). Median time to obliteration was 50 months after S2. An excellent outcome (no new neurologic deficiencies, complete obliteration) was reached in 47%. Eleven patients (73%) showed a MRS ≤ 1. Radiation-induced complications occurred in 20%, of which 13% occurred after S2. No (re-)bleedings were encountered during 137-patient years
at risk

The gold standard for diagnosing complete obliteration is DSA. DSA has a low, but definite risk of neurological complications. Therefore in **Chapter 8** we assessed if MRI/MRA can be used reliably to predict obliteration, and if MRI/MRA can replace DSA in the follow-up after radiosurgery. From a cohort of 120 patients three independent observers were asked to comment on the patency of the bAVM on follow up MR images and DSA images after stereotactic radiosurgery on a five point scale of confidence. Consensus reading of the post radiosurgery DSA was considered the gold standard for assessment of nidus patency. Using ROC analysis the area under curve for all three observers was 0.85 – 0.86 indicating similar diagnostic performance for all three observers. The positive and negative predictive values for 'true obliteration', defined as a not patent, or probably not patent nidus, varied between 0.89 – 0.93 and 0.63 – 0.70, respectively. Using MRI/MRA obliteration was falsely diagnosed in 16%, conversely obliteration was missed in 21%. We concluded that MRI is an adequate investigation to diagnose obliteration in the follow-up of bAVMs after radiosurgery. When there is doubt about the presence of obliteration on MRI/MRA it is probably not useful to perform a DSA yet. Regarding the potential consequences of misdiagnosing a patent nidus we highly recommend follow-up DSA for definitive diagnosis of complete obliteration.

In **Chapter 9** new developments which may be used to decrease the amount of interobserver variation when delineating bAVMs are discussed and it elaborates further on different ways and future developments which may decrease the interval between delineation and obliteration.

In the **Appendix** a method is presented that may decrease the aforementioned interobserver variation. This method uses different colors to codes the time that contrast arrives at any location in the brain vasculature in a single composite image. The use of such color-coded images could enhance the discrimination of the nidus from feeding arteries and draining veins, even when these are projected over the nidus, which may improve the target definition for radiosurgery of bAVMs.

Chapter 11

Appendix: Color Intensity Projections of Digital Subtraction Angiography

K.S. Cover
F.J. Lagerwaard
R. van den Berg
D.R. Buis
B.J. Slotman

Adapted from: Cover KS, Lagerwaard FJ, van den Berg R, Buis DR, Slotman BJ. Color intensity projection of digitally subtracted angiography for the visualization of brain arteriovenous malformations. Neurosurgery. 2007 Mar;60(3):511-4; discussion 514-5.

Abstract

Objective

Reliable and rapid delineation of arteriovenous malformations enables the application of effective treatments such as stereotactic radiosurgery. We describe a new method to improve the speed and reliability of visualizing the flow of contrast images with digital subtraction angiography.

Methods

In line with current practices, digital subtraction angiography was used to produce a sequence of grayscale images. The new method combines the standard grayscale images produced by digital subtraction angiography into a single composite color image that encodes the contrast arrival time at each point of the brain's circulatory system. The algorithm is simple, fast, and easy to implement.

Results

The technique allows the flow of contrast from a series of angiography images to be summarized in a single color image.

Conclusion

This visualization method promises to improve the speed of manual delineation of arteriovenous malformations. Further studies are required to evaluate the clinical value of the use of color intensity projection images, supplemented by grayscale images as necessary, in comparison with contouring on grayscale images only.

Key words

Angiography • Intracranial arteriovenous malformations • Maximum intensity projections • Radiosurgery • Stereotactic techniques

Introduction

Stereotactic radiosurgery is an established modality for the treatment of brain arteriovenous malformations (bAVM). Accurate target definition of the bAVM nidus is essential to ensure full coverage of the nidus by the high-dose region of radiation and, equally important, to limit radiation exposure to surrounding healthy brain tissue[58, 132, 138, 250, 371, 399]. Although bAVMs can be visualized with three-dimensional imaging techniques such as computed tomographic angiography and magnetic resonance angiography (MRA), these modalities lack the temporal information that is essential for discriminating the bAVM nidus from feeding arteries and draining veins. Because stereotactic digital subtraction angiography (DSA) series provide temporal information regarding the filling of the brain vasculature, this technique is still considered the 'gold standard' for contouring bAVMs for the purpose of radiosurgery[331].

In clinical practice, detailed examination of numerous consecutive DSA images is needed to study the various components of the bAVM. Usually, a single early phase of DSA is selected for delineation of the nidus in the radiosurgery planning system. However, practical considerations limit the reliability of contouring the bAVM in a single biplanar DSA phase because not all shunt areas in the nidus exhibit the same pace of flow and, more importantly, because biplanar DSA is a two-dimensional imaging modality, overprojecting arteries and veins may sometimes obscure the actual bAVM nidus. This can result in significant intra- and interobserver variations in contouring[58].

In this article, we present a simple but effective method for color coding the time that contrast arrives at any location in the brain vasculature in a single composite image. The method, arrival-time color intensity projection (CIP), combines the information contained in a number of sequential DSA images into a single composite color image. This composite image represents the arrival time of contrast at each pixel with each pixel's hue, brightness, and saturation conveying the intensity and intensity variation, respectively, of the pixel over the DSA component images. The use of color-coded images could enhance the discrimination of the bAVM nidus from feeding arteries and draining veins, even when these are projected over the nidus, which may improve the target definition for radiosurgery of bAVMs.

Methods

The method for summarizing the contrast arrival time in a single color image is based on the percentage-time CIP algorithm, which was developed to simplify and speed up the analysis of the mobility of lung tumors[86]. In percentage-time CIP, the hue of the color is used to encode the percentage of time there is tissue in a particular location. Before applying the percentage-time algorithm to a series of DSA images, a new image sequence must be calculated from the original DSA, which simulates a continuous flow of contrast after the contrast injection has started.

This new image sequence represents a cumulative minimum intensity projection (MinIP) sequence of all DSA images and is simple to calculate. The first image of the cumulative MinIP sequence is the first image of the original DSA image sequence. The second image of the cumulative MinIP sequence is the pixel-by-pixel minimum of the first two images of the original DSA image sequence. The third image of the cumulative MinIP sequence is the pixel-by-pixel minimum of the first three images of the original DSA image sequence. Following the same pattern, all images of the cumulative MinIP sequence can be easily calculated (Figure 11.1).

Finally, the arrival-time CIP composite image is derived by applying the percentage-time CIP algorithm to this cumulative MinIP sequence. Although the percentage-time CIP algorithm has been presented in detail previously[86], it is also presented here for convenience. The first step is to scale the pixel values of the cumulative MinIP sequence to values between 0 and 1. This new image sequence, the normalized cumulative MinIP sequence, is calculated by dividing each pixel in each cumulative MinIP image by the maximum value of all pixels in all images. The second step is to calculate, on a pixel-by-pixel basis, the maximum (MaxIP), mean (MeanIP), and minimum (MinIP) of the normalized cumulative MinIP sequence. The MaxIP, MeanIP, and MinIP are then combined on a pixel-by-pixel basis with the following equations to determine the hue, saturation, and brightness of the composite color image:

- Brightness = MaxIP
- Saturation = (MaxIP - MinIP)/MaxIP
- Hue = $^{2}/_{3} \times$ (MeanIP - MinIP)/(MaxIP - MinIP)

The hue, saturation, and brightness for each pixel is then converted to the standard red, green, and blue presentation of color using widely available subroutines. Applying this method to the cumulative MinIP sequence results in the arrival-time CIP composite image. Early phases of the DSA series appear in red, intermediate phases appear in yellow, and late phases appear in green and blue (Figure 11.2). If desired, the saturation can be multiplied by a constant larger than unity before conversion to red, green, and blue. This will distinguish the colors more conspicuously on the composite image. In addition, the hue may be scaled to emphasize early, mid, or late arrival times. The arrival time CIP images were calculated on an AMD Duron processor (Advanced Micro Devices, Inc., Sunnyvale, CA) running at 1 GHz and took less than 10 seconds to calculate.

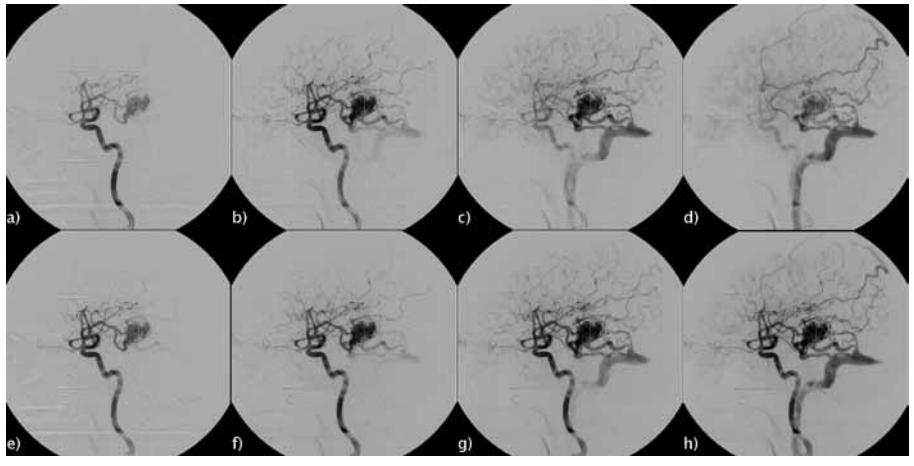

Figure 11.1
Regularly spaced images from the original DSA sequence (**A–D**) and the cumulative MinIP images at the corresponding times (**E–H**). As expected, the contrast seen entering in the brain in A does not appear in C or D, but does appear in all of the cumulative MinIP images (**E–H**).

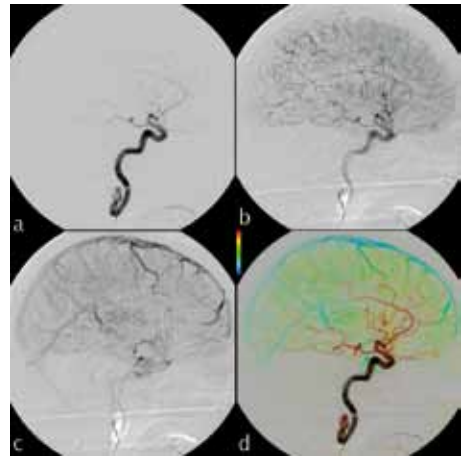

Figure 11.2
Early (**A**), intermediate (**B**), and late (**C**) single phases of a DSA study. The corresponding composite CIP image (**D**) illustrates the color differentiation of the temporal information.

Results

The generation of arrival-time CIP images is illustrated with two patients.

Illustrative cases

Patient 1

The first patient is a 46-year-old man who experienced epilepsy as a result of a Spetzler-Martin Grade II bAVM feeding from the middle cerebral artery in the left temporal lobe of the brain. For the purpose of stereotactic irradiation of this bAVM, selective angiography of the left internal carotid artery was performed at a frame rate of six images per second. The sequential DSA images and the cumulative MinIP sequence of this patient are shown in Figure 11.1. The corresponding arrival-time CIP image is shown in Figure 11.3, with the color bar in the upper left corner indicating the ordering of colors; red indicates the earliest arrival time, and blue indicates the latest arrival time. For generation of this CIP image, the saturation was multiplied by 1.5 and any resulting saturation values greater than 1 were set to 1. In addition, the hue values were windowed between 0.2 and 0.8, indicating that hue values of 0.2 or less were set to 0, values of 0.8 and above were set to 1, and values between 0.2 and 0.8 were linearly scaled to between 0 and 1. The red color of the bAVM and feeding middle cerebral artery (bright red) can be clearly distinguished from the early draining vein of Labbé (yellow) and late draining veins and sinus (green and blue).

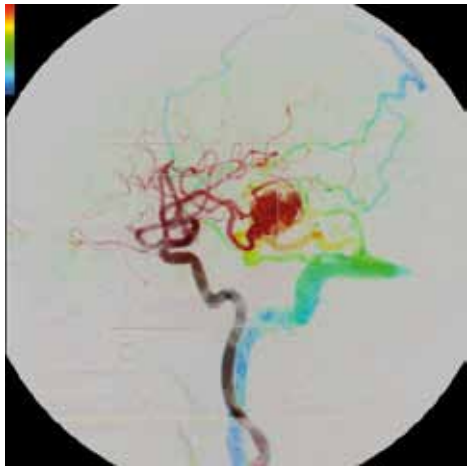

Figure 11.3
Arrival-time CIP image of the DSA images shown in Figure 11.1. The color bar in the upper right corner shows the ordering of the colors, with red indicating the earliest arrival time and blue indicating the latest. The progress of the contrast from the feeding arteries (red), through the bAVM (bright red), on to the early (yellow) and late (green and blue) draining veins is illustrated.

Patient 2

The second patient illustrates the potential impact of the use of arrival-time CIP images for delineating the bAVM for the purpose of high-precision radiosurgery. This 52-year-old patient developed focal epilepsy in the right leg as a result of a small Spetzler-Martin Grade I bAVM. Before stereotactic treatment, DSA of the left internal carotid artery was performed. Figure 11.4 shows the arrival-time CIP of the DSA, feeding of the bAVM by the left pericallosal artery, and drainage into the superior sagittal sinus. The top panel shows the initial contouring of the bAVM in the treatment planning system by the treating clinician, which can only be performed on a single grayscale DSA image. The bottom panel shows the subsequent contouring of the bAVM on the arrival-time CIP image. When comparing the contour derived from a single grayscale DSA image with the contour from a CIP image, using the full set of grayscale DSA images as the standard of reference, the smaller contour derived from the CIP image seemed more appropriate. The color coding of the CIP enabled the differentiation of the vein from the nidus. Because computed tomographic angiography and MRA lack the temporal resolution of DSA series, this differentiation could not be obtained using these three-dimensional imaging techniques. The detail of the bAVM shows that the more posterior part of the originally contoured target volume actually consists of looping feeding arteries and draining veins. In this case, the additional information from the CIP image led to a smaller radiosurgery target volume and potentially less toxicity of the stereotactic treatment.

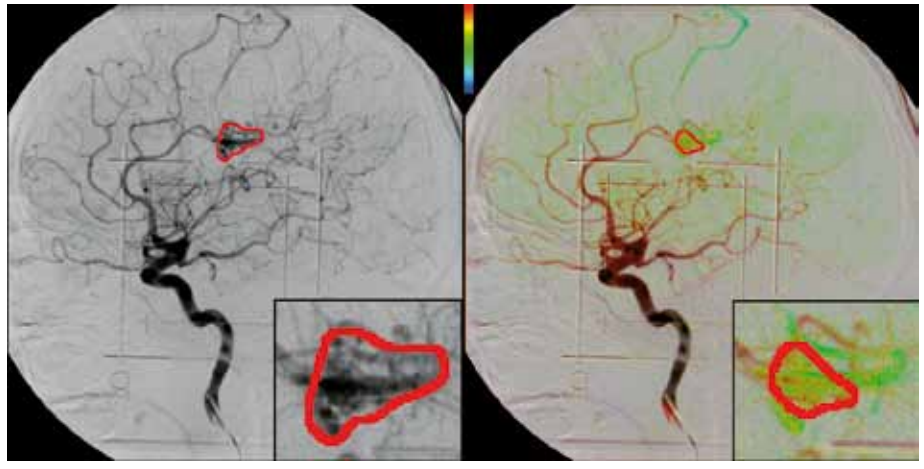

Figure 11.4
Example of the advantages of contouring an bAVM on an arrivaltime CIP image over DSA images. The arrival-time CIP enables the contour to be drawn smaller with much more confidence compared with the routinely used grayscale image.

Discussion

The use of CIP images that summarize all temporal information of a DSA series within a single composite image may have an advantage over the use of a single early phase image of the DSA for stereotactic treatment planning. The overprojection of feeding arteries and enlarged draining veins can obscure the boundaries of the bAVM nidus on conventional biplanar angiography series. However, these can be better discriminated on CIP images. It remains to be determined whether or not the CIP display technique, supplemented by the series of grayscale images as necessary, can diminish intra- and interobserver variations in contouring bAVMs, which can be substantial. The latter is the subject of ongoing research at our center.

Although the arrival-time CIP algorithm has been demonstrated for imaging the flow of contrast in the brain, it has potential applications in a wide range of fields in which there is a need to summarize the changes over a series of grayscale images in a single color image. Some possible fields of application include other medical imaging modalities, astronomy, engineering, and geophysics.

References

1. Abdulrauf SI, Malik GM, Awad IA: Spontaneous angiographic obliteration of cerebral arteriovenous malformations. **Neurosurgery 44**:280-287, 1999
2. Abu-Salma Z, Nataf F, Ghossoub M, et al: The protective status of subtotal obliteration of arteriovenous malformations after radiosurgery: significance and risk of hemorrhage. **Neurosurgery 65**:709-717, 2009
3. Achrol AS, Pawlikowska L, McCulloch CE, et al: Tumor necrosis factor-alpha-238G>A promoter polymorphism is associated with increased risk of new hemorrhage in the natural course of patients with brain arteriovenous malformations. **Stroke 37**:231-234, 2006
4. Akakin A, Ozkan A, Akgun E, et al: Endovascular treatment increases but gamma knife radiosurgery decreases angiogenic activity of arteriovenous malformations: an in vivo experimental study using a rat cornea model. **Neurosurgery 66**:121-129, 2010
5. Al-Shahi R, Bhattacharya JJ, Currie DG, et al: Prospective, population-based detection of intracranial vascular malformations in adults: the Scottish Intracranial Vascular Malformation Study (SIVMS). **Stroke 34**:1163-1169, 2003
6. Al-Shahi R, Fang JS, Lewis SC, et al: Prevalence of adults with brain arteriovenous malformations: a community based study in Scotland using capture-recapture analysis. **J Neurol Neurosurg Psychiatry 73**:547-551, 2002
7. Al-Shahi R, Pal N, Lewis SC, et al: Observer agreement in the angiographic assessment of arteriovenous malformations of the brain. **Stroke 33**:1501-1508, 2002
8. Al-Shahi R, Warlow CP: Interventions for treating brain arteriovenous malformations in adults. **Cochrane Database Syst Rev**CD003436, 2006
9. Al-Shahi R, Stapf C: The Prognosis and Treatment of Arteriovenous Malformations of the Brain. **Pract Neurol 5**:194-205, 2005
10. Ali MJ, Bendok BR, Rosenblatt S, et al: Recurrence of pediatric cerebral arteriovenous malformations after angiographically documented resection. **Pediatr Neurosurg 39**:32-38, 2003
11. Altschuler EM, Lunsford LD, Coffey RJ, et al: Gamma knife radiosurgery for intracranial arteriovenous malformations in childhood and adolescence. **Pediatr Neurosci 15**:53-61, 1989
12. Amendola BE, Wolf A, Coy SR, et al: Radiosurgery for Intracranial Arteriovenous Malformations in Children. **Radiosurg 3**:159-164, 2000
13. Andaluz N, Myseros JS, Sathi S, et al: Recurrence of cerebral arteriovenous malformations in children: Report of two cases and review of the literature. **Surg Neurol 62**:324-330, 2004

14. Andrade-Souza YM, Ramani M, Beachey DJ, et al: Liquid embolisation material reduces the delivered radiation dose: a physical experiment. **Acta Neurochir (Wien) 150**:161-164, 2008
15. Andrade-Souza YM, Ramani M, Scora D, et al: Embolization before radiosurgery reduces the obliteration rate of arteriovenous malformations. **Neurosurgery 60**:443-451, 2007
16. Angelie E, Oost ER, Hendriksen D, et al: Automated contour detection in cardiac MRI using active appearance models: the effect of the composition of the training set. **Invest Radiol 42**:697-703, 2007
17. Anzalone N, Scomazzoni F, Strada L, et al: Intracranial vascular malformations. **Eur Radiol 8**:685-690, 1998
18. Aoki S, Yoshikawa T, Hori M, et al: MR digital subtraction angiography for the assessment of cranial arteriovenous malformations and fistulas. **AJR Am J Roentgenol 175**:451-453, 2000
19. Aoyama H, Shirato H, Katoh N, et al: Comparison of imaging modalities for the accurate delineation of arteriovenous malformation, with reference to stereotactic radiosurgery. **Int J Radiat Oncol Biol Phys 62**:1232-1238, 2005
20. Aoyama H, Shirato H, Nishioka T, et al: Treatment outcome of single or hypofractionated single-isocentric stereotactic irradiation (STI) using a linear accelerator for intracranial arteriovenous malformation. **Radiother Oncol 59**:323-328, 2001
21. ApSimon HT, Reef H, Phadke RV, et al: A population-based study of brain arteriovenous malformation: long-term treatment outcomes. **Stroke 33**:2794-2800, 2002
22. Asahi M, Wang X, Mori T, et al: Effects of matrix metalloproteinase-9 gene knock-out on the proteolysis of blood-brain barrier and white matter components after cerebral ischemia. **J Neurosci 21**:7724-7732, 2001
23. Auzou P, Callonnec F, Hannequin D, et al: [Spontaneous thrombosis of cerebral arteriovenous malformation]. **J Radiol 78**:219-222, 1997
24. Ayad M, Eskioglu E, Mericle RA: OnyxR: a unique neuroembolic agent. **Expert Rev Med Devices 3**:705-715, 2006
25. Back AG, Vollmer D, Zeck O, et al: Retrospective analysis of unstaged and staged Gamma Knife surgery with and without preceding embolization for the treatment of arteriovenous malformations. **J Neurosurg 109 Suppl**:57-64, 2008
26. Bahram A, Bitaraf MA, Mavroidis P, et al: Vascular structure and binomial statistics for response modeling in radiosurgery of cerebral arteriovenous malformations. **Phys.Med. Biol. 55**:2057, 2010 (Abstract)
27. Barker CS, Anslow PL: Spontaneous thrombosis of a cerebral arteriovenous malformation. **Clin Radiol 42**:130-132, 1990
28. Barker FG, Butler WE, Lyons S, et al: Dose-volume prediction of radiation-related complications after proton beam radiosurgery for cerebral arteriovenous malformations. **J Neurosurg 99**:254-263, 2003

29. Bednarz G, Downes MS, Werner-Wasik M, et al: Combining stereotactic angiography and 3D time-of-flight magnetic resonance angiography in treatment planning for arteriovenous malformation radiosurgery. **Int J Radiat Oncol Biol Phys 46**:1149-1154, 2000
30. Beijnum Jv, Worp HBvd, Schippers HM, et al: Familial occurrence of brain arteriovenous malformations: a systematic review. **J Neurol Neurosurg Psychiatry 78**:1213-1217, 2007
31. Bendszus M, Koltzenburg M, Burger R, et al: Silent embolism in diagnostic cerebral angiography and neurointerventional procedures: a prospective study. **Lancet 354**:1594-1597, 1999
32. Berenstein A, Lasjaunias P, TerBrugge KG: Cerebral vascular malformations: incidence, classification, angioarchitecture, and symptomatology of brain arteriovenous and venous malformations., in Berenstein A, Lasjaunias P, TerBrugge KG (eds): **Surgical Neuroangiography 2.2 Clinical and endovascular treatment aspect in adults.** Berlin: Springer Verlag, 2004, pp 609-694
33. Berg Rvd, Buis DR, Lagerwaard FJ, et al: Extensive white matter changes after stereotactic radiosurgery for brain arteriovenous malformations: a prognostic sign for obliteration? **Neurosurgery 63**:1064-1069, 2008
34. Berger MO, Anxionnat R, Kerrien E, et al: A methodology for validating a 3D imaging modality for brain AVM delineation: Application to 3DRA. **Comput Med Imaging Graph 32**:544-553, 2008
35. Bernstein M, Ginsberg H, Glen J: Protection of iodine-125 brachytherapy brain injury in the rat with the 21-aminosteroid U-74389F. **Neurosurgery 31**:923-927, 1992
36. Bhattacharya J.J., Luo C.B., Suh D.C., et al: Wyburn-Mason or Bonnet-Dechaume-Blanc as Cerebrofacial Arteriovenous Metameric Syndromes (CAMS): A new concept and a new classification. **Interv Neuroradiol 7**:5-17, 2001
37. Bidaut LM, Laurent C, Piotin M, et al: Second-generation three-dimensional reconstruction for rotational three-dimensional angiography. **Acad Radiol 5**:836-849, 1998
38. Blamek S, Boba M, Larysz D, et al: The Incidence of Imaging Abnormalities after Stereotactic Radiosurgery for Cerebral Arteriovenous and Cavernous Malformations, **Brain Edema XIV.** Wien: Springer Vienna, 2009, pp 187-190
39. Blanchard N, Bernier V, Anxionnat R, et al: [Radiosurgery of cerebral arteriovenous malformations: a prescription algorithm]. **Cancer Radiother 13**:1-10, 2009
40. Blatt DR, Friedman WA, Bova FJ: Modifications based on computed tomographic imaging in planning the radiosurgical treatment of arteriovenous malformations. **Neurosurgery 33**:588-595, 1993
41. Bogren H, Svalander C, Wickbom I: Angiography in intracranial cavernous hemangiomas. **Acta Radiol Diagn (Stockh) 10**:81-89, 1970

42. Bollet MA, Anxionnat R, Buchheit I, et al: Efficacy and morbidity of arc-therapy radiosurgery for cerebral arteriovenous malformations: a comparison with the natural history. **Int J Radiat Oncol Biol Phys 58**:1353-1363, 2004
43. Bova FJ, Friedman WA: Stereotactic angiography: an inadequate database for radiosurgery? **Int J Radiat Oncol Biol Phys 20**:891-895, 1991
44. Bowden P, Fisher R, Mac Manus M, et al: Measurement of lung tumor volumes using three-dimensional computer planning software. **Int J Radiat Oncol Biol Phys 53**:566-573, 2002
45. Brennan RL: **Generalizability theory**. New York: Springer Verlag, 2010,
46. Brenner DJ, Martel MK, Hall EJ: Fractionated regimens for stereotactic radiotherapy of recurrent tumors in the brain. **Int J Radiat Oncol Biol Phys 21**:819-824, 1991
47. Bridcut RR, Winder RJ, Workman A, et al: Assessment of distortion in a three-dimensional rotational angiography system. **Br J Radiol 75**:266-270, 2002
48. Bristol RE, Albuquerque FC, McDougall CG: The evolution of endovascular treatment for intracranial arteriovenous malformations. **Neurosurg Focus 20**:E6, 2006
49. Bristol RE, Albuquerque FC, Spetzler RF, et al: Surgical management of arteriovenous malformations in children. **J Neurosurg 105**:88-93, 2006
50. Brocheriou I, Capron F: [Intracranial arteriovenous malformations: histopathological features.]. **J Neuroradiol 31**:359-361, 2004
51. Brown RD, Jr.: Simple risk predictions for arteriovenous malformation hemorrhage. **Neurosurgery 46**:1024, 2000
52. Brown RD, Jr.: Unruptured brain AVMs: to treat or not to treat. **Lancet Neurol 7**:195-196, 2008
53. Brown RD, Jr., Wiebers DO, Forbes G, et al: The natural history of unruptured intracranial arteriovenous malformations. **J Neurosurg 68**:352-357, 1988
54. Bruner JM, Tien RD, McLendon RE: Tumors of vascular origin, in Bigner DD, McLendon RE, Bruner JM (eds): **Russell & Rubinstein's pathology of tumors of the nervous system.** London: Arnold, 1998, pp 239-293
55. Buatti JM, Friedman WA, Theele DP, et al: The lazaroid U74389G protects normal brain from stereotactic radiosurgery-induced radiation injury. **Int J Radiat Oncol Biol Phys 34**:591-597, 1996
56. Buis DR, Berg Rvd, Lycklama G, et al: Spontaneous regression of brain arteriovenous malformations--a clinical study and a systematic review of the literature. **J Neurol 251**:1375-1382, 2004
57. Buis DR, Dirven CM, Lagerwaard FJ, et al: Radiosurgery of brain arteriovenous malformations in children. **J Neurol 255**:551-560, 2008

58. Buis DR, Lagerwaard FJ, Barkhof F, et al: Stereotactic radiosurgery for brain AVMs: role of interobserver variation in target definition on digital subtraction angiography. **Int J Radiat Oncol Biol Phys 62**:246-252, 2005
59. Buis DR, Lagerwaard FJ, Dirven CM, et al: Delineation of brain AVMs on MR-Angiography for the purpose of stereotactic radiosurgery. **Int J Radiat Oncol Biol Phys 67**:308-316, 2007
60. Carrasco JL, Jover L: Estimating the generalized concordance correlation coefficient through variance components. **Biometrics 59**:849-858, 2003
61. Carter BS, Brisman JL, Ogilvy CS: Spontaneous obliteration of an arteriovenous malformation associated with head trauma. Case illustration. **J Neurosurg 94**:139, 2001
62. Cashen TA, Carr JC, Shin W, et al: Intracranial time-resolved contrast-enhanced MR angiography at 3T. **AJNR Am J Neuroradiol 27**:822-829, 2006
63. Castaigne P, Buge A, Pertuiset B, et al: [Radiologically excluded, thrombosed angioma.]. **Bull Mem Soc Med Hop Paris 77**:923-930, 1961
64. Castro Pena P, Kirova YM, Campana F, et al: Anatomical, clinical and radiological delineation of target volumes in breast cancer radiotherapy planning: individual variability, questions and answers. **Br J Radiol 82**:595-599, 2009
65. Celli P, Ferrante L, Palma L, et al: Cerebral arteriovenous malformations in children. Clinical features and outcome of treatment in children and in adults. **Surg Neurol 22**:43-49, 1984
66. Chang SD, Marcellus ML, Marks MP, et al: Multimodality treatment of giant intracranial arteriovenous malformations. **Neurosurgery 53**:1-11, 2003
67. Chang SD, Shuster DL, Steinberg GK, et al: Stereotactic radiosurgery of arteriovenous malformations: pathologic changes in resected tissue. **Clin Neuropathol 16**:111-116, 1997
68. Chang TC, Shirato H, Aoyama H, et al: Stereotactic irradiation for intracranial arteriovenous malformation using stereotactic radiosurgery or hypofractionated stereotactic radiotherapy. **Int J Radiat Oncol Biol Phys 60**:861-870, 2004
69. Chapman PH, Ogilvy CS, Loeffler JS: The relationship between occlusive hyperemia and complications associated with the radiosurgical treatment of arteriovenous malformations: report of two cases. **Neurosurgery 55**:228-233, 2004
70. Chen JW, Kerber C, HS U: Spontaneous regression of large bilateral basal ganglia arteriovenous malformations. **AJNR Am J Neuroradiol 12**:835-837, 1991
71. Chen Y, Pawlikowska L, Yao JS, et al: Interleukin-6 involvement in brain arteriovenous malformations. **Ann Neurol 59**:72-80, 2006
72. Chin LS, Ma L, DiBiase S: Radiation necrosis following gamma knife surgery: a case-controlled comparison of treatment parameters and long-term clinical follow up. **J Neurosurg 94**:899-904, 2001
73. Choi JH, Mast H, Hartmann A, et al: Clinical and morphological determinants of focal neurological deficits in patients with unruptured brain arteriovenous malformation. **J Neurol Sci 287**:126-130, 2009

74. Choi JH, Mast H, Sciacca RR, et al: Clinical outcome after first and recurrent hemorrhage in patients with untreated brain arteriovenous malformation. **Stroke 37**:1243-1247, 2006
75. Cloft HJ: Spontaneous regression of cerebral arteriovenous malformation in hereditary hemorrhagic telangiectasia. **AJNR Am J Neuroradiol 23**:1049-1050, 2002
76. Cloft HJ, Joseph GJ, Dion JE: Risk of cerebral angiography in patients with subarachnoid hemorrhage, cerebral aneurysm, and arteriovenous malformation: a meta-analysis. **Stroke 30**:317-320, 1999
77. Cockroft KM: Unruptured cerebral arteriovenous malformations: to treat or not to treat. **Stroke 37**:1148-1149, 2006
78. Cockroft KM: Unruptured brain arteriovenous malformations should be treated conservatively: no. **Stroke 38**:3310-3311, 2007
79. Cohen T, Nahari D, Cerem LW, et al: Interleukin 6 induces the expression of vascular endothelial growth factor. **J Biol Chem 271**:736-741, 1996
80. Cohen-Gadol AA, Pollock BE: Radiosurgery for arteriovenous malformations in children. **J Neurosurg 104**:388-391, 2006
81. Colombo F, Cavedon C, Casentini L, et al: Early results of CyberKnife radiosurgery for arteriovenous malformations. **J Neurosurg 111**:807-819, 2009
82. Colombo F, Cavedon C, Francescon P, et al: Three-dimensional angiography for radiosurgical treatment planning for arteriovenous malformations. **J Neurosurg 98**:536-543, 2003
83. Conforti P: Spontaneous disappearance of cerebral arteriovenous angioma. Case report. **J Neurosurg 34**:432-434, 1971
84. Coutinho JM, Stam J: How to treat cerebral venous and sinus thrombosis. **J Thromb Haemost** 2010
85. Cover KS, Lagerwaard FJ, van den Berg R, et al: Color intensity projection of digitally subtracted angiography for the visualization of brain arteriovenous malformations. **Neurosurgery 60**:511-514, 2007
86. Cover KS, Lagerwaard FJ, Senan S: Color intensity projections: A rapid approach for evaluating four-dimensional CT scans in treatment planning. **Int J Radiat Oncol Biol Phys 64**:954-961, 2006
87. Cover K, Lagerwaard F, Senan S: Color Intensity Projections: A Simple Way to Display Changes in Astronomical Images. **PASP 119**:523-526, 2007
88. Crawford PM, West CR, Chadwick DW, et al: Arteriovenous malformations of the brain: natural history in unoperated patients. **J Neurol Neurosurg Psychiatry 49**:1-10, 1986
89. Cronqvist M, Wirestam R, Ramgren B, et al: Endovascular treatment of intracerebral arteriovenous malformations: procedural safety, complications, and results evaluated by MR imaging, including diffusion and perfusion imaging. **AJNR Am J Neuroradiol 27**:162-176, 2006

90. Cronqvist S, Granholm L, Lundstrom NR: Hydrocephalus and congestive heart failure caused by intracranial arteriovenous malformations in infants. **J Neurosurg 36**:249-254, 1972
91. Da Costa L, Wallace MC, ter Brugge KG, et al: The Natural History and Predictive Features of Hemorrhage From Brain Arteriovenous Malformations. **Stroke 40**:100-105, 2009
92. Davidson ASM, Morgan MK: How Safe Is Arteriovenous Malformation Surgery? A Prospective, Observational Study of Surgery As First-Line Treatment for Brain Arteriovenous Malformations. **Neurosurgery 66**: 2010
93. Davie CA, O'Brien P: Stroke and pregnancy. **J Neurol Neurosurg Psychiatry 79**:240-245, 2008
94. Dawkins AA, Evans AL, Wattam J, et al: Complications of cerebral angiography: a prospective analysis of 2,924 consecutive procedures. **Neuroradiology 49**:753-759, 2007
95. De Lange SA: [A case of spontaneous thrombosis of an arteriovenous aneurysm in the brain]. **Ned Tijdschr Geneeskd 99**:944-946, 1955
96. Deorah S, Lynch CF, Sibenaller ZA, et al: Trends in brain cancer incidence and survival in the United States: Surveillance, Epidemiology, and End Results Program, 1973 to 2001. **Neurosurg Focus 20**:E1, 2006
97. Desal HA, uffray-Calvier E, Guillon B, et al: [Emergency imaging of cerebrovascular accidents]. **J Neuroradiol 31**:327-333, 2004
98. Di Rocco C, Tamburrini G, Rollo M: Cerebral arteriovenous malformations in children. **Acta Neurochir (Wien) 142**:145-156, 2000
99. Dias MS: Neurovascular emergencies in pregnancy. **Clin Obstet Gynecol 37**:337-354, 1994
100. Dias MS, Sekhar LN: Intracranial hemorrhage from aneurysms and arteriovenous malformations during pregnancy and the puerperium. **Neurosurgery 27**:855-865, 1990
101. Dion JE, Gates PC, Fox AJ, et al: Clinical events following neuroangiography: a prospective study. **Stroke 18**:997-1004, 1987
102. Doby T: Cerebral angiography and Egas Moniz. **AJR Am J Roentgenol 159**:364, 1992
103. Douglas JG, Goodkin R: Treatment of arteriovenous malformations using Gamma Knife surgery: the experience at the University of Washington from 2000 to 2005. **J Neurosurg 109 Suppl**:51-56, 2008
104. Duong DH, Young WL, Vang MC, et al: Feeding artery pressure and venous drainage pattern are primary determinants of hemorrhage from cerebral arteriovenous malformations. **Stroke 29**:1167-1176, 1998
105. Duran M, Schoenberg SO, Yuh WT, et al: Cerebral arteriovenous malformations: morphologic evaluation by ultrashort 3D gadolinium-enhanced MR angiography. **Eur Radiol 12**:2957-2964, 2002
106. Dyck P: Spontaneous thrombosis of an arteriovenous malformation. **Neurosurgery 1**:287-290, 1977

107. Earnest F, Forbes G, Sandok BA, et al: Complications of cerebral angiography: prospective assessment of risk. **AJR Am J Roentgenol 142**:247-253, 1984
108. Eddleman CS, Jeong HJ, Hurley MC, et al: 4D radial acquisition contrast-enhanced MR angiography and intracranial arteriovenous malformations: quickly approaching digital subtraction angiography. **Stroke 40**:2749-2753, 2009
109. Edmister WB, Lane JI, Gilbertson JR, et al: Tumefactive Cysts: A Delayed Complication following Radiosurgery for Cerebral Arterial Venous Malformations. **AJNR Am J Neuroradiol 26**:1152-1157, 2005
110. Eisenman JI, Alekoumbides A, Pribram H: Spontaneous thrombosis of vascular malformations of the brain. **Acta Radiol Diagn (Stockh) 13**:77-85, 1972
111. Engenhart R, Wowra B, Debus J, et al: The role of high-dose, single-fraction irradiation in small and large intracranial arteriovenous malformations. **Int J Radiat Oncol Biol Phys 30**:521-529, 1994
112. Ezura M, Kagawa S: Spontaneous disappearance of a huge cerebral arteriovenous malformation: case report. **Neurosurgery 30**:595-599, 1992
113. Fee D, Grzybicki D, Dobbs M, et al: Interleukin 6 promotes vasculogenesis of murine brain microvessel endothelial cells. **Cytokine 12**:655-665, 2000
114. Finnerty JJ, Chisholm CA, Chapple H, et al: Cerebral arteriovenous malformation in pregnancy: Presentation and neurologic, obstetric, and ethical significance, . **Am J Obstet Gynecol 181**:296-303, 1999
115. Fiorella D, Albuquerque FC, Woo HH, et al: The role of neuroendovascular therapy for the treatment of brain arteriovenous malformations. **Neurosurgery 59**:S163-S177, 2006
116. Fischer G, Brunon G, Thierry A, et al: [Thrombosis during the development of cerebral arteriovenous aneurysms (a propos of 2 cases]. **J Med Lyon 50**:613-625, 1969
117. Fleetwood IG, Marcellus ML, Levy RP, et al: Deep arteriovenous malformations of the basal ganglia and thalamus: natural history. **J Neurosurg 98**:747-750, 2003
118. Fleetwood IG, Steinberg GK: Arteriovenous malformations. **Lancet 359**:863-873, 2002
119. Flickinger JC: An integrated logistic formula for prediction of complications from radiosurgery. **Int J Radiat Oncol Biol Phys 17**:879-885, 1989
120. Flickinger JC, Kondziolka D, Lunsford LD, et al: Development of a model to predict permanent symptomatic postradiosurgery injury for arteriovenous malformation patients. Arteriovenous Malformation Radiosurgery Study Group. **Int J Radiat Oncol Biol Phys 46**:1143-1148, 2000
121. Flickinger JC, Kondziolka D, Maitz AH, et al: An analysis of the dose-response for arteriovenous malformation radiosurgery and other factors affecting obliteration. **Radiother Oncol 63**:347-354, 2002
122. Flickinger JC, Pollock BE, Kondziolka D, et al: A dose-response analysis of arteriovenous malformation obliteration after radiosurgery. **Int J Radiat Oncol Biol Phys 36**:873-879, 1996

123. Flickinger JC, Schell MC, Larson DA: Estimation of complications for linear accelerator radiosurgery with the integrated logistic formula. **Int J Radiat Oncol Biol Phys 19**:143-148, 1990
124. Flickinger JC, Kondziolka D, Pollock BE, et al: Complications from arteriovenous malformation radiosurgery: Multivariate analysis and risk modeling. **Int J Radiat Oncol Biol Phys 38**:485-490, 1997
125. Foote KD, Friedman WA, Ellis TL, et al: Salvage retreatment after failure of radiosurgery in patients with arteriovenous malformations. **J Neurosurg 98**:337-341, 2003
126. Forster DM, Kunkler IH, Hartland P: Risk of cerebral bleeding from arteriovenous malformations in pregnancy: the Sheffield experience. **Stereotact Funct Neurosurg 61 Suppl 1**:20-22, 1993
127. Forster DM, Steiner L, Hakanson S: Arteriovenous malformations of the brain. A long-term clinical study. **J Neurosurg 37**:562-570, 1972
128. Freudenstein D, Duffner F, Ernemann U, et al: Recurrence of a cerebral arteriovenous malformation after surgical excision. **Cerebrovasc Dis 11**:59-64, 2001
129. Friedlander RM: Clinical practice. Arteriovenous malformations of the brain. **N Engl J Med 356**:2704-2712, 2007
130. Friedman WA, Blatt DL, Bova FJ, et al: The risk of hemorrhage after radiosurgery for arteriovenous malformations. **J Neurosurg 84**:912-919, 1996
131. Friedman WA, Bova FJ, Bollampally S, et al: Analysis of factors predictive of success or complications in arteriovenous malformation radiosurgery. **Neurosurgery 52**:296-307, 2003
132. Friedman WA, Bova FJ, Mendenhall WM: Linear accelerator radiosurgery for arteriovenous malformations: the relationship of size to outcome. **J Neurosurg 82**:180-189, 1995
133. Fullerton HJ, Achrol AS, Johnston SC, et al: Long-term hemorrhage risk in children versus adults with brain arteriovenous malformations. **Stroke 36**:2099-2104, 2005
134. Fults D, Kelly DL, Jr.: Natural history of arteriovenous malformations of the brain: a clinical study. **Neurosurgery 15**:658-662, 1984
135. Fuss M, Salter BJ, Caron JL, et al: Intensity-modulated radiosurgery for childhood arteriovenous malformations. **Acta Neurochir (Wien) 147**:1141-1149, 2005
136. Gabriel EM, Sampson JH, Wilkins RH: Recurrence of a cerebral arteriovenous malformation after surgical excision. **J Neurosurg 84**:879-882, 1996
137. Gabriel RA, Kim H, Sidney S, et al: Ten-Year Detection Rate of Brain Arteriovenous Malformations in a Large, Multiethnic, Defined Population. **Stroke 41**:21-26, 2010
138. Gallina P, Merienne L, Meder JF, et al: Failure in radiosurgery treatment of cerebral arteriovenous malformations. **Neurosurgery 42**:996-1002, 1998

139. Gallina P, Nataf F, Merienne L, et al: [Retrospective analysis of failures in radiosurgery treatment of cerebral arteriovenous malformations]. **Neurochirurgie 47**:311-317, 2001
140. Ganz JC, Reda WA, Abdelkarim K, et al: A simple method for predicting imaging-based complications following gamma knife surgery for cerebral arteriovenous malformations. **J Neurosurg 102 Suppl**:4-7, 2005
141. Garcia-Monaco R, Rodesch G, TerBrugge K, et al: Multifocal dural arteriovenous shunts in children. **Childs Nerv Syst 7**:425-431, 1991
142. Gaspar LE, Ding M: A review of intensity-modulated radiation therapy. **Curr Oncol Rep 10**:294-299, 2008
143. Gault J, Sarin H, Awadallah NA, et al: Pathobiology of human cerebrovascular malformations: basic mechanisms and clinical relevance. **Neurosurgery 55**:1-16, 2004
144. Gauvrit JY, Leclerc X, Oppenheim C, et al: Three-dimensional dynamic MR digital subtraction angiography using sensitivity encoding for the evaluation of intracranial arteriovenous malformations: a preliminary study. **AJNR Am J Neuroradiol 26**:1525-1531, 2005
145. Gauvrit JY, Oppenheim C, Nataf F, et al: Three-dimensional dynamic magnetic resonance angiography for the evaluation of radiosurgically treated cerebral arteriovenous malformations. **Eur Radiol 16**:583-591, 2006
146. Geest RJvd, Lelieveldt BP, Angelie E, et al: Evaluation of a new method for automated detection of left ventricular boundaries in time series of magnetic resonance images using an Active Appearance Motion Model. **J Cardiovasc Magn Reson 6**:609-617, 2004
147. George EJ, Butler P, Plowman PN: Can magnetic resonance imaging alone accurately define the arteriovenous nidus for gamma knife radiosurgery? **J Neurosurg 97 Suppl**:464-470, 2002
148. Gerszten PC, Adelson PD, Kondziolka D, et al: Seizure outcome in children treated for arteriovenous malformations using gamma knife radiosurgery. **Pediatr Neurosurg 24**:139-144, 1996
149. Ghossoub M, Nataf F, Merienne L, et al: [Characteristics of headache associated with cerebral arteriovenous malformations]. **Neurochirurgie 47**:177-183, 2001
150. Gibb PA, Gullan RW, Sandhu N: Spontaneous angiographic disappearance of an intracranial arteriovenous malformation. **Br J Neurosurg 2**:529-533, 1988
151. Gobin YP, Laurent A, Merienne L, et al: Treatment of brain arteriovenous malformations by embolization and radiosurgery. **J Neurosurg 85**:19-28, 1996
152. Graf CJ, Perret GE, Torner JC: Bleeding from cerebral arteriovenous malformations as part of their natural history. **J Neurosurg 58**:331-337, 1983
153. Griffiths PD, Beveridge CJ, Gholkar A: Angiography in non-traumatic brain haematoma. An analysis of 100 cases. **Acta Radiol 38**:797-802, 1997

154. Grzyska U, Freitag J, Zeumer H: Selective cerebral intraarterial DSA. Complication rate and control of risk factors. **Neuroradiology 32**:296-299, 1990
155. Guazzo EP, Xuereb JH: Spontaneous thrombosis of an arteriovenous malformation. **J Neurol Neurosurg Psychiatry 57**:1410-1412, 1994
156. Guglielmi G: Analysis of the hemodynamic characteristics of brain arteriovenous malformations using electrical models: baseline settings, surgical extirpation, endovascular embolization, and surgical bypass. **Neurosurgery 63**:1-10, 2008
157. Guo WY, Lindquist C, Karlsson B, et al: Gamma knife surgery of cerebral arteriovenous malformations: serial MR imaging studies after radiosurgery. **Int J Radiat Oncol Biol Phys 25**:315-323, 1993
158. Guo WY, Nordell B, Karlsson B, et al: Target delineation in radiosurgery for cerebral arteriovenous malformations. Assessment of the value of stereotaxic MR imaging and MR angiography. **Acta Radiol 34**:457-463, 1993
159. Hademenos GJ, Massoud TF: Risk of intracranial arteriovenous malformation rupture due to venous drainage impairment. A theoretical analysis. **Stroke 27**:1072-1083, 1996
160. Hadizadeh DR, von FM, Gieseke J, et al: Cerebral arteriovenous malformation: Spetzler-Martin classification at subsecond-temporal-resolution four-dimensional MR angiography compared with that at DSA. **Radiology 246**:205-213, 2008
161. Halim AX, Johnston SC, Singh V, et al: Longitudinal risk of intracranial hemorrhage in patients with arteriovenous malformation of the brain within a defined population. **Stroke 35**:1697-1702, 2004
162. Halim AX, Singh V, Johnston SC, et al: Characteristics of brain arteriovenous malformations with coexisting aneurysms: a comparison of two referral centers. **Stroke 33**:675-679, 2002
163. Hamada J, Yonekawa Y: Spontaneous disappearance of a cerebral arteriovenous malformation: case report. **Neurosurgery 34**:171-173, 1994
164. Hamann GF, Okada Y, del Zoppo GJ: Hemorrhagic transformation and microvascular integrity during focal cerebral ischemia/reperfusion. **J Cereb Blood Flow Metab 16**:1373-1378, 1996
165. Hamm KD, Klisch J, Surber G, et al: Special aspects of diagnostic imaging for radiosurgery of arteriovenous malformations. **Neurosurgery 62**:A44-A52, 2008
166. Han JH, Kim DG, Chung HT, et al: Clinical and neuroimaging outcome of cerebral arteriovenous malformations after Gamma Knife surgery: analysis of the radiation injury rate depending on the arteriovenous malformation volume. **J Neurosurg 109**:191-198, 2008
167. Han PP, Ponce FA, Spetzler RF: Intention-to-treat analysis of Spetzler-Martin grades IV and V arteriovenous malformations: natural history and treatment paradigm. **J Neurosurg 98**:3-7, 2003

168. Hara H, Burrows PE, Flodmark O, et al: Neonatal superficial cerebral arteriovenous malformations. **Pediatr Neurosurg 20**:126-136, 1994
169. Hartmann A, Mast H, Mohr JP, et al: Morbidity of intracranial hemorrhage in patients with cerebral arteriovenous malformation. **Stroke 29**:931-934, 1998
170. Hartmann A, Mast H, Mohr JP, et al: Determinants of staged endovascular and surgical treatment outcome of brain arteriovenous malformations. **Stroke 36**:2431-2435, 2005
171. Hartmann A, Stapf C, Hofmeister C, et al: Determinants of neurological outcome after surgery for brain arteriovenous malformation. **Stroke 31**:2361-2364, 2000
172. Hashimoto N, Nozaki K: Do cerebral arteriovenous malformations recur after angiographically confirmed total extirpation? **Crit Rev Neurosurg 9**:141-146, 1999
173. Hashimoto T, Emala CW, Joshi S, et al: Abnormal pattern of Tie-2 and vascular endothelial growth factor receptor expression in human cerebral arteriovenous malformations. **Neurosurgery 47**:910-918, 2000
174. Hashimoto T, Matsumoto MM, Li JF, et al: Suppression of MMP-9 by doxycycline in brain arteriovenous malformations. **BMC Neurol 5**:1, 2005
175. Hatt M, Cheze le RC, Turzo A, et al: A fuzzy locally adaptive Bayesian segmentation approach for volume determination in PET. **IEEE Trans Med Imaging 28**:881-893, 2009
176. Hatt M, Cheze le Rest C, Descourt P, et al: Accurate Automatic Delineation of Heterogeneous Functional Volumes in Positron Emission Tomography for Oncology Applications. **Int J Radiat Oncol Biol Phys 77**:301-308, 2010
177. Haw CS, TerBrugge K, Willinsky R, et al: Complications of embolization of arteriovenous malformations of the brain. **J Neurosurg 104**:226-232, 2006
178. Hayashi T, Noshita N, Sugawara T, et al: Temporal profile of angiogenesis and expression of related genes in the brain after ischemia. **J Cereb Blood Flow Metab 23**:166-180, 2003
179. Heeres JG, Hekster RE, Thomeer RA: [Spontaneous thrombosis of arteriovenous malformation in cerebral vessels, 10 years after manifestation of lesion]. **Ned Tijdschr Geneeskd 120**:57-61, 1976
180. Heffez DS, Osterdock RJ, Alderete L, et al: The effect of incomplete patient follow-up on the reported results of AVM radiosurgery. **Surg Neurol 49**:373-381, 1998
181. Heidenreich JO, Schilling AM, Unterharnscheidt F, et al: Assessment of 3D-TOF-MRA at 3.0 Tesla in the characterization of the angioarchitecture of cerebral arteriovenous malformations: a preliminary study. **Acta Radiol 48**:678-686, 2007
182. Heiserman JE, Dean BL, Hodak JA, et al: Neurologic complications of cerebral angiography. **AJNR Am J Neuroradiol 15**:1401-1407, 1994
183. Heros RC: Spetzler-Martin grades IV and V arteriovenous malformations. **J Neurosurg 98**:1-2, 2003
184. Heros RC: Re: Multimodality treatment of posterior fossa arteriovenous malformations. **J Neurosurg 108**:1148-1151, 2008

185. Heros RC, Korosue K, Diebold PM: Surgical excision of cerebral arteriovenous malformations: late results. **Neurosurgery 26**:570-577, 1990
186. Hillman J: Population-based analysis of arteriovenous malformation treatment. **J Neurosurg 95**:633-637, 2001
187. Hino A, Fujimoto M, Yamaki T, et al: Value of repeat angiography in patients with spontaneous subcortical hemorrhage. **Stroke 29**:2517-2521, 1998
188. Hino A, Fujimoto M, Iwamoto Y, et al: An adult case of recurrent arteriovenous malformation after "complete" surgical excision: a case report. **Surg Neurol 52**:156-159, 1999
189. Hofmeister C, Stapf C, Hartmann A, et al: Demographic, morphological, and clinical characteristics of 1289 patients with brain arteriovenous malformation. **Stroke 31**:1307-1310, 2000
190. Hoh BL, Chapman PH, Loeffler JS, et al: Results of multimodality treatment for 141 patients with brain arteriovenous malformations and seizures: factors associated with seizure incidence and seizure outcomes. **Neurosurgery 51**:303-309, 2002
191. Hoh BL, Ogilvy CS, Butler WE, et al: Multimodality treatment of nongalenic arteriovenous malformations in pediatric patients. **Neurosurgery 47**:346-357, 2000
192. Hoh DJ, Liu CY, Chen JC, et al: Chained lightning, part II: neurosurgical principles, radiosurgical technology, and the manipulation of energy beam delivery. **Neurosurgery 61**:433-446, 2007
193. Hoh DJ, Liu CY, Chen JC, et al: Chained lightning: part III--Emerging technology, novel therapeutic strategies, and new energy modalities for radiosurgery. **Neurosurgery 61**:1111-1129, 2007
194. Hook O, Johanson C: Intracranial arteriovenous aneurysms; a follow-up study with particular attention to their growth. **AMA Arch Neurol Psychiatry 80**:39-54, 1958
195. Horton JC, Chambers WA, Lyons SL, et al: Pregnancy and the risk of hemorrhage from cerebral arteriovenous malformations. **Neurosurgery 27**:867-871, 1990
196. Huston J, III, Rufenacht DA, Ehman RL, et al: Intracranial aneurysms and vascular malformations: comparison of time-of-flight and phase-contrast MR angiography. **Radiology 181**:721-730, 1991
197. Iizuka Y, Rodesch G, Garcia-Monaco R, et al: Multiple cerebral arteriovenous shunts in children: report of 13 cases. **Childs Nerv Syst 8**:437-444, 1992
198. Im SH, Han MH, Kwon BJ, et al: Venous-predominant parenchymal arteriovenous malformation: a rare subtype with a venous drainage pattern mimicking developmental venous anomaly. **J Neurosurg 108**:1142-1147, 2008
199. Imbesi SG, Knox K, Kerber CW: Reproducibility analysis of a new objective method for measuring arteriovenous malformation nidus size at angiography. **AJNR Am J Neuroradiol 23**:412-415, 2002

200. Inoue HK, Ohye C: Hemorrhage risks and obliteration rates of arteriovenous malformations after gamma knife radiosurgery. **J Neurosurg 97 Suppl**:474-476, 2002
201. Intensity Modulated Radiation Therapy Collaborative Working Group: Intensity-modulated radiotherapy: current status and issues of interest. **Int J Radiat Oncol Biol Phys 51**:880-914, 2001
202. Isoda K, Fukuda H, Takamura N, et al: Arteriovenous malformation of the brain -- histological study and micrometric measurement of abnormal vessels. **Acta Pathol Jpn 31**:883-893, 1981
203. Itoyama Y, Uemura S, Ushio Y, et al: Natural course of unoperated intracranial arteriovenous malformations: study of 50 cases. **J Neurosurg 71**:805-809, 1989
204. Izawa M, Hayashi M, Chernov M, et al: Long-term complications after gamma knife surgery for arteriovenous malformations. **J Neurosurg 102 Suppl**:34-37, 2005
205. Jabbour MN, Elder JB, Samuelson CG, et al: Aberrant angiogenic characteristics of human brain arteriovenous malformation endothelial cells. **Neurosurgery 64**:139-146, 2009
206. Jayaraman MV, Marcellus ML, Do HM, et al: Hemorrhage rate in patients with Spetzler-Martin grades IV and V arteriovenous malformations: is treatment justified? **Stroke 38**:325-329, 2007
207. Jayaraman MV, Marcellus ML, Hamilton S, et al: Neurologic complications of arteriovenous malformation embolization using liquid embolic agents. **AJNR Am J Neuroradiol 29**:242-246, 2008
208. Jessurun GA, Kamphuis DJ, van der Zande FH, et al: Cerebral arteriovenous malformations in The Netherlands Antilles. High prevalence of hereditary hemorrhagic telangiectasia-related single and multiple cerebral arteriovenous malformations. **Clin Neurol Neurosurg 95**:193-198, 1993
209. Jones J, Jang S, Getch CC, et al: Advances in the radiosurgical treatment of large inoperable arteriovenous malformations. **Neurosurg Focus 23**:E6, 2007
210. Kader A, Goodrich JT, Sonstein WJ, et al: Recurrent cerebral arteriovenous malformations after negative postoperative angiograms. **J Neurosurg 85**:14-18, 1996
211. Kader A, Young WL, Pile-Spellman J, et al: The influence of hemodynamic and anatomic factors on hemorrhage from cerebral arteriovenous malformations. **Neurosurgery 34**:801-807, 1994
212. Kakar M, Olsen DR: Automatic segmentation and recognition of lungs and lesion from CT scans of thorax. **Comput Med Imaging Graph 33**:72-82, 2009
213. Karlsson B, Kihlström L, Lindquist C, et al: Gamma knife surgery for previously irradiated arteriovenous malformations. **Neurosurgery 42**:1-5, 1998
214. Karlsson B, Lax I, Soderman M: Factors influencing the risk for complications following Gamma Knife radiosurgery of cerebral arteriovenous malformations. **Radiother Oncol 43**:275-280, 1997

215. Karlsson B, Lax I, Soderman M: Risk for hemorrhage during the 2-year latency period following gamma knife radiosurgery for arteriovenous malformations. **Int J Radiat Oncol Biol Phys 49**:1045-1051, 2001
216. Karlsson B, Lindquist C, Johansson A, et al: Annual risk for the first hemorrhage from untreated cerebral arteriovenous malformations. **Minim Invasive Neurosurg 40**:40-46, 1997
217. Karlsson B, Lindquist C, Steiner L: Prediction of obliteration after gamma knife surgery for cerebral arteriovenous malformations. **Neurosurgery 40**:425-430, 1997
218. Kasliwal MK, Kale SS, Gupta A, et al: Outcome after hemorrhage following Gamma Knife surgery for cerebral arteriovenous malformations. **J Neurosurg 110**:1003-1009, 2009
219. Kaspari N, Michaelis B, Gademann G: Using an Artificial Neural Network to Define the Planning Target Volume in Radiotherapy. **J Med Syst 21**:389-401, 1997
220. Katsaridis V, Papagiannaki C, Aimar E: Curative embolization of cerebral arteriovenous malformations (AVMs) with Onyx in 101 patients. **Neuroradiology 50**:589-597, 2008
221. Kaufmann TJ, Huston J, III, Mandrekar JN, et al: Complications of diagnostic cerebral angiography: evaluation of 19,826 consecutive patients. **Radiology 243**:812-819, 2007
222. Kelly ME, Guzman R, Sinclair J, et al: Multimodality treatment of posterior fossa arteriovenous malformations. **J Neurosurg 108**:1152-1161, 2008
223. Ketkar M, Shrier D: An allergic reaction to intraarterial nonionic contrast material. **AJNR Am J Neuroradiol 24**:292, 2003
224. Kihlström L, Guo WY, Karlsson B, et al: Magnetic resonance imaging of obliterated arteriovenous malformations up to 23 years after radiosurgery. **J Neurosurg 86**:589-593, 1997
225. Kim BS, Sarma D, Lee SK, et al: Brain edema associated with unruptured brain arteriovenous malformations. **Neuroradiology 51**:327-335, 2009
226. Kim EJ, Halim AX, Dowd CF, et al: The relationship of coexisting extranidal aneurysms to intracranial hemorrhage in patients harboring brain arteriovenous malformations. **Neurosurgery 54**:1349-1357, 2004
227. Kim H, Pawlikowska L, Chen Y, et al: Brain arteriovenous malformation biology relevant to hemorrhage and implication for therapeutic development. **Stroke 40**:S95-S97, 2009
228. Kim LJ, Albuquerque FC, Spetzler RF, et al: Postembolization neurological deficits in cerebral arteriovenous malformations: stratification by arteriovenous malformation grade. **Neurosurgery 59**:53-59, 2006
229. King-Im JM, Trivedi R, Cross J, et al: Conventional digital subtraction x-ray angiography versus magnetic resonance angiography in the evaluation of carotid disease: patient satisfaction and preferences. **Clin Radiol 59**:358-363, 2004

230. Kiran N, Kale S, Kasliwal M, et al: Gamma knife radiosurgery for arteriovenous malformations of basal ganglia, thalamus and brainstemΓÇöa retrospective study comparing the results with that for AVMs at other intracranial locations. **Acta Neurochirurgica**
231. Kjellberg RN, Hanamura T, Davis KR, et al: Bragg-peak proton-beam therapy for arteriovenous malformations of the brain. **N Engl J Med 309**:269-274, 1983
232. Klimo P, Jr., Rao G, Brockmeyer D: Pediatric arteriovenous malformations: a 15-year experience with an emphasis on residual and recurrent lesions. **Childs Nerv Syst 23**:31-37, 2007
233. Klopfenstein JD, Spetzler RF: Cerebral arteriovenous malformations: when is surgery indicated? **Acta Neurochir (Wien) 147**:693-695, 2005
234. Kokkinis C, Vlychou M, Zavras GM, et al: The role of 3D-computed tomography angiography (3D-CTA) in investigation of spontaneous subarachnoid haemorrhage: comparison with digital subtraction angiography (DSA) and surgical findings. **Br J Neurosurg 22**:71-78, 2008
235. Komiyama M, Yamanaka K, Nishikawa M, et al: Prospective analysis of complications of catheter cerebral angiography in the digital subtraction angiography and magnetic resonance era. **Neurol Med Chir (Tokyo) 38**:534-539, 1998
236. Kondziolka D, Humphreys RP, Hoffman HJ, et al: Arteriovenous malformations of the brain in children: a forty year experience. **Can J Neurol Sci 19**:40-45, 1992
237. Kondziolka D, Lunsford LD, Kanal E, et al: Stereotactic magnetic resonance angiography for targeting in arteriovenous malformation radiosurgery. **Neurosurgery 35**:585-590, 1994
238. Kondziolka D, McLaughlin MR, Kestle JR: Simple risk predictions for arteriovenous malformation hemorrhage. **Neurosurgery 37**:851-855, 1995
239. Kondziolka D, Mori Y, Martinez AJ, et al: Beneficial effects of the radioprotectant 21-aminosteroid U-74389G in a radiosurgery rat malignant glioma model. **Int J Radiat Oncol Biol Phys 44**:179-184, 1999
240. Kondziolka D, Somaza S, Martinez AJ, et al: Radioprotective effects of the 21-aminosteroid U-74389G for stereotactic radiosurgery. **Neurosurgery 41**:203-208, 1997
241. Krapf H, Siekmann R, Freudenstein D, et al: Spontaneous occlusion of a cerebral arteriovenous malformation: angiography and MR imaging follow-up and review of the literature. **AJNR Am J Neuroradiol 22**:1556-1560, 2001
242. Krings T, Hans F: New developments in MRA: time-resolved MRA. **Neuroradiology 46 Suppl 2**:s214-s222, 2004
243. Krings T, Ozanne A, Chng SM, et al: Neurovascular phenotypes in hereditary haemorrhagic telangiectasia patients according to age. Review of 50 consecutive patients aged 1 day-60 years. **Neuroradiology 47**:711-720, 2005
244. Kubicek GJ, Machtay M: New advances in high-technology radiotherapy for head and neck cancer. **Hematol Oncol Clin North Am 22**:1165-80, viii, 2008

245. Kubo HD, Wilder RB, Pappas CT: Impact of collimator leaf width on stereotactic radiosurgery and 3D conformal radiotherapy treatment plans. **Int J Radiat Oncol Biol Phys 44**:937-945, 1999
246. Kunieda E, Kawaguchi O, Onozuka S, et al: Intra-arterial CT-angiography for cerebral arteriovenous malformation--initial experiences for treatment planning of radiosurgery. **Int J Radiat Oncol Biol Phys 54**:1121-1133, 2002
247. Kunishima K, Mori H, Itoh D, et al: Assessment of arteriovenous malformations with 3-Tesla time-resolved, contrast-enhanced, three-dimensional magnetic resonance angiography. **J Neurosurg 110**:492-499, 2009
248. Kurita H, Shin M, Ueki K, et al: Congestive brain oedema associated with a pial arteriovenous malformation with impaired venous drainage. **Acta Neurochir (Wien) 143**:339-342, 2001
249. Kushner J, Alexander E Jr: Partial spontaneous regressive arteriovenous malformation; case report with angiographic evidence. **J Neurosurg 32**:360-366, 1970
250. Kwon Y, Jeon SR, Kim JH, et al: Analysis of the causes of treatment failure in gamma knife radiosurgery for intracranial arteriovenous malformations. **J Neurosurg 93 Suppl 3**:104-106, 2000
251. Lang CT, King JC: Maternal mortality in the United States. **Best Pract Res Clin Obstet Gynaecol 22**:517-531, 2008
252. Langer DJ, Lasner TM, Hurst RW, et al: Hypertension, small size, and deep venous drainage are associated with risk of hemorrhagic presentation of cerebral arteriovenous malformations. **Neurosurgery 42**:481-486, 1998
253. Lanzino G, Jensen ME, Cappelletto B, et al: Arteriovenous malformations that rupture during pregnancy: a management dilemma. **Acta Neurochir (Wien) 126**:102-106, 1994
254. Lasjaunias P: A revised concept of the congenital nature of cerebral arteriovenous malformations. **Interv Neuroradiol 3**:275-281, 1997
255. Lasjaunias P, Hui F, Zerah M, et al: Cerebral arteriovenous malformations in children. Management of 179 consecutive cases and review of the literature. **Childs Nerv Syst 11**:66-79, 1995
256. Lasjaunias P, Piske R, TerBrugge K, et al: Cerebral arteriovenous malformations (C. AVM) and associated arterial aneurysms (AA). Analysis of 101 C. AVM cases, with 37 AA in 23 patients. **Acta Neurochir (Wien) 91**:29-36, 1988
257. Lasjaunias P, TerBrugge KG, Berenstein A: Cerebral arteriovenous malformations, in Lasjaunias P, TerBrugge KG, Berenstein A (eds): **Surgical neuroangiography 3: Clinical and interventional aspects in children.** Berlin: Springer, 2006, pp 291-358
258. Lasjaunias PL, Landrieu P, Rodesch G, et al: Cerebral proliferative angiopathy: clinical and angiographic description of an entity different from cerebral AVMs. **Stroke 39**:878-885, 2008

259. Lawton MT: Spetzler-Martin Grade III arteriovenous malformations: surgical results and a modification of the grading scale. **Neurosurgery 52**:740-748, 2003
260. Leclerc X, Gauvrit JY, Trystram D, et al: Imagerie vasculaire non invasive et malformations artérioveineuses cérébrales. **J Neuroradiol 31**:349-358, 2004
261. Ledezma CJ, Hoh BL, Carter BS, et al: Complications of cerebral arteriovenous malformation embolization: multivariate analysis of predictive factors. **Neurosurgery 58**:602-611, 2006
262. Lee BC, Herzberg L, Zimmerman RD, et al: MR imaging of cerebral vascular malformations. **AJNR Am J Neuroradiol 6**:863-870, 1985
263. Lee CZ, Xue Z, Zhu Y, et al: Matrix metalloproteinase-9 inhibition attenuates vascular endothelial growth factor-induced intracerebral hemorrhage. **Stroke 38**:2563-2568, 2007
264. Lee KE, Choi CG, Choi JW, et al: Detection of residual brain arteriovenous malformations after radiosurgery: diagnostic accuracy of contrast-enhanced three-dimensional time of flight MR angiography at 3.0 Tesla. **Korean J Radiol 10**:333-339, 2009
265. Lee SK, Vilela P, Willinsky R, et al: Spontaneous regression of cerebral arteriovenous malformations: clinical and angiographic analysis with review of the literature. **Neuroradiology 44**:11-16, 2002
266. Leffers AM, Wagner A: Neurologic complications of cerebral angiography. A retrospective study of complication rate and patient risk factors. **Acta Radiol 41**:204-210, 2000
267. Leksell L: A stereotaxic apparatus for intracerebral surgery. **Acta Chir Scand 99**:229-233, 1949
268. Leksell L: The stereotaxic method and radiosurgery of the brain. **Acta Chir Scand 102**:316-319, 1951
269. Leramo OB, Clarke WF: Complete spontaneous regression of a cerebral arteriovenous malformation. **South Med J 80**:529-532, 1987
270. Levegrün S, Hof H, Essig M, et al: Radiation-Induced Changes of Brain Tissue after Radiosurgery in Patients with Arteriovenous Malformations: Dose/Volume-Response Relations. **Strahlenther Onkol 180**:758-767, 2004
271. Levegrün S, Hof H, Essig M, et al: Radiation-induced changes of brain tissue after radiosurgery in patients with arteriovenous malformations: correlation with dose distribution parameters. **Int J Radiat Oncol Biol Phys 59**:796-808, 2004
272. Levine J, Misko JC, Seres JL, et al: Spontaneous angiographic disapparance of a cerebral arteriovenous malformation. Third reported case. **Arch Neurol 28**:195-196, 1973
273. Levy EI, Niranjan A, Thompson TP, et al: Radiosurgery for childhood intracranial arteriovenous malformations. **Neurosurgery 47**:834-841, 2000
274. Liang CC, Chang SD, Lai SL, et al: Stroke complicating pregnancy and the puerperium. **Eur J Neurol 13**:1256-1260, 2006
275. Lidegaard O, Edstrom B, Kreiner S: Oral contraceptives and venous thromboembolism: a five-year national case-control study. **Contraception 65**:187-196, 2002

276. Lidegaard O, Kreiner S: Cerebral thrombosis and oral contraceptives. A case-control study. **Contraception 57**:303-314, 1998
277. Ligon BL: The mystery of angiography and the "unawarded" Nobel Prize: Egas Moniz and Hans Christian Jacobaeus. **Neurosurgery 43**:602-611, 1998
278. Lin LI: A concordance correlation coefficient to evaluate reproducibility. **Biometrics 45**:255-268, 1989
279. Lindquist C, Steiner L: Stereotactic radiosurgical treatment of arteriovenous malformations, in Lunsford LD (ed): **Modern Stereotactic Neurosurgery.** Boston: Martinus Nijhoff, 1988, pp 491-505
280. Lindqvist M, Karlsson B, Guo WY, et al: Angiographic long-term follow-up data for arteriovenous malformations previously proven to be obliterated after gamma knife radiosurgery. **Neurosurgery 46**:803-808, 2000
281. Lindvall P, Bergstrom P, Lofroth PO, et al: Hypofractionated conformal stereotactic radiotherapy for arteriovenous malformations. **Neurosurgery 53**:1036-1042, 2003
282. Liscak R, Vladyka V, Simonova G, et al: Arteriovenous malformations after Leksell gamma knife radiosurgery: rate of obliteration and complications. **Neurosurgery 60**:1005-1014, 2007
283. Loeffler JS, Niemierko A, Chapman PH: Second tumors after radiosurgery: tip of the iceberg or a bump in the road? **Neurosurgery 52**:1436-1440, 2003
284. Loeffler JS, Rossitch E Jr, Siddon R, et al: Role of stereotactic radiosurgery with a linear accelerator in treatment of intracranial arteriovenous malformations and tumors in children. **Pediatrics 85**:774-782, 1990
285. Lynn M, Friedman WA: Hyperbaric oxygen in the treatment of a radiosurgical complication: technical case report. **Neurosurgery 60**:E579, 2007
286. Mabe H, Furuse M: Spontaneous disappearance of a cerebral arteriovenous malformation in infancy. Case report. **J Neurosurg 46**:811-815, 1977
287. Maity A, Shu HK, Tan JE, et al: Treatment of pediatric intracranial arteriovenous malformations with linear-accelerator-based stereotactic radiosurgery: the University of Pennsylvania experience. **Pediatr Neurosurg 40**:207-214, 2004
288. Maitz AH, Niranjan A, Jungreis CA, et al: Tube angulation improves angiographic targeting of arteriovenous malformations during stereotactic radiosurgery. **Comput Aided Surg 6**:225-229, 2001
289. Mandybur TI, Nazek M: Cerebral arteriovenous malformations. A detailed morphological and immunohistochemical study using actin. **Arch Pathol Lab Med 114**:970-973, 1990
290. Marconi F, Parenti G, Puglioli M: Spontaneous regression of intracranial arteriovenous malformation. **Surg Neurol 39**:385-391, 1993
291. Maruyama K, Kawahara N, Shin M, et al: The risk of hemorrhage after radiosurgery for cerebral arteriovenous malformations. **N Engl J Med 352**:146-153, 2005

292. Maruyama K, Shin M, Tago M, et al: Radiosurgery to reduce the risk of first hemorrhage from brain arteriovenous malformations. **Neurosurgery 60**:453-458, 2007
293. Mast H, Mohr JP, Osipov A, et al: 'Steal' is an unestablished mechanism for the clinical presentation of cerebral arteriovenous malformations. **Stroke 26**:1215-1220, 1995
294. Mathiesen T: Arguments against the proposed randomised trial (ARUBA). **Neuroradiology 50**:469-471, 2008
295. Matsumoto H, Takeda T, Kohno K, et al: Delayed hemorrhage from completely obliterated arteriovenous malformation after gamma knife radiosurgery. **Neurol Med Chir (Tokyo) 46**:186-190, 2006
296. Mattle HP, Schroth G, Seiler RW: Dilemmas in the management of patients with arteriovenous malformations. **J Neurol 247**:917-928, 2000
297. McIver JI, Pollock BE: Radiation-induced tumor after stereotactic radiosurgery and whole brain radiotherapy: case report and literature review. **J Neurooncol 66**:301-305, 2004
298. Megison P, Batjer HH, Purdy PD, et al: Spontaneous resolution of arteriovenous malformation without hemorrhage. **AJNR Am J Neuroradiol 10**:204, 1989
299. Meisel HJ, Mansmann U, Alvarez H, et al: Cerebral arteriovenous malformations and associated aneurysms: analysis of 305 cases from a series of 662 patients. **Neurosurgery 46**:793-800, 2000
300. Meisel HJ, Mansmann U, Alvarez H, et al: Effect of partial targeted N-butyl-cyano-acrylate embolization in brain AVM. **Acta Neurochir (Wien) 144**:879-887, 2002
301. Metz C: ROC analysis in medical imaging: a tutorial review of the literature. **Radiol Phys Technol 1**:2-12, 2008
302. Minakawa T, Tanaka R, Koike T, et al: Angiographic follow-up study of cerebral arteriovenous malformations with reference to their enlargement and regression. **Neurosurgery 24**:68-74, 1989
303. Miyamoto S, Hashimoto N, Nagata I, et al: Posttreatment sequelae of palliatively treated cerebral arteriovenous malformations. **Neurosurgery 46**:589-594, 2000
304. Miyawaki L, Dowd C, Wara W, et al: Five year results of LINAC radiosurgery for arteriovenous malformations: outcome for large AVMS. **Int J Radiat Oncol Biol Phys 44**:1089-1106, 1999
305. Miyazaki M, Shima T, Yokoyama N, et al: [Spontaneous, and postirradiation complete regression of arteriovenous malformations (AVM) of the brain proved by angiography (author's transl)]. **No Shinkei Geka 6**:195-203, 1978
306. Mizutani T, Tanaka H, Aruga T: Total recanalization of a spontaneously thrombosed arteriovenous malformation. Case report. **J Neurosurg 82**:506-508, 1995
307. Mohr JP: A randomized trial of unruptured brain arteriovenous malformations (ARUBA). **Acta Neurochir Suppl 103**:3-4, 2008
308. Monk JE, Perks JR, Doughty D, et al: Comparison of a micro-multileaf collimator with a 5-mm-leaf-width collimator for intracranial stereotactic radiotherapy. **Int J Radiat Oncol Biol Phys 57**:1443-1449, 2003
309. Montaner J, varez-Sabin J, Molina CA, et al: Matrix metalloproteinase expression is related to hemorrhagic transformation after cardioembolic stroke. **Stroke 32**:2762-2767, 2001
310. Morcos SK, Thomsen HS: Adverse reactions to iodinated contrast media. **Eur Radiol 11**:1267-1275, 2001
311. Morgan M, Sekhon L, Rahman Z, et al: Morbidity of intracranial hemorrhage in patients with cerebral arteriovenous malformation. **Stroke 29**:2001-2002, 1998
312. Morgan MK, Rochford AM, Tsahtsarlis A, et al: Surgical risks associated with the management of Grade I and II brain arteriovenous malformations. **Neurosurgery 54**:832-837, 2004
313. Morgan MK, Sekhon LH, Finfer S, et al: Delayed neurological deterioration following resection of arteriovenous malformations of the brain. **J Neurosurg 90**:695-701, 1999
314. Mori H, Aoki S, Okubo T, et al: Two-dimensional thick-slice MR digital subtraction angiography in the assessment of small to medium-size intracranial arteriovenous malformations. **Neuroradiology 45**:27-33, 2003
315. Mori K, Murata T, Hashimoto N, et al: Clinical analysis of arteriovenous malformations in children. **Childs Brain 6**:13-25, 1980
316. Mourik AMv, Elkhuizen PHM, Minkema D, et al: Multiinstitutional study on target volume delineation variation in breast radiotherapy in the presence of guidelines. **Radiother Oncol 94**:286-291, 2010
317. Mukherji SK, Quisling RG, Kubilis PS, et al: Intracranial arteriovenous malformations: quantitative analysis of magnitude contrast MR angiography versus gradient-echo MR imaging versus conventional angiography. **Radiology 196**:187-193, 1995
318. Mullan S, Mojtahedi S, Johnson DL, et al: Embryological basis of some aspects of cerebral vascular fistulas and malformations. **J Neurosurg 85**:1-8, 1996
319. Murphy PA, Lam MTY, Wu X, et al: Endothelial Notch4 signaling induces hallmarks of brain arteriovenous malformations in mice. **Proc Natl Acad Sci U S A 105**:10901-10906, 2008
320. Nakstad PH, Nornes H: Superselective angiography, embolisation and surgery in treatment of arteriovenous malformations of the brain. **Neuroradiology 36**:410-413, 1994
321. Nataf F, Ghossoub M, Schlienger M, et al: Bleeding after radiosurgery for cerebral arteriovenous malformations. **Neurosurgery 55**:298-305, 2004
322. Nataf F, Schlienger M, Bayram M, et al: Microsurgery or radiosurgery for cerebral arteriovenous malformations? A study of two paired series. **Neurosurgery 61**:39-49, 2007
323. Nataf F, Schlienger M, Lefkopoulos D, et al: Radiosurgery of cerebral arteriovenous malformations in children: a series of 57 cases. **Int J Radiat Oncol Biol Phys 57**:184-195, 2003

324. Nehls DG, Pittman HW: Spontaneous regression of arteriovenous malformations. **Neurosurgery 11**:776-780, 1982
325. Ng J, Kitchen N: Neurosurgery and pregnancy. **J Neurol Neurosurg Psychiatry 79**:745-752, 2008
326. Nicolato A, Foroni R, Seghedoni A, et al: Leksell gamma knife radiosurgery for cerebral arteriovenous malformations in pediatric patients. **Childs Nerv Syst 21**:301-307, 2005
327. Nicolato A, Gerosa M, Ferraresi P, et al: Stereotactic radiosurgery for the treatment of arteriovenous malformations in childhood. **J Neurosurg Sci 41**:359-371, 1997
328. Nicolato A, Lupidi F, Sandri MF, et al: Gamma knife radiosurgery for cerebral arteriovenous malformations in children/adolescents and adults. Part I: Differences in epidemiologic, morphologic, and clinical characteristics, permanent complications, and bleeding in the latency period. **Int J Radiat Oncol Biol Phys 64**:904-913, 2006
329. Nicolato A, Lupidi F, Sandri MF, et al: Gamma Knife radiosurgery for cerebral arteriovenous malformations in children/adolescents and adults. Part II: Differences in obliteration rates, treatment-obliteration intervals, and prognostic factors. **Int J Radiat Oncol Biol Phys 64**:914-921, 2006
330. Niranjan A, Gobbel GT, Kondziolka D, et al: Experimental radiobiological investigations into radiosurgery: present understanding and future directions. **Neurosurgery 55**:495-504, 2004
331. Niranjan A, Maitz A, Kondziolka D: Radiosurgery: current techniques. **Tech Neurosurg 9**:119-127, 2003
332. Niranjan A, Kondziolka D, Lunsford LD: Neoplastic Transformation After Radiosurgery or Radiotherapy: Risk and Realities. **Otolaryngol Clin North Am 42**:717-729, 2009
333. Njeh C: Tumor delineation: The weakest link in the search for accuracy in radiotherapy. **J Med Phys 33**:136-140, 2008
334. Nukui H, Miyagi O, Tamada J, et al: [Long-term follow-up study by cerebral angiography in cases with arteriovenous malformation of the brain. With special reference to spontaneous disappearance of arteriovenous malformation in cerebral angiography (author's transl)]. **Neurol Med Chir (Tokyo) 22**:125-132, 1982
335. Ogilvy CS: Radiation therapy for arteriovenous malformations: a review. **Neurosurgery 26**:725-735, 1990
336. Ogilvy CS, Stieg PE, Awad I, et al: AHA Scientific Statement: Recommendations for the management of intracranial arteriovenous malformations: a statement for healthcare professionals from a special writing group of the Stroke Council, American Stroke Association. **Stroke 32**:1458-1471, 2001
337. Oh BC, Liu CY, Wang MY, et al: Stereotactic radiosurgery: adjacent tissue injury and response after high-dose single fraction radiation. Part II: Strategies for therapeutic enhancement, brain injury mitigation, and brain injury repair. **Neurosurgery 60**:799-814, 2007

338. Ohara S, Umemura S, Wakabayashi S, et al: [Totally thrombosed large arteriovenous malformation--a case report]. **No Shinkei Geka 10**:1233-1237, 1982
339. Omojola MF, Fox AJ, Vinuela FV, et al: Spontaneous regression of intracranial arteriovenous malformations. Report of three cases. **J Neurosurg 57**:818-822, 1982
340. Ondra SL, Troupp H, George ED, et al: The natural history of symptomatic arteriovenous malformations of the brain: a 24-year follow-up assessment. **J Neurosurg 73**:387-391, 1990
341. Oost E, Koning G, Sonka M, et al: Automated contour detection in X-ray left ventricular angiograms using multiview active appearance models and dynamic programming. **IEEE Trans Med Imaging 25**:1158-1171, 2006
342. Oppenheim C, Meder JF, Trystram D, et al: Radiosurgery of cerebral arteriovenous malformations: is an early angiogram needed? **AJNR Am J Neuroradiol 20**:475-481, 1999
343. Osborn AG: Vascular malformations, **Diagnostic cerebral angiography.** Philadelphia: Lippincott Williams & Wilkins, 1999, pp 277-312
344. Osborn AG: Arteriovenous malformation, in Osborn AG (ed): **Diagnostic Imaging: Brain.** Salt Lake City, Utah: Amirsys Inc, 2005, pp I-5-4-I-5-7
345. Osipov A, Koennecke H-C, Hartmann A, et al: Seizures in cerebral arteriovenous aalformations: type, clinical course and medical management. **Interventional Neuroradiology 3**:37-41, 1997
346. Ozsarlak O, Van Goethem JW, Maes M, et al: MR angiography of the intracranial vessels: technical aspects and clinical applications. **Neuroradiology 46**:955-972, 2004
347. Panciani PP, Fontanella M, Carlino C, et al: Progressive spontaneous occlusion of a cerebellar AVM: Pathogenetic hypothesis and review of literature. **Clin Neurol Neurosurg 110**:502-510, 2008
348. Papadias A, Taha A, Sgouros S, et al: Incidence of vascular malformations in spontaneous intra-cerebral haemorrhage in children. **Childs Nerv Syst 23**:881-886, 2007
349. Park YS, Kwon JT: Recurrent cerebral arteriovenous malformation in a child : case report and review of the literature. **J Korean Neurosurg Soc 45**:401-404, 2009
350. Parmar H, Ivancevic MK, Dudek N, et al: Neuroradiologic applications of dynamic MR angiography at 3 T. **Magn Reson Imaging Clin N Am 17**:63-75, 2009
351. Pascual-Castroviejo I, Pascual-Pascual JI, Blazquez MG, et al: Spontaneous occlusion of an intracranial arteriovenous malformation. **Childs Brain 3**:169-179, 1977
352. Pasqualin A, Vivenza C, Rosta L, et al: Spontaneous disappearance of intracranial arteriovenous malformations. **Acta Neurochir (Wien) 76**:50-57, 1985
353. Patel MC, Hodgson TJ, Kemeny AA, et al: Spontaneous obliteration of pial arteriovenous malformations: a review of 27 cases. **AJNR Am J Neuroradiol 22**:531-536, 2001
354. Patil AA: Angiographic disappearance and reappearance of an arteriovenous malformation of the cerebellum and brain stem, and its surgical excision. A case report. **Acta Neurochir (Wien) 62**:247-252, 1982

355. Pavesi G, Rustemi O, Berlucchi S, et al: Acute surgical removal of low-grade (Spetzler-Martin I-II) bleeding arteriovenous malformations. **Surg Neurol 72**:662-667, 2009
356. Pawlikowska L, Poon KY, Achrol AS, et al: Apolipoprotein E epsilon 2 is associated with new hemorrhage risk in brain arteriovenous malformations. **Neurosurgery 58**:838-843, 2006
357. Pawlikowska L, Tran MN, Achrol AS, et al: Polymorphisms in transforming growth factor-beta-related genes ALK1 and ENG are associated with sporadic brain arteriovenous malformations. **Stroke 36**:2278-2280, 2005
358. Pawlikowska L, Tran MN, Achrol AS, et al: Polymorphisms in genes involved in inflammatory and angiogenic pathways and the risk of hemorrhagic presentation of brain arteriovenous malformations. **Stroke 35**:2294-2300, 2004
359. Pearlstein RD, Higuchi Y, Moldovan M, et al: Metalloporphyrin antioxidants ameliorate normal tissue radiation damage in rat brain. **Int J Radiat Oncol Biol Phys 86**:145-163, 2010
360. Perquin DA, Kloet A, Tans JT, et al: [Intracranial arteriovenous malformations in pregnant women]. **Ned Tijdschr Geneeskd 143**:497-500, 1999
361. Petereit D, Mehta M, Turski P, et al: Treatment of arteriovenous malformations with stereotactic radiosurgery employing both magnetic resonance angiography and standard angiography as a database. **Int J Radiat Oncol Biol Phys 25**:309-313, 1993
362. Petkova M, Gauvrit JY, Trystram D, et al: Three-dimensional dynamic time-resolved contrast-enhanced MRA using parallel imaging and a variable rate k-space sampling strategy in intracranial arteriovenous malformations. **J Magn Reson Imaging 29**:7-12, 2009
363. Pinker K, Stavrou I, Knosp E, et al: Are cerebral cavernomas truly nonenhancing lesions and thereby distinguishable from arteriovenous malformations?: MRI findings and histopathological correlation. **Magnetic Resonance Imaging 24**:631-637, 2006
364. Plowman PN: Stereotactic radiosurgery. VIII. The classification of postradiation reactions. **Br J Neurosurg 13**:256-264, 1999
365. Pollock BE: Stereotactic radiosurgery for arteriovenous malformations. **Neurosurg Clin N Am 10**:281-290, 1999
366. Pollock BE: Occlusive hyperemia: a radiosurgical phenomenon? **Neurosurgery 47**:1178-1182, 2000
367. Pollock BE, Brown RD, Jr.: Management of cysts arising after radiosurgery to treat intracranial arteriovenous malformations. **Neurosurgery 49**:259-264, 2001
368. Pollock BE, Flickinger JC: A proposed radiosurgery-based grading system for arteriovenous malformations. **J Neurosurg 96**:79-85, 2002
369. Pollock BE, Flickinger JC: Modification of the radiosurgery-based arteriovenous malformation grading system. **Neurosurgery 63**:239-243, 2008
370. Pollock BE, Flickinger JC, Lunsford LD, et al: Factors that predict the bleeding risk of cerebral arteriovenous malformations. **Stroke 27**:1-6, 1996

371. Pollock BE, Flickinger JC, Lunsford LD, et al: Factors associated with successful arteriovenous malformation radiosurgery. **Neurosurgery 42**:1239-1244, 1998
372. Pollock BE, Gorman DA, Coffey RJ: Patient outcomes after arteriovenous malformation radiosurgical management: results based on a 5- to 14-year follow-up study. **Neurosurgery 52**:1291-1296, 2003
373. Pollock BE, Kline RW, Stafford SL, et al: The rationale and technique of staged-volume arteriovenous malformation radiosurgery. **Int J Radiat Oncol Biol Phys 48**:817-824, 2000
374. Pollock BE, Kondziolka D, Flickinger JC, et al: Magnetic resonance imaging: an accurate method to evaluate arteriovenous malformations after stereotactic radiosurgery. **J Neurosurg 85**:1044-1049, 1996
375. Pollock BE, Kondziolka D, Lunsford LD, et al: Repeat stereotactic radiosurgery of arteriovenous malformations: factors associated with incomplete obliteration. **Neurosurgery 38**:318-324, 1996
376. Pott M, Huber M, Assheuer J, et al: Comparison of MRI, CT and angiography in cerebral arteriovenous malformations. **Bildgebung 59**:98-102, 1992
377. Prat R, Galeano I, Conde R, et al: Surgical removal after first bleeding of an arteriovenous malformation previously obliterated with radiosurgery: case report. **Surg Neurol 71**:211-214, 2009
378. Prince MR: Contrast-enhanced MR angiography: theory and optimization. **Magn Reson Imaging Clin N Am 6**:257-267, 1998
379. Raabe A, Nakaji P, Beck J, et al: Prospective evaluation of surgical microscope-integrated intraoperative near-infrared indocyanine green videoangiography during aneurysm surgery. **J Neurosurg 103**:982-989, 2005
380. Raelson CA, Kanal KM, Vavilala MS, et al: Radiation dose and excess risk of cancer in children undergoing neuroangiography. **Am J Roentgenol 193**:1621-1628, 2009
381. Rajamani K, Fisher M: An overview of atherosclerosis, in Welch KMA, Caplan LR, Reis DJ, et al (eds): **Primer on cerebrovascular diseases.** San Diego: Academic Press, 1997, pp 145-148
382. Raza SM, Jabbour S, Thai QA, et al: Repeat stereotactic radiosurgery for high-grade and large intracranial arteriovenous malformations. **Surg Neurol 68**:24-34, 2007383. Reinacher PC, Stracke P, Reinges MH, et al: Contrast-enhanced time-resolved 3-D MRA: applications in neurosurgery and interventional neuroradiology. **Neuroradiology 49 Suppl 1**:S3-13, 2007
384. Reyns N, Blond S, Gauvrit JY, et al: Role of radiosurgery in the management of cerebral arteriovenous malformations in the pediatric age group: data from a 100-patient series. **Neurosurgery 60**:268-276, 2007
385. Rieger J, Hosten N, Neumann K, et al: Initial clinical experience with spiral CT and 3D arterial reconstruction in intracranial aneurysms and arteriovenous malformations. **Neuroradiology 38**:245-251, 1996

386. Riva D, Pantaleoni C, Devoti M, et al: Radiosurgery for cerebral AVMs in children and adolescents: the neurobehavioral outcome. **J Neurosurg 86**:207-210, 1997
387. Robinson JL, Hall CS, Sedzimir CB: Arteriovenous malformations, aneurysms, and pregnancy. **J Neurosurg 41**:63-70, 1974
388. Rodesch G, Malherbe V, Alvarez H, et al: Nongalenic cerebral arteriovenous malformations in neonates and infants. Review of 26 consecutive cases (1982-1992). **Childs Nerv Syst 11**:231-241, 1995
389. Rodriguez-Arias C, Martinez R, Rey G, et al: Recurrence in a different location of a cerebral arteriovenous malformation in a child after radiosurgery. **Childs Nerv Syst 16**:363-365, 2000
390. Rooij WJv, Sluzewski M, Beute GN: Brain AVM Embolization with Onyx. **AJNR Am J Neuroradiol 28**:172-177, 2007
391. Saleh RS, Lohan DG, Villablanca JP, et al: Assessment of Craniospinal Arteriovenous Malformations at 3T with Highly Temporally and Highly Spatially Resolved Contrast-Enhanced MR Angiography. **AJNR Am J Neuroradiol 29**:1024-1031, 2008
392. Saleh RS, Singhal A, Lohan D, et al: Assessment of Cerebral Arteriovenous Malformations With High Temporal and Spatial Resolution Contrast-Enhanced Magnetic Resonance Angiography: A Review From Protocol to Clinical Application. **Top Magn Reson Imaging 19**: 2008
393. Salpietro FM, Cipri S, Tomasello F, et al: Late onset of a large cavernous aneurysm after spontaneous disappearance of cerebral arteriovenous malformation. Case report. **J Neurosurg Sci 33**:211-214, 1989
394. Sanchez-Mejia RO, Chennupati SK, Gupta N, et al: Superior outcomes in children compared with adults after microsurgical resection of brain arteriovenous malformations. **J Neurosurg 105**:82-87, 2006
395. Sartor K: Spontaneous closure of cerebral arteriovenous malformation demonstrated by angiography and computed tomography. **Neuroradiology 15**:95-98, 1978
396. Sasaki U, Itagaki T, Shimizu H, et al: [Almost complete regression of cerebral arteriovenous malformation--report of a case (author's transl)]. **No Shinkei Geka 4**:175-181, 1976
397. Sawlani V, Handique A, Phadke RV: Spontaneous regression of cerebral AVM due to thrombosis of draining vein--angiographic and MRI demonstration. **J Neurol Sci 223**:195-198, 2004
398. Schaller C, Schramm J: Arteriovenous malformations and magnetic resonance imaging. **J Neurosurg 87**:647-649, 1997
399. Schlienger M, Atlan D, Lefkopoulos D, et al: Linac radiosurgery for cerebral arteriovenous malformations: results in 169 patients. **Int J Radiat Oncol Biol Phys 46**:1135-1142, 2000
400. Schlienger M, Nataf F, Lefkopoulos D, et al: Repeat linear accelerator radiosurgery for cerebral arteriovenous malformations. **Int J Radiat Oncol Biol Phys 56**:529-536, 2003

401. Schneider BF, Eberhard DA, Steiner LE: Histopathology of arteriovenous malformations after gamma knife radiosurgery. **J Neurosurg 87**:352-357, 1997
402. Schwartz ED, Hurst RW, Sinson G, et al: Complete regression of intracranial arteriovenous malformations. **Surg Neurol 58**:139-147, 2002
403. Sedzimir CB, Robinson J: Intracranial hemorrhage in children and adolescents. **J Neurosurg 38**:269-281, 1973
404. Senan S, van Sörnsen de Koste J, Samson M, et al: Evaluation of a target contouring protocol for 3D conformal radiotherapy in non-small cell lung cancer. **Radiother Oncol 53**:247-255, 1999
405. Sharshar T, Lamy C, Mas JL: Incidence and causes of strokes associated with pregnancy and puerperium. A study in public hospitals of Ile de France. Stroke in Pregnancy Study Group. **Stroke 26**:930-936, 1995
406. Shavelson RJ, Webb NM: **Generalizability Theory: A Primer (Measurement Methods for the Social Science)**. Newbury Park, CA: Sage Publications, 1991,
407. Shaw E, Kline R, Gillin M, et al: Radiation Therapy Oncology Group: radiosurgery quality assurance guidelines. **Int J Radiat Oncol Biol Phys 27**:1231-1239, 1993
408. Sheikh BY, Hassounah M, Al-Moutare K, et al: Childhood intracranial arteriovenous malformation in Saudi Arabia. **Childs Nerv Syst 15**:262-266, 1999
409. Shin M, Kawahara N, Maruyama K, et al: Risk of hemorrhage from an arteriovenous malformation confirmed to have been obliterated on angiography after stereotactic radiosurgery. **J Neurosurg 102**:842-846, 2005
410. Shin M, Kawamoto S, Kurita H, et al: Retrospective analysis of a 10-year experience of stereotactic radio surgery for arteriovenous malformations in children and adolescents. **J Neurosurg 97**:779-784, 2002
411. Shin M, Maruyama K, Kurita H, et al: Analysis of nidus obliteration rates after gamma knife surgery for arteriovenous malformations based on long-term follow-up data: the University of Tokyo experience. **J Neurosurg 101**:18-24, 2004
412. Shuey HM, Jr., Day AL, Quisling RG, et al: Angiographically cryptic cerebrovascular malformations. **Neurosurgery 5**:476-479, 1979
413. Sirin S, Kondziolka D, Niranjan A, et al: Prospective staged volume radiosurgery for large arteriovenous malformations: indications and outcomes in otherwise untreatable patients. **Neurosurgery 58**:17-27, 2006
414. Slotman BJ, Lagerwaard FJ, Senan S: 4D imaging for target definition in stereotactic radiotherapy for lung cancer. **Acta Oncol 45**:966-972, 2006
415. Smith HJ, Strother CM, Kikuchi Y, et al: MR imaging in the management of supratentorial intracranial AVMs. **Am J Roentgenol 150**:1143-1153, 1988

416. Smith KA, Shetter A, Speiser B, et al: Angiographic follow-up in 37 patients after radiosurgery for cerebral arteriovenous malformations as part of a multimodality treatment approach. **Stereotact Funct Neurosurg 69**:136-142, 1997
417. Smyth MD, Sneed PK, Ciricillo SF, et al: Stereotactic radiosurgery for pediatric intracranial arteriovenous malformations: the University of California at San Francisco experience. **J Neurosurg 97**:48-55, 2002
418. Soderman M, Andersson T, Karlsson B, et al: Management of patients with brain arteriovenous malformations. **Eur J Radiol 46**:195-205, 2003
419. Soderman M: **Volume determination and predictive models in the management of cerebral arteriovenous malformations**. Thesis: Stockholm, Karolinska Hospital, 2000,
420. Sohn CH, Sevick RJ, Frayne R: Contrast-enhanced MR angiography of the intracranial circulation. **Magn Reson Imaging Clin N Am 11**:599-614, 2003
421. Sorimachi T, Koike T, Takeuchi S, et al: Embolization of cerebral arteriovenous malformations achieved with polyvinyl alcohol particles: angiographic reappearance and complications. **AJNR Am J Neuroradiol 20**:1323-1328, 1999
422. Spetzler RF: Arteriovenous malformation grading system. **J Neurosurg 108**:185, 2008
423. Spetzler RF, Martin NA: A proposed grading system for arteriovenous malformations. **J Neurosurg 65**:476-483, 1986
424. Spetzler RF, Martin NA: A proposed grading system for arteriovenous malformations. 1986. **J Neurosurg 108**:186-193, 2008
425. Spetzler RF, Martin NA, Carter LP, et al: Surgical management of large AVM's by staged embolization and operative excision. **J Neurosurg 67**:17-28, 1987
426. Spetzler RF, Wilson CB, Weinstein P, et al: Normal perfusion pressure breakthrough theory. **Clin Neurosurg 25**:651-672, 1978
427. Spiegelmann R, Friedman WA, Bova FJ: Limitations of angiographic target localization in planning radiosurgical treatment. **Neurosurgery 30**:619-623, 1992
428. Spoelstra FO, Senan S: Novel tools in radiotherapy. **Ann Oncol 19 Suppl 7**:vii294-vii299, 2008
429. Stapf C: The rationale behind "A Randomized Trial of Unruptured Brain AVMs" (ARUBA). **Acta Neurochir Suppl 107**:83-85, 2010
430. Stapf C, Khaw AV, Sciacca RR, et al: Effect of age on clinical and morphological characteristics in patients with brain arteriovenous malformation. **Stroke 34**:2664-2669, 2003
431. Stapf C, Labovitz DL, Sciacca RR, et al: Incidence of adult brain arteriovenous malformation hemorrhage in a prospective population-based stroke survey. **Cerebrovasc Dis 13**:43-46, 2002
432. Stapf C, Mast H, Sciacca RR, et al: The New York Islands AVM Study: design, study progress, and initial results. **Stroke 34**:e29-e33, 2003

433. Stapf C, Mast H, Sciacca RR, et al: Predictors of hemorrhage in patients with untreated brain arteriovenous malformation. **Neurology 66**:1350-1355, 2006
434. Stapf C, Mohr JP, Pile-Spellman J, et al: Concurrent arterial aneurysms in brain arteriovenous malformations with haemorrhagic presentation. **J Neurol Neurosurg Psychiatry 73**:294-298, 2002
435. Stapf C, Mohr JP, Choi JH, et al: Invasive treatment of unruptured brain arteriovenous malformations is experimental therapy. **Current Opinion in Neurology 19**: 2006
436. Stefani MA, Porter PJ, TerBrugge KG, et al: Angioarchitectural factors present in brain arteriovenous malformations associated with hemorrhagic presentation. **Stroke 33**:920-924, 2002
437. Stefani MA, Porter PJ, TerBrugge KG, et al: Large and deep brain arteriovenous malformations are associated with risk of future hemorrhage. **Stroke 33**:1220-1224, 2002
438. Stein SC, Burnett MG, Zager EL, et al: Completion angiography for surgically treated cerebral aneurysms: an economic analysis. **Neurosurgery 61**:1162-1167, 2007
439. Steinberg GK, Chang SD, Levy RP, et al: Surgical resection of large incompletely treated intracranial arteriovenous malformations following stereotactic radiosurgery. **J Neurosurg 84**:920-928, 1996
440. Steinberg GK, Fabrikant JI, Marks MP, et al: Stereotactic heavy-charged-particle Bragg-peak radiation for intracranial arteriovenous malformations. **N Engl J Med 323**:96-101, 1990
441. Suzuki M, Matsui O, Kobayashi K, et al: Contrast-enhanced MRA for investigation of cerebral arteriovenous malformations. **Neuroradiology 45**:231-235, 2003
442. Swoboda NA, Armstrong DG, Smith J, et al: Pediatric patient surface doses in neuroangiography. **Pediatric Radiology 35**:859-866, 2005
443. Takano S, Nose T, Maki Y, et al: [Spontaneous occlusion of a cerebral arteriovenous malformation--report of a case]. **No Shinkei Geka 15**:991-996, 1987
444. Tanabe S, Uede T, Nonaka T, et al: Diagnosis of cerebral arteriovenous malformations with three-dimensional CT angiography. **J Clin Neurosci 5**:33-38, 1998
445. Tanaka H, Numaguchi Y, Konno S, et al: Initial experience with helical CT and 3D reconstruction in therapeutic planning of cerebral AVMs: comparison with 3D time-of-flight MRA and digital subtraction angiography. **J Comput Assist Tomogr 21**:811-817, 1997
446. Tanaka R, Miyasaka Y, Fujii K, et al: Vascular structure of arteriovenous malformations. **Journal of Clinical Neuroscience 7**:24-28, 2000
447. Tanaka T, Kobayashi T, Kida Y, et al: Comparison between adult and pediatric arteriovenous malformations treated by Gamma Knife radiosurgery. **Stereotact Funct Neurosurg 66 Suppl 1**:288-295, 1996

448. Taschner CA, Gieseke J, Le T, V, et al: Intracranial arteriovenous malformation: time-resolved contrast-enhanced MR angiography with combination of parallel imaging, keyhole acquisition, and k-space sampling techniques at 1.5 T. **Radiology 246**:871-879, 2008
449. The Arteriovenous Malformation Study Group: Arteriovenous malformations of the brain in adults. **N Engl J Med 340**:1812-1818, 1999
450. Thierry-Chef I, Simon SL, Land CE, et al: Radiation Dose to the Brain and Subsequent Risk of Developing Brain Tumors in Pediatric Patients Undergoing Interventional Neuroradiology Procedures. **Radiation Research 170**:553-565, 2009
451. Thierry-Chef I, Simon S, Miller D: Radiation dose and cancer risk among pediatric patients undergoing interventional neuroradiology procedures. **Pediatric Radiology 36**:159-162, 2006
452. Touboul E, Al HA, Buffat L, et al: Single-fraction stereotactic radiotherapy: a dose-response analysis of arteriovenous malformation obliteration. **Int J Radiat Oncol Biol Phys 41**:855-861, 1998
453. Trivedi RA, Kirkpatrick PJ: Arteriovenous malformations of the cerebral circulation that rupture in pregnancy. **J Obstet Gynaecol 23**:484-489, 2003
454. Tsuchiya K, Katase S, Yoshino A, et al: MR digital subtraction angiography of cerebral arteriovenous malformations. **AJNR Am J Neuroradiol 21**:707-711, 2000
455. Unlu E, Temizoz O, Albayram S, et al: Contrast-enhanced MR 3D angiography in the assessment of brain AVMs. **Eur J Radiol 60**:367-378, 2006
456. Uno M, Satoh K, Matsubara S, et al: Does multimodality therapy of arteriovenous malformations improve patient outcome? **Neurol Res 26**:50-54, 2004
457. Valavanis A, Schubiger O, Wichmann W: Classification of brain arteriovenous malformation nidus by magnetic resonance imaging. **Acta Radiol Suppl 369**:86-89, 1986
458. Vinuela F, Dion JE, Duckwiler G, et al: Combined endovascular embolization and surgery in the management of cerebral arteriovenous malformations: experience with 101 cases. **J Neurosurg 75**:856-864, 1991
459. Vinuela F, Fox AJ, Pelz D, et al: Angiographic follow-up of large cerebral AVMs incompletely embolized with isobutyl-2-cyanoacrylate. **AJNR Am J Neuroradiol 7**:919-925, 1986
460. Voges J, Treuer H, Lehrke R, et al: Risk analysis of LINAC radiosurgery in patients with arteriovenous malformation (AVM). **Acta Neurochir Suppl 68**:118-123, 1997
461. Vorwerk H, Beckmann G, Bremer M, et al: The delineation of target volumes for radiotherapy of lung cancer patients. **Radiother Oncol 91**:455-460, 2009
462. Wakai S, Chen CH, Wu KY, et al: Spontaneous regression of a cerebral arteriovenous malformation. Report of a case and review of the literature. **Arch Neurol 40**:377-380, 1983

463. Watanabe H, Nakamura H, Matsuo Y, et al: [Spontaneous regression of cerebral arteriovenous malformation following major artery thrombosis proximal to dominant feeders: a case report]. **No Shinkei Geka 23**:371-376, 1995
464. Weber F, Knopf H: Incidental findings in magnetic resonance imaging of the brains of healthy young men. **J Neurol Sci 240**:81-84, 2006
465. Weber W, Kis B, Siekmann R, et al: Preoperative embolization of intracranial arteriovenous malformations with Onyx. **Neurosurgery 61**:244-252, 2007
466. Wedderburn CJ, van BJ, Bhattacharya JJ, et al: Outcome after interventional or conservative management of unruptured brain arteriovenous malformations: a prospective, population-based cohort study. **Lancet Neurol 7**:223-230, 2008
467. Wei LH, Kuo ML, Chen CA, et al: Interleukin-6 promotes cervical tumor growth by VEGF-dependent angiogenesis via a STAT3 pathway. **Oncogene 22**:1517-1527, 2003
468. Weintraub MI, Khoury A, Cole SP: Biologic effects of 3 Tesla (T) MR imaging comparing traditional 1.5 T and 0.6 T in 1023 consecutive outpatients. **J Neuroimaging 17**:241-245, 2007
469. Weiss E, Hess CF: The Impact of Gross Tumor Volume (GTV) and Clinical Target Volume (CTV) Definition on the Total Accuracy in Radiotherapy. **Stralenther Onkol 179**:21-30, 2003
470. Wiebers DO: Subarachnoid hemorrhage in pregnancy. **Semin Neurol 8**:226-229, 1988
471. Wilkins RH: Natural history of intracranial vascular malformations: a review. **Neurosurgery 16**:421-430, 1985
472. Williamson R, Kondziolka D, Kanaan H, et al: Adverse Radiation Effects after Radiosurgery May Benefit from Oral Vitamin E and Pentoxifylline Therapy: A Pilot Study. **Stereotact Funct Neurosurg 86**:359-366, 2008
473. Willinsky RA, Fitzgerald M, TerBrugge K, et al: Delayed angiography in the investigation of intracerebral hematomas caused by small arteriovenous malformations. **Neuroradiology 35**:307-311, 1993
474. Willinsky RA, Taylor SM, TerBrugge K, et al: Neurologic complications of cerebral angiography: prospective analysis of 2,899 procedures and review of the literature. **Radiology 227**:522-528, 2003
475. Wolfe SQ, Heros RC: Developmental venous anomalies with arterial supply. **J Neurosurg 108**:1139-1141, 2008
476. Wong EK, Truong PT, Kader HA, et al: Consistency in seroma contouring for partial breast radiotherapy: Impact of guidelines. **Int J Radiat Oncol Biol Phys 66**:372-376, 2006
477. Wong JH, Awad IA, Kim JH: Ultrastructural pathological features of cerebrovascular malformations: a preliminary report. **Neurosurgery 46**:1454-1459, 2000
478. Yamada S, Takagi Y, Nozaki K, et al: Risk factors for subsequent hemorrhage in patients with cerebral arteriovenous malformations. **J Neurosurg 107**:965-972, 2007

479. Yamamoto M, Jimbo M, Hara M, et al: Gamma knife radiosurgery for arteriovenous malformations: long-term follow-up results focusing on complications occurring more than 5 years after irradiation. **Neurosurgery 38**:906-914, 1996
480. Yamamoto M, Jimbo M, Ide M, et al: Long-term follow-up of radiosurgically treated arteriovenous malformations in children: report of nine cases. **Surg Neurol 38**:95-100, 1992
481. Yang GY, Xu B, Hashimoto T, et al: Induction of focal angiogenesis through adenoviral vector mediated vascular endothelial cell growth factor gene transfer in the mature mouse brain. **Angiogenesis 6**:151-158, 2003
482. Yao JS, Zhai W, Young WL, et al: Interleukin-6 triggers human cerebral endothelial cells proliferation and migration: the role for KDR and MMP-9. **Biochem Biophys Res Commun 342**:1396-1404, 2006
483. Yaşargil MG: Hemodynamics, in Yaşargil MG (ed): **Microneurosurgery IIIA. AVM of the Brain: History, Embryology, Pathological Considerations, Hemodynamics, Diagnostic Studies, Microsurgical Anatomy.** Stuttgart New York: Thieme Verlag, 1987, pp 213-239
484. Yaşargil MG: History, in Yaşargil MG (ed): **Microneurosurgery IIIA. AVM of the Brain: History, Embryology, Pathological Considerations, Hemodynamics, Diagnostic Studies, Microsurgical Anatomy.** Stuttgart New York: Thieme Verlag, 1987, pp 3-22
485. Yen CP, Varady P, Sheehan J, et al: Subtotal obliteration of cerebral arteriovenous malformations after gamma knife surgery. **J Neurosurg 106**:361-369, 2007
486. Yu C, Petrovich Z, Apuzzo ML, et al: Study of magnetic resonance imaging-based arteriovenous malformation delineation without conventional angiography. **Neurosurgery 54**:1104-discussion, 2004
487. Zabel A, Milker-Zabel S, Huber P, et al: Treatment outcome after linac-based radiosurgery in cerebral arteriovenous malformations: retrospective analysis of factors affecting obliteration. **Radiother Oncol 77**:105-110, 2005
488. Zabel-du Bois A, Milker-Zabel S, Huber P, et al: Pediatric cerebral arteriovenous malformations: the role of stereotactic linac-based radiosurgery. **Int J Radiat Oncol Biol Phys 65**:1206-1211, 2006
489. Zabel-du Bois A, Milker-Zabel S, Huber P, et al: Risk of hemorrhage and obliteration rates of LINAC-based radiosurgery for cerebral arteriovenous malformations treated after prior partial embolization. **Int J Radiat Oncol Biol Phys 68**:999-1003, 2007
490. Zabel-du Bois A, Stefanie M, Peter H, et al: Stereotactic linac-based radiosurgery in the treatment of cerebral arteriovenous malformations located deep, involving corpus callosum, motor cortex, or brainstem. **Int J Radiat Oncol Biol Phys 64**:1044-1048, 2006 (Abstract)

491. Zabel-du Bois A, Milker-Zabel S, Huber P, et al: Linac-based radiosurgery or hypofractionated stereotactic radiotherapy in the treatment of large cerebral arteriovenous malformations. **Int J Radiat Oncol Biol Phys 64**:1049-1054, 2006
492. Zabel-du Bois A, Wagner-Ecker M, Milker-Zabel S, et al: Gene Expression Signatures in the Peripheral Blood After Radiosurgery of Human Cerebral Arteriovenous Malformations. **Stralenther Onkol 186**:91-98, 2010
493. Zhang H, Maki JH, Prince MR: 3D contrast-enhanced MR angiography. **J Magn Reson Imaging 25**:13-25, 2007
494. Zhang XQ, Shirato H, Aoyama H, et al: Clinical significance of 3D reconstruction of arteriovenous malformation using digital subtraction angiography and its modification with CT information in stereotactic radiosurgery. **Int J Radiat Oncol Biol Phys 57**:1392-1399, 2003
495. Zhang ZG, Zhang L, Jiang Q, et al: VEGF enhances angiogenesis and promotes blood-brain barrier leakage in the ischemic brain. **J Clin Invest 106**:829-838, 2000
496. Zhao J, Wang S, Li J, et al: Clinical characteristics and surgical results of patients with cerebral arteriovenous malformations. **Surg Neurol 63**:156-161, 2005
497. Zipfel GJ, Bradshaw P, Bova FJ, et al: Do the morphological characteristics of arteriovenous malformations affect the results of radiosurgery? **J Neurosurg 101**:393-401, 2004

Publications

1. Buis DR, Meijer OW, van den Berg R, Lagerwaard FJ, Bot JC, Slotman BJ, Vandertop WP. Clinical outcome after repeated radiosurgery for brain arteriovenous malformations. **Radiother Oncol**. 2010 May;95(2):250-6.
2. Van den Berg R, Buis DR, Lagerwaard FJ, Lycklama à Nijeholt GJ, Vandertop WP. Extensive white matter changes after stereotactic radiosurgery for brain arteriovenous malformations: a prognostic sign for obliteration? **Neurosurgery**. 2008 Dec;63(6):1064-9; discussion 1069-70.
3. Buis DR, Vandertop WP. Gamma knife surgery and arteriovenous malformations. **J Neurosurg Pediatr**. 2008 Sep;2(3):229.
4. Buis DR, Buis CR, Feller RE, Mandl ES, Peerdeman SM. A basic model for practice of intracranial microsurgery. **Surg Neurol**. 2009 Feb;71(2):254-6.
5. Buis DR, Dirven CM, Lagerwaard FJ, Mandl ES, Lycklama à Nijeholt GJ, Eshghi DS, Van den Berg R, Baayen JC, Meijer OW, Slotman BJ, Vandertop WP. Radiosurgery of brain arteriovenous malformations in children. **J Neurol**. 2008 Apr;255(4):551-60.
6. Mandl ES, Dirven CM, Buis DR, Postma TJ, Vandertop WP. Repeated surgery for glioblastoma multiforme: only in combination with other salvage therapy. **Surg Neurol**. 2008 May;69(5):506-9; discussion 509.
7. Cover KS, Lagerwaard FJ, van den Berg R, Buis DR, Slotman BJ. Color intensity projection of digitally subtracted angiography for the visualization of brain arteriovenous malformations. **Neurosurgery**. 2007 Mar;60(3):511-4; discussion 514-5.
8. Buis DR, Lagerwaard FJ, Dirven CM, Barkhof F, Knol DL, van den Berg R, Slotman BJ, Vandertop WP. Delineation of brain AVMs on MR-Angiography for the purpose of stereotactic radiosurgery**. Int J Radiat Oncol Biol Phys**. 2007 Jan 1;67(1):308-16.
9. Mandl ES, Buis DR, Heimans JJ, Peerdeman SM. Acquired encephaloceles and epilepsy in osteopetrosis. **Acta Neurochir (Wien)**. 2007 Jan;149(1):79-81; discussion 81.
10. Buis DR, Dirven CM, van den Berg R, Manoliu RA, Vandertop WP. Air in the carotid canal as a predictor of distal internal carotid artery laceration. **Acta Neurochir (Wien)**. 2006 Nov;148(11):1201-3; discussion 1203.
11. Buis DR, van Ouwerkerk WJ, Takahata H, Vandertop WP. Intracranial aneurysms in children under 1 year of age: a systematic review of the literature. **Childs Nerv Syst**. 2006 Nov;22(11):1395-409.
12. Buis DR, Lagerwaard FJ, Barkhof F, Dirven CM, Lycklama à Nijeholt GJ, Meijer OW, van den Berg R, Langendijk HA, Slotman BJ, Vandertop WP. Stereotactic radiosurgery for brain AVMs: role of interobserver variation in target definition on digital subtraction angiography. **Int J Radiat Oncol Biol Phys.** 2005 May 1;62(1):246-52.
13. Buis DR, van den Berg R, Lycklama G, van der Worp HB, Dirven CM, Vandertop WP. Spontaneous regression of brain arteriovenous malformations--a clinical study and a systematic review of the literature. **J Neurol**. 2004 Nov;251(11):1375-82.
14. Buis DR, Peerdeman SM, Vandertop WP. Metastatic adenocarcinoma in the cerebellopontine angle, presenting as a meningioma: a case report of rare occurrence. **Acta Neurochir (Wien).** 2004 Dec;146(12):1369-72; discussion 1372.

Dankwoord

Dit proefschrift is het resultaat van een intensieve samenwerking tussen de afdelingen neurochirurgie, radiotherapie en radiologie van het VU Medisch Centrum. Graag wil ik iedereen bedanken die direct of indirect heeft bijgedragen aan de totstandkoming van dit proefschrift. Een aantal personen wil ik graag in het bijzonder bedanken.

Mijn promotoren en co-promotoren:
Prof. dr. W.P. Vandertop, *Geachte professor, ik prijs me zeer gelukkig met het feit dat u mij negen jaar geleden de gelegenheid hebt gegeven om klinisch onderzoek te combineren met werk als arts op de afdeling neurochirurgie van het VUmc. En ik ben u zeer dankbaar dat u mij wilde opleiden tot neurochirurg. U wordt voor mij het meest gekenmerkt door een groot gevoel voor humor en een prettige laagdrempelige toegankelijkheid voor het bespreken van klinische en wetenschappelijke problemen. Ik heb uw positieve blik op situaties en anders dan verwachte uitkomsten zeer gewaardeerd en hoop ooit iets mee te krijgen van uw vermogen om een doorbraak te bereiken in lastige onderhandelingen en omstandigheden. Hartelijk dank hiervoor! Ik hoop op en buiten de OK nog veel van u te leren.*

Prof. dr. C.M.F. Dirven, *Beste Clemens, met jouw vertrek naar Rotterdam is het VUmc niet alleen een groot neurochirurg, maar ook een 'Renaissance Man' armer. Naast neurochirurgie en wetenschap leerde ik van jou ook de grondbeginselen van jagen en de kenmerken van Italiaanse opera's. Dank je wel!*

Prof.dr. B.J. Slotman en prof. dr. F.D.R.K. Barkhof, *Beste professor Slotman, dank u wel voor de kritische beoordeling van de manuscripten. Wat voor artikel ik ook geschreven had, u had altijd een positieve en optimistische feedback. Beste Frederik, dank je wel voor de kritische beoordeling van de manuscripten en het intekenen van talloze AVMs. Ik heb van jou bij uitstek geleerd om 'materiaal en methoden' voor het starten van het feitelijke onderzoek helemaal uit te werken. Beiden heel veel dank hiervoor.*

Dr. F.J. Lagerwaard, *Beste Frank, toen jij uit Rotterdam naar het VUmc kwam was ik al ongeveer een jaar, zonder succes, bezig om een interobserver studie op te zetten. Pas toen ik mensen van de medische fysica sprak kwam ik er achter dat jij veel wist over het opzetten van interobserver studies. Jouw hulp, inzicht, ideeën en het vermogen om ideeën in concrete plannen om te zetten, en vervolgens nieuwe ideeën te genereren zijn onmisbaar geweest in het opzetten van de belangrijkste studies in dit proefschrift. Ik ben je hier zeer dankbaar voor en denk dat zonder jouw bemoeienis dit proefschrift niet in deze vorm tot stand was gekomen.*

Alle mede-auteurs, ben ik dankbaar voor waardevolle suggesties, het beoordelen van de manuscripten en foto's, aanvullingen, nieuwe ideeën en statistische berekeningen.
Dr. R. van den Berg, dr. G.J. Lycklama à Nijeholt en dr. J. Bot wil ik graag bedanken voor het beoordelen van alle MRI-beelden en het intekenen van tientallen AVMs. Beste René, heel veel dank voor de hulp bij het 'de puntjes op de i zetten' in het laatste stadium van dit proefschrift. Beste Geert, ik ben je heel dankbaar voor de suggestie dat een, toen nog AGNIO neurochirurgie, best een Master-degree in Neurovascular Disease zou kunnen behalen, q.e.d.

De leden van de leescommissie, prof. dr. J.J. Heimans, dr. C. Majoie, prof. dr. K. Van Overbeeke, prof. dr. S. Senan en prof. dr. R.M. Verdaasdonk, hartelijk dank voor het beoordelen van het manuscript en de bereidheid zitting te nemen in de beoordelingscommissie.
Alle stafleden van het Neurochirurgisch Centrum Amsterdam wil ik bedanken voor het in mij gestelde vertrouwen en voor het opleiden tot neurochirurg.

Alle artsen van het Neurochirurgisch Centrum Amsterdam, ben ik dankbaar voor de fijne samenwerking de afgelopen jaren. Daarnaast ben ik speciaal dank verschuldigd aan mijn kamergenoot Friso Hoefnagels voor de eindeloze discussies over relevante en irrelevante onderwerpen. Het feit dat een zeiler en snowboarder een kamer kan delen met een waterskiër en alpine-skiër schept hoop voor de toekomst.

De stereotaxie laboranten: Kim, Corinne, Gilian en Sietse, wil ik graag bedanken voor de hulp met importeren van foto's en voor het samen op- en afschroeven van meer dan 300 stereotactische ringen.

Alle medewerkers van de afdeling neurochirurgie, dank jullie wel voor de samenwerking. Ik wil in het bijzonder de verpleegkundigen bedanken voor de gezelligheid en voor het keer op keer mogelijk maken van opnames. Daarnaast wil ik de medewerkers van de klinische en poliklinische secretariaten neurochirurgie bedanken voor al hun inspanningen, tijd, aandacht en gezelligheid en voor het uitwerken van brieven op onmogelijke tijdstippen

Ik ben er trots op dat een aantal mensen mij vertrouwde hun paranimf te zijn: dr. R.J.L. Stuyt, internist en MDL-arts, dr. R.F.J. Schop, internist-hematoloog, en dr. R. Nandoe, neurochirurg i.o. Jullie konden niet mijn paranimf zijn omdat ik daar reeds op de Langebrug blijvende afspraken over had gemaakt. Desalniettemin ben ik zeer vereerd jullie paranimf te zijn geweest! Ik wens jullie ieder toekomstig succes.

Mijn eigen paranimfen: Ellen Mandl en Okke Snieders ben ik veel dank verschuldigd. Ellen, je bent de beste en meest betrokken dokter die ik ken. Daarnaast ben je ook mijn beste vriendin en de op één na beste neurochirurg ter wereld! Okke, na alle Langebrug avonturen lag het voor de hand dat je mijn paranimf zou worden. Ik beschouw het als een grote eer.

Mijn broer(tje) Kevin wil ik bedanken voor alle hulp en gezelligheid de afgelopen jaren. Ik ben zo blij dat je naast me woont!

Het meest van alles wil ik mijn ouders bedanken voor alles wat jullie voor mij gedaan hebben.
Zonder jullie was ik nooit zo ver gekomen...

Curriculum Vitae

The author was born on July 28th, 1973 in Amsterdam, The Netherlands. After finishing secondary school at the 'Veenlanden College' in Mijdrecht. He entered law school at Leiden University in 1993. His medical training started in 1994 at the same university. During medical training he performed basic research after the permeability of the blood-brain-barrier at the Department of Pharmacology 1 of the University of Nagasaki, Japan (dr. M.A. Deli and prof. M. Niwa). During the final two years of his medical training in the Leiden University Medical Center he followed a clerkship in Gynaecology and Obstetrics in Paramaribo, Surinam and a clerkship in pediatric neurosurgery at the Institute for Neurology and Neurosurgery, Beth Israel Medical Center in New York, NY (prof. F.J. Epstein). He obtained the Master of Laws degree in 2000, and the Medical Doctor degree in 2001. In 2001 he started as a resident-not-in-training at the department of Neurosurgery of the VU University Medical Center. During this residency he started the research described in this thesis under supervision of prof. dr. W.P. Vandertop and prof. dr. B.J. Slotman. In 2006 he was international fellow at the Department of Neurosurgery of the Barrow's Neurological Institute in Phoenix, AZ (prof. R.F. Spetzler). In the same year he obtained a Master of Science degree in Neurovascular Diseases at the Faculty of Medicin, University of Paris XI. He started neurosurgical training in May 2006 at the Neurosurgical Center Amsterdam (head: prof. dr. W.P. Vandertop, supervisor: dr. S.M. Peerdeman). In 2007 he was trained in neurology for one year at the Academic Medical Center (prof. dr. J. Stam and prof. dr. M. Vermeulen). In 2008 he was trained in Intensive Care medicine in the VU University Medical Center (prof. dr. A.R.J. Girbes), and in 2010 in spinal surgery at the Neurosurgical Spine Center of the St. Lucas Andreas Hospital (dr. G.J. Bouma). He hopes to complete his neurosurgical training in November 2011. His interests in neurosurgery are directed towards pediatric and vascular neurosurgery.

Now this is not the end. It is not even the beginning of the end.
But it is, perhaps, the end of the beginning.

Sir Winston S. Churchill, Mansion House, London, 10th November 1942